NUREG/CR-2897

Calculations of Hydrogen Detonations in Nuclear Containments by the Random Choice Method

RECEIVED BY TIC OCT 06 1982

MASTER

DO NOT MICROFILM
COVER

Prepared by M. A. Delichatsios, M. B. Genadry, M. N. Fardis

Department of Civil Engineering
Massachusetts Institute of Technology

Prepared for
U.S. Nuclear Regulatory
Commission

DISTRIBUTION OF THIS DOCUMENT IS UNLIMITED

DISCLAIMER

This report was prepared as an account of work sponsored by an agency of the United States Government. Neither the United States Government nor any agency thereof, nor any of their employees, makes any warranty, express or implied, or assumes any legal liability or responsibility for the accuracy, completeness, or usefulness of any information, apparatus, product, or process disclosed, or represents that its use would not infringe privately owned rights. Reference herein to any specific commercial product, process, or service by trade name, trademark, manufacturer, or otherwise does not necessarily constitute or imply its endorsement, recommendation, or favoring by the United States Government or any agency thereof. The views and opinions of authors expressed herein do not necessarily state or reflect those of the United States Government or any agency thereof.

DISCLAIMER

Portions of this document may be illegible in electronic image products. Images are produced from the best available original document.

NOTICE

This report was prepared as an account of work sponsored by an agency of the United States Government. Neither the United States Government nor any agency thereof, or any of their employees, makes any warranty, expressed or implied, or assumes any legal liability of responsibility for any third party's use, or the results of such use, of any information, apparatus, product or process disclosed in this report, or represents that its use by such third party would not infringe privately owned rights.

Availability of Reference Materials Cited in NRC Publications

Most documents cited in NRC publications will be available from one of the following sources:

1. The NRC Public Document Room, 1717 H Street, N.W.
   Washington, DC 20555
2. The NRC/GPO Sales Program, U.S. Nuclear Regulatory Commission,
   Washington, DC 20555
3. The National Technical Information Service, Springfield, VA 22161

Although the listing that follows represents the majority of documents cited in NRC publications, it is not intended to be exhaustive.

Referenced documents available for inspection and copying for a fee from the NRC Public Document Room include NRC correspondence and internal NRC memoranda; NRC Office of Inspection and Enforcement bulletins, circulars, information notices, inspection and investigation notices; Licensee Event Reports; vendor reports and correspondence; Commission papers; and applicant and licensee documents and correspondence.

The following documents in the NUREG series are available for purchase from the NRC/GPO Sales Program: formal NRC staff and contractor reports, NRC-sponsored conference proceedings, and NRC booklets and brochures. Also available are Regulatory Guides, NRC regulations in the *Code of Federal Regulations*, and *Nuclear Regulatory Commission Issuances*.

Documents available from the National Technical Information Service include NUREG series reports and technical reports prepared by other federal agencies and reports prepared by the Atomic Energy Commission, forerunner agency to the Nuclear Regulatory Commission.

Documents available from public and special technical libraries include all open literature items, such as books, journal and periodical articles, and transactions. *Federal Register* notices, federal and state legislation, and congressional reports can usually be obtained from these libraries.

Documents such as theses, dissertations, foreign reports and translations, and non-NRC conference proceedings are available for purchase from the organization sponsoring the publication cited.

Single copies of NRC draft reports are available free upon written request to the Division of Technical Information and Document Control, U.S. Nuclear Regulatory Commission, Washington, DC 20555.

Copies of industry codes and standards used in a substantive manner in the NRC regulatory process are maintained at the NRC Library, 7920 Norfolk Avenue, Bethesda, Maryland, and are available there for reference use by the public. Codes and standards are usually copyrighted and may be purchased from the originating organization or, if they are American National Standards, from the American National Standards Institute, 1430 Broadway, New York, NY 10018.

GPO Printed copy price: $7.50

NUREG/CR--2897

DE83 900138

NUREG/CR-2897
RD

Calculations of Hydrogen Detonations in Nuclear Containments by the Random-Choice Method

MASTER

Manuscript Completed: December 1981
Date Published: September 1982

Prepared by
M. A. Delichatsios, M. B. Genadry, M. N. Fardis

Department of Civil Engineering
Massachusetts Institute of Technology
Cambridge MA 02139

Prepared for
Division of Engineering Technology
Office of Nuclear Regulatory Research
U.S. Nuclear Regulatory Commission
Washington, D.C. 20555
NRC FIN B7085

NOTICE

PORTIONS OF THIS REPORT ARE ILLEGIBLE. It has been reproduced from the best available copy to permit the broadest possible availability.

DISTRIBUTION OF THIS DOCUMENT IS UNLIMITED

ABSTRACT

Computer codes which simulate hydrogen detonators in planar, cylindrical, spherical and two-dimensional axisymmetric geometries have been developed. The computational method is based on the Random Choice Technique which can handle accurately sharp discontinuities. The detonation front is represented in the model as a discontinuity which changes the still unburnt gas to a completely burnt one, according to the Chapman-Jouguet conditions. Numerical results for one-dimensional geometries show good agreement with available analytical solutions. The one-dimensional code was modified to include coupling with an elastically deformable wall and the modified version was used to demonstrate that for typical concrete containment structures interaction of the waves with wall deformations has insignificant effects on the wave properties, and can be neglected. The two-dimensional axisymmetric code was used to calculate pressure time histories at the wall of a cylindrical containment capped with a semi-spherical dome. Dimensions were similar to the ones of the containment of the Indian Point Nuclear Power Plant. The detonations simulated had initiation at either the center of the base mat or at a point on the axis at approximately two-thirds the cylinder height, and were for two different intensities. Computed pressures included repeated reflections at the walls and died out within a few tenths of a second.

TABLE OF CONTENTS (CONTINUED)

TABLE OF CONTENTS

Blank Page

LIST OF FIGURES

CHAPTER I

INTRODUCTION

1.1 Background Information

After the Three Mile Island accident of March 28, 1979, questions haye been raised concerning the safety of Nuclear Power Plants if a rapid hydrogen explosion occurs.

Internal explosions are a severe test for the integrity of the containment structure of Nuclear Power Plants. In Light-Water-Reactors (LWR) such events may result from hydrogen detonations (due to exothermic chemical reactions between hydrogen and oxygen) or steam explosions. Hydrogen is generated from the coolant water, both during normal operations and during accidents. Sources of hydrogen during normal operation include aqueous corrosion of core metals, electrolysis and radiolysis. During an accident that involves core heatup, hydrogen may be produced in the core by the high-temperature reaction of water with metals, namely with zirconium from the zircaloy fuel cladding and with iron from the molten steel. Large quantities of hydrogen gas may thus accumulate in the reactor pressure vessel, as was actually the case in the Three Mile Island accident. The sources of oxygen are primarily in-leakage of air, and again, water electrolysis and radiolysis.

In the event of such internal explosions, the consequences could be catastrophic as they may cause the failure of several Engineering Safety Systems and hence, the containment structure is the last line of defense against early release of radioactive fission-products to the atmosphere.

1.2 Hydrogen Combustion

If the hydrogen is homogeneously distributed in a containment, deflagrations or detonations may occur if the composition of the hydrogen-air mixture falls within the corresponding range on the Shapiro and Moffette [1.1] tripartite diagram. Flammability limits depend on the pressure, temperature and direction of the flame. Considerable uncertainty exists on the exact location of the detonability limits. Shapiro and Moffette assumed these limits to be 19% and 45% hydrogen for air-hydrogen mixtures and drew the limits conservatively, almost parallel to the flammability limits. Detonation limits also depend on the pressure and were found to be equal to 20% and 65% in hydrogen-air mixtures at room pressure and temperature [1.2].

Detonation is a shock wave driven and sustained by the chemical energy released from oxygen-hydrogen reaction. The shock wave and the chemical reaction propagate together at a supersonic speed relative to the burnt medium. The shock front is characterized by an abrupt increase in pressure, temperature and density of the gas and by a net forward movement of the gas particles.

Detonation may start as a result of minor sparks, contact to metal surface, temperature above the spontaneous ignition temperature, minor shock propagating in the gas or by transition from deflagration. Although a detonation is very unlikely to happen in a LWR containment, the possibility should not be disregarded because of the high temperature and pressure, and the intense radiation in case of an accident.

1.3 Previous Work in the Area

The effect of the quasi-static increase of pressure (resulting from slow burning) on containments integrity has been studied by the U.S.N.R.C. [1.3] and Fardis [1.4]; however, little has been done on the effect of a detonation on the containment structure.

Morrison et al., [1.5] have treated the hydrogen detonation and steam explosion in an over-simplified manner. They modeled these phenomena as TNT explosions occurring at the center of a containment (idealized as a sphere), through an equivalence between released energy and TNT mass. Then they computed the peak overpressure at a distance equal to the containment radius. They neglected the effect of the reflection at the wall pressure (the reflection can increase the overpressure by a factor of the order of 2 to 3).

In a better attempt, Carbiener et al. [1.6] tried to solve the same problem; however, they neglected the fact that the

shock pressure takes a finite time to decay from its Chapman-Jouguet plane to the steady state pressure (the Chapman-Jouguet plane is the detonation front plane); thus, the impulse calculated on the basis of this assumption may be 300-400 times smaller. They also neglected the effect of repeated reflections.

After the Three Mile Island accident, the interest in this area rose again; Byers [1.7] studied the effect of the hydrogen detonation on the containment structure using a code based on "artificial viscosity". The code was originally used for continuum mechanics problems and it is difficult to adapt it to hydrogen detonations. Running such a program requires a large amount of CPU time.

1.4 Objective

Development of a numerical model able to predict correctly the behavior of the gas in an axisymmetric containment in case of an explosion is required in order to assess the capability of the structure to contain the explosion. Because of many uncertainties in the physical models, it is very difficult to develop a computer program to predict the initiation and development of a hydrogen detonation. It has been assumed in this work that a hydrogen detonation can be developed instantaneously after ignition. Such conditions present a higher challenge for the containment structure since pressure waves induced by detonation are expected to be larger than pressure waves induced by a slow combustion (deflagration).

In this research, a reliable computer code is developed capable of solving the hydrogen detonation problem for axisymmetric geometries.

The gas dynamics equations for planar, cylindrical and axisymmetric geometries are derived in Chapter II; the following assumptions are made:

1) homogeneous mixing of the hydrogen with steam and air in the containment volume,

2) the energy due to radiation is negligible

3) heating of the containment wall by the gases is negligible.

The Random Choice Technique is used for solving numerically the equations of motion. Chapter III includes the principles, the advantages and the implementation of the method for planar, spherical and axisymmetric geometries. Validation of the method, pressure histories and interactions with the wall are included in Chapter IV. Chapter V presents the application of the two-dimensional code in computing the pressure histories generated by a hydrogen detonation in a realistic nuclear containment building. The conclusions are summarized in Chapter VI.

Blank Page

CHAPTER II

COMPRESSIBLE FLOW EQUATIONS

In this chapter the basic gas dynamics equations which constitute the starting point of the analysis are presented. The derivation can be found in any gas dynamics book (see for example Landau & Lifshitz [2.1]).

The equations describing the motion of a compressible inviscid gas are:

$$\frac{\partial \rho}{\partial t} + \rho \nabla \cdot \underset{\sim}{u} = 0, \tag{2.1a}$$

$$\frac{\partial \underset{\sim}{u}}{\partial t} + \underset{\sim}{u} \cdot \nabla \underset{\sim}{u} = - \frac{1}{\rho} \nabla p, \tag{2.1b}$$

$$\frac{\partial e}{\partial t} + \nabla \cdot (e+p) \underset{\sim}{u} = \rho Q, \tag{2.1c}$$

where ρ is the density, $\underset{\sim}{u}$ is the velocity, p is the pressure, e is the total energy per unit volume, and t is time. The energy due to external sources or sinks, Q, is considered to be equal to zero. The total energy, e, is given by

$$e = \rho \varepsilon + \frac{1}{2} \rho \, |\underset{\sim}{u}|^2, \tag{2.2}$$

where

$$\varepsilon = \varepsilon_i + q, \tag{2.3}$$

and

$$\varepsilon_i = \frac{1}{\gamma-1} \frac{p}{\rho} . \qquad (2.4)$$

In equations (2.2), (2.3) and (2.4) ε_i is the internal energy per unit mass, γ is a gas constant equal to C_p/C_v, $\gamma > 1$ and q is the energy released by chemical reactions.

2.1 One-Dimensional Cartesian Coordinate System

The equations in one-dimensional cartesian coordinate system follow directly from equations (2.1). The gradient and divergence are

$$\nabla\phi = \frac{\partial\phi}{\partial x} \underset{\sim}{i} , \qquad (2.1.1)$$

and

$$\nabla\cdot\underset{\sim}{u} = \frac{\partial u_x}{\partial x} , \qquad (2.1.2)$$

where $\underset{\sim}{i}$ is the unit vector in the x direction , and $\underset{\sim}{u} = u_x\underset{\sim}{i}$. After rearranging the gas dynamics equations, we get:

$$\frac{\partial\rho}{\partial t} + \frac{\partial m}{\partial x} = 0, \qquad (2.1.3a)$$

$$\frac{\partial m}{\partial t} + \frac{\partial}{\partial x}\left(\frac{m^2}{\rho} + p\right) = 0, \qquad (2.1.3b)$$

$$\frac{\partial e}{\partial t} + \frac{\partial}{\partial x}\left(\frac{m}{\rho}(e+p)\right) = 0, \qquad (2.1.3c)$$

where $m = \rho u_x$ is the momentum flux. Observe that the equations in one-dimensional cartesian system can be written in a conservation form without source or sink terms.

2.2 One-Dimensional Spherical and Cylndrical Coordinate Systems

$$\nabla\phi = \frac{\partial\phi}{\partial r}\,\underset{\sim}{j}\,, \qquad (2.2.1)$$

and

$$\nabla \cdot \underset{\sim}{u}\ \frac{\partial u_r}{\partial r} + (\eta-1)\,\frac{u_r}{r}\,, \qquad (2.2.2)$$

where $\underset{\sim}{j}$ is the unit vector in the r direction and $\eta = 3$ for spherical, $\eta = 2$ for cylindrical coordinates.

By inserting these relations in the gas dynamics equations (2.1), we obtain

$$\frac{\partial\rho}{\partial t} + \frac{\partial m}{\partial r} = -(\eta-1)\,\frac{m}{r}\,, \qquad (2.2.3a)$$

$$\frac{\partial m}{\partial t} + \frac{\partial}{\partial r}\left(\frac{m^2}{\rho} + p\right) = -(\eta-1)\frac{m^2}{\rho r}, \qquad (2.2.3b)$$

$$\frac{\partial e}{\partial t} + \frac{\partial}{\partial r}\left(\frac{m}{\rho}(e+p)\right) = -(\eta-1)\,\frac{m}{\rho r}(e+p), \qquad (2.2.3c)$$

where in this case, $m = \rho u_r$ is the momentum flux and u_r is the radial velocity. Observe that in cylindrical or spherical coordinates, the equations have sink terms.

2.3 Axisymmetric (Two-Dimensional Cylindrical) Coordinate System

In a two-dimensional cylindrical coordinate system, the gradient and the divergence are

$$\nabla\phi = \frac{\partial\phi}{\partial r}\ \underset{\sim}{j} + \frac{\partial\phi}{\partial z}\ \underset{\sim}{k}\ , \tag{2.3.1}$$

$$\nabla \cdot \underset{\sim}{u} = \frac{\partial u_r}{\partial r} + \frac{\partial u_z}{\partial z} + \frac{u_z}{r}\ , \tag{2.3.2}$$

where $\underset{\sim}{j}$ and $\underset{\sim}{k}$ are unit vectors in the r and z directions and

$$\underset{\sim}{u} = u_r\underset{\sim}{j} + u_z\underset{\sim}{k}.$$

The gas dynamics equations for the axisymmetric problem become

$$\frac{\partial\rho}{\partial t} + \frac{\partial m_r}{\partial r} + \frac{\partial m_z}{\partial z} = -\frac{m_r}{r}, \tag{2.3.3a}$$

$$\frac{\partial m_r}{\partial t} + \frac{\partial}{\partial r}\left(\frac{m_r^2}{\rho} + p\right) + \frac{\partial}{\partial z}\left(\frac{m_r m_z}{\rho}\right) = -\frac{m_r^2}{\rho r}\ , \tag{2.3.3b}$$

$$\frac{\partial m_z}{\partial t} + \frac{\partial}{\partial r}\left(\frac{m_r m_z}{\rho}\right) + \frac{\partial}{\partial z}\left(\frac{m_z^2}{\rho} + p\right) = -\frac{m_r m_z}{\rho r}\ , \tag{2.3.3c}$$

$$\frac{\partial e}{\partial t} + \frac{\partial}{\partial r}\left(\frac{m_r}{\rho}(e+p)\right) + \frac{\partial}{\partial z}\left(\frac{m_z}{\rho}(e+p)\right) = -\frac{m_r}{\rho r}(e+p), \tag{2.3.3d}$$

where $m_r = \rho u_r$ is the momentum flux in the radial direction and $m_z = \rho u_z$ is the momentum flux in the z direction.

Equations (2.3.3) can be written in the general vector form used by Sod (1980)

$$\underset{\sim}{U}_t + \underset{\sim}{F}(\underset{\sim}{U})_r + \underset{\sim}{G}(\underset{\sim}{U})_z = -\underset{\sim}{W}(\underset{\sim}{U}), \qquad (2.3.4)$$

where subscripts indicate differentiation. In equation (2.3.4)

$$\underset{\sim}{U} = \begin{bmatrix} \rho \\ m_r \\ m_z \\ e \end{bmatrix}, \quad \underset{\sim}{F}(\underset{\sim}{U}) = \begin{bmatrix} m_r \\ m_r^2/\rho + p \\ m_r m_z/\rho \\ m_r(e+p)/\rho \end{bmatrix}, \quad \underset{\sim}{G}(\underset{\sim}{U}) = \begin{bmatrix} m_z \\ m_r m_z/\rho \\ m_z^2/\rho + p \\ m_z(e+p)/\rho \end{bmatrix}, \quad \underset{\sim}{W}(\underset{\sim}{U}) = \begin{bmatrix} m_r/r \\ m_r^2/\rho r \\ m_r m_z/\rho r \\ m_z(e+p)/\rho r \end{bmatrix}$$

It is worth noticing at this point that equations (2.1.3) for the one-dimensional cartesian problem can be recovered from equation (2.3.4) by setting $\underset{\sim}{G}(\underset{\sim}{U}) = \underset{\sim}{W}(\underset{\sim}{U}) = 0$. Similarly, equations (2.2.3) can be obtained by taking $\underset{\sim}{G}(\underset{\sim}{U}) = 0$.

2.4 Chapman-Jouguet (C-J) Conditions

The one-dimensional cartesian equations (section 2.1) can be solved in a closed form (see Williams [2.2]) or Courant and Friedrich [2.3]).

In the following discussion the subscript u refers to the unburnt gas (i.e., gas which has not yet undergone chemical reaction) and the subscript b refers to the burnt gas. By defining

$$w_b = u_b - U \text{ and } w_u = u_u - U,$$

where U is the velocity of the reaction zone and u is the particle velocity in the Eulerian reference frame, we can express the continuity and momentum equation by

$$\rho_b w_b = \rho_u w_b = -M, \tag{2.4.1}$$

$$\rho_u w_u^2 + p_u = \rho_b w_b^2 + p_b. \tag{2.4.2}$$

From these relations we can deduce

$$-M^2 = (p_b - p_u)/(\tau_b - \tau_u), \tag{2.4.3}$$

where $\tau = 1/\rho$. From the energy equation an expression for τ_b in function of τ_u, γ, q, p_u and p_b can be derived

$$\tau_b = \tau_u\left(\frac{p_u + \mu^2 p_b}{\mu^2 p_u + p_b}\right) + \frac{2\mu^2 q}{\mu^2 p_u + p_b}, \tag{2.4.4}$$

where $\mu^2 = \frac{\gamma - 1}{\gamma + 1}$; in deriving equation (2.4.4), it has been assumed that $\gamma_b = \gamma_u = \gamma$.

A C-J detonation moves with respect to the burnt gas with a velocity equal to the velocity of sound in the burnt gas, i.e.,

$$|w_b| = c_b = \left(\frac{\gamma p_b}{\rho_b}\right)^{1/2} \tag{2.4.5}$$

Using equations (2.4.1), (2.4.2) and (2.4.5) we can find an expression for p_b,

$$p_b^2 + 2bp_b + c = 0, \tag{2.4.6}$$

where

$$b = -p_u - q\rho_u(\gamma-1),^{+} \tag{2.4.7a}$$

and

$$c = p_u^2 + 2\mu^2 p_u \rho_u q; \tag{2.4.7b}$$

A trivial calculation shows that $b^2 - c \geq 0$ if $\gamma \geq 1$ and $q \leq 0$ (exothermic reaction). Thus,

$$p_{cj} = p_b = -b + (b^2 - c)^{1/2}, \tag{2.4.8}$$

where the + sign is mandatory since a detonation is compressive. Therefore, given the properties of the unburnt gas and the energy per unit mass released by the combustion, we can find the pressure behind a C-J. detonation; equation (2.4.4) is used to find the density ρ_{cj}. From equation (2.4.1) we find the expression for the detonation speed,

$$u_{cj} = (\rho_u u_u + (\gamma p_{cj}/\rho_{cj})^{1/2})/\rho_u, \tag{2.4.9}$$

and then,

$$u_{cj} = U_{cj} - c_{cj}. \tag{2.4.10}$$

If a C-J detonation occurs, it is followed by a rarefaction wave to adjust to the boundary conditions. For a still wall behind the detonation, the gas has to adjust itself to a zero velocity at the wall. A non-dimensional analysis has been performed by Taylor [2.5] to deter-

---

+Notice that in Chorin [2.4] the second term of this expression is multiplied by 2 which is incorrect.

mine the behavior of the gas behind a detonation if bounded by a wall. The resulting curves are shown in Figures 2.4.1-3. The solution of this planar problem was obtained by taking into account the consistency of the Riemann invariants in the rarefaction region. The solution is hence dependent on the gas constant γ. It is seen from the figures that the gas has constant properties until about a mid-distance between the wall and the detonation front; at this point a discontinuity occurs and the velocity starts increasing linearly towards the C-J velocity; the equations describing the pressure and density curves are polynomials of order 5 and 7.

An analysis similar to Taylor's has been performed for radially symmetric detonations by Barenblatt et al.[2.6]. For $\gamma = 1.4$ the results are shown in Figures 2.4.1-3. It can be seen that the gradients of the velocity, pressure and density near the detonation front are larger in the cylindrical coordinate system than in the planar one. They become even larger for a spherical detonation.

In the next chapter we will present the numerical techniques used for solving the equations of motion.

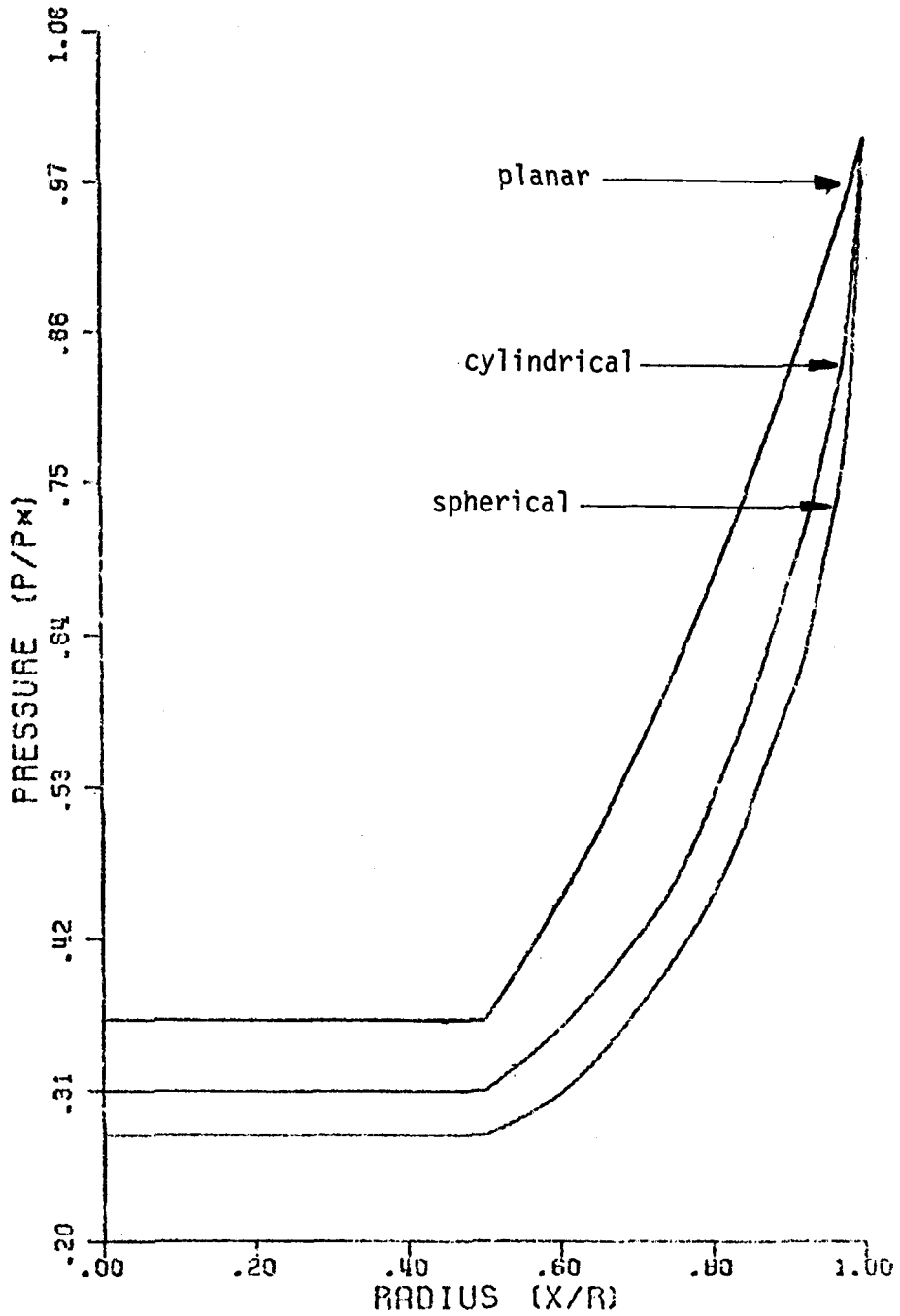

FIGURE 2.4.1: PRESSURE DISTRIBUTION BEHIND PLANAR, CYLINDRICAL AND SPHERICAL DETONATION FRONTS WHEN $\gamma = 1.4$

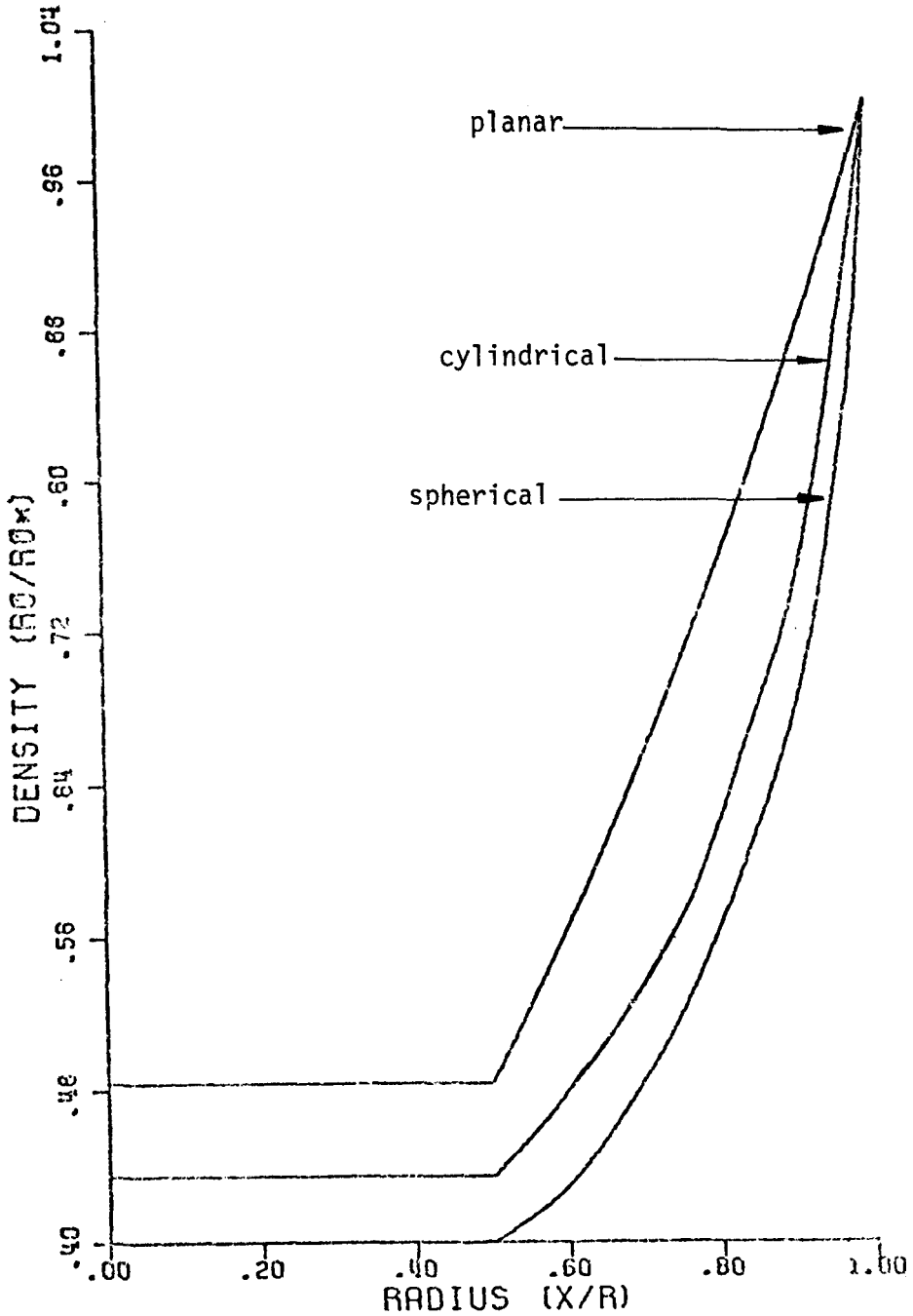

FIGURE 2.4.2: DENSITY DISTRIBUTION BEHIND PLANAR, CYLINDRICAL AND SPHERICAL DETONATION FRONTS WHEN $\gamma = 1.4$

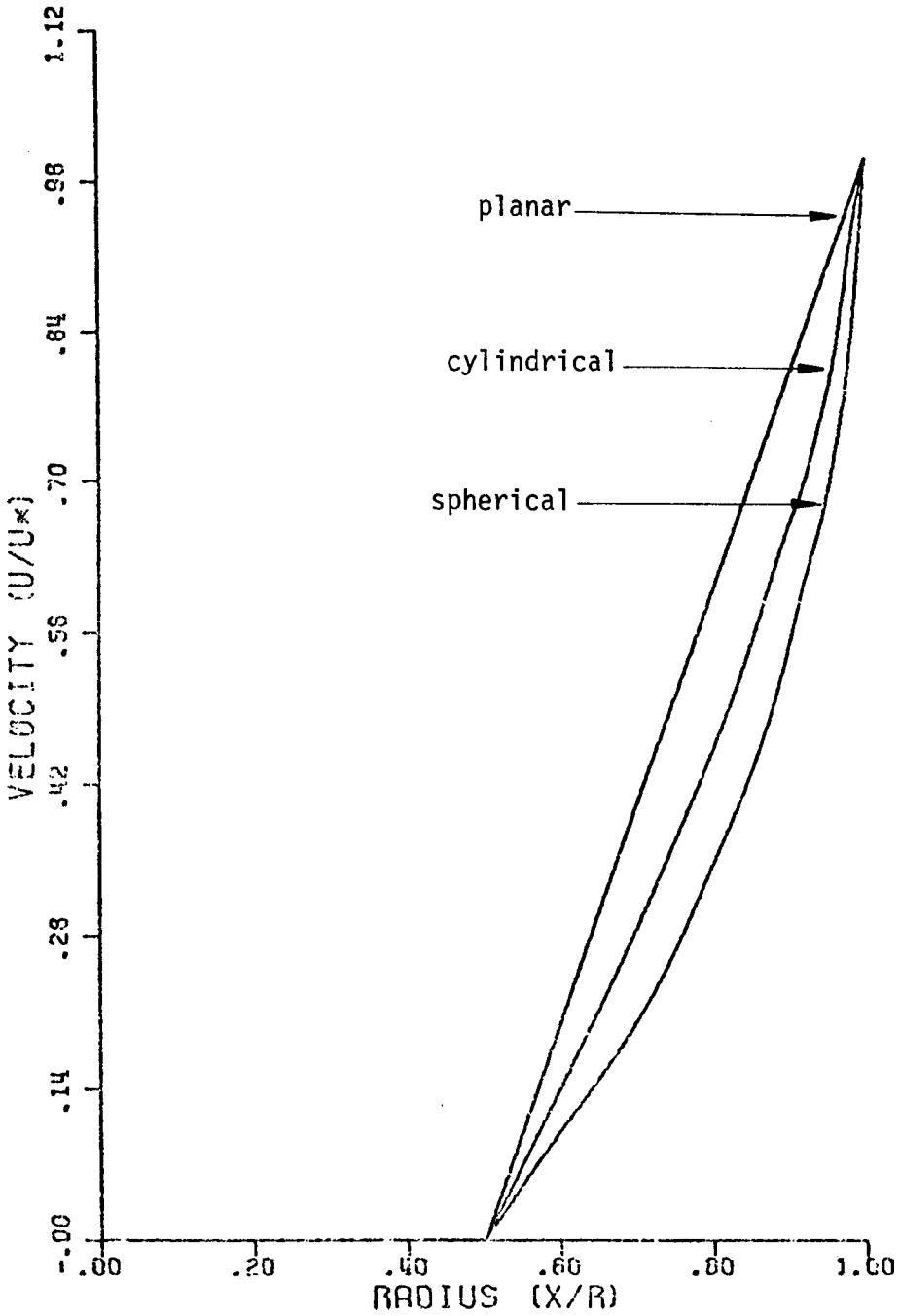

FIGURE 2.4.3: VELOCITY DISTRIBUTION BEHIND PLANAR, CYLINDRICAL AND SPHERICAL DETONATION FRONTS WHEN $\gamma = 1.4$

Blank Page

CHAPTER III

NUMERICAL SOLUTION OF HYDROGEN DETONATION BY THE RANDOM CHOICE METHOD

The gas dynamics equation (see Chapter II) form a non-linear unsteady hyperbolic system. A general analytic solution of the gas dynamics equations is not possible for an arbitrary geometry including repeated reflections from walls. Various numerical methods have been developed to solve these equations (see e.g. Sod [3.1]):

1) Finite-difference methods;

2) The random choice method; and recently:

3) Spectral transformation and finite element methods.

The finite-difference methods have the disadvantage to broaden, a time increases, expected discontinuities (like shock waves) of the flow. Recently correction terms have been proposed to counteract the diffusion of the width of a discontinuity (see Boris and Book [3.2]). Spectral and finite element methods are promising because they may reduce considerably the computation time; however, they are still in an experimental stage.

A method that produces infinitely sharp shocks is the method of Glimm [3.3]. Alexander Chorin [2.4] developed and applied Glimm's method for the fluid dynamical part of a combusting gas flow; here an artificial amount of diffusion would grossly distort those phenomena, like flame propagation, which depend on the rage of energy production. For

these reasons, we have decided to use in this program the random choice method to calculate the pressure histories generated by hydrogen detonations in a nuclear reactor containment.

The random choice method is described in the following sections, for one-dimensional plane, spherical and axisymmetric geometries.

3.1 One-Dimensional Plane Geometry

3.1a Gas dynamic flows without detonations

For one-dimensional plane geometry, the equations can be written in the following form:

$$\underset{\sim}{U}_t + \underset{\sim}{F}(\underset{\sim}{U})_x = 0 \qquad (3.1.1)$$

where

$$\underset{\sim}{U} = \begin{bmatrix} \rho \\ m \\ e \end{bmatrix} \quad \text{and} \quad \underset{\sim}{F}(\underset{\sim}{U}) = \begin{bmatrix} m \\ m^2/\rho + p \\ (m/\rho)(e+p) \end{bmatrix}$$

We discretize the time in intervals of length Δt and the space in intervals Δx. The solution advances at each grid point in time from t to $t + \Delta t$ by first calculating the values of the variables at mid grid points at time $t + \Delta t/2$ and then, advancing in a similar fashion the solution to time $t + \Delta t$. The solution at each half time step is found by solving a Riemann problem between adjacent grid points. The solution is evaluated at times $n\Delta t$, where n is a positive integer, at the spacial grid points $i\Delta x$, where $i = 0, \pm 1, \pm 2, \ldots$, and at times $(n + \frac{1}{2})\Delta t$ at $(i + \frac{1}{2})\Delta x$.

Let u_i^n approximate $\underset{\sim}{U}(i\Delta x, n\Delta t)$ and $u_{i+1/2}^{n+1/2}$ approximate $\underset{\sim}{U}((i + \frac{1}{2})\Delta x, (n + \frac{1}{2})\Delta t)$. To find $u_{i+1/2}^{n+1/2}$, consider the system (3.1.1) assuming piecewise constant initial data (time $t \equiv n\Delta t$)

$$\underset{\sim}{U}(x, n\Delta t) = u_{i+1}^n , \quad x \geq (i + \tfrac{1}{2})\Delta x,$$

$$= u_i^n , \quad x < (i + \tfrac{1}{2})\Delta x.$$

This defines a sequence of Riemann problems. If $\Delta t < \Delta x/2(|u|+c)$, where c is the local sound speed and $|u|$ is the absolute value of the particle velocity, the waves generated will not interact. Hence, the solution V(x,t) to the Riemann problem can be combined into a single exact solution (see Figure 3.1.1). The solution at the time step $t + \Delta t/2$ is found, following Glimm's method, by sampling the exact solution to the Riemann problem V(x,t) at time $t + \Delta t/2$. Let ξ_n be a uniformly distributed random variable in the interval $[-\frac{1}{2}, \frac{1}{2}]$. Define

$$u_{i+1/2}^{n+1/2} = V((i + \xi_n)\Delta x, (n + \tfrac{1}{2})\Delta t); \quad (3.1.3)$$

(see Figure 3.1.2).

At each time step the solution is approximated by a piecewise constant function. The solution is then advanced in time exactly and the new values are sampled.

A method of choosing the random variable ξ_n has been studied by Chorin [2.4, 3.4]. He suggested choosing one random variable ξ

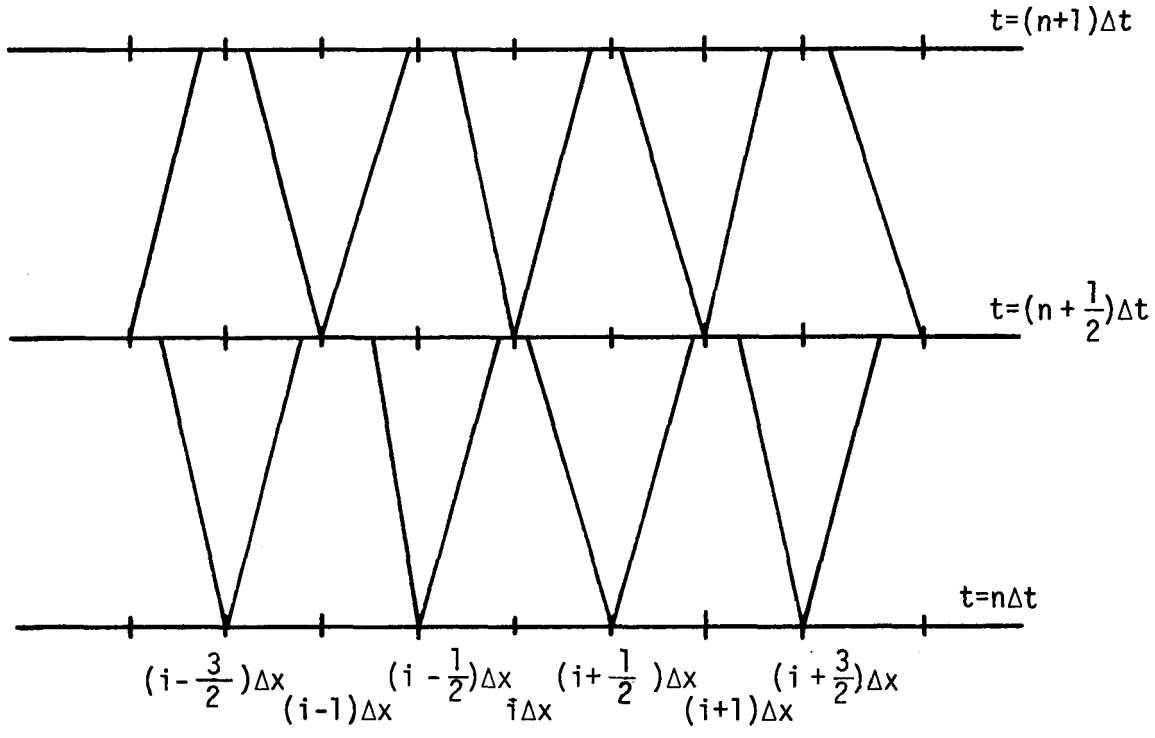

FIGURE 3.1.1: SEQUENCE OF RIEMANN PROBLEMS ON GRID

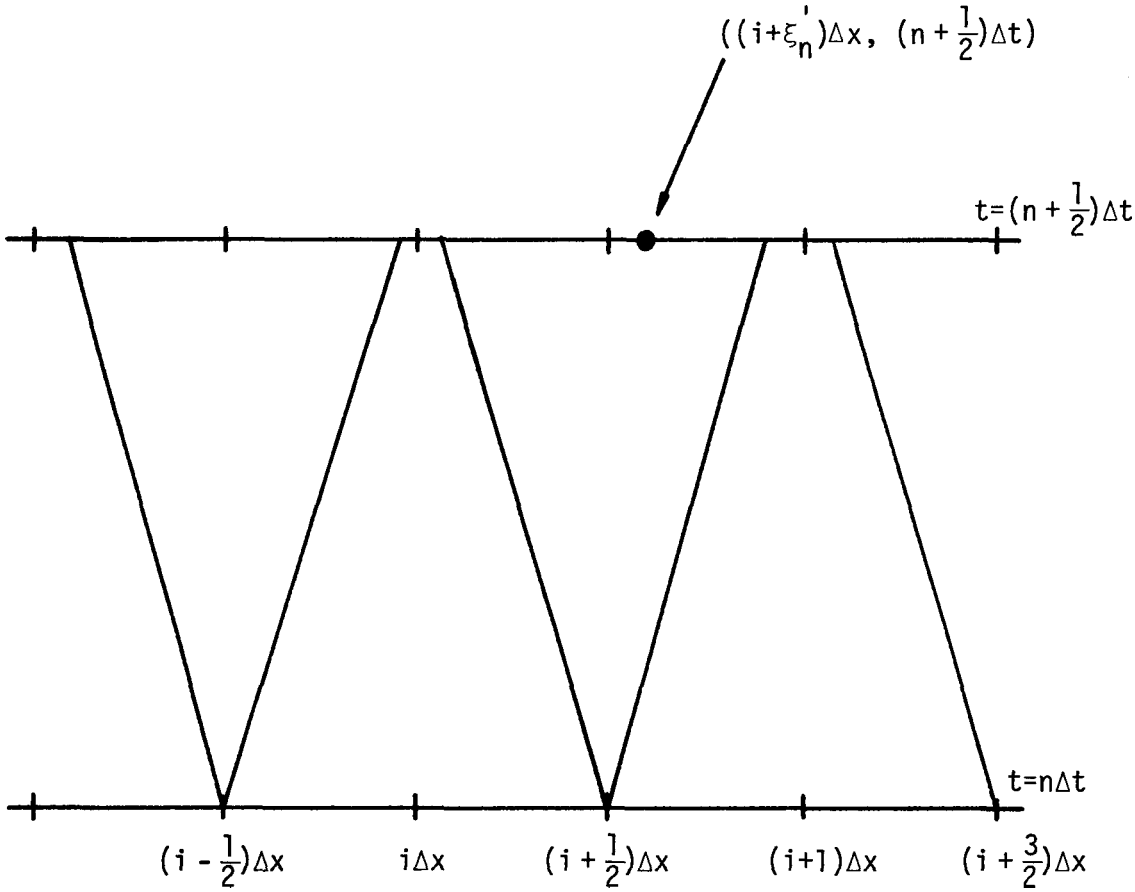

FIGURE 3.1.2: SAMPLING PROCEDURE FOR THE GLIMM'S METHOD

per time level rather than one for each point and each time level. In order that the variance of the solution be further reduced by making ξ reach approximate equidistribution over $[-\frac{1}{2}, \frac{1}{2}]$ at a faster rate, Chorin [2.4] suggested the following procedure. Let m_1, m_2, $m_1 < m_2$ be two mutually prime integers. Consider the sequence of integrers

$$n_0 \text{ given}, \quad n_0 < m_2,$$

$$n_{j+1} = (n_j + m_1)(\text{mod } m_2),$$

then,

$$\xi_j' = (n_j + \xi_j)/m_2,$$

where ξ_j is the random number and ξ_j' is the pseudorandom number which is actually used for sampling; j indexes the time.

In each time step, the solution consists of three states: S_r, S_ℓ, and a middle state S_* with $u = u_*$, $p = p_*$, separated by waves which may be either shock or rarefaction waves. A slip line $\frac{dx}{dt} = u_*$ separates the gas initially at $x < (i + \frac{1}{2})\Delta x$ from the gas initially at $x \geq (i + \frac{1}{2})\Delta x$ with possibly different values of ρ_* but equal values of u_* and p_* (see Figure 3.1.3).

The first step is to calculate the pressure p_* and the velocity u_* in state S_*. This is done by a method due to Godunov [3.5]. The outline of this method can be found in Appendix A. Now there are four cases to be considered:

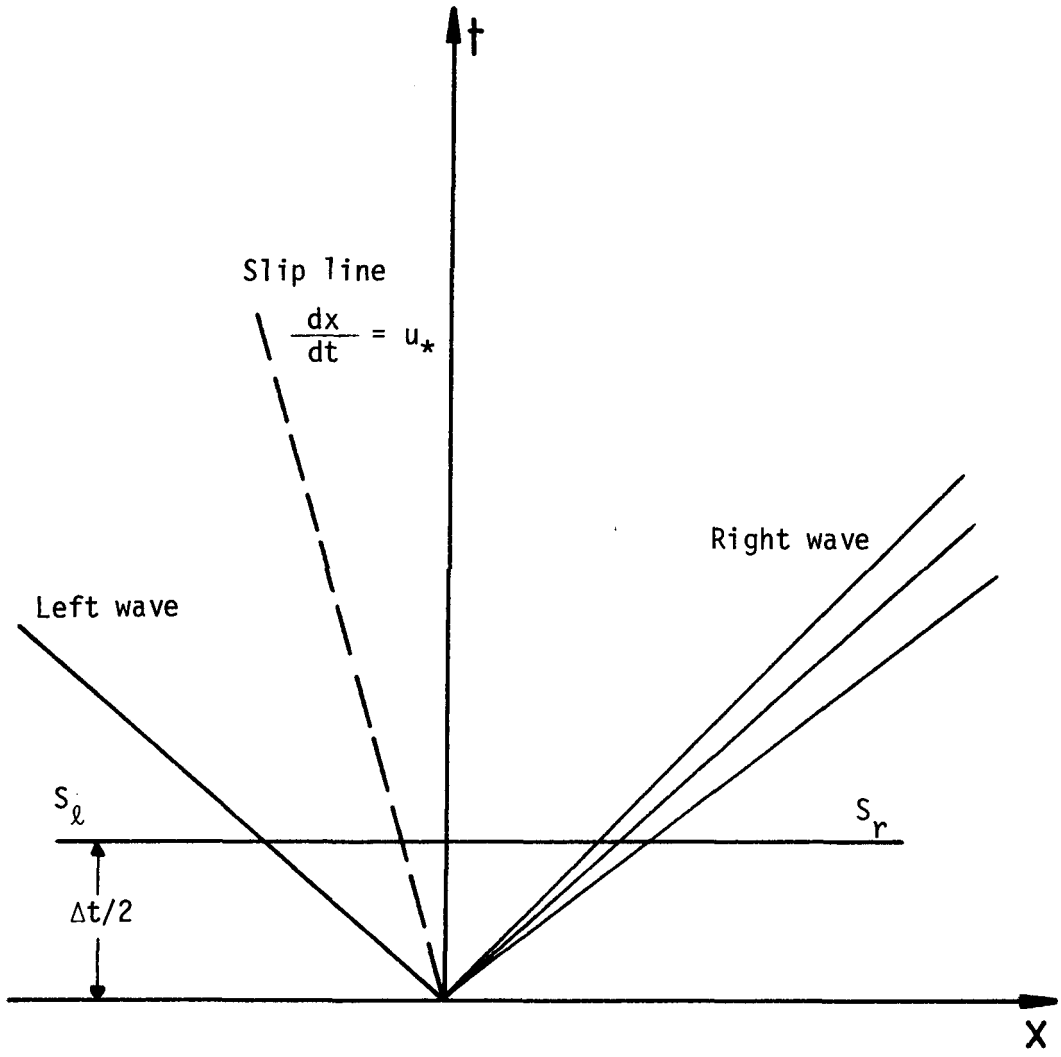

FIGURE 3.1.3: SOLUTION OF THE RIEMANN PROBLEM

Case 1 The sample point P lies to the right of the slip line ($\xi'\Delta x \geq u_* \frac{\Delta t}{2}$), and the right wave is a shock ($p_* > p_r$);

Case 2 P lies to the right of the slip line and the right wave is a rarefaction wave ($\xi'\Delta x \geq u_* \frac{\Delta t}{2}$ and $p_* \leq p_r$);

Case 3 P lies to the left of the slip line and the left wave is a shock ($\xi'\Delta x < u_* \frac{\Delta t}{2}$ and $p_* > p_\ell$); and

Case 4 P lies to the left of the slip line and the left wave is a rarefaction wave ($\xi'\Delta x < u_* \frac{\Delta t}{2}$ and $p_* \leq p_\ell$).

For Case 1, the velocity, U_r of the right shock can be found by using equation (A.2). If P lies to the right of the shock line $dx/dt = U_r$, we have $\rho_p = \rho_r$, $u_p = u_r$, $p_p = p_r$. If P lies to the left of the shock, $u_p = u_*$, $p_p = p_*$; $\rho_r = \rho_*$ can be found from equation (A.2). In solving Case 2 we let $c = (\gamma p/\rho)^{1/2}$ be the sound speed. If P lies to the right of the rarefaction, $\rho_p = \rho_r$, $u_p = u_r$, $p_p = p_r$; If P lies to the left of the rarefaction $\rho_p = \rho_*$, $u_p = u_*$, $p_p = p_*$; ρ_* is found from the constancy of the Riemann invariant

$$\Gamma_r = 2c_*(\gamma-1)^{-1} - u_* = 2c_r(\gamma-1)^{-1} - u_r.$$

If P lies inside the rarefaction, ρ_p, u_p and p_p can be derived by equating the slope of the characteristic $dx/dt = u+c$ to the slope of the line defined by the origin (which in this case is the grid point) and P

$$u_p + c_p = 2\xi' \quad \frac{\Delta x}{\Delta t} ,$$

then using the constancy of the Riemann invariant and the isentropic law $p\rho^{-\gamma}$ = constant.

Cases 3 and 4 are essentially identical to cases 1 and 2.

3.1.b A method to incorporate the detonation discontinuity in the random choice method

The objective of the present work was to predict pressure histories generated by hydrogen detonations in an enclosure. It is assumed that a hydrogen detonation will be initiated and developed if the hydrogen concentrations are within the detonability limits (Herzberg [3.6]. To avoid treating the chemical kinetics of combustion, we decided to represent the detonation as a sharp discontinuity which changes the still unburnt gas to a completely burnt gas according to the Chapman-Jouguet conditions (see section 2.4). This proposition is consistent with the observation that the chemical kinetic reaction rates are very large.

For each hydrogen concentration within the detonability limits, the Chapman-Jouguet state behind the detonation can be calculated (see section 2.4). For the numerical solution, we associate a variable ϕ = 1 if the gas is unburnt and ϕ = 0 otherwise. The

propagation of the detonation is calculated numerically by using the random choice method. Consider two adjacent grid points with their states represented at time $t = n\Delta t$ by

$$S_\ell = (\rho_\ell, u_\ell, p_\ell, \phi_\ell), \quad x < (i + \tfrac{1}{2})\Delta x,$$

$$S_r = (\rho_r, u_r, p_r, \phi_r), \quad x \geq (i + \tfrac{1}{2})\Delta x. \qquad (3.1.4)$$

If $\phi_\ell = \phi_r$, detonation does not occur between these points and Glimm's method (see section 3.1a) is used to advance the solution; if $\phi_\ell = 0$ and $\phi_r = 1$ a detonation wave will propagate from left to right (see Figure 3.1.4). Its speed will be (see section 2.4)

$$U_{cj} = u_{cj} + c_{cj} \qquad (3.1.5)$$

where $u_{cj} = u_\ell$ is the particle velocity and $c_{cj} = c_\ell$ is the sound speed corresponding to Chapman-Jouguet conditions corresponding to the state of the unburnt gas (ρ_r, u_r, p_r).

The solution is advanced in a similar way as in the Riemann problem (see section 3.1a) by sampling the detonation discontinuity (see Figure 3.1.4) using the same random numbers as in the Riemann problem.

The computer program CRTDET for solving the one-dimensional plane gas dynamics equations including detonation is listed in Appendix B.

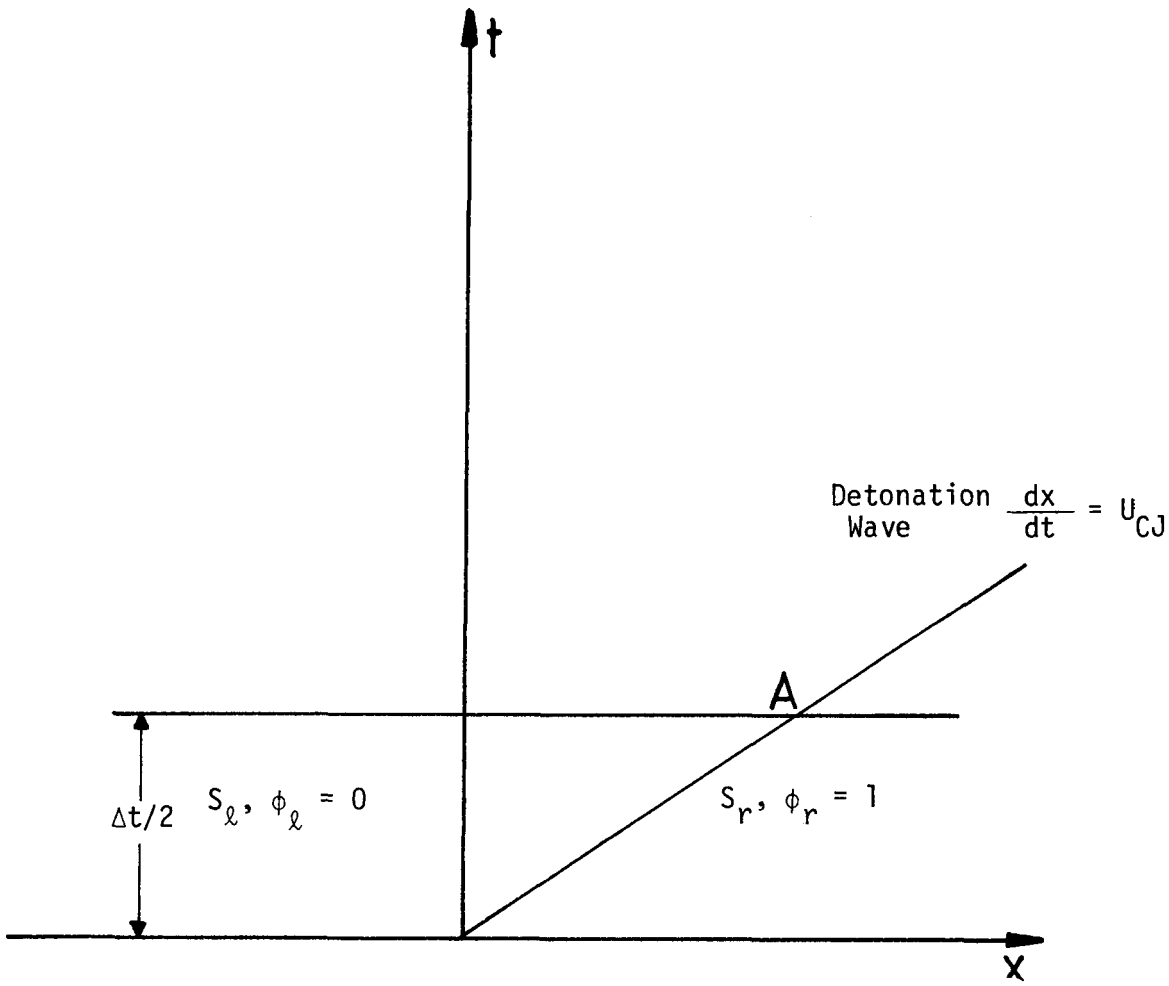

FIGURE 3.1.4: SOLUTION OF THE DETONATION PROBLEM

3.2 Boundary Conditions

Particular attention should be given to the boundary conditions especially as far as sampling is concerned. Assume the location of the boundary point is to the right of the region of flow at $x = i_0\Delta x$ and moving with a certain velocity V. To model the reflection at the wall we create a fake state to the right of x at $(i_0 + \frac{1}{2})\Delta x$ such that

$$\rho_{i_0 + 1/2} = \rho_{i_0 - 1/2}\,, \tag{3.2.1a}$$

$$u_{i_0 + 1/2} = 2V - u_{i_0 - 1/2} \tag{3.2.1b}$$

$$p_{i_0 + 1/2} = p_{i_0 - 1/2} \tag{3.2.1c}$$

(see Chorin [3.4]or Courant [2.3]). This will make a simple wave to propagate on both sides of the boundary point; the constant state in the middle of the Riemann solution is the wall state.

Special care should be taken in the sampling procedure. If ξ_1' and ξ_2' are the values of ξ' at two successive time steps, we should make sure that the resulting physical point does not lie to the right of the wall line $\frac{dx}{dt} = V$, so that no information is lost at the wall. This condition can be satisfied in different ways depending on each problem.

To satisfy the previous condition in the present case, ξ'_1 and ξ'_2 can be chosen as follows: pick ξ'_1 in the interval $[-\frac{\Delta x}{2}, \frac{\Delta x}{2}]$ according to the usual procedure and choose $\xi'_2 = -\xi'_1$. This method also ensures the physical point to lie within the boundary and avoids the problem of singular points.

3.3 One-Dimensional Spherical Geometry

The system of differential equations for the one-dimensional spherical problem is given by the set of differential equations (2.2.3). These equations can be written in the vector form

$$\underset{\sim}{U}_t + \underset{\sim}{F}(\underset{\sim}{U})_r = -2\,\underset{\sim}{W}(\underset{\sim}{U}); \qquad (3.3.1)$$

$\underset{\sim}{U}$, $\underset{\sim}{F}$ and $\underset{\sim}{W}$ were defined in section 2.3.

To solve the equations (3.3.1), we use the method of operator splitting used by Sod [3.7]. In a first step we remove the inhomogeneous term $-2\underset{\sim}{W}(\underset{\sim}{U})$ thus, we solve the homogeneous system

$$\underset{\sim}{U}_t + \underset{\sim}{F}(\underset{\sim}{U})_r = 0, \qquad (3.3.2)$$

which represents the one-dimensional equations of gas dynamics in cartesian coordinates and whose solution was presented in detail in the previous two sections.

The second step consists of solving the system of ordinary differential equations

$$\underset{\sim}{U}_t = -2\underset{\sim}{W}(\underset{\sim}{U}),$$

using the results of the solution of equation (3.3.2). This is done as follows: Once the solution $\tilde{u}_i^{n+1}$ of (3.3.2) is found, equation (3.3.3) is approximated by

$$\frac{u_i^{n+1} - \tilde{u}_i^{n+1}}{\Delta t} = -2\,\underset{\sim}{W}(\tilde{u}_i^{n+1}), \qquad (3.3.4)$$

or

$$u_i^{n+1} = \tilde{u}_i^{n+1} - 2\Delta t\,\underset{\sim}{W}(\tilde{u}_i^{n+1}). \qquad (3.3.5)$$

This scheme is only first order accurate, however there is no reason to use a higher order method since the random choice method is also at the most first order accurate.

The boundary conditions at the wall was chosen to be similar to the cartesian case, i.e., $\xi_2' = 0$ at the wall. The center of the detonation is treated similarly to the wall problem however, because of the singularity at the center, the appropriate sampling scheme discussed in section 3.2 should be used.

SPHDET is the computer program which is used to solve the one-dimensional spherical detonation problem (see Appedix C).

3.4 Axisymmetric (Two-Dimensional Cylindrical) Geometry

The numerical technique of solving the equations of the axisymmetric problem (2.3.4) is an extension of the one-dimensional case. Chorin [2.4] and Sod [3.8, 3.9] have already used it for the shock problem.

The basic procedure consists of two major steps:

1. use the operator splitting technique in the spatial coordinates and solve the equation

$$\underset{\sim}{U}_t + \underset{\sim}{F}(\underset{\sim}{U})_r + \underset{\sim}{G}(\underset{\sim}{U})_z = 0, \qquad (3.4.1)$$

2. solve the equation

$$\underset{\sim}{U}_t = -\underset{\sim}{W}(\underset{\sim}{U}). \qquad (3.4.2)$$

Solving the ordinary differential equation (3.4.2) is exactly identical to solving equation (3.3.3). Equation (3.4.1) is solved using an extended version of Glimm's method. At each time step, four quarter time steps of duration $\frac{\Delta t}{2}$ are performed; each quarter time step is a sweep in either r or z direction. Again, the operator splitting technique in the spatial coordinates is used to reduce the system of two-dimensional equations into two sets of one-dimensional ones. Hence, the equations to be solved in the r sweeps are

$$\frac{\partial \rho}{\partial t} + \frac{\partial}{\partial r}(\rho u_r) = 0, \qquad (3.4.3a)$$

$$\frac{\partial}{\partial t}(\rho u_r) + \frac{\partial}{\partial r}(\rho u_r^2 + p) = 0, \qquad (3.4.3b)$$

$$\frac{\partial}{\partial t}(\rho u_z) + \frac{\partial}{\partial r}(\rho u_r u_z) = 0, \qquad (3.4.3c)$$

$$\frac{\partial e}{\partial t} + \frac{\partial}{\partial r}((e+p)u_r) = 0. \qquad (3.4.3d)$$

Equation (3.4.3c) can be written in the form

$$\frac{\partial u_z}{\partial t} + u_r \frac{\partial u_z}{\partial r} = 0 \qquad (3.4.4)$$

i.e., the convective derivative of u_z is equal to zero and hence, in the r sweeps u_z is transported as a passive scalar. Similar equations hold in the z sweeps.

Now, given equations (3.4.3a, b, d) coupled with equation (3.4.4), the Glimm's method can be used. At each partial step, the solution vector is approximated by a piecewise constant vector. In the r sweeps the resulting waves in the r direction are found and in the z sweeps the waves in the z direction are found. In order to account properly for the interaction of the r and z waves, the follow-

ing scheme is used: at the beginning of the time step ρ, p, u_r and u_z are known at point ($i\Delta r$, $j\Delta z$). After an r sweep, the solution is found at $((i + \frac{1}{2})\Delta r, j\Delta z)$ (see Figure 3.4.1). $((i + \frac{1}{2})\Delta r, j\Delta z)$ and $((i + \frac{1}{2})\Delta r, (j + 1)\Delta z)$ can then be used to find the solution at $((1 + \frac{1}{2})\Delta r, (j + \frac{1}{2})\Delta z)$ by a z sweep. An r sweep then leads to $(i\Delta r, (j + \frac{1}{2})\Delta z)$ and a z sweep back to $(i\Delta r, j\Delta z)$. One pseudorandom variable is used per quarter step.

The detonation conditions are handled in a similar way as in the one-dimensional case, however, one should bear in mind that the C-J velocity represents the total velocity which should be splitted into its r and z components. For example, consider two points $i\Delta r$ and $(i+1)\Delta r$ (z the same) with $\phi=0$ at $i\Delta r$ and $\phi=1$ at $(i+1)\Delta r$. In accordance with our approach, a detonation is expected between these points. The conditions behind the detonation are known as a function of hydrogen concentration. By using the operator splitting technique in space, the two components of particle velocity can be calculated. Then, the solution is advanced by using the random choice method.

The boundary conditions are handled in the same way as in the one-dimensional problem. A curved boundary is represented by a stepwise line parallel to the mesh.

The computer prgram TWODIM (see Appendix D) uses the method outlined to solve the axisymmetric problem.

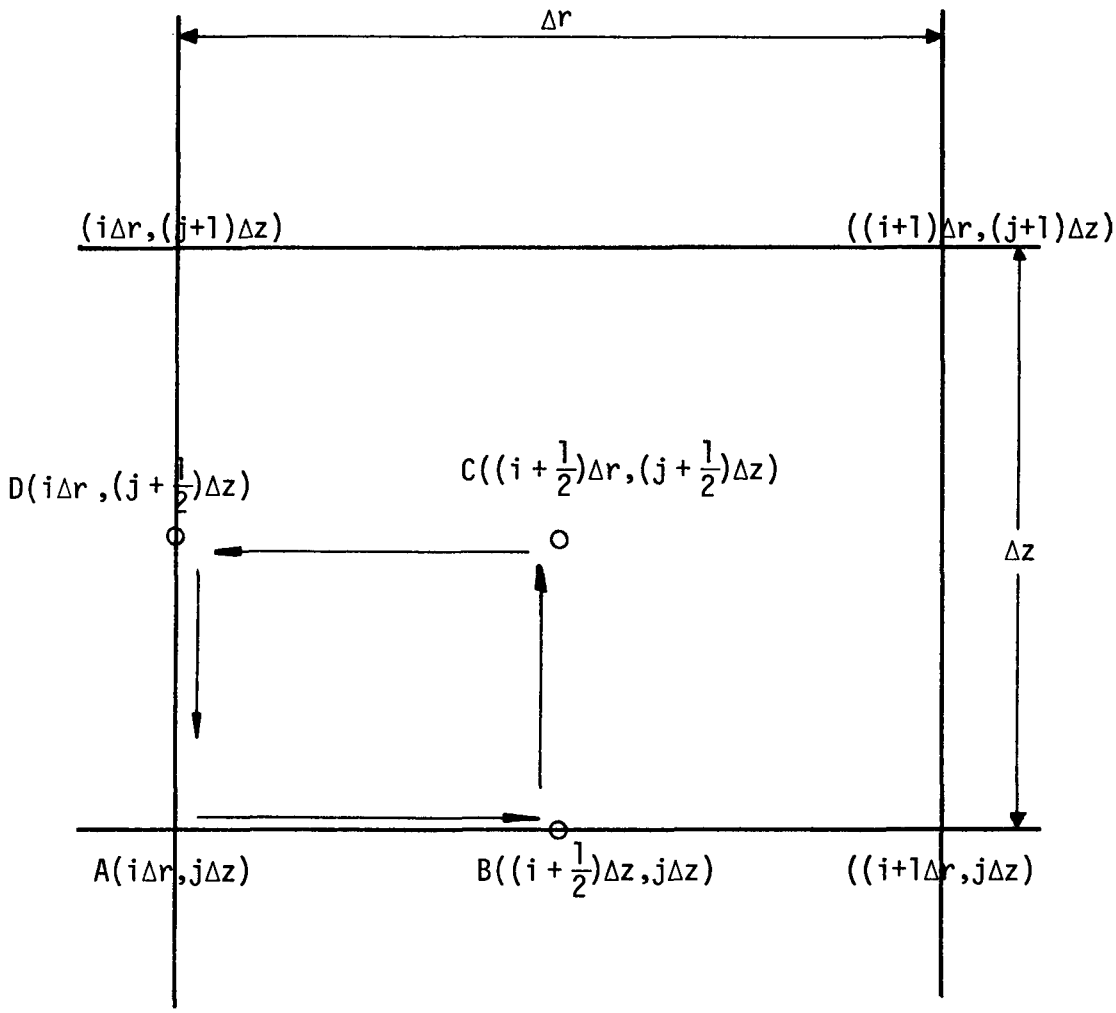

FIGURE 3.4.1: DIRECTION OF THE COMPUTATION AT EACH TIME STEP FOR THE AXISYMMETRIC PROBLEM

CHAPTER IV

COMPUTER CODE DEVELOPMENT AND RESULTS

4.1 One-Dimensional Planar Geometry

The main task of this section is to verify the validity of the numerical method described previously. To achieve this goal, the pressure, density and velocity histories of a hydrogen detonation in a one-dimensional cartesian coordinate system have been studied. The numerical results were compared with existing analytical solutions prior to reflections (see Figures 2.4.1, 2.4.2 and 2.4.3).

The first problem we investigated simulates a detonation initiated at the center of a shock tube, 2m long, bounded by a wall at both sides. As a result of the symmetry with respect to the initiation plane, the study was limited to half the length, the origin behaving as a wall. A mesh of one hundred and one grid points, equally spaced, was used. The time intervals were of variable length to meet the condition of non-interaction between the waves (see Section 3.1.a). Initially the unburnt gas was considered to be at rest, with a pressure of 10100 N/m^2 and a density of 0.1188 Kg/m^3. The hydrogen concentration was considered to be stoichiometric. The detonation was assumed to have reached the second grid point from the origin. Those grid points were assigned the values corresponding to the Taylor curves (Figures 2.4.1 to 2.4.3). The detonation front propagates with constant gas properties (The Chapman-Jouguet condi-

tions); the C-J pressure is approximately 15 times the pressure of the unburnt gas.

The computer program CRTDET (see Appendix B) was used to solve this problem. After 0.47 ms, the detonation wave progressed in the cylinder and was ready to contact the wall. Non-dimensional plots for the pressure, density and velocity as a function of the non-dimensional distance (defined as $x/U_{cj}t$), are shown in Figures 4.1.1-4.1.3. These are close to the analytical Taylor curves; the gas reaches steady conditions with zero velocity at approximately half distance between the origin and the detonation front; however, as noted by Sod [3.8], because of the randomness of the sampling, the rarefaction waves occurring just behind the detonation front are not reproduced by a smooth curve. Figures 4.1.4 to 4.1.6 show the pressure, density and velocity distributions in the shock tube at five different times. After the wave is reflected by the wall, there is an increase of pressure; the pressure exerted on the wall becomes 2.3 times higher than the C-J pressure or 37 times the initial one. These results are in agreement with the analytical equation given by Landau and Lifshitz [2.1] to determine the reflected pressure. After the wave has reached the wall, all the gas in the shock tube has already been burnt and the reflected wave is a strong shock which decreases in strength as it goes back towards the origin. When it reflects at the center the shock increases in strength and travels again towards the wall. Eventually, the wave decays and the gas reaches steady state conditions.

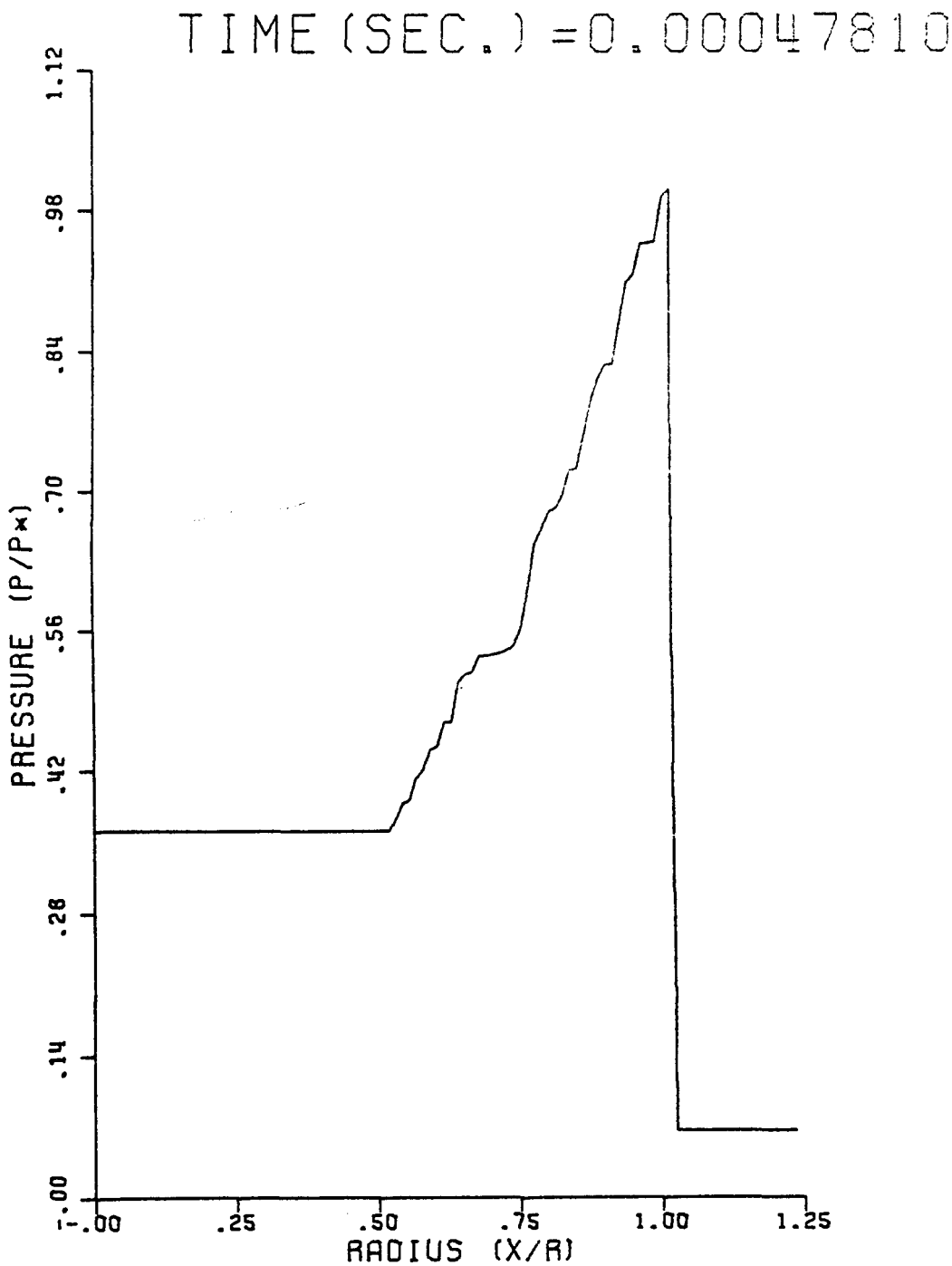

FIGURE 4.1.1: NON-DIMENSIONAL PRESSURE DISTRIBUTION (planar geometry) FOR A 1m RADIUS; 2 INITIAL GRID POINTS, SIGMA=0.8, $R=U_{CJ}t$

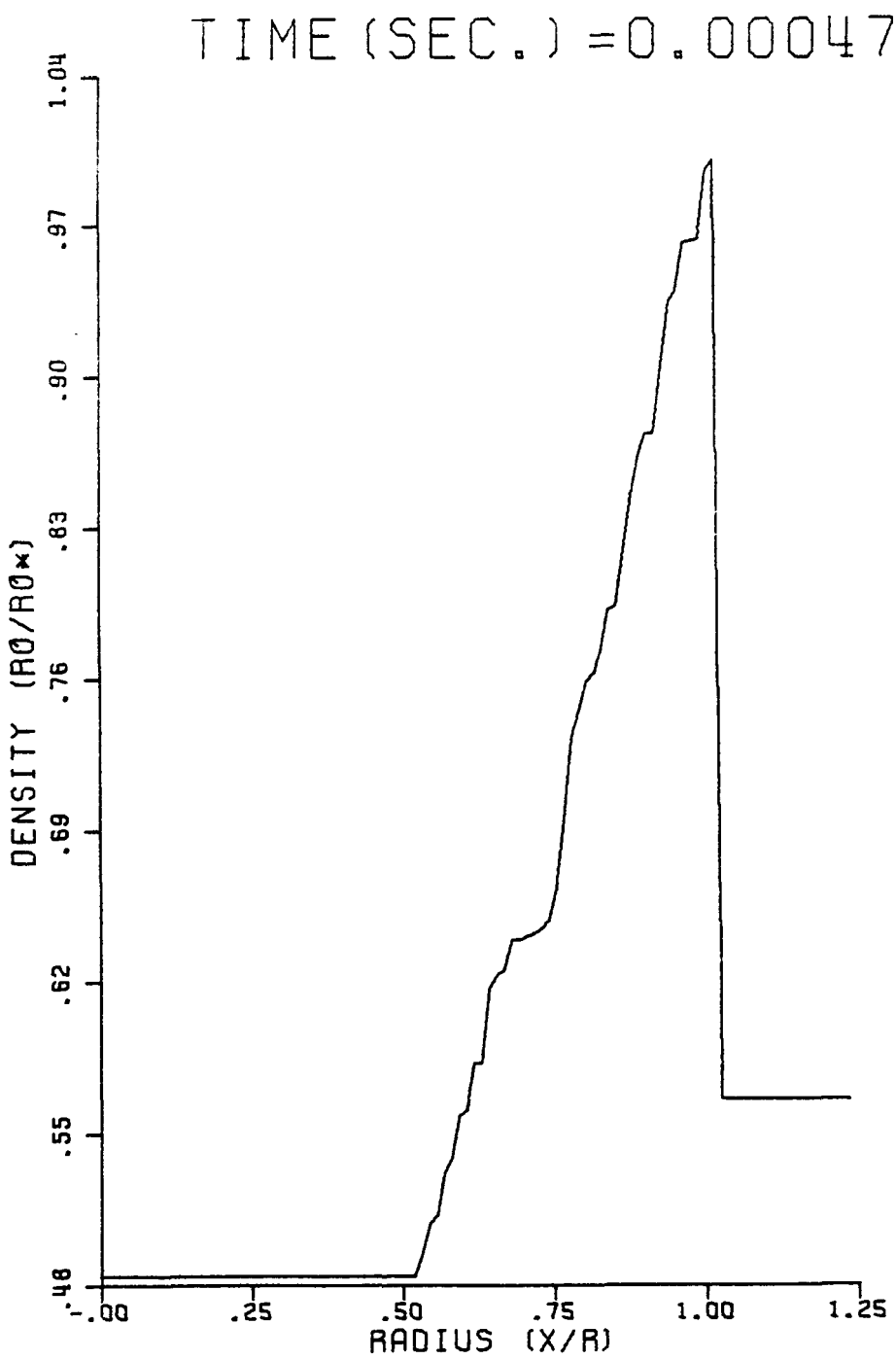

FIGURE 4.1.2: NON-DIMENSIONAL DENSITY DISTRIBUTION (planar geometry) FOR A 1m RADIUS; 2 Initial Grid Points, SIGMA=0.8

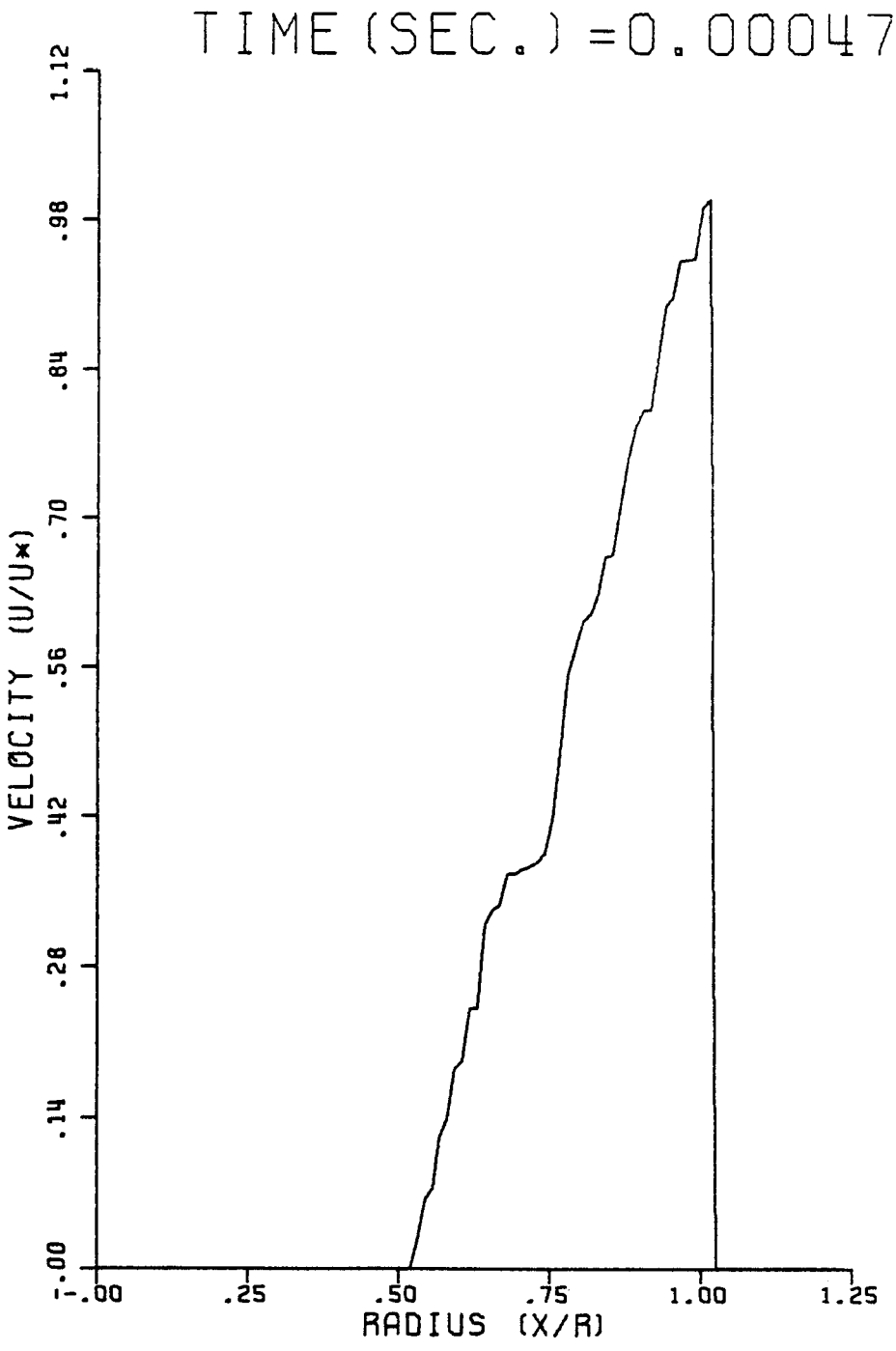

FIGURE 4.1.3: NON-DIMENSIONAL VELOCITY DISTRIBUTION (planar geometry) FOR A 1m RADIUS; 2 TWO GRID POINTS, SIGMA=0.8

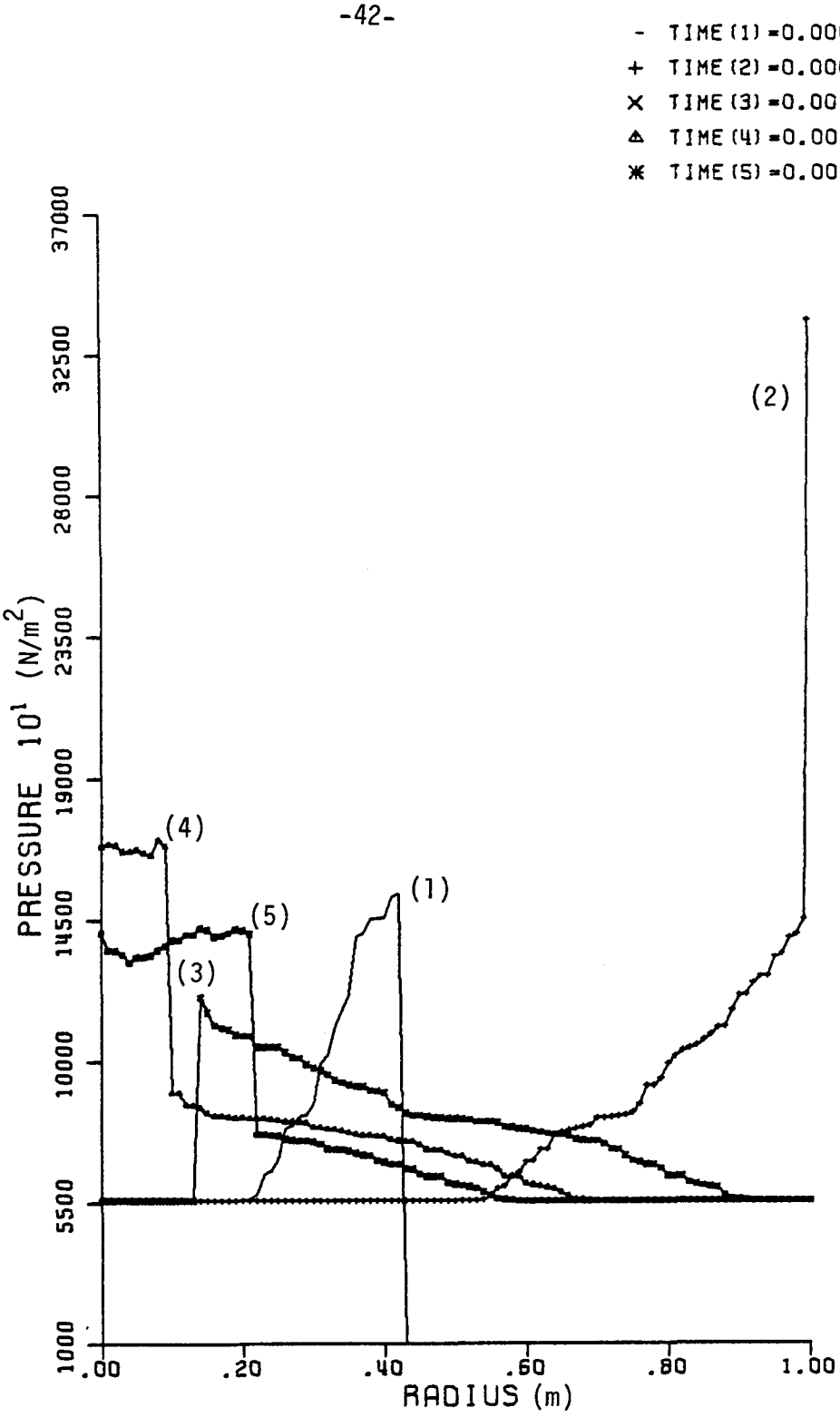

FIGURE 4.1.4: PRESSURE DISTRIBUTION (planar geometry) FOR A 1m RADIUS AT FIVE DIFFERENT TIMES; 2 INITIAL GRID POINTS, SIGMA=0.8

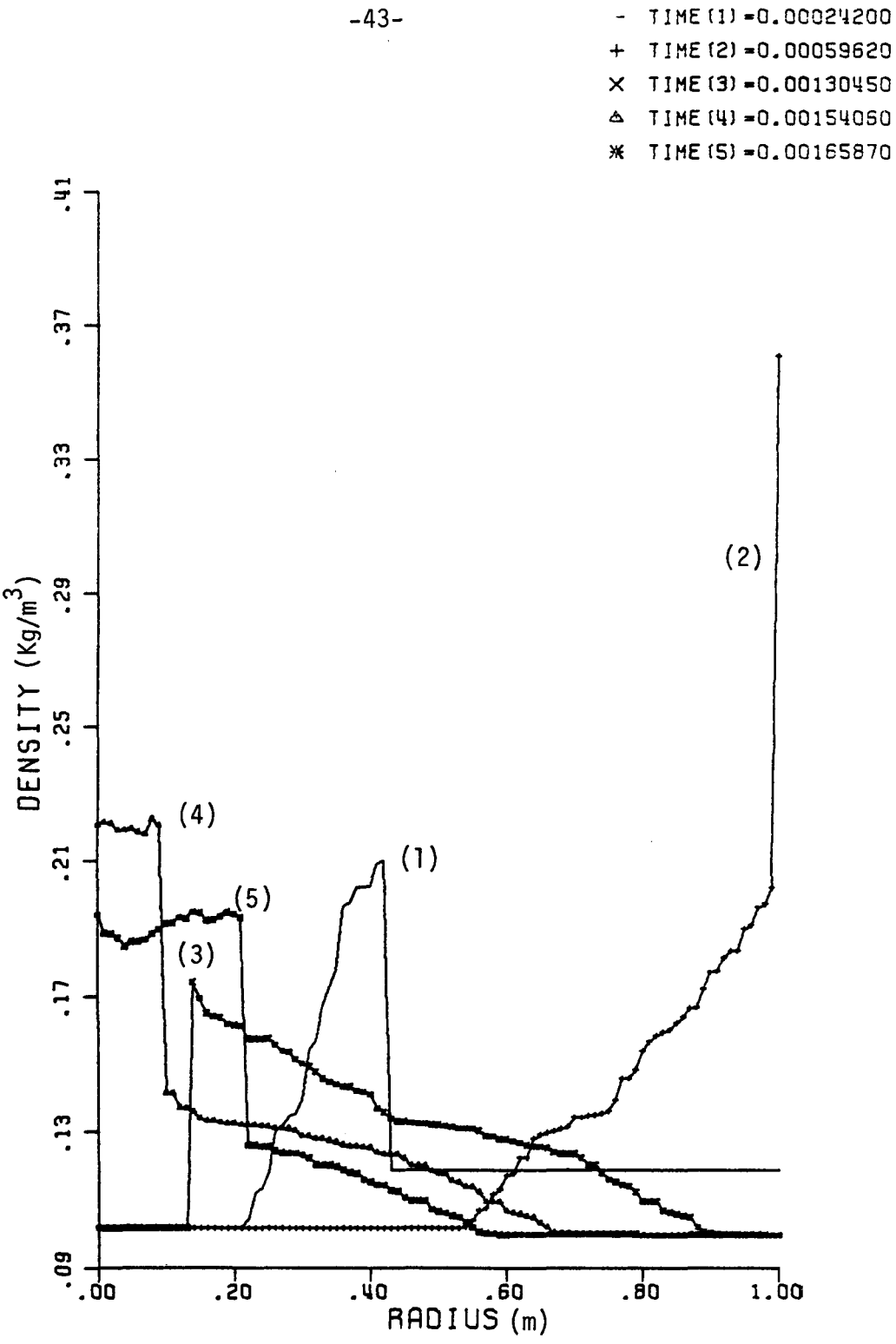

FIGURE 4.1.5: DENSITY DISTRIBUTION (planar geometry) FOR A 1m RADIUS AT FIVE DIFFERENT TIMES; 2 INITIAL GRID POINTS, SIGMA=0.8

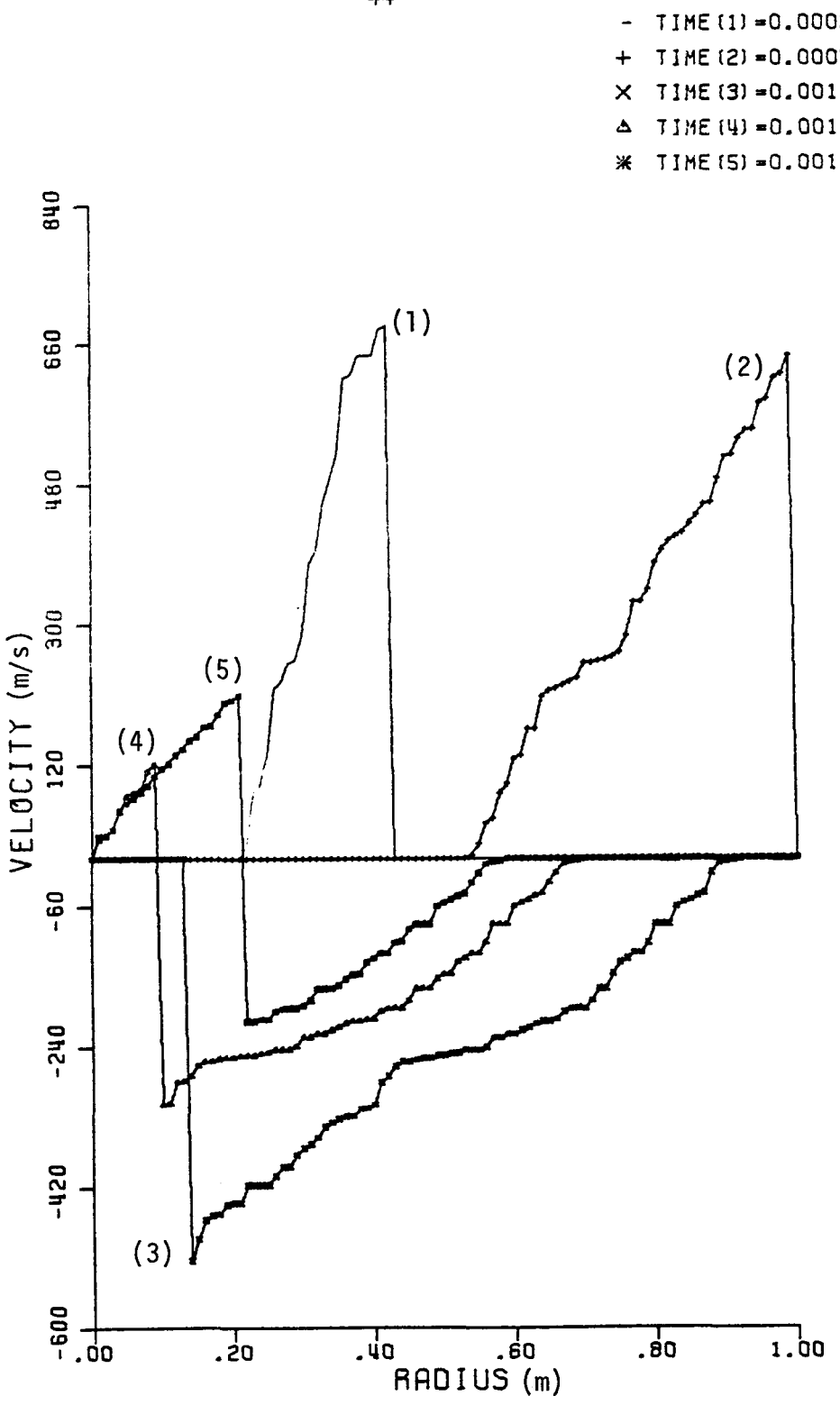

FIGURE 4.1.6: VELOCITY DISTRIBUTION (planar geometry) FOR A 1m RADIUS AT FIVE DIFFERENT TIMES; 2 INITIAL GRID POINTS, SIGMA=0.8

As previously noted, to ensure that waves do not interact, $\Delta t < \Delta x/(|u|+c)$ must hold true. The effect of choosing different time intervals was studied next. Figures 4.1.7 to 4.1.9 show that a time step (SIGMA = 0.4; see Appendix B) equal to half the previous one (SIGMA = 0.8; see Appendix B) has little effect on the solution (Figures 4.1.1-4.1.3). The only difference noted was in reproduction of the rarefaction wave; this is due to the randomness of the sampling. The time steps should not be very small because the explicit technique used can lead to numerical instabilities, causing the wave to move backward. Hence, to ensure the stability of the solution it was found that

$$0.3 < \frac{\Delta t}{\Delta x}(|u|+c) < 1.0.$$

Next we examined the effect on the numerical solution of the number of the initial grid points behind the detonation wave. In Figures 4.1.10 to 4.1.15, at the beginning of the computation, eight initial grid points were assigned in accordance with the Taylor solution. The pressure, density and velocity histories agree with those in Figures 4.1.1 - 4.1.6 where only two initial grid points were employed before the detonation wave started to expand.

The most important output of the numerical analysis was the evaluation of the variation of the pressure with time, close to the wall. For the problem described above, the pressure and density profiles at a still wall, 1m distant from the origin of the detonation, are shown in Figures 4.1.16 and 4.1.17. At a time 0.58 ms after the

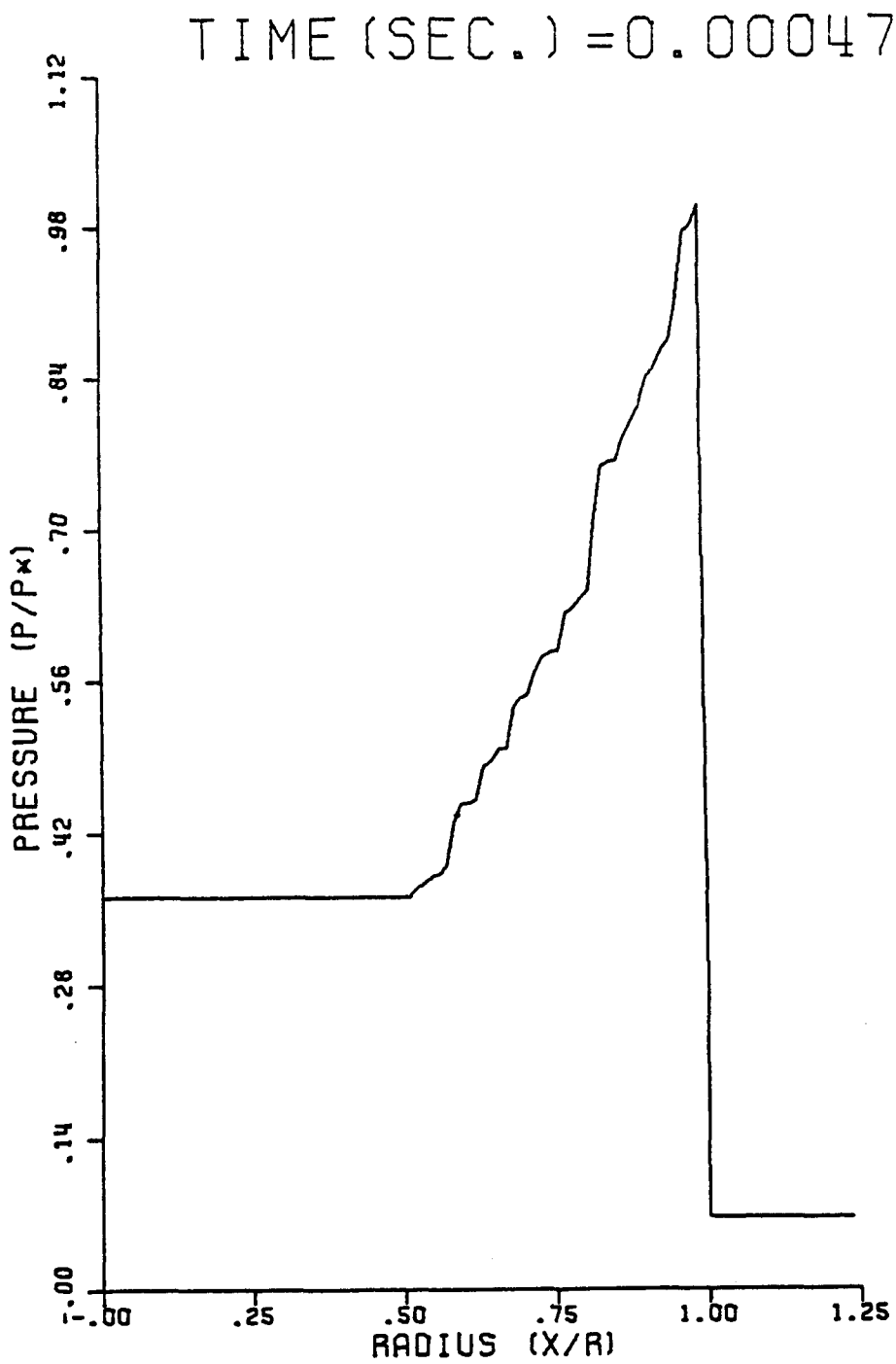

FIGURE 4.1.7: NON-DIMENSIONAL PRESSURE DISTRIBUTION (planar geometry) FOR A 1m RADIUS; 2 INITIAL GRID POINTS, SIGMA=0.4

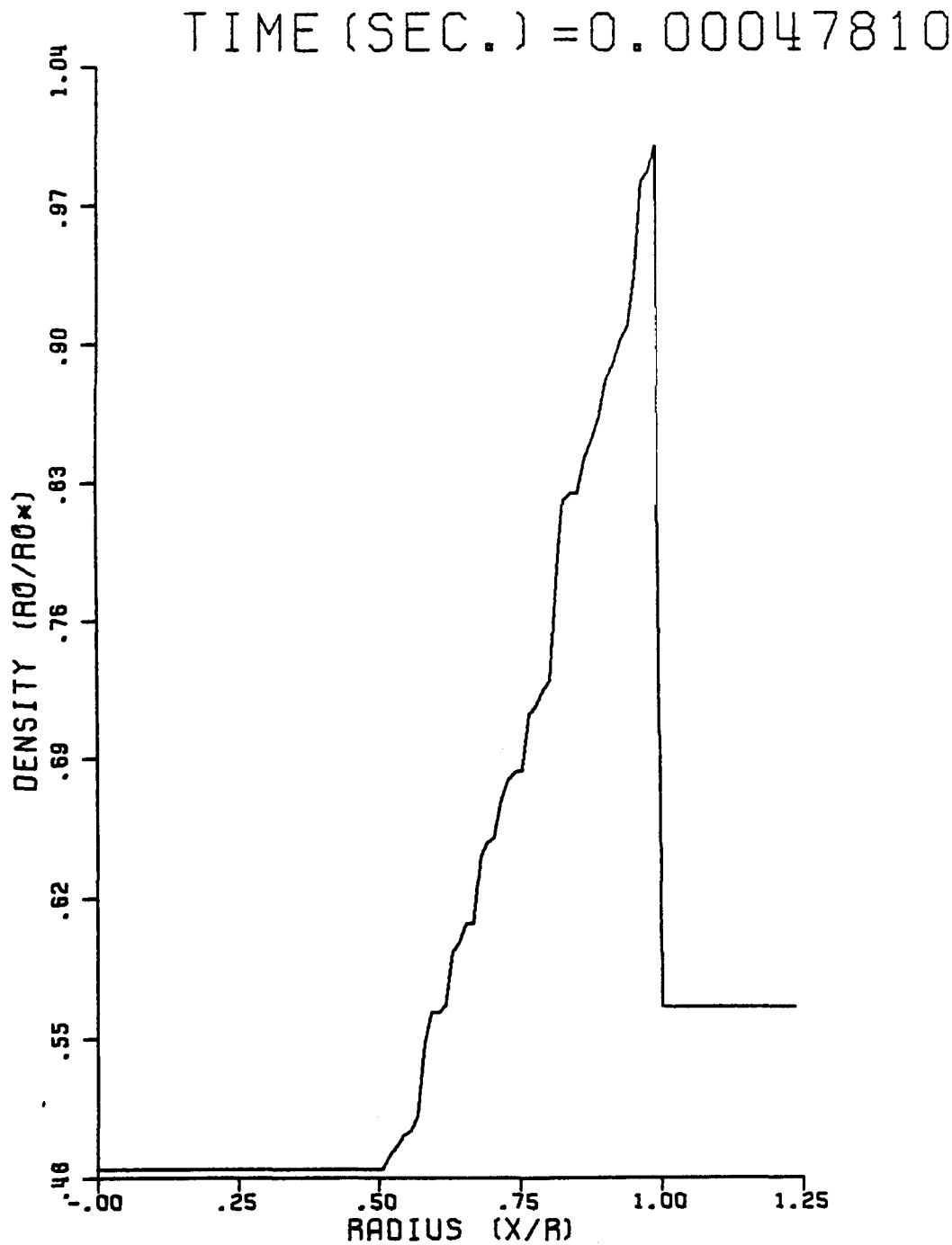

FIGURE 4.1.8: NON-DIMENSIONAL DENSITY DISTRIBUTION (planar geometry) FOR 1m RADIUS; 2 INITIAL GRID POINTS, SIGMA=0.4

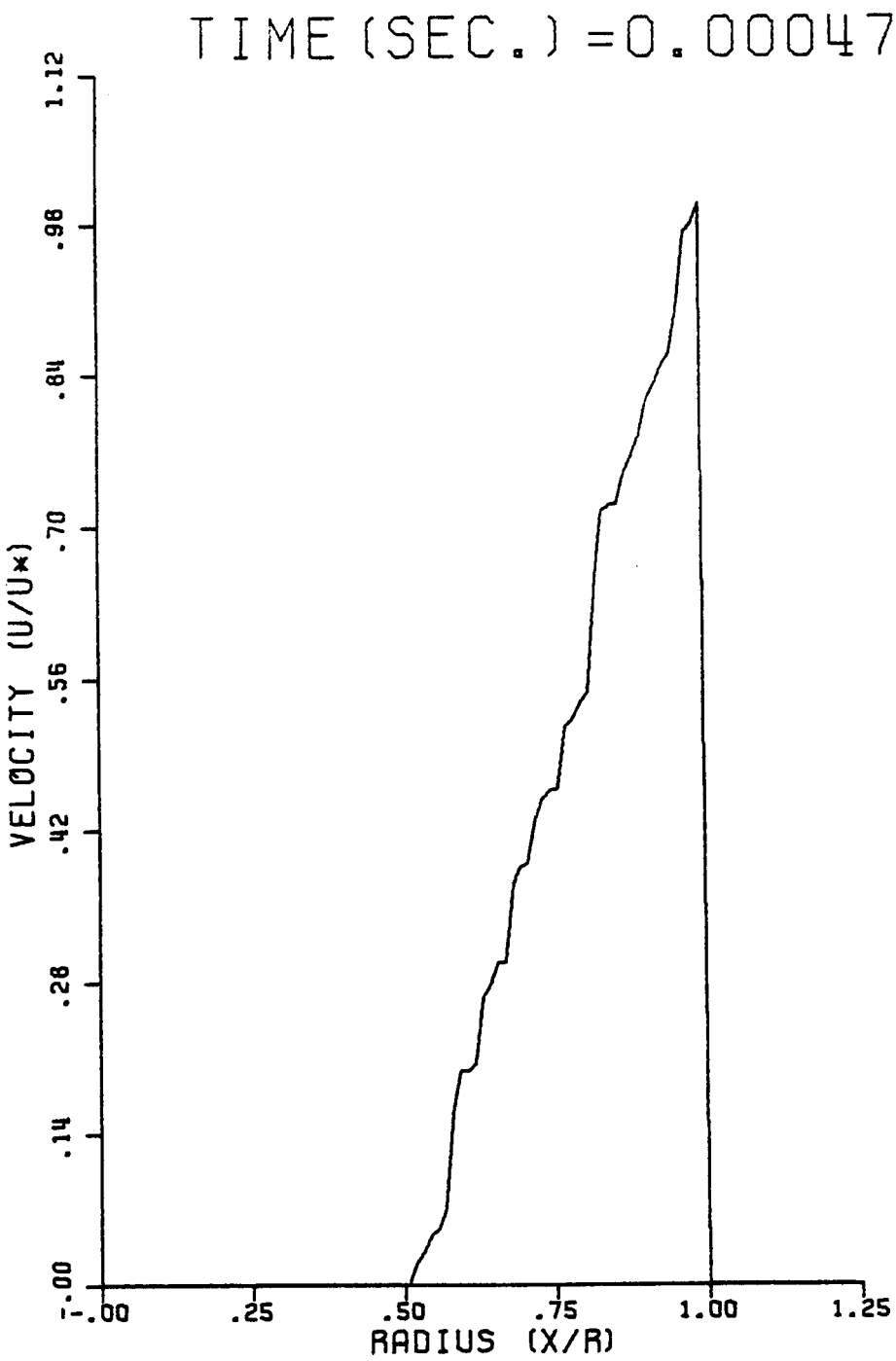

FIGURE 4.1.9: NON-DIMENSIONAL PRESSURE DISTRIBUTION (planar geometry) FOR A 1m RADIUS; 2 INITIAL GRID POINTS, SIGMA=0.4

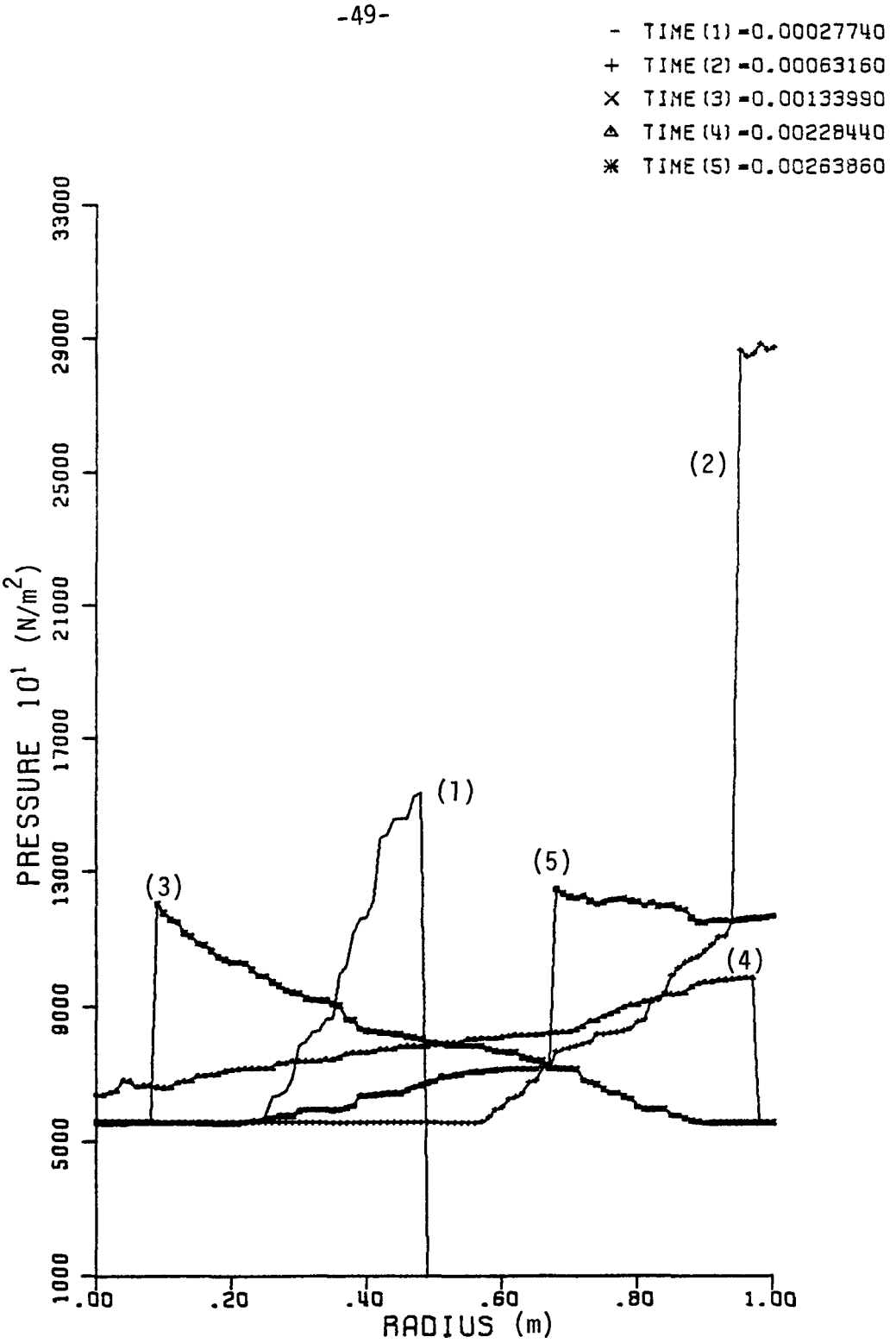

FIGURE 4.1.10: PRESSURE DISTRIBUTION (planar geometry) FOR A 1m RADIUS AT FIVE DIFFERENT TIMES; 8 INITIAL GRID POINTS, SIGMA=0.8

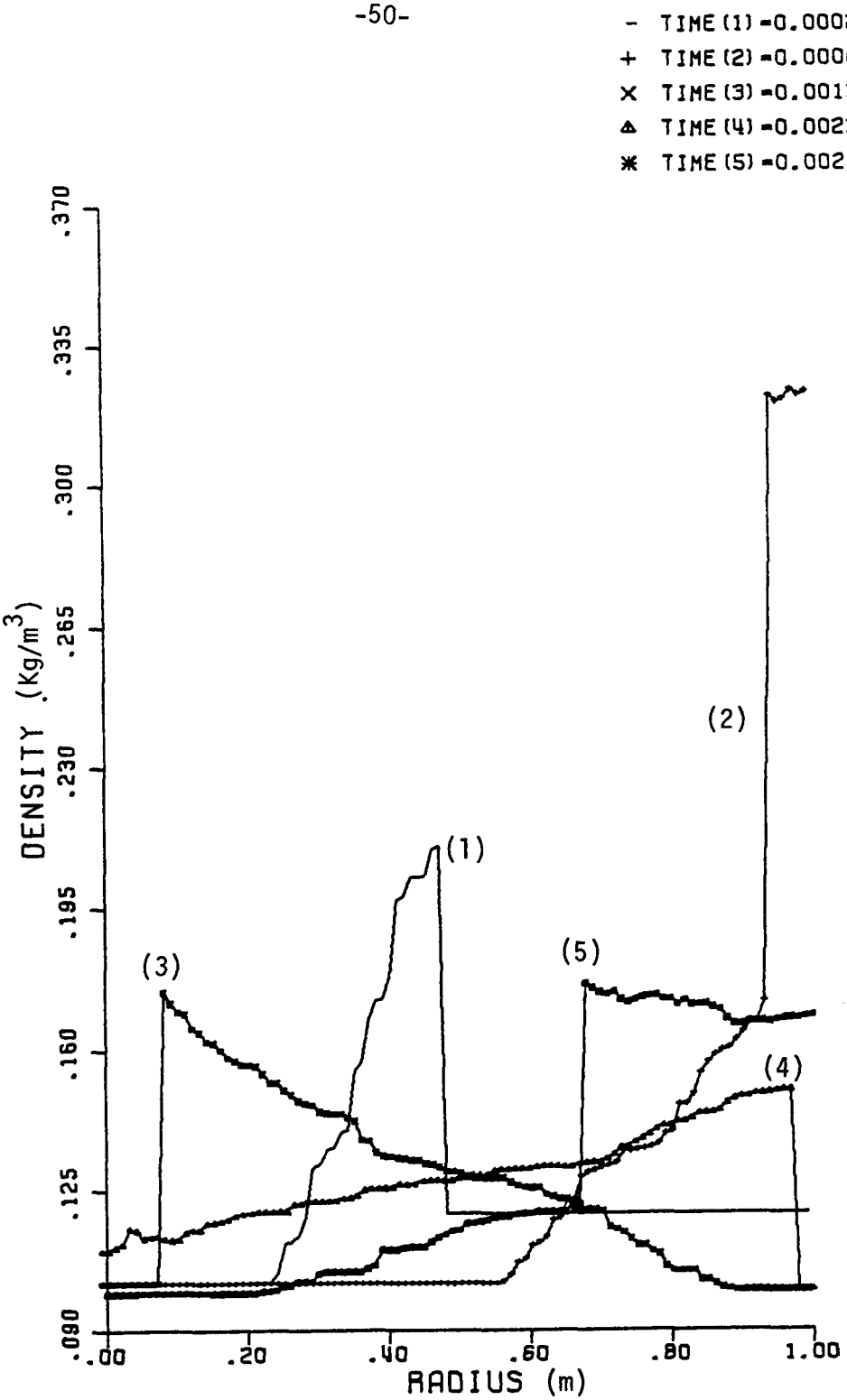

FIGURE 4.1.11: DENSITY DISTRIBUTION (planar geometry) FOR A 1m RADIUS AT FIVE DIFFERENT TIMES; 8 INITIAL GRID POINTS, SIGMA=0.8

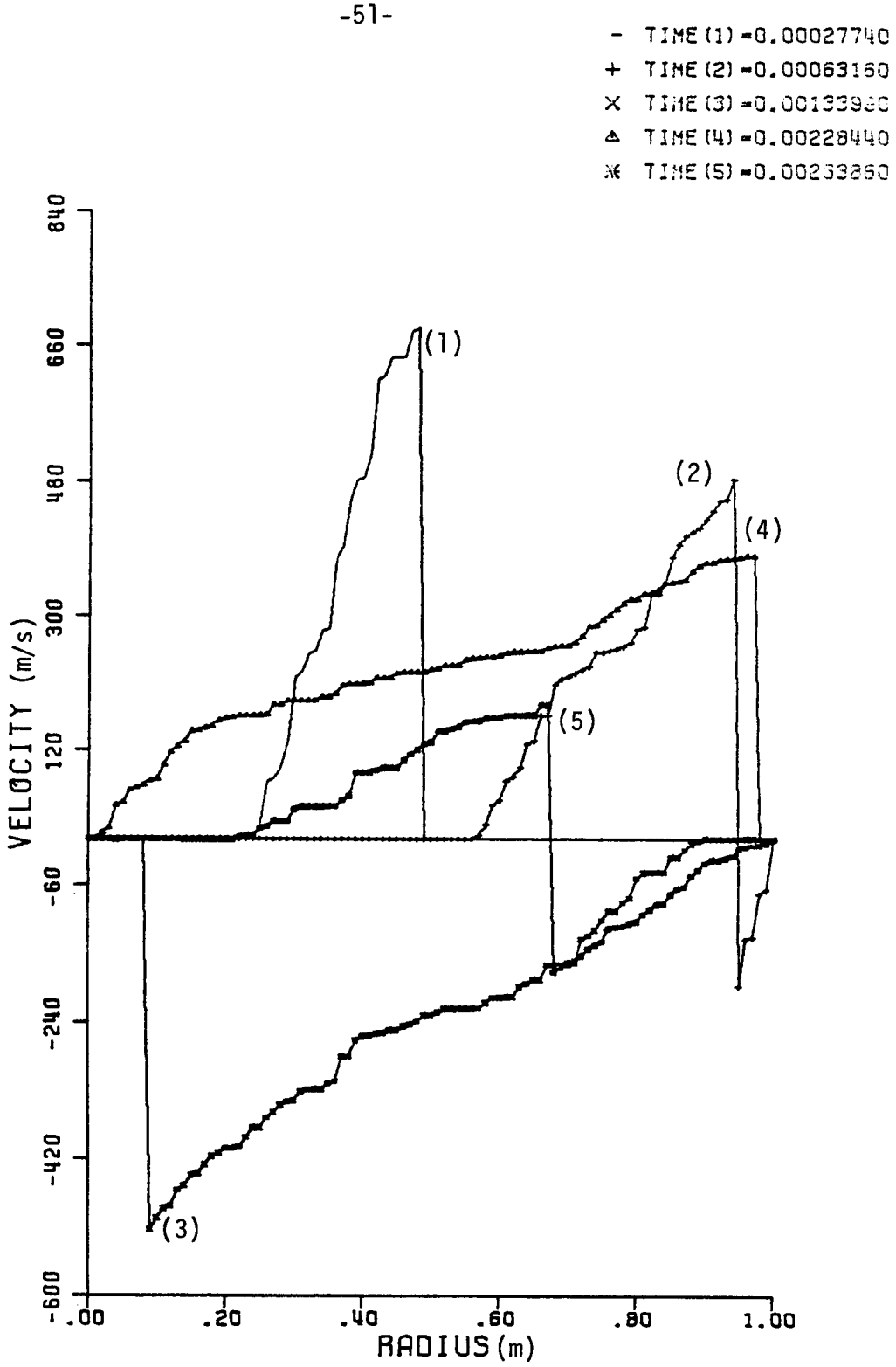

FIGURE 4.1.12: VELOCITY DISTRIBUTION (planar geometry) FOR A 1m RADIUS AT FIVE DIFFERENT TIMES; 8 INITIAL GRID POINTS, SIGMA=0.8

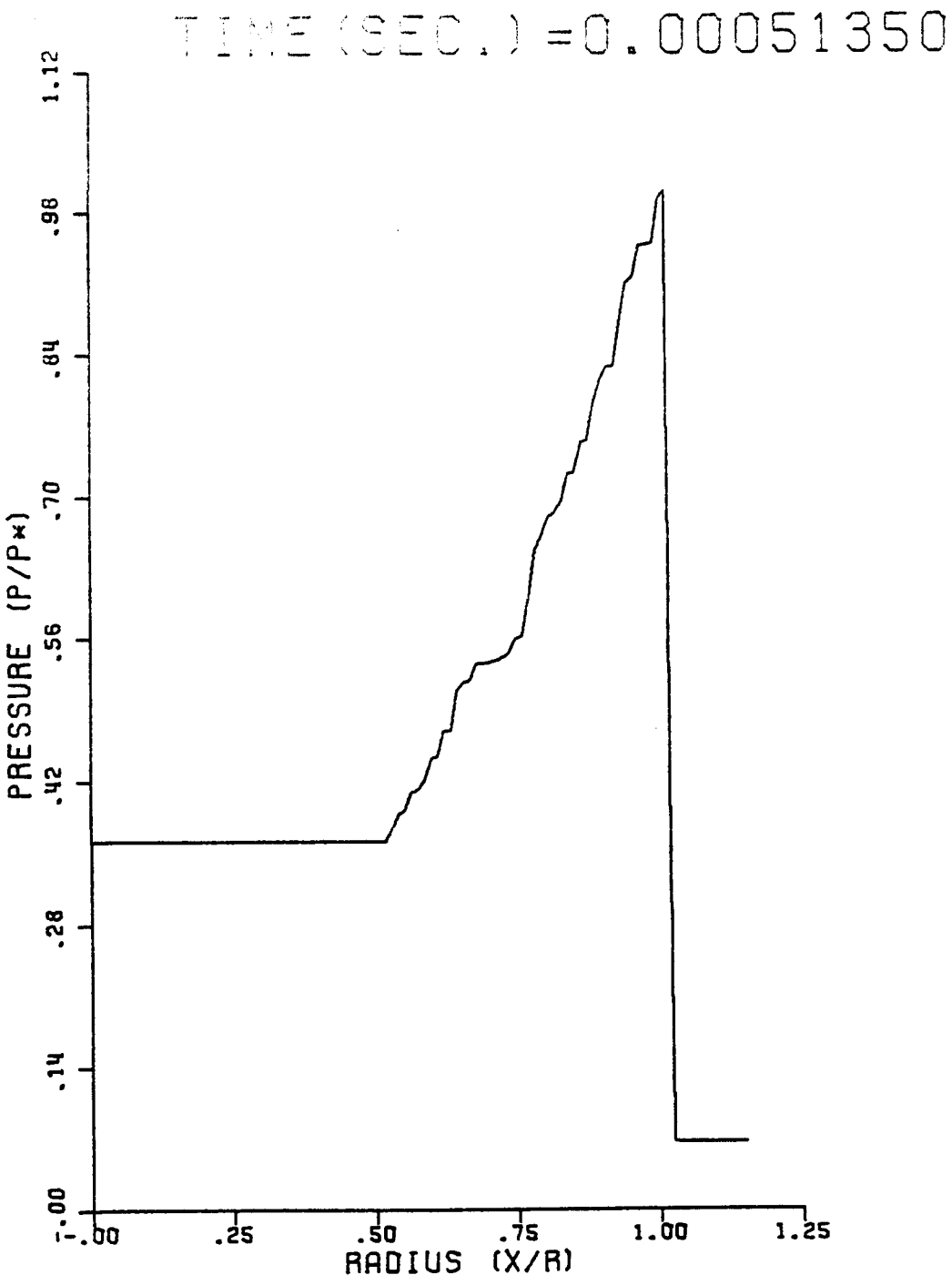

FIGURE 4.1.13: NON-DIMENSIONAL PRESSURE DISTRIBUTION (planar geometry) FOR A 1m RADIUS; 8 INITIAL GRID POINTS, SIGMA=0.8

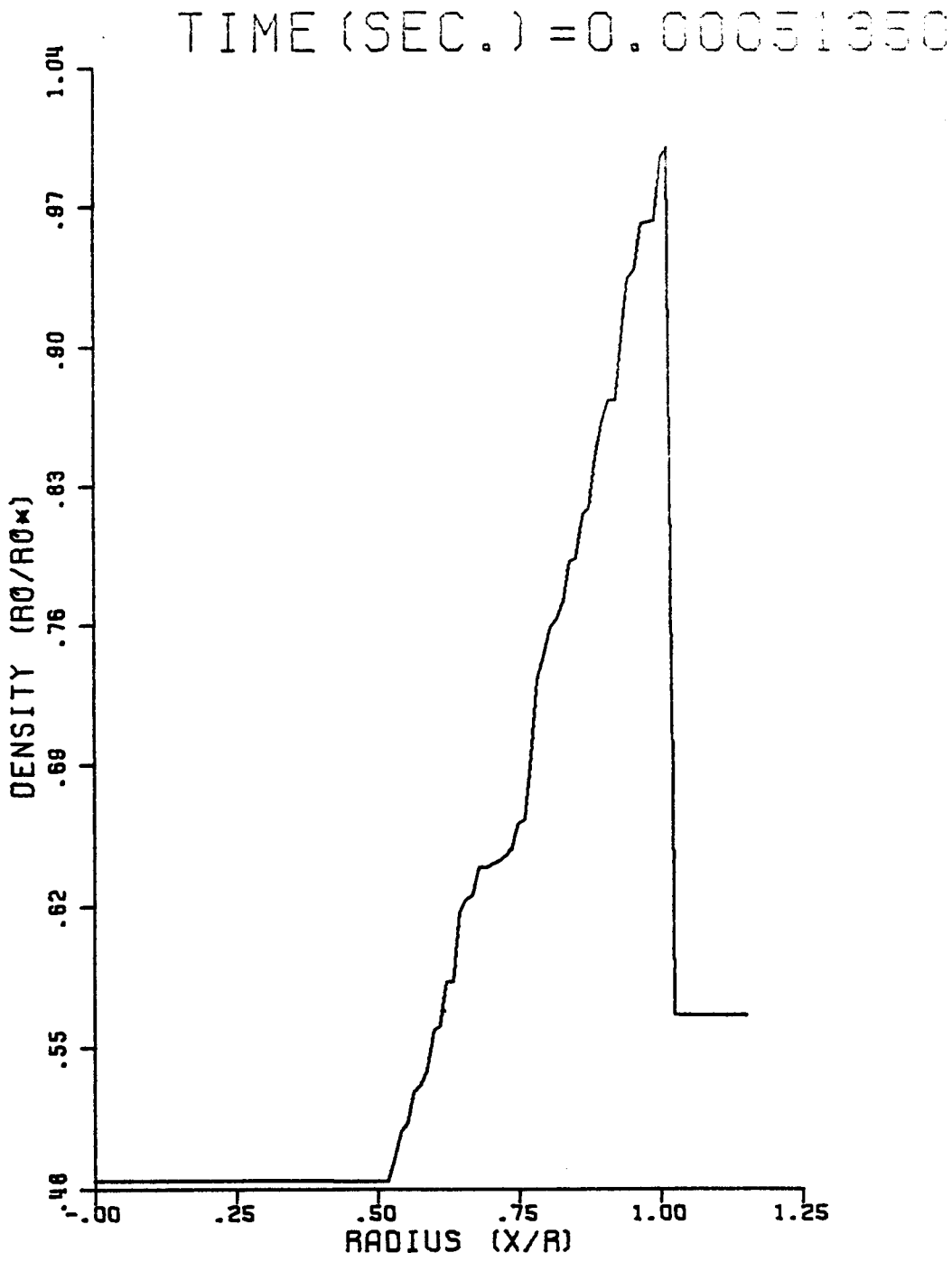

FIGURE 4.1.14: NON-DIMENSIONAL DENSITY DISTRIBUTION (planar geometry) FOR A 1m RADIUS; 8 INITIAL GRID POINTS, SIGMA=0.8

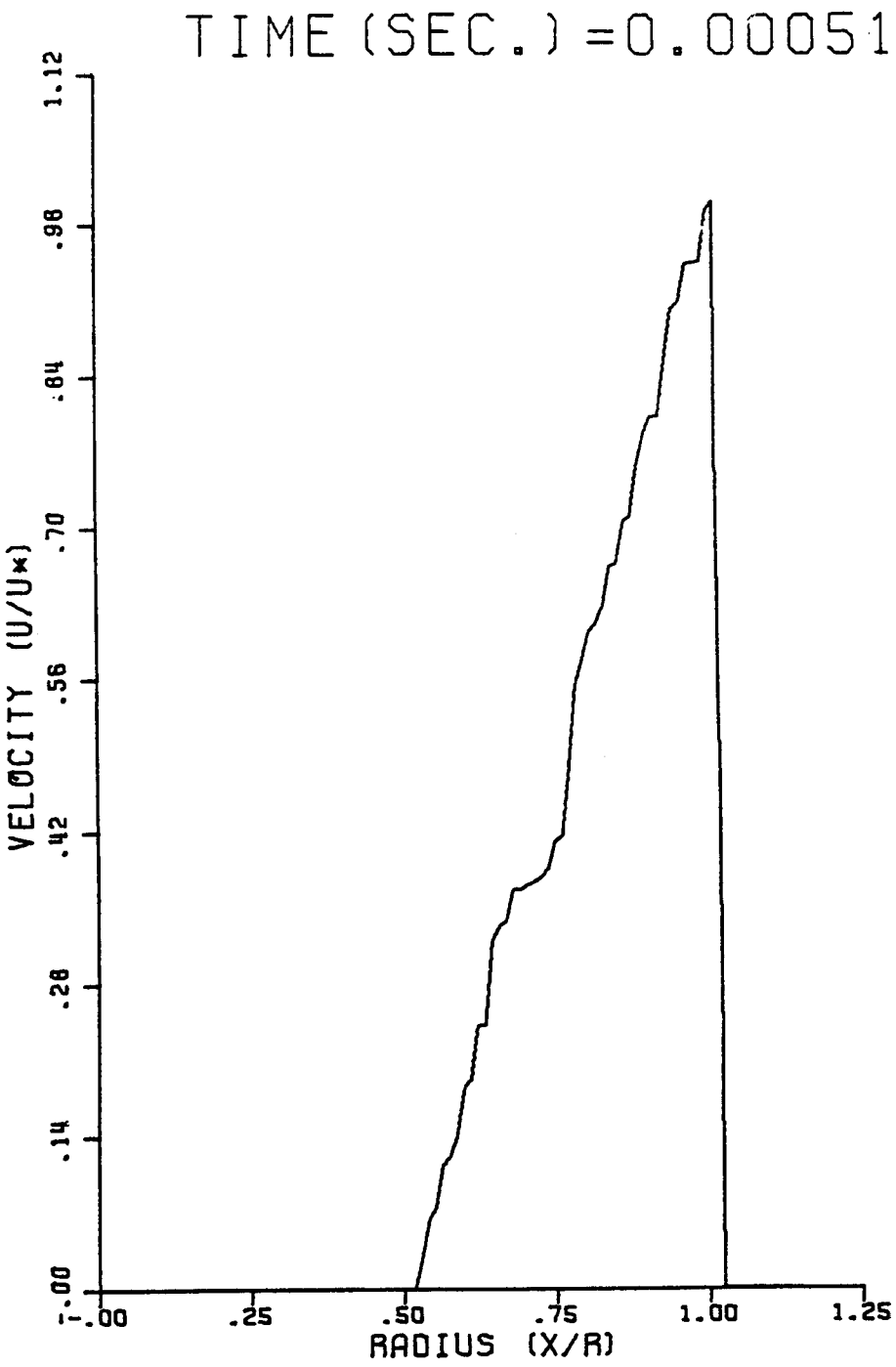

FIGURE 4.1.15: NON-DIMENSIONAL VELOCITY DISTRIBUTION (planar geometry) FOR A 1m RADIUS; 8 INITIAL GRID POINTS, SIGMA=0.8

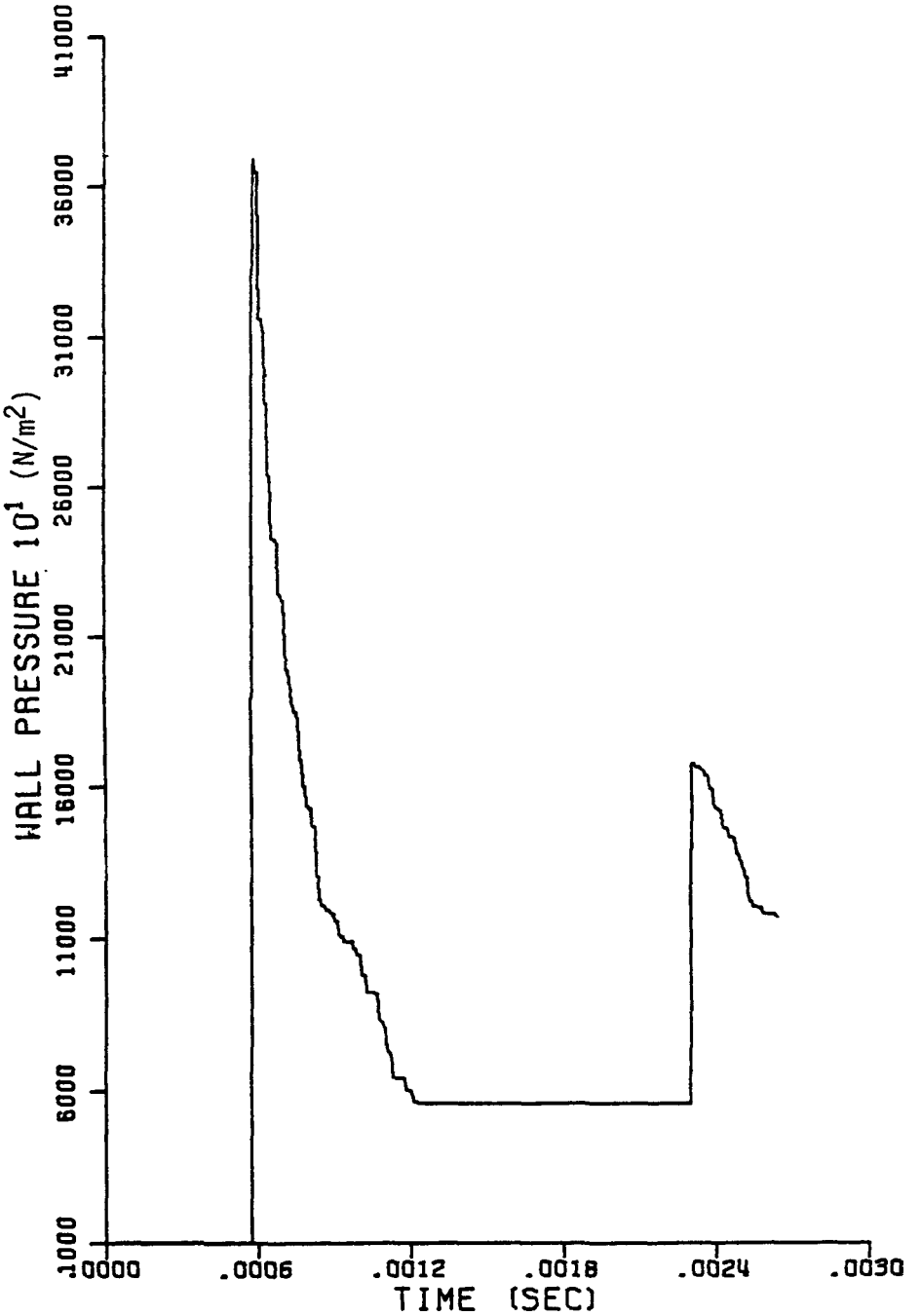

FIGURE 4.1.16: WALL PRESSURE HISTORY FOR A 1m RADIUS (planar geometry) 2 INITIAL GRID POINTS, SIGMA=0.8, Δx=0.01.

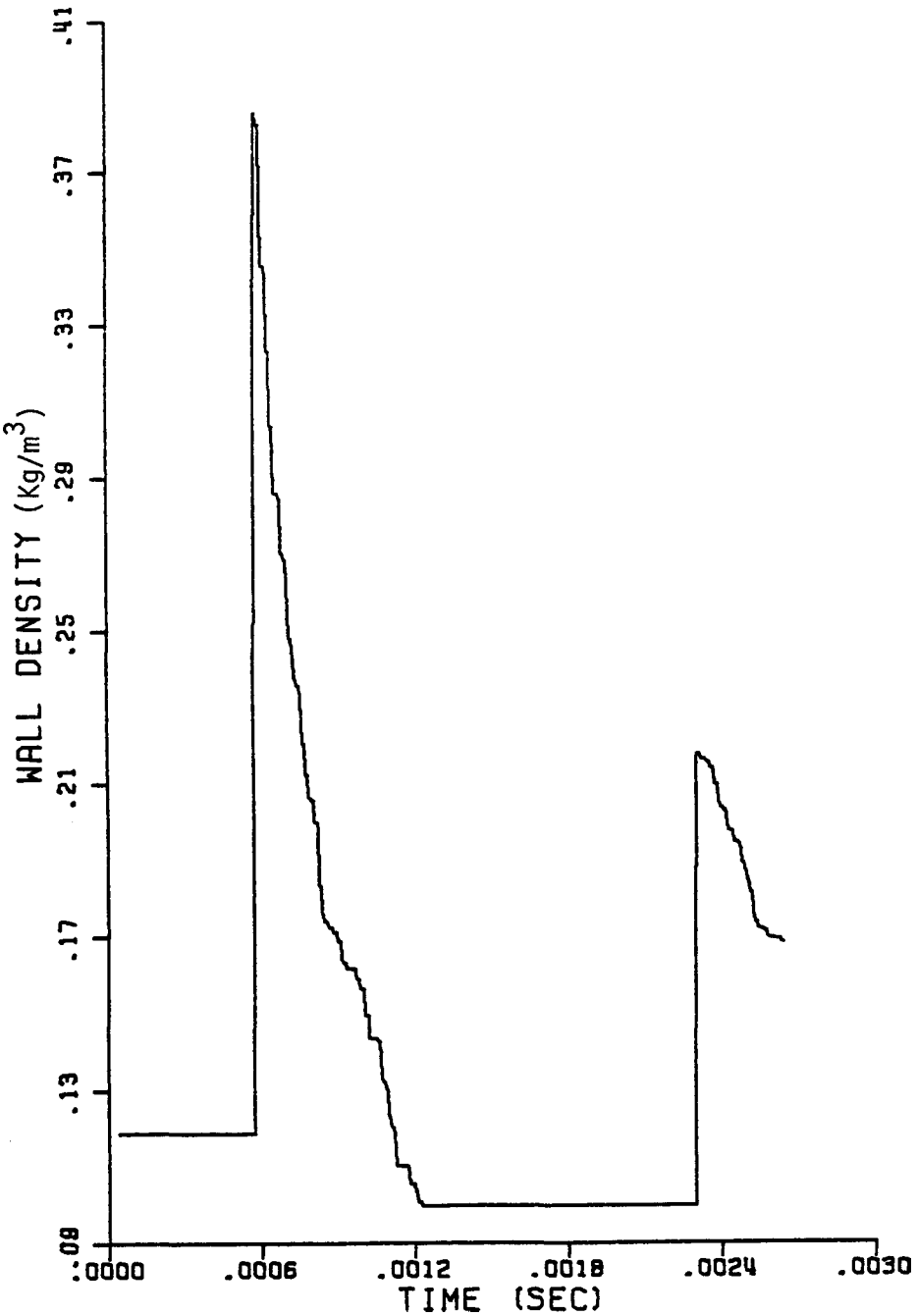

FIGURE 4.1.17: WALL DENSITY HISTORY FOR A 1m RADIUS (planar geometry) 2 INITIAL GRID POINTS, SIGMA=0.8, Δx=0.01

initiation of the detonation, the detonation front is reflected by the wall which results in an increase in pressure (approximately 37 times the pressure of the unburnt gas). Then, the pressure starts to decrease until it reaches a constant value at t = 1.2 ms. This value of the pressure is close to the pressure of an expanding detonation close to the center where the velocity of the gas equals zero. At t = 1.3 ms, the wave gets reflected at the center (Figures 4.1.18 and 4.1.19). At the origin, the shock increases in strength and the pressure reaches a value 23 times greater than the initial pressure. Then the wave moves back towards the wall. At t = 2.3 ms, a second reflection against the wall occurs; this reflection is much weaker than the first reflection; the pressure is 16 times the initial pressure of the unburnt gas.

Next, a detonation was investigated in a plane geometry of size comparable to a nuclear reactor containment. The gas was confined by walls at a distance of 20 m apart. The initial pressure and density of the gas in the containment was considered to be atmospheric. The mesh was composed of 201 grid points 0.1 meter apart. We let the programs run for 100 time steps (t = 45 ms); the computational time on an IBM - 370 was approximately 8 CPU minutes. The results for the pressure and density profiles at the wall and at the centerline are shown in Figures 4.1.20 to 4.1.23. The shape of the curves are, as expected, similar to those shown in Figures 4.1.16 - 4.1.19. We should also note here, that the relative pressures are almost identical in both problems studied in this sec-

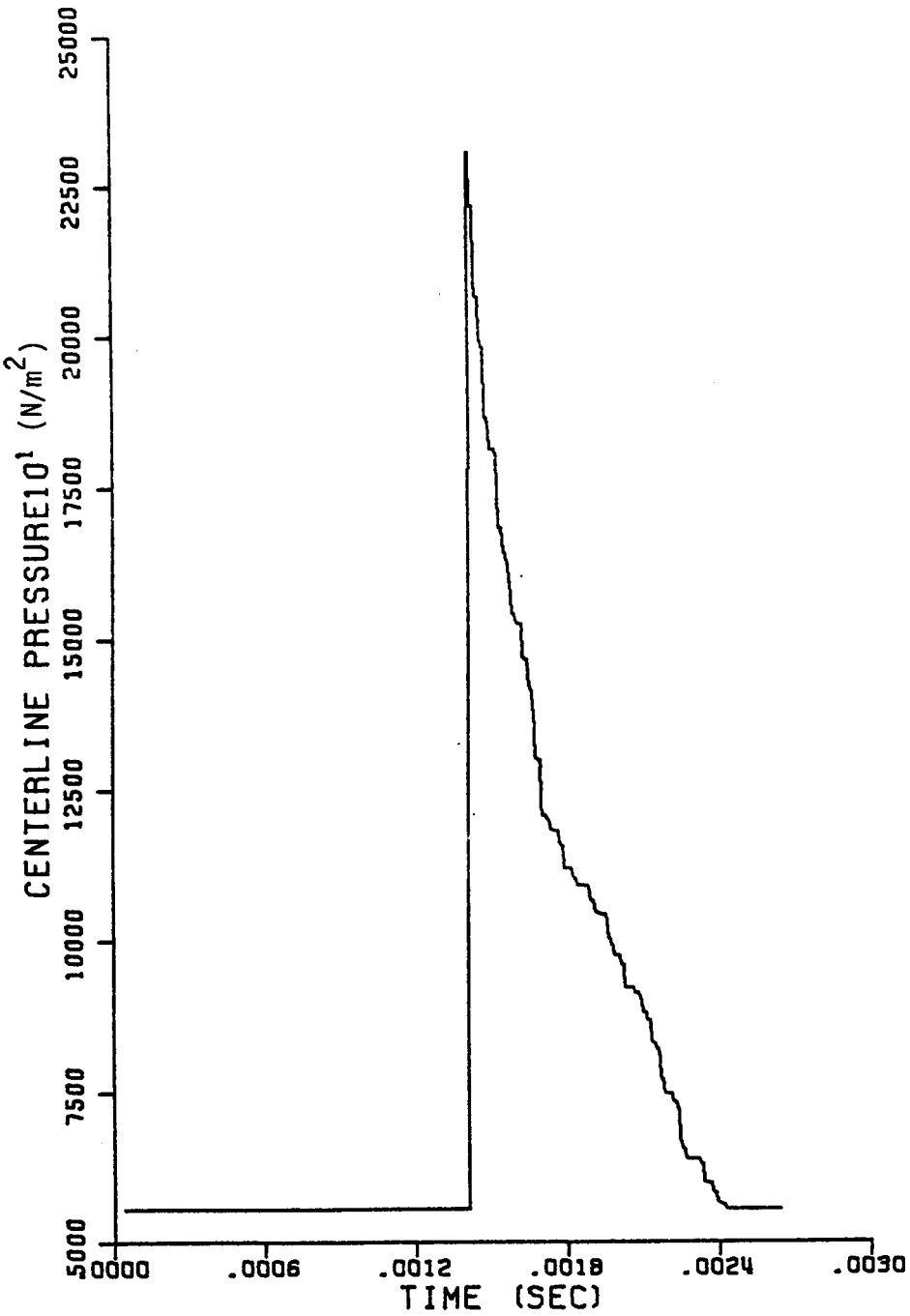

FIGURE 4.1.18: CENTERLINE PRESSURE HISTORY FOR A 1m RADIUS (planar geometry) 2 INITIAL GRID POINTS, SIGMA=0.8, Δx=0.01

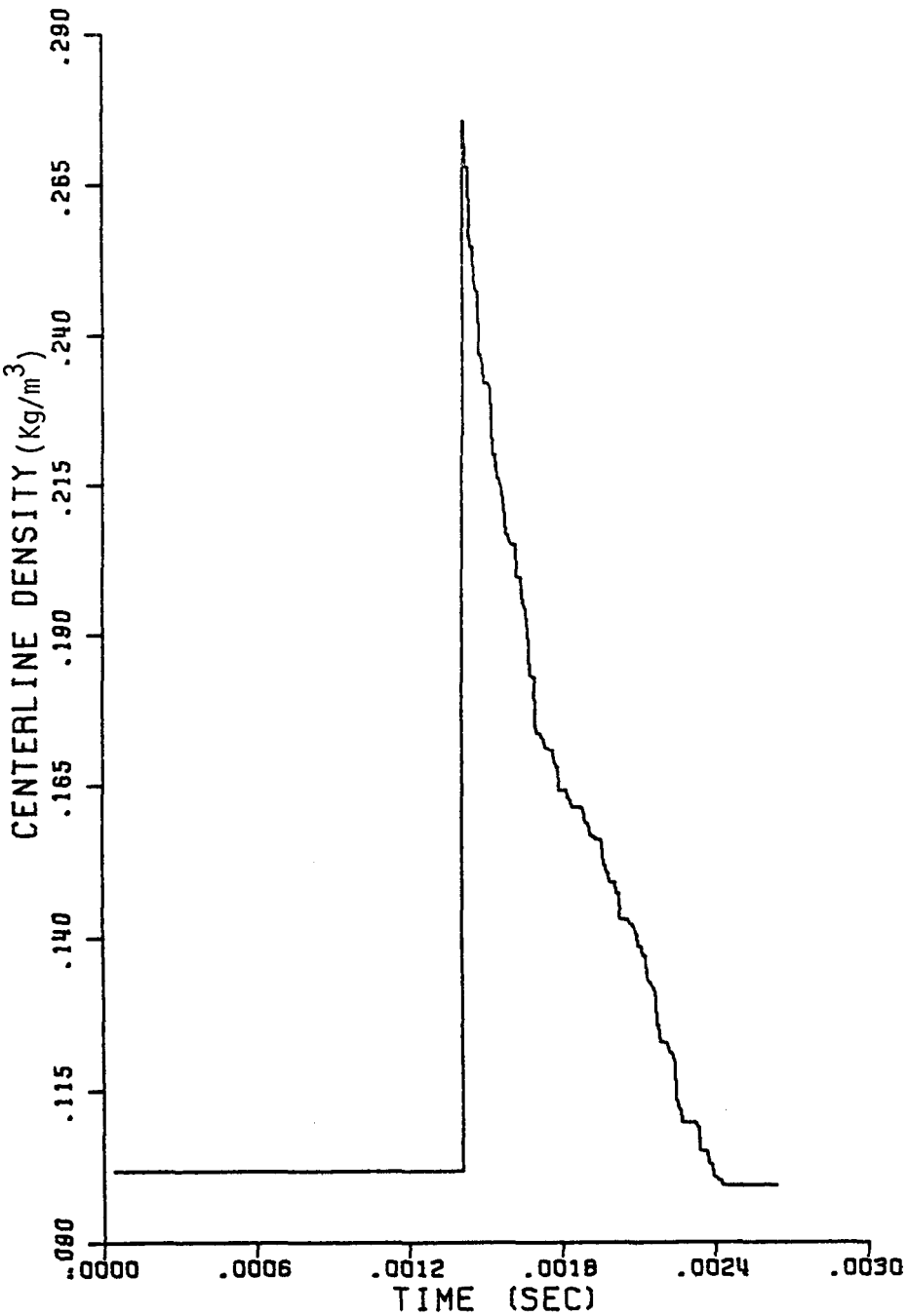

FIGURE 4.1.19: CENTERLINE DENSITY HISTORY FOR A 1m RADIUS (planar geometry) 2 INITIAL GRID POINTS, SIGMA=0.8, Δx=0.01

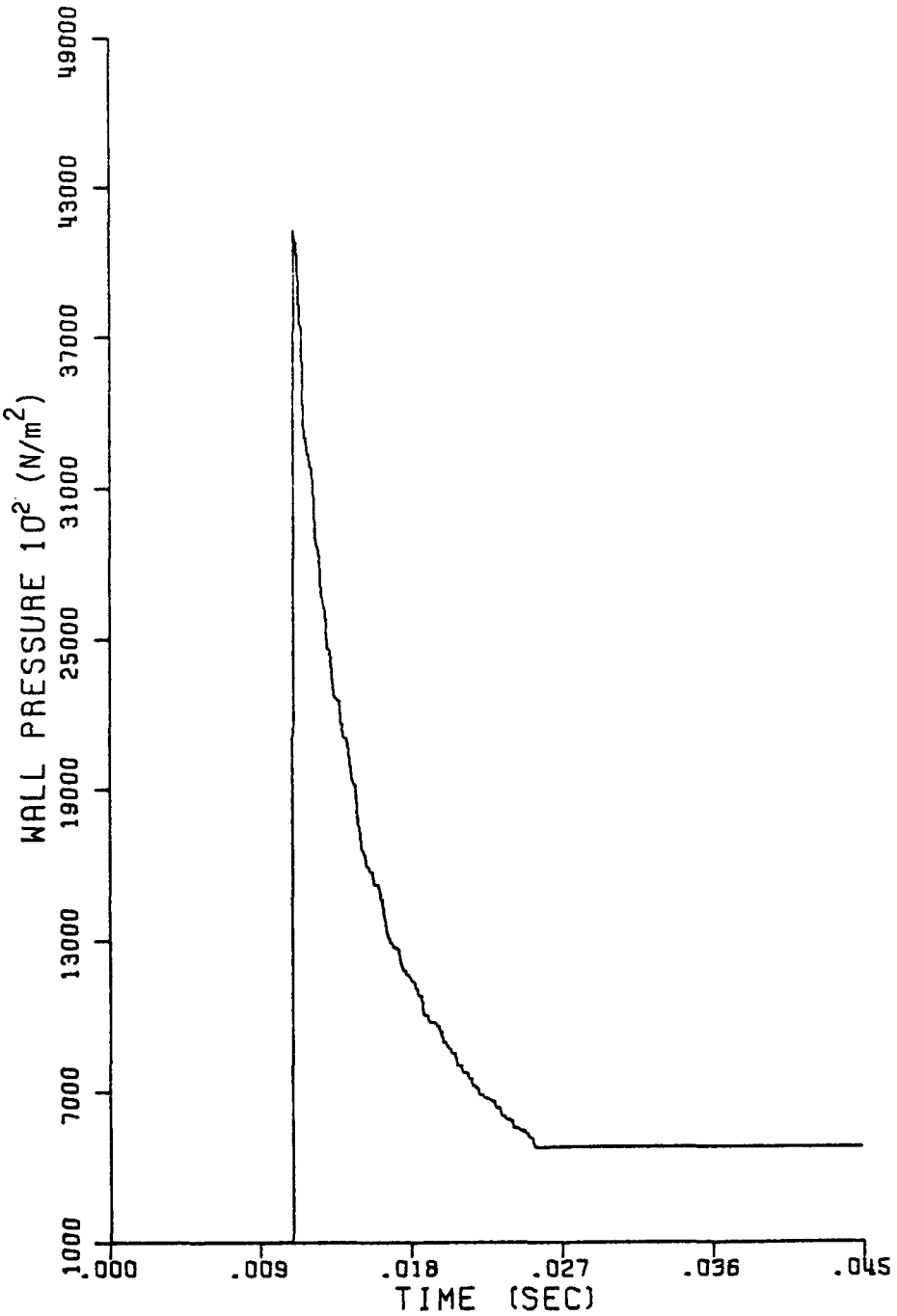

FIGURE 4.1.20: WALL PRESSURE HISTORY FOR A 20 m RADIUS$_3$(planar geometry) Δx=0.1, p_u=1 atm, ρ_u=1.19 Kg/m^3

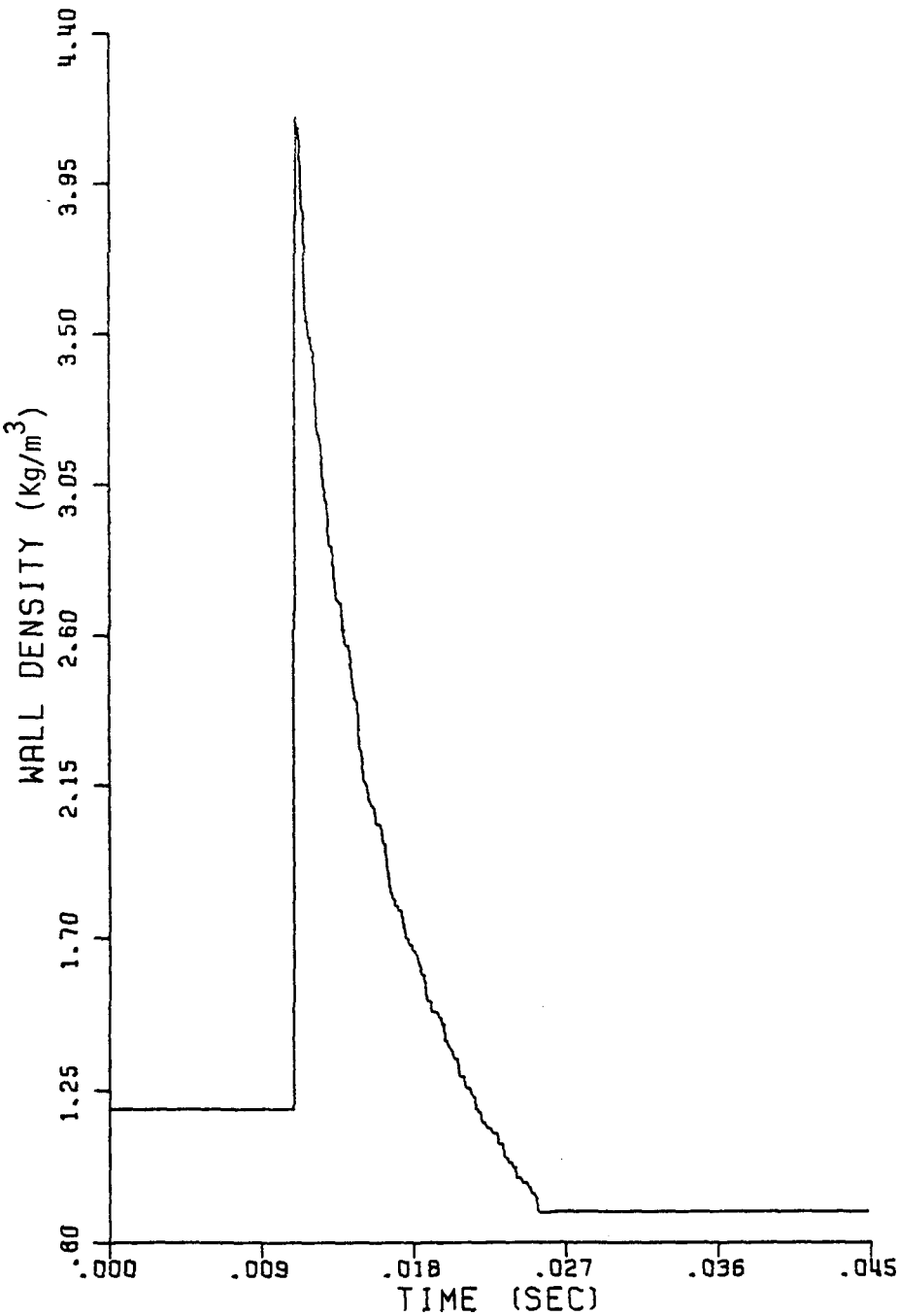

FIGURE 4.1.21: WALL DENSITY HISTORY FOR A 20m RADIUS (planar geometry) Δx=0.1, p_u=1 atm, ρ_u=1.19 Kg/m^3

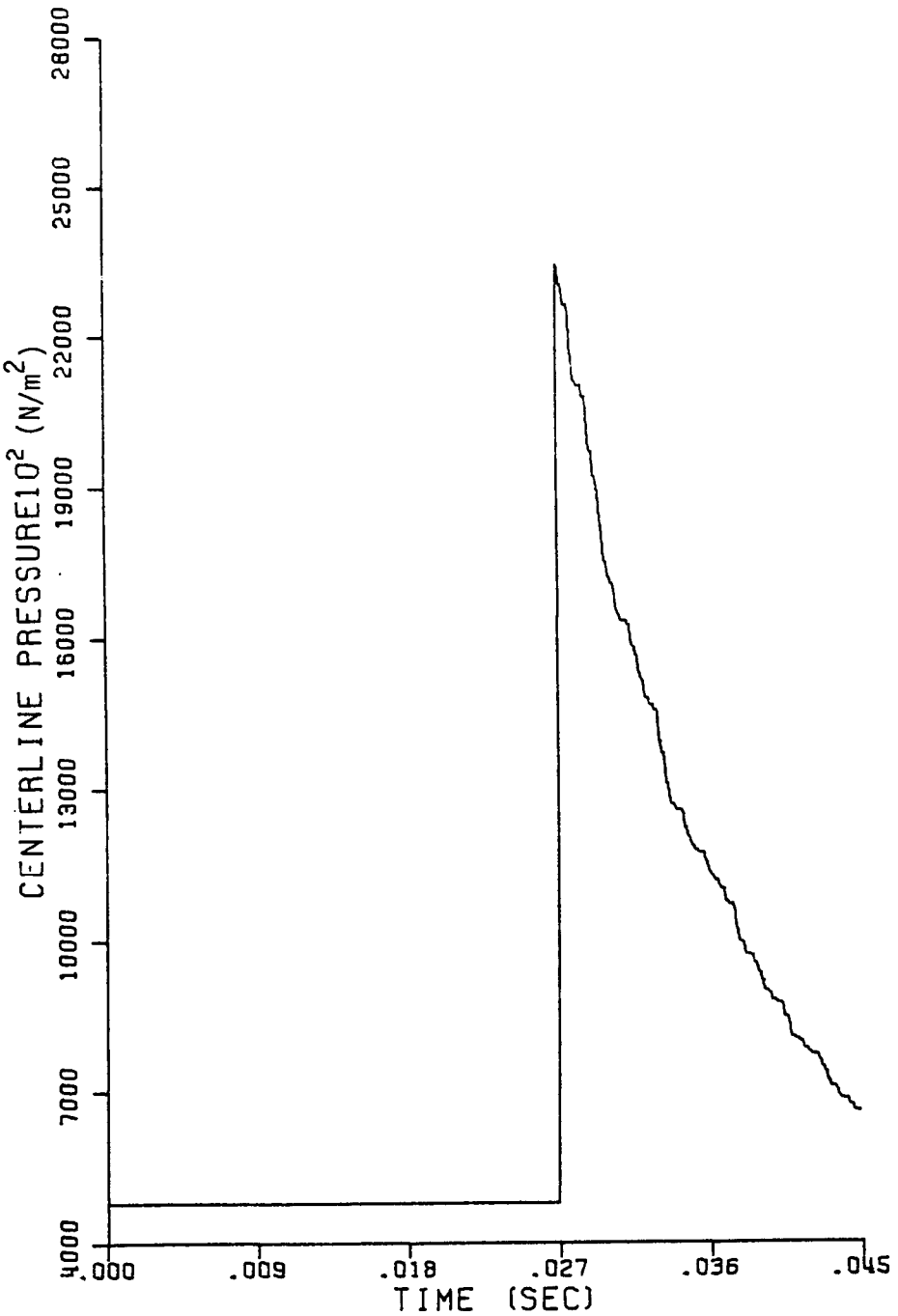

FIGURE 4.1.22: CENTERLINE PRESSURE HISTORY FOR A 20 m RADIUS (planar geometry) $\Delta x=0.1$, $p_u=1$ atm, $\rho_u=19$ Kg/m^3

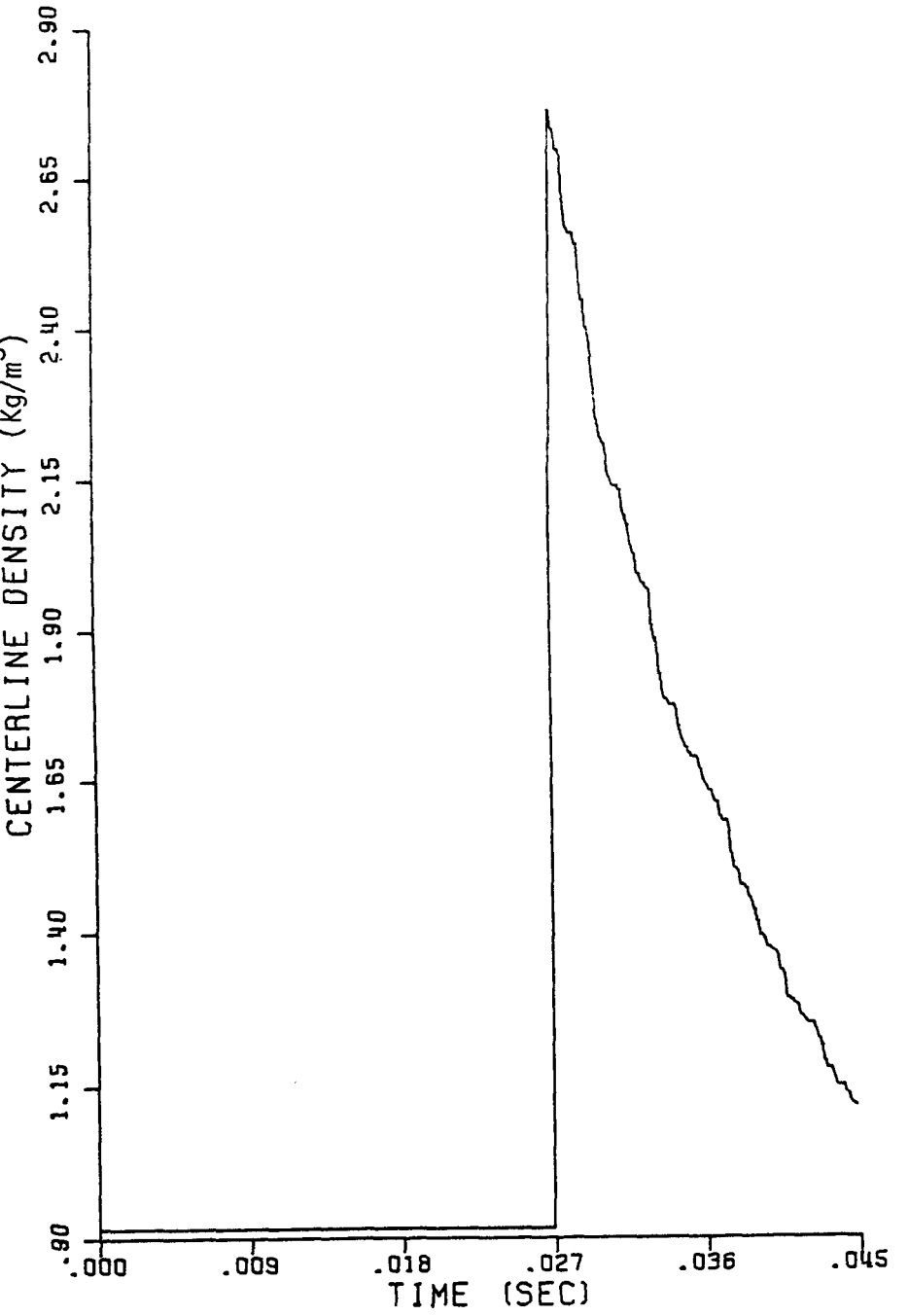

FIGURE 4.1.23: CENTERLINE DENSITY HISTORY FOR A 20 m RADIUS (planar geometry) Δx=0.1, p_u=1 atm, ρ_u=1.19 Kg/m^3

tion; this is a result of considering in both cases the same hydrogen concentration.

4.2 Deformable Wall

In the problems discussed in Section 4.1, we assumed the walls to be rigid; however, if the increase of pressure, due to the detonation and reflected waves, is very large, the wall may start to deform and vibrate because of the elasticity of the material. The velocity of the wall, if it becomes large enough, might have some effects on the properties of the flow. These effects are studied in this section.

The equations governing the motion of the wall can be written as

$$M\ddot{w} + K\, w = P, \tag{4.2.1}$$

where $M = t\rho$, and for the elastic part of the stress-strain curve of the wall material, $K = (\eta-1)\frac{E}{R^2}(A_R + A_L)$; the symbols in equation (4.2.1) are defined as follows:

w = wall displacement from its equilibrium position

P = pressure exerted on the wall,

t = wall thickness,

ρ = wall density,

η = 2 for cylindrical wall, 3 for spherical wall,

E = Young's modulus of steel,

R = radius,

A_R = area of hoop reinforcing bars, per unit wall height,

A_L = liner thickness.

Equation (4.2.1) can be discretized in time, to become

$$\frac{w_n - 2w_{n-1} + w_{n-2}}{\Delta t^2} + \frac{K}{M} w_n = \frac{P}{M}, \qquad (4.2.2)$$

where w_n is the dsiplacement of the wall at time $n\Delta t$. The velocity of the wall can be approximated by

$$V = \dot{w} = \frac{w_n - w_{n-1}}{\Delta t} \qquad (4.2.3)$$

Equation (4.2.2) can be easily incorporated in the algorithm described in Chapter III; equation (4.2.3) can be combined with equation (3.2.1b).

In the application, the values of K and M in Equation (4.2.2) were selected equal to those of an 1 m-high segment of the cylindrical wall of the Indian Point containment. The 1.37 m-thick reinforced concrete wall was considered cracked, and only the contribution of the horizontal steel bars and the liner plate were taken into account. These latter steel components were considered elastic. The distance between the initiation axis and the wall was taken equal to the internal radius of the containment (20.7 m). Results are shown in Figures 4.2.1 - 4.2.3: When the detonation starts, the wall is at rest with zero displacement and zero velocity. It remains in this condition until t = 11 ms, when the detonation wave contacts the wall. The increase in pressure is transmitted to the wall, which acquires a small velocity; this velocity increases until it reaches its maximum value of 4.5 m/s at t = 20 ms, before it starts decreasing. This sinusoidal behavior of the velocity seems to have negligible effects on the pressure and on the density of the gas (less than 1%). The corresponding graphs (Figures 4.2.2 and 4.2.3) are almost identical to those of the rigid wall problem (Figures 4.1.20 and 4.1.21); the reason for this similarity is mainly the fact that the velocity of the wall is negligible compared to the

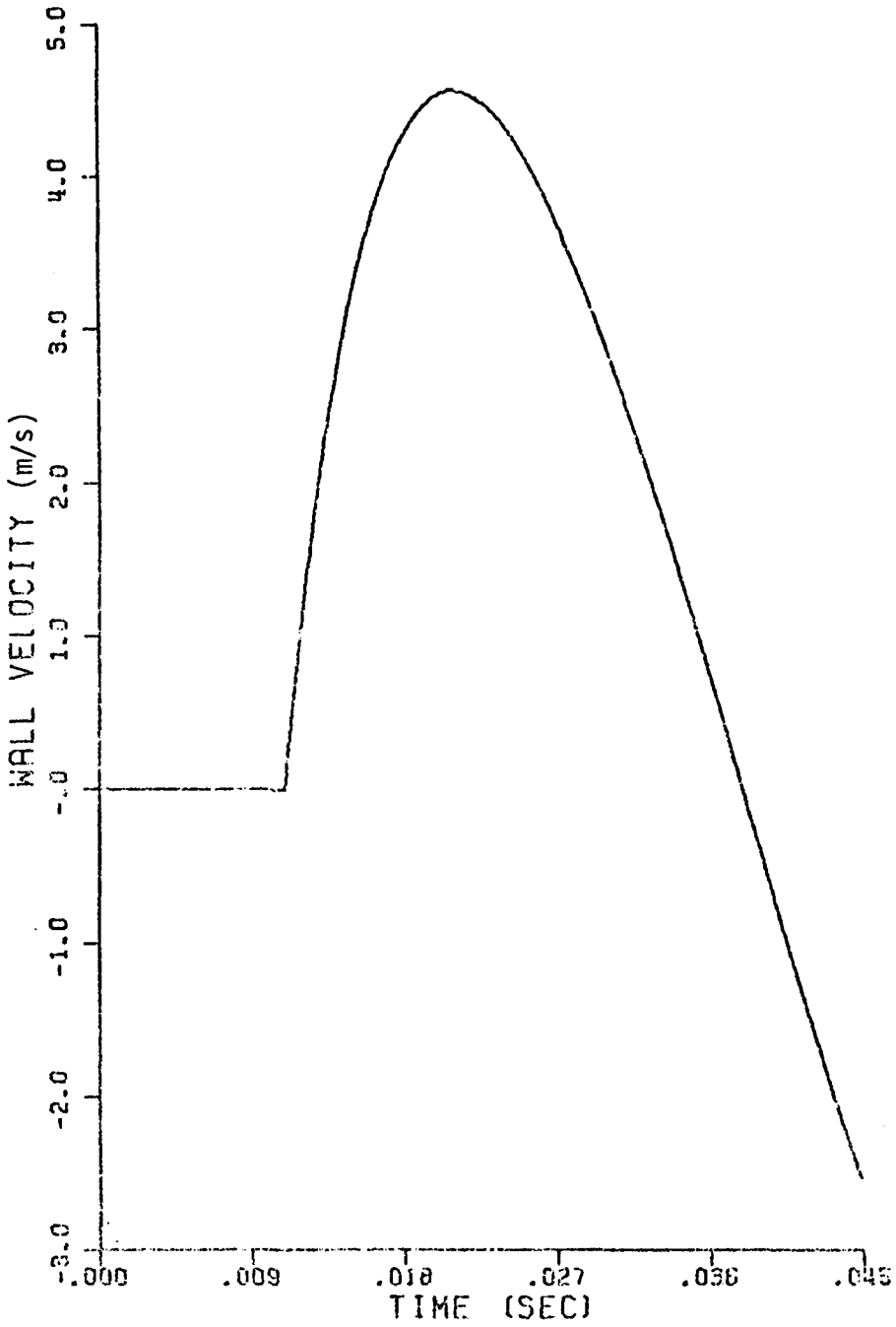

FIGURE 4.2.1: VELOCITY PROFILE OF THE DEFORMABLE WALL

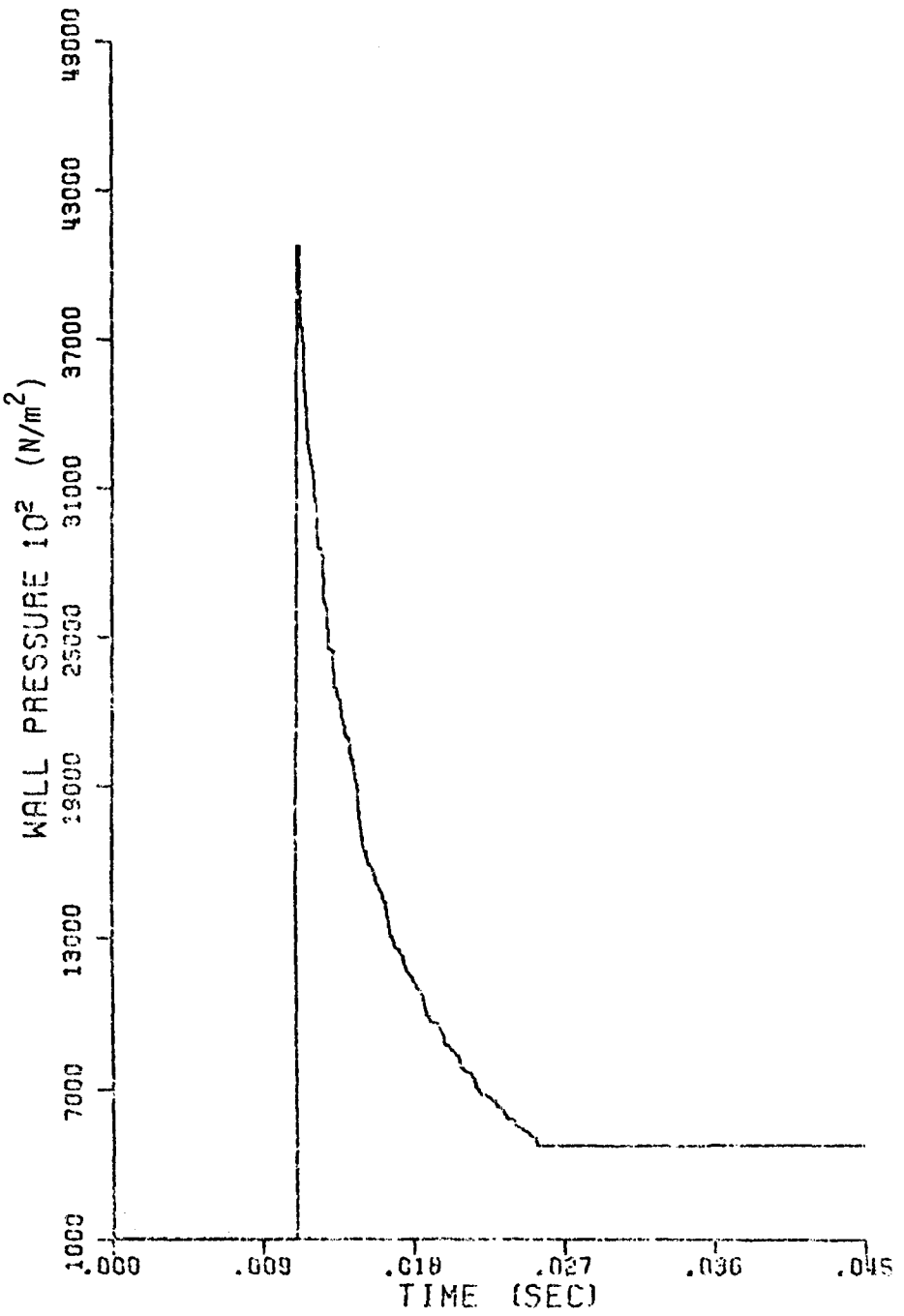

FIGURE 4.2.2: PRESSURE HISTORY AT THE DEFORMABLE WALL

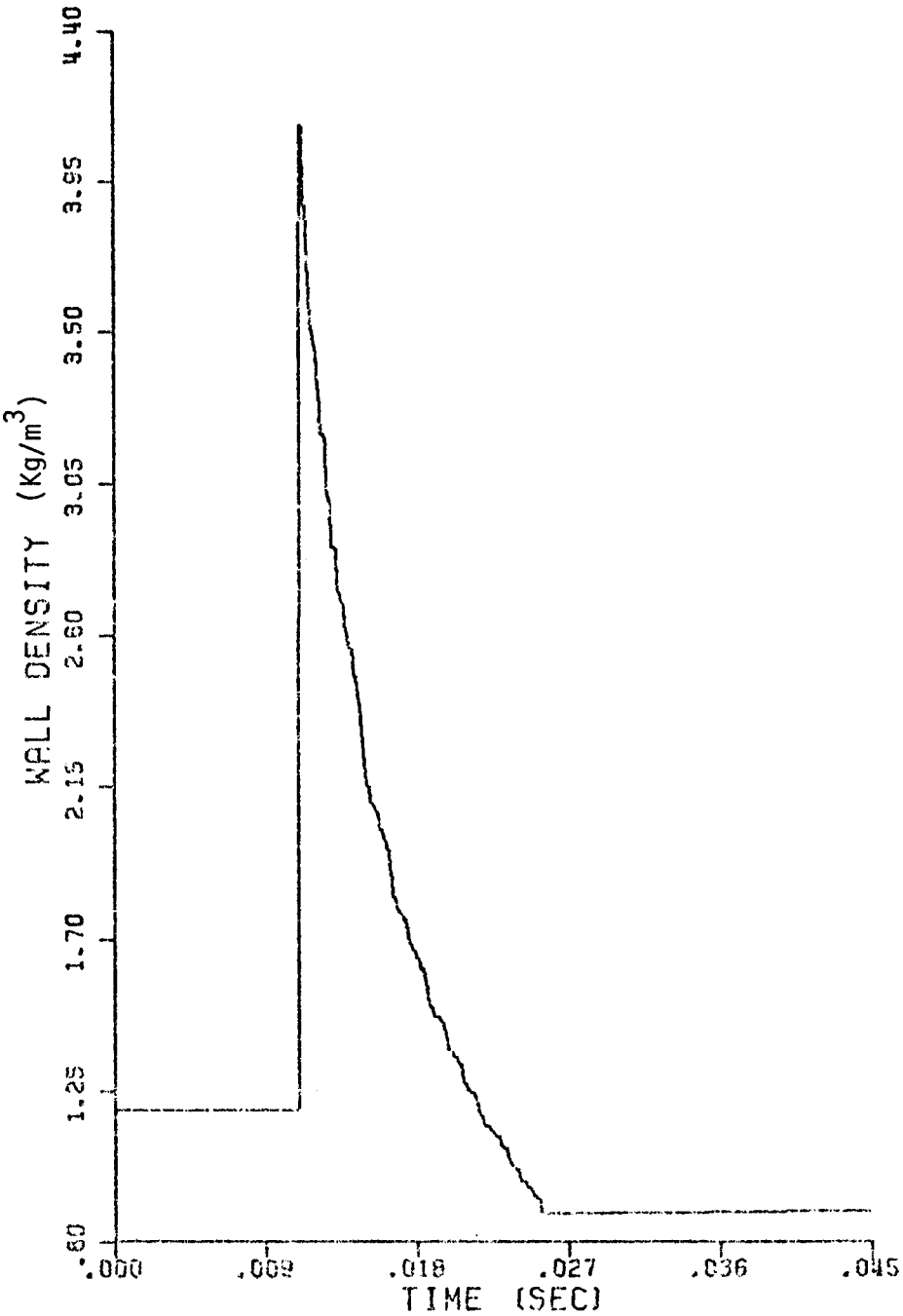

FIGURE 4.2.3: DENSITY HISTORY AT THE DEFORMABLE WALL

wave velocity (1787 m/s). This lack of shock-wall interaction is expected to hold even when multiple reflections are considered, since the interarrival time of waves ($\sim$0.04 sec.) is much shorter than the period of the wall ($\sim$0.1 sec.). Sensitivity studies have shown that increasing or decreasing the value of K by 2 orders of magnitude do not change the conclusions above.

4.3 One-Dimensional Spherical Geometry

An approach similar to the one followed in section 4.1 has been adopted here to test the one-dimensional spherical algorithm in the computer program SPHDET (see Appendix C).

The first problem studied is that of a detonation wave initiated at the origin of a 1 m radius sphere bounded by a rigid wall. A mesh of 101 grid points, 0.01 m apart was constructed. Initially the gas is at rest at a pressure p_u = 10100 N/m^2 and a density ρ_u = 0.1188 Kg/m^3. The chemical composition is stoichiometric.

It was necessary to assign the Taylor conditions to a minimum of 20 grid points. This is due to two reasons: Glimm's method is basically the solution of the one-dimensional planar problem; and the gradient of the pressure, density and velocity profiles just behind the detonation front are very large (see Figures 2.4.1, 2.4.3 and 2.4.3).

The non-dimensional graphs (Figures 4.3.1 - 4.3.3) at t = 0.55 ms show the good agreement of the solution with the Taylor curves; however, because of the randomness of the sampling, the curves are not reproduced smoothly. It is worth noting that the values

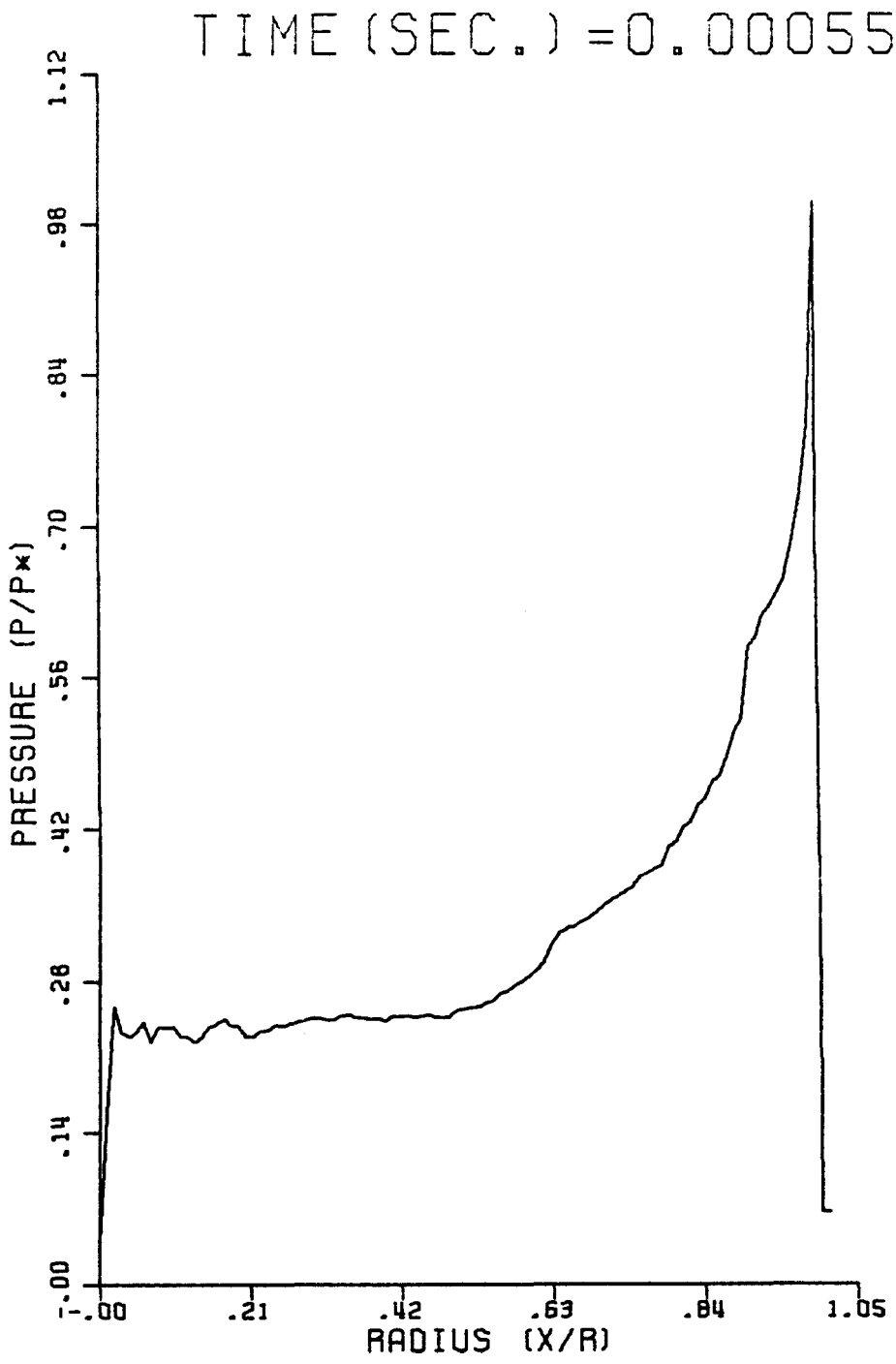

FIGURE 4.3.1: NON-DIMENSIONAL PRESSURE DISTRIBUTION; SPHERICAL GEOMETRY, 1m RADIUS

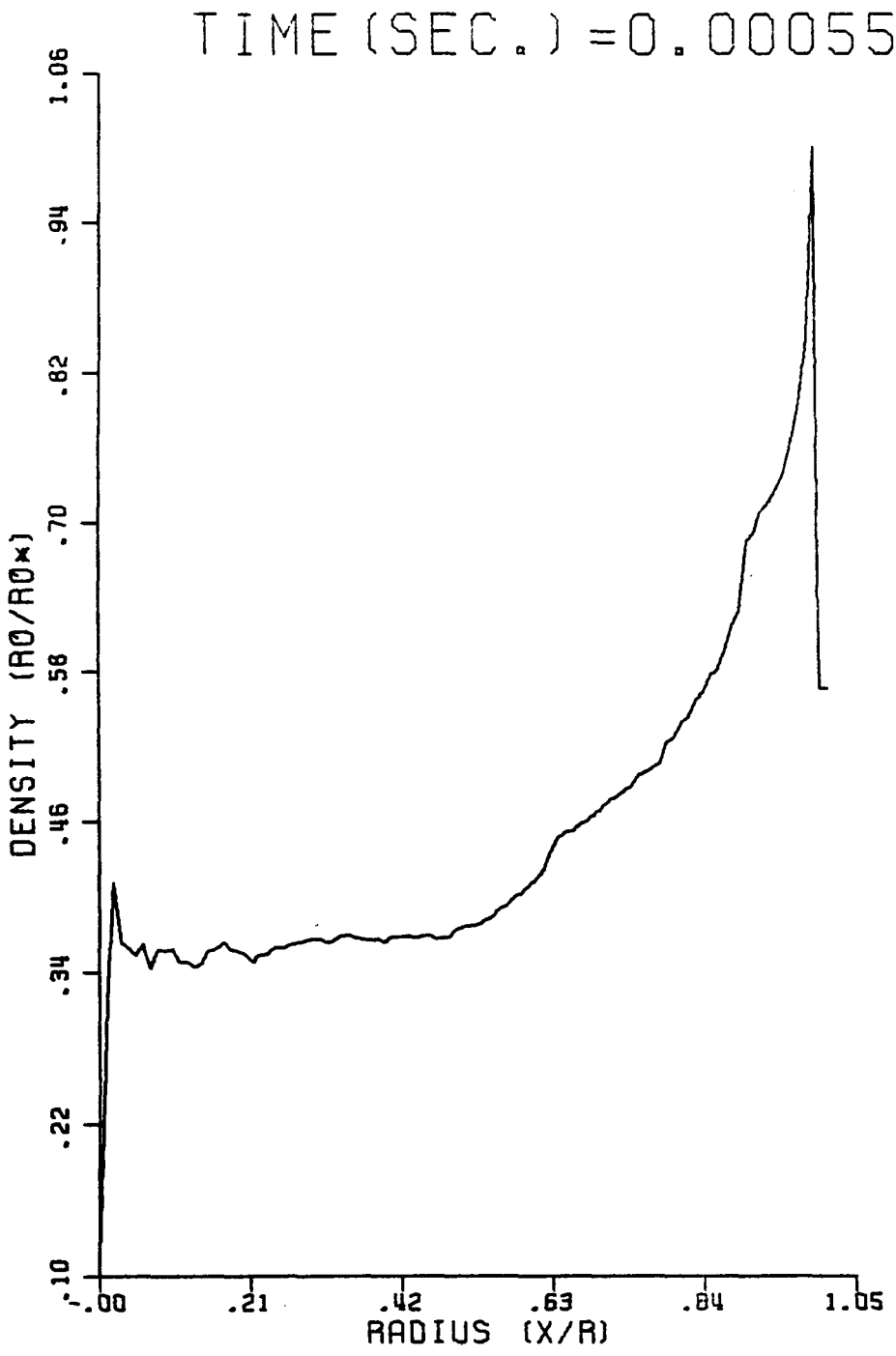

FIGURE 4.3.2: NON-DIMENSIONAL DENSITY DISTRIBUTION; SPHERICAL GEOMETRY, 1 m RADIUS

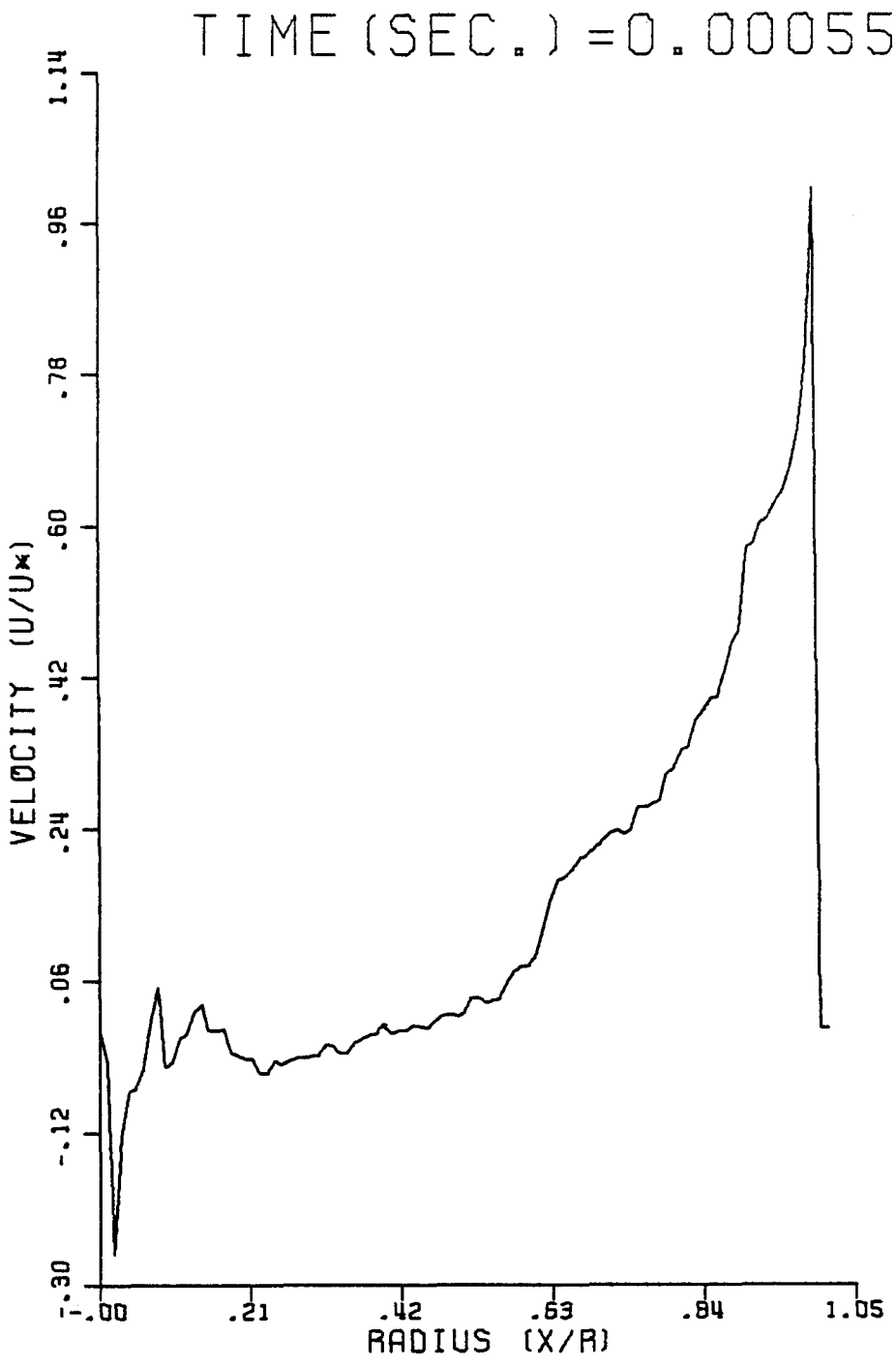

FIGURE 4.3.3: NON-DIMENSIONAL VELOCITY DISTRIBUTION; SPHERICAL GEOMETRY, 1m RADIUS

near the center do not follow the prediction of the Taylor solution.

The pressure, density and velocity histories inside the sphere are shown in Figures 4.3.4 - 4.3.6, for five different times. It can be seen how the detonation wave propagates inside the sphere (times (1) and (2)); then, the wave is reflected by the wall. The resulting shock wave travels back towards the center. First, the shock decreases in strength but as it approaches the center, the shock front properties increase steadily until the wave reaches the origin; there, the pressure behind the reflected wave becomes 43 times the pressure of the initial unburnt gas. This implosion phenomenon, for spherical and cylindrical converging waves has already been noticed experimentally by Perry and Kantrowitz [3.10] and analytically by Oswatitsh [3.11] and Sod [3.7].

The pressure and density profiles at the still wall (Figures 4.3.7 and 4.3.8) are similar to the cartesian problem. The wall remains at the constant initial pressure (10100 N/m^2) and density (0.1188 Kg/m^3) until the combustion wave is reflected by the wall at t = 0.53 ms; then, the pressure rises to approximately 40 times the initial pressure. It starts decreasing to reach a stable pressure of 65000 N/m^2, for the remaining of the interval of time shown.

The computer analysis was extended to conditions expected in a nuclear containment of spherical geometry: the initial pressure was set at 1 atm, the initial density was set at 1.19 Kg/m^3, the gas was bounded by a 20 m radius sphere. The results are shown in Figures

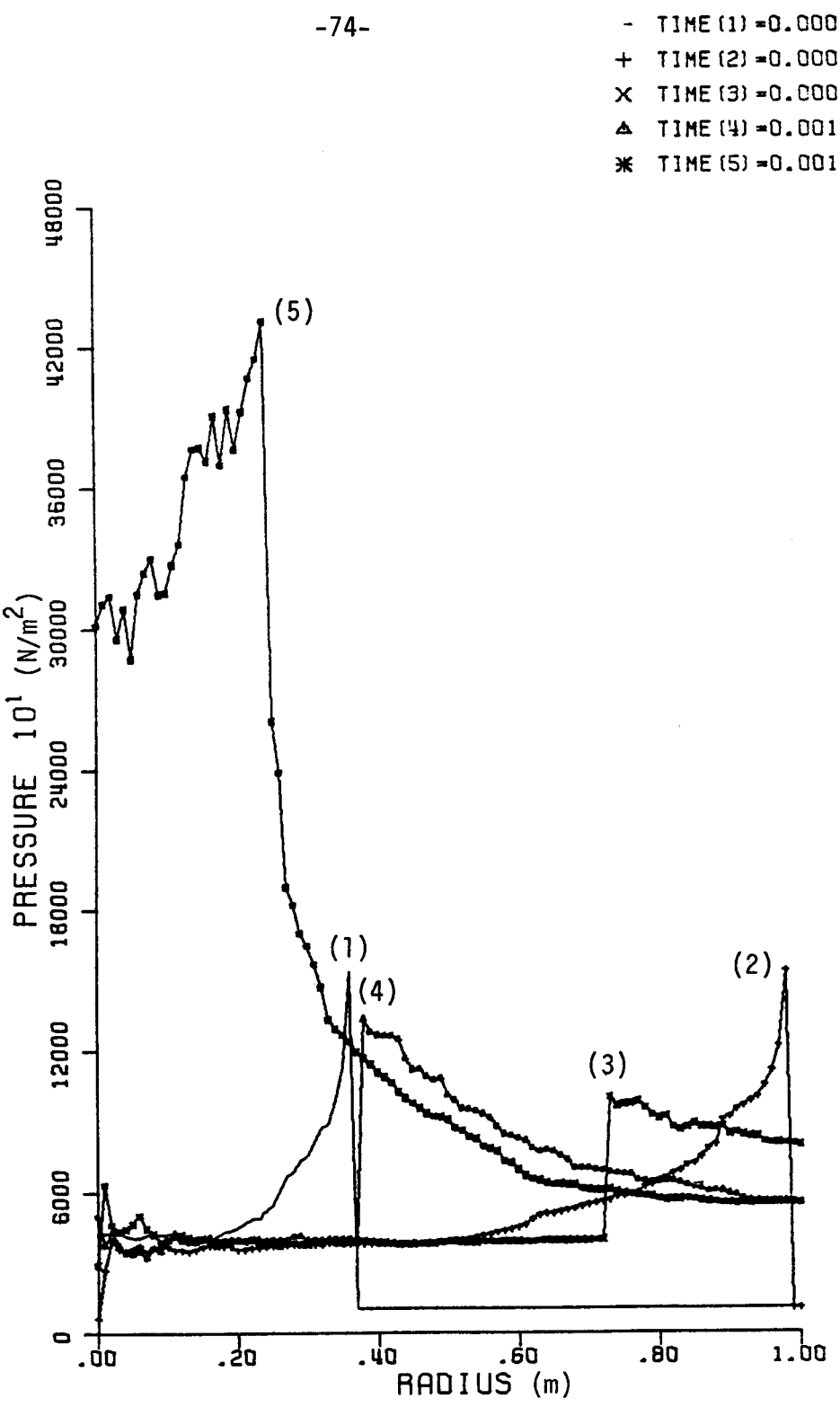

FIGURE 4.3.4: PRESSURE DISTRIBUTION IN A 1m RADIUS SPHERE AT FIVE DIFFERENT TIMES

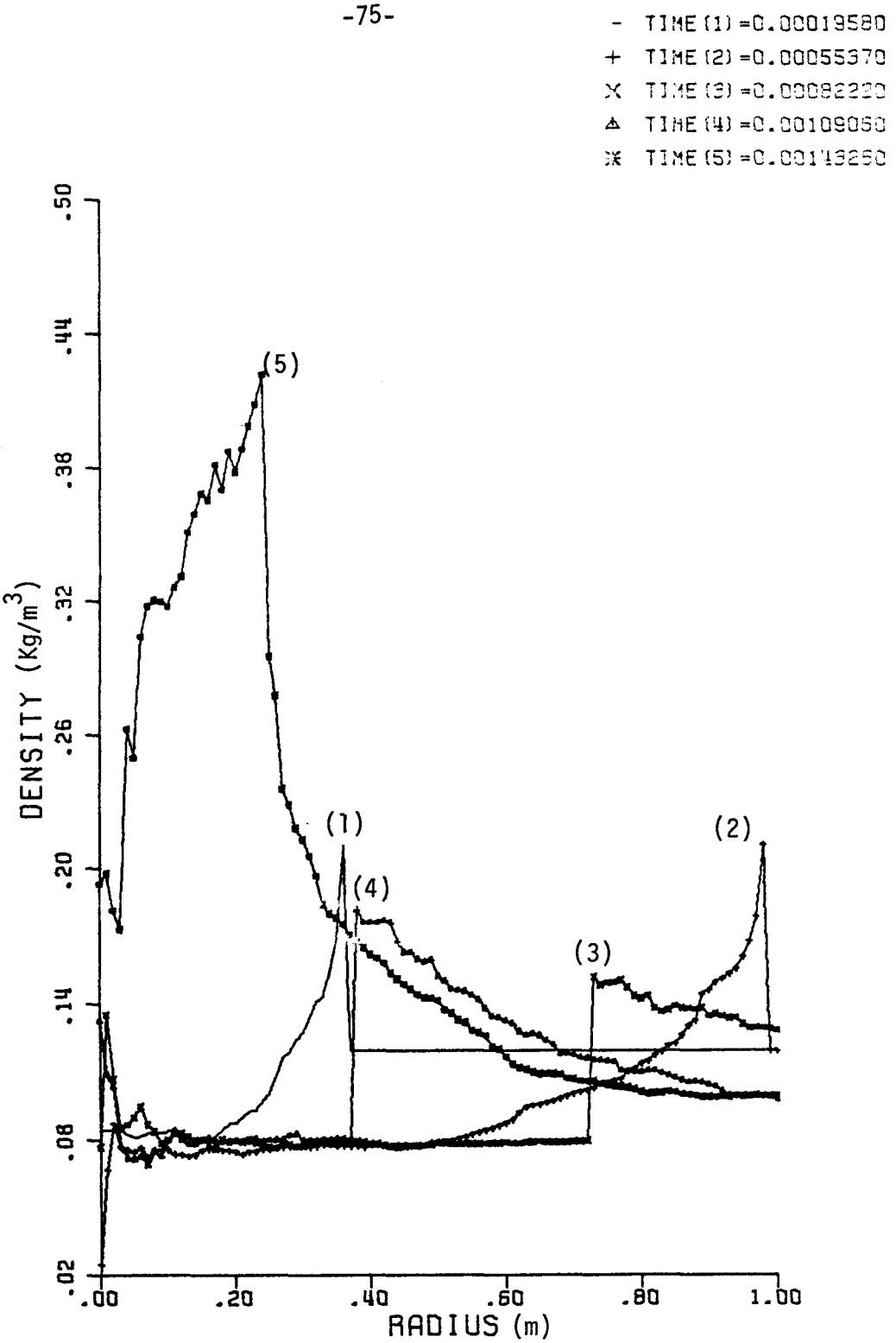

FIGURE 4.3.5: DENSITY DISTRIBUTION IN A 1m RADIUS SPHERE AT FIVE DIFFERENT TIMES

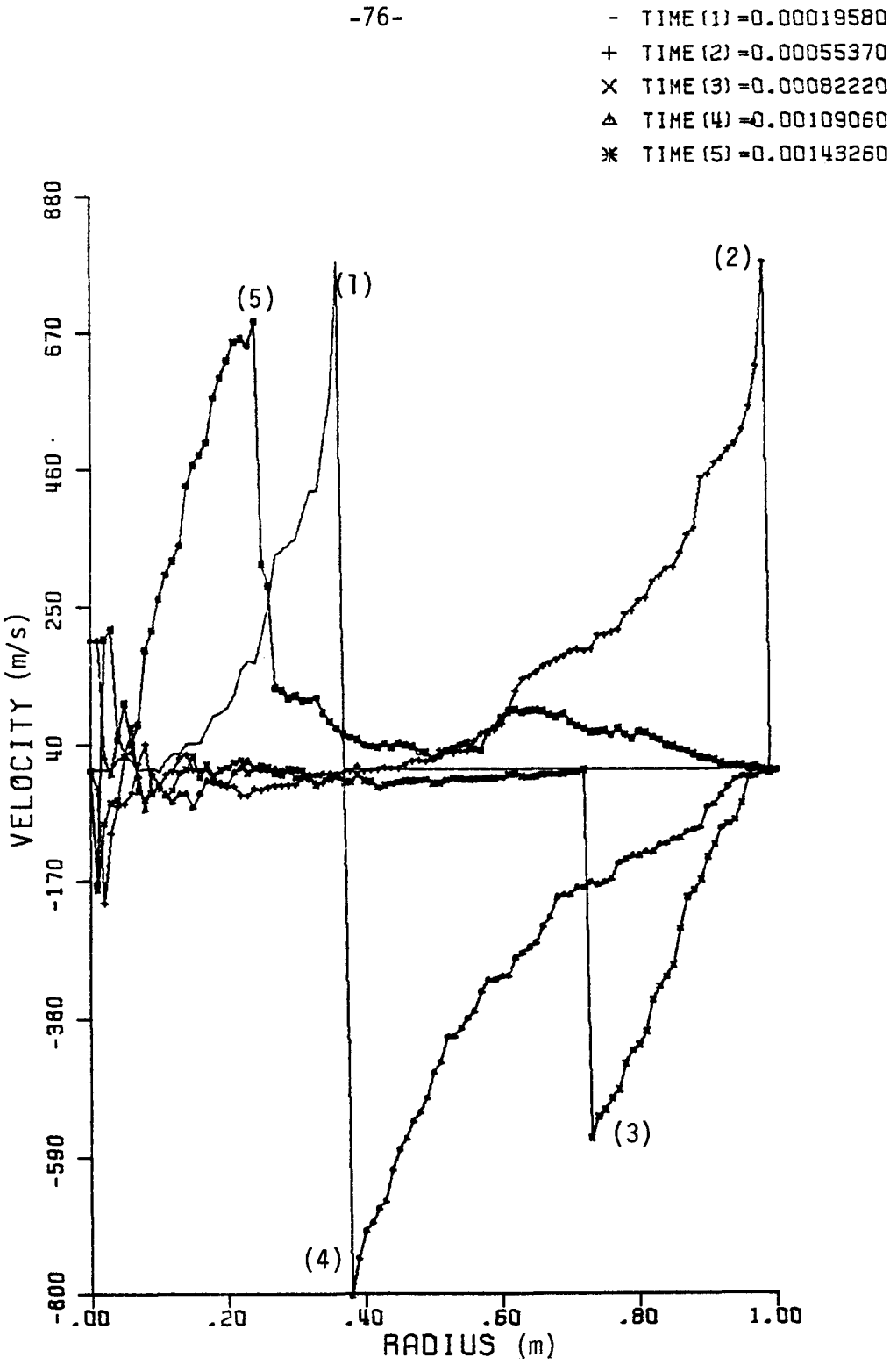

FIGURE 4.3.6: VELOCITY DISTRIBUTION IN A 1m RADIUS SPHERE AT FIVE DIFFERENT TIMES

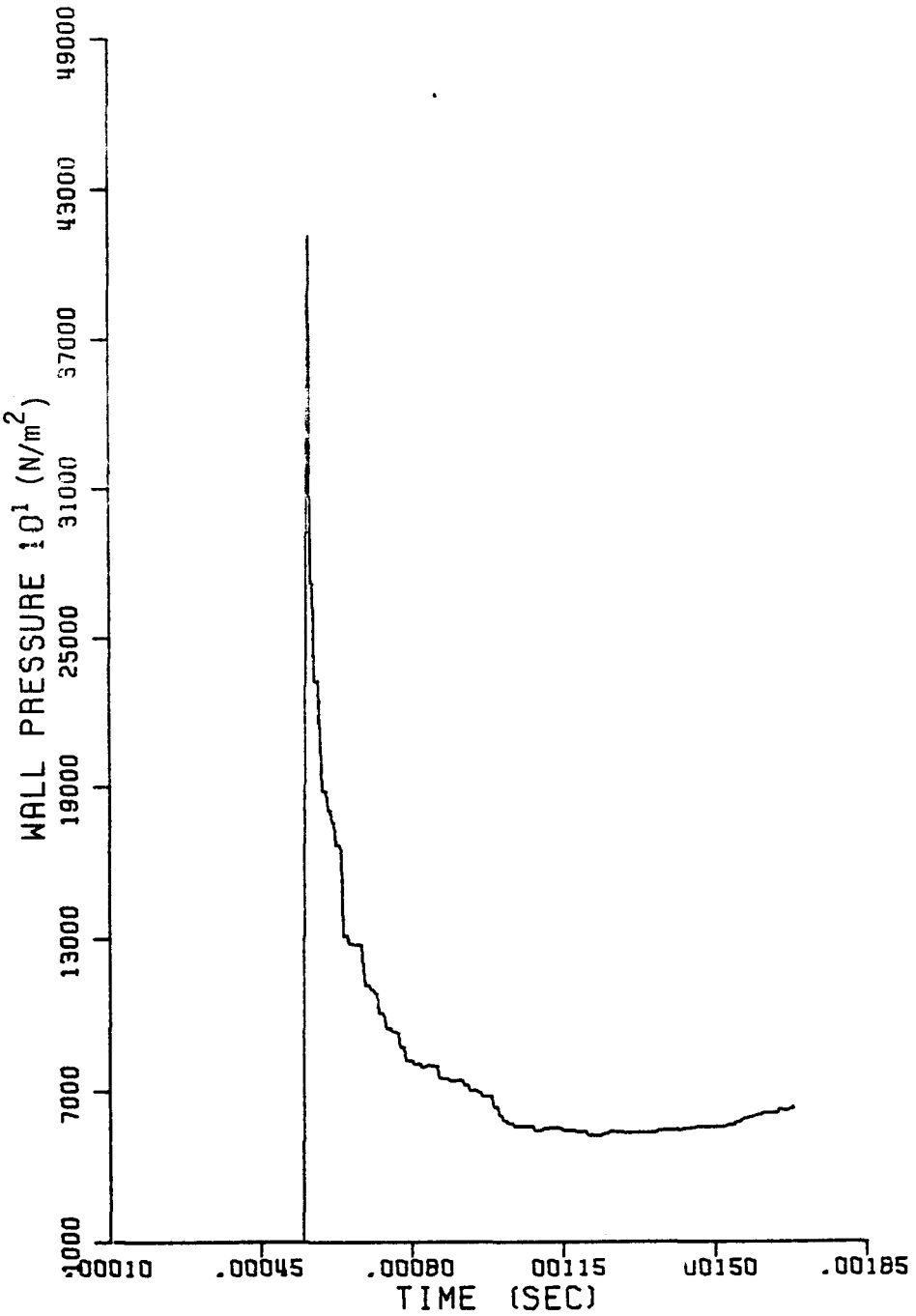

FIGURE 4.3.7: PRESSURE PROFILE AT THE WALL OF A 1m RADIUS SPHERE
p_u = 10100 N/m^2, ρ_u = 0.1188 Kg/m^3

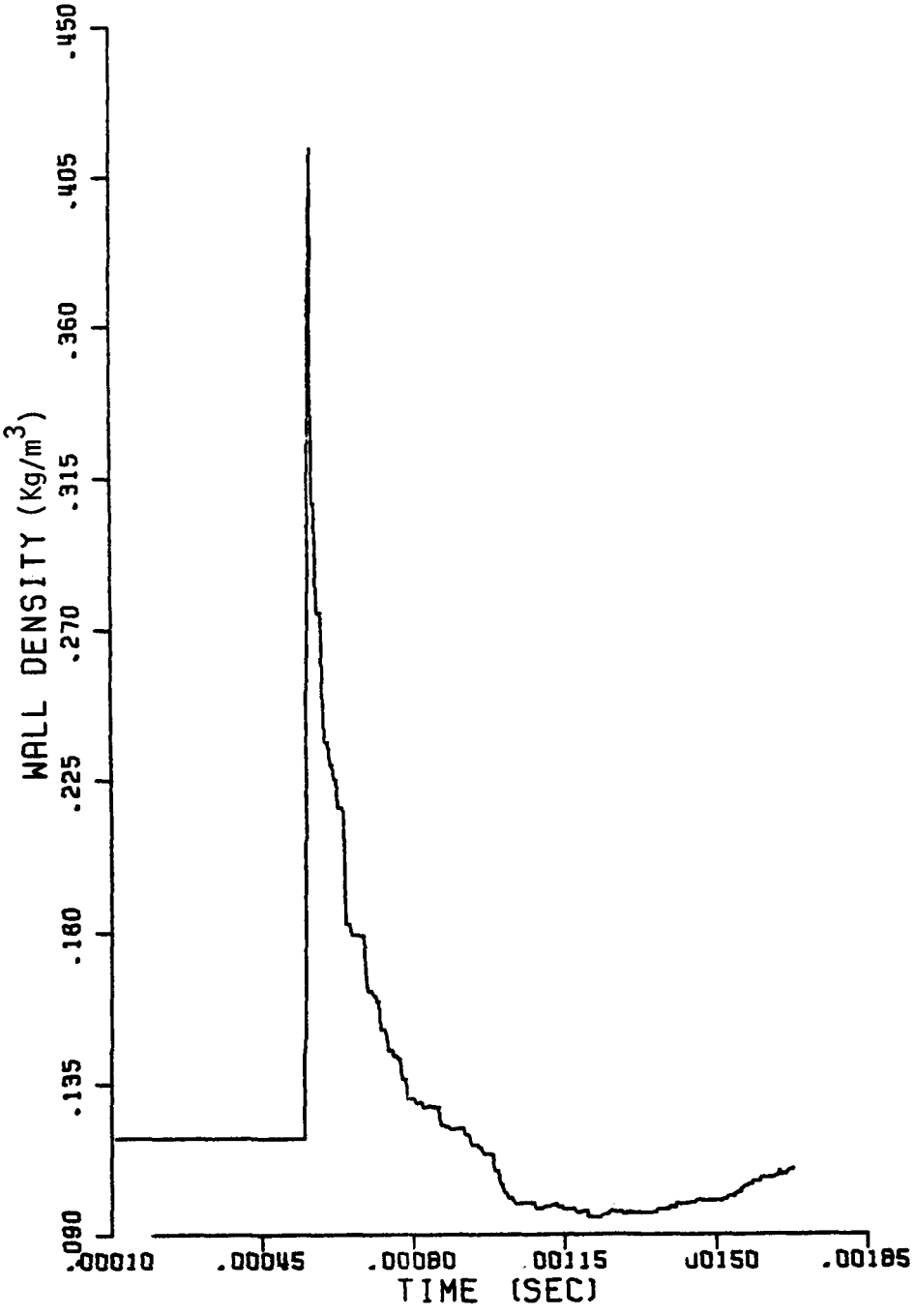

FIGURE 4.3.8: DENSITY PROFILE AT THE WALL OF A 1m RADIUS SPHERE
p_u = 10100 N/m^2, ρ_u = 0.1188 Kg/m^3

4.3.9 and 4.3.10. The shape of the curves are similar to the previous case; the pressure rises to 40.5 atm at t = 11 ms, when the wave contacts the wall, and decreases to 6.5 atm at t = 23 ms.
For an interval of time longer than that shown, it is expected that another reflection takes place at the wall; another spike, with smaller magnitude than the first one would be recorded. For 1500 time steps (t=40 ms) the computation time was 22 CPU minutes.

4.4 Axisymmetric Geometry

In this section we consider the axisymmetric program TWODIM (see Appendix D). For this purpose we evaluated the capability of this program to reproduce a one-dimensional spherical detonation (whose solution can be obtained using SPHDET).

The non-dimensional pressure, density and velocity profiles of a spherical detonation in a 1 m radius sphere (p_u = 10100 N/m^2, ρ_u = 0.1188 Kg/m^3) can be seen in Figures 4.4.1 - 4.4.3.

To solve the equivalent problem in an axisymmetric coordinate system we took 101 grid points in the x and y directions, 0.01 m apart. We assigned the initial conditions to all the grid points within a 0.2 m radius according to the Taylor [2.5] solution; the program was run for 80 time steps (t = 0.4 ms). The properties were recorded at the grid points lying on the 45° diagonal line. The non-dimensional plots of these properties are shown in Figures 4.4.4 - 4.4.6. These graphs compare well enough with the graphs obtained from the

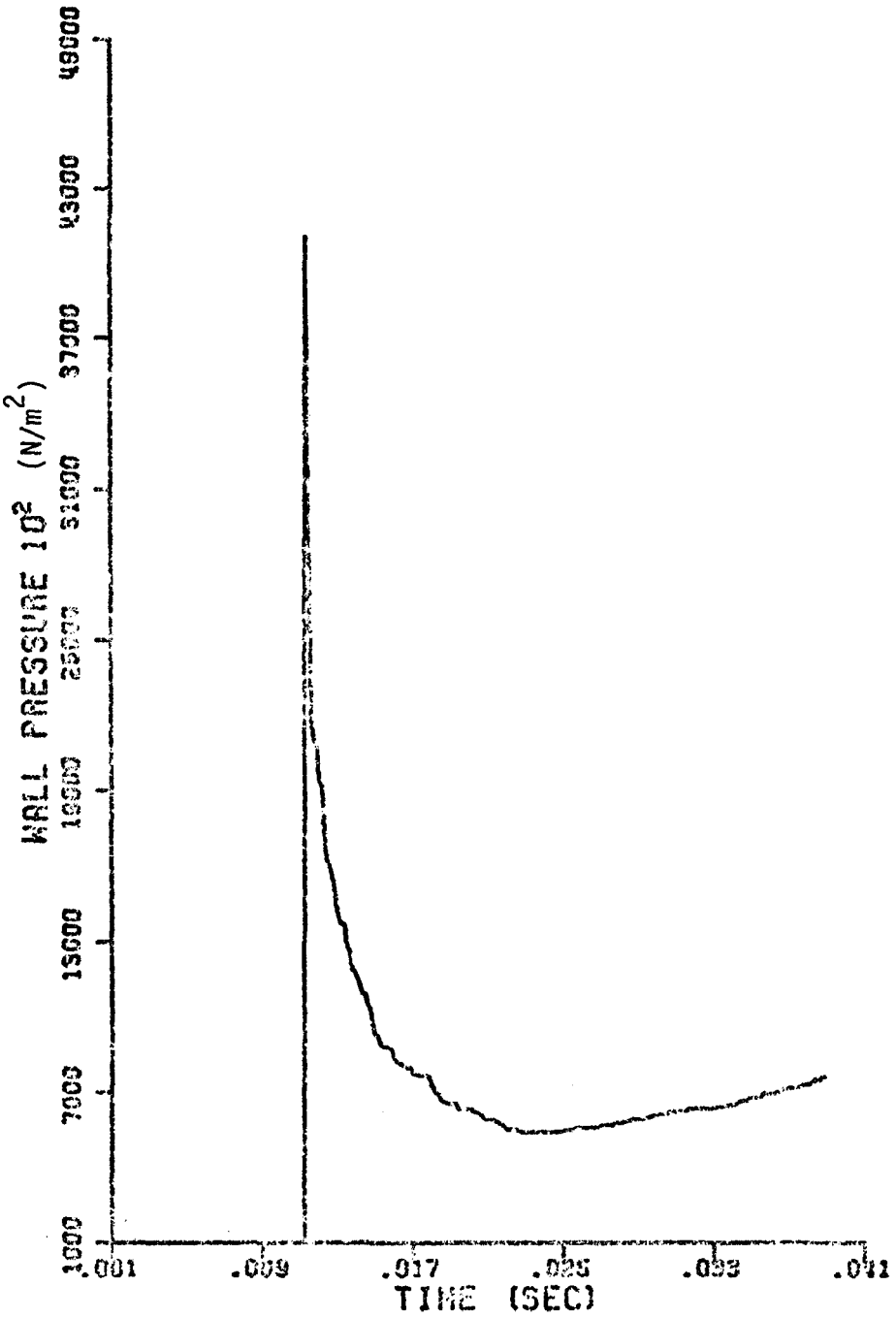

FIGURE 4.3.9: PRESSURE PROFILE AT THE WALL OF A 20 m RADIUS SPHERE
p_u = 1 atm, ρ_u = 1.19 Kg/m^3

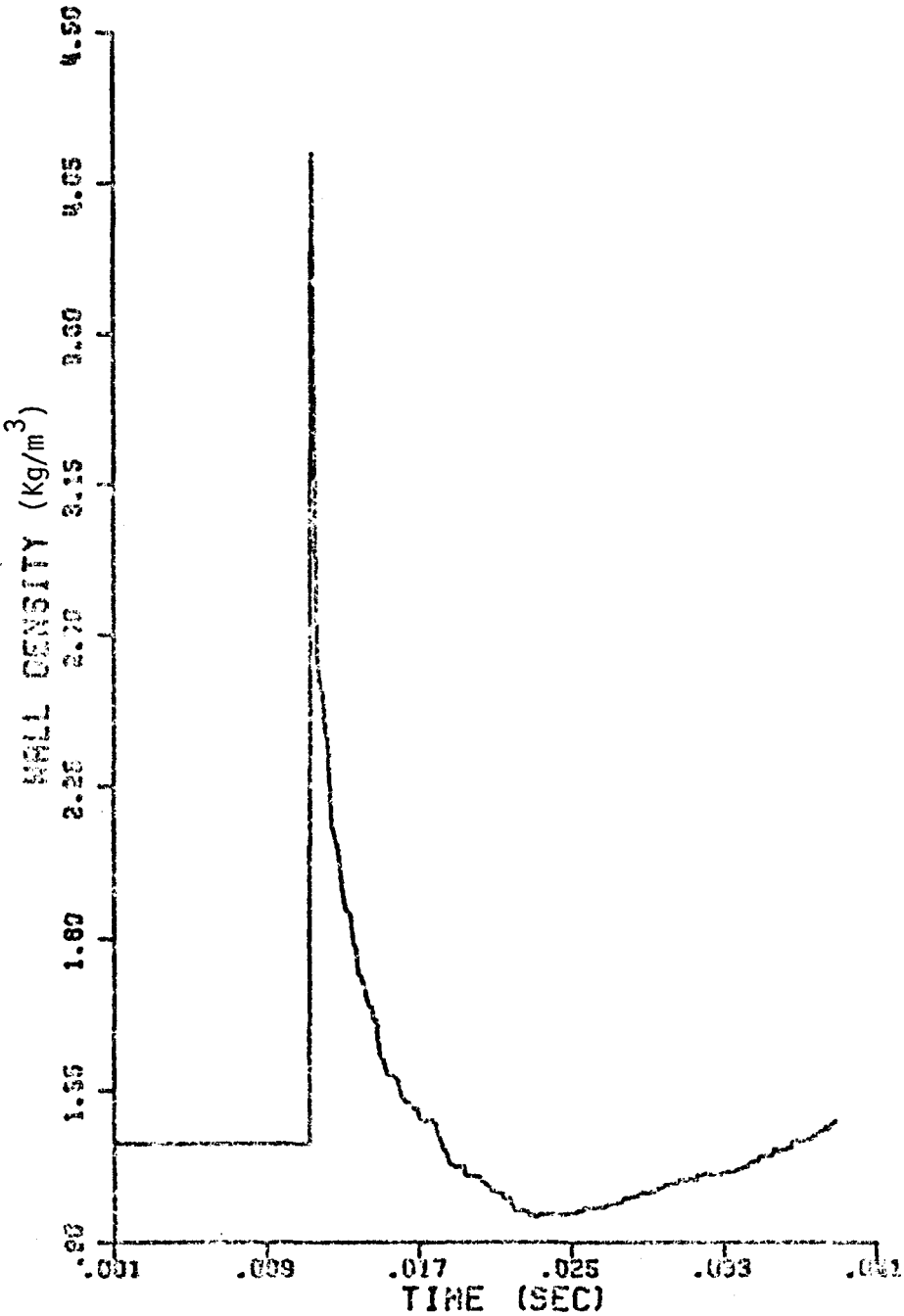

FIGURE 4.3.10: DENSITY PROFILE AT THE WALL OF A 20 m RADIUS SPHERE
p_u = 1 atm, ρ_u = 1.19 Kg/m^3

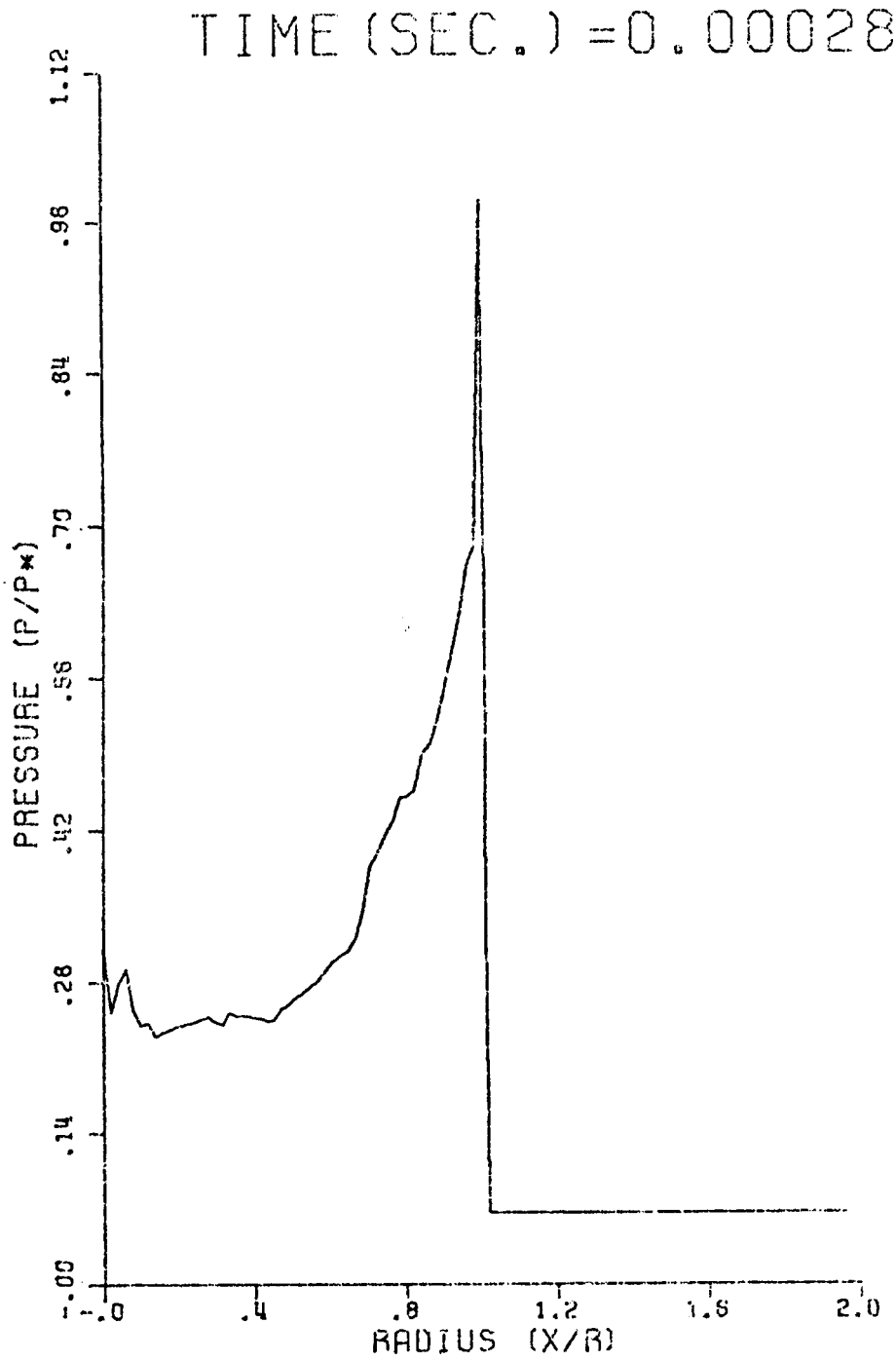

FIGURE 4.4.1: NON-DIMENSIONAL PRESSURE DISTRIBUTION FOR THE ONE-DIMENSIONAL SPHERICAL PROBLEM USING SPHDET

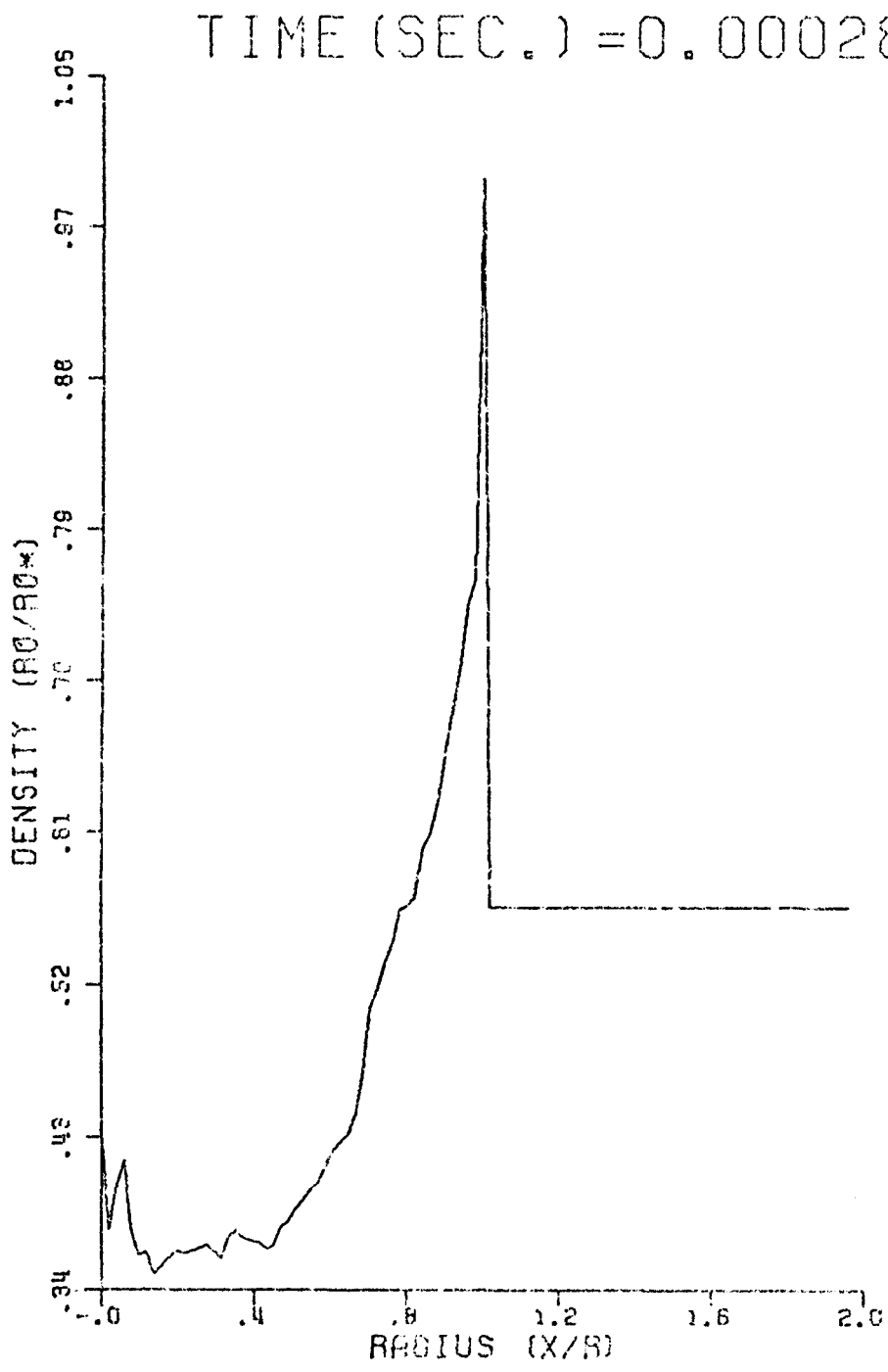

FIGURE 4.4.2: NON-DIMENSIONAL DENSITY DISTRIBUTION FOR THE ONE-DIMENSIONAL SPHERICAL PROBLEM USING SPHDET

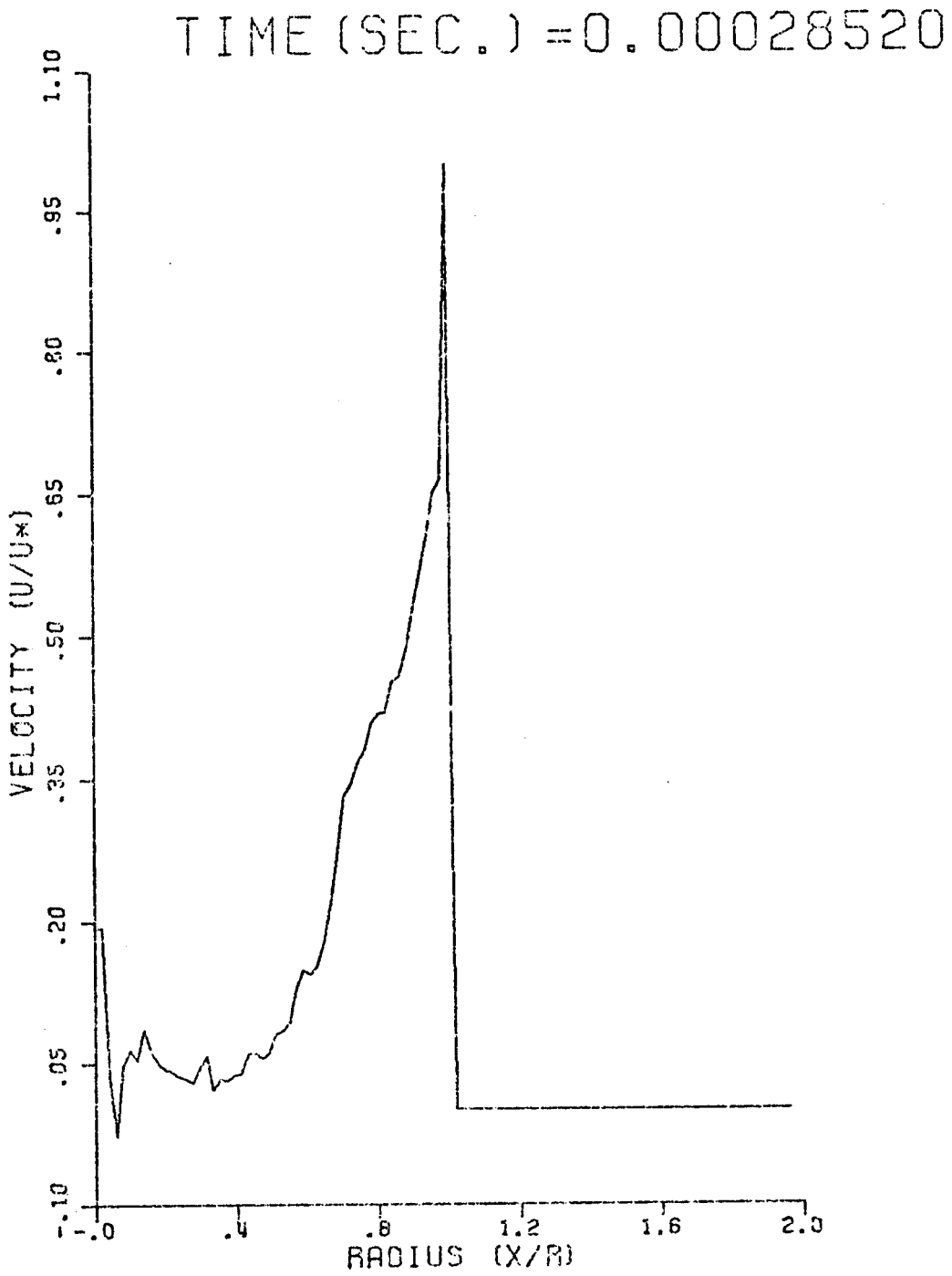

FIGURE 4.4.3: NON-DIMENSIONAL VELOCITY DISTRIBUTION FOR THE ONE-DIMENSIONAL SPHERICAL PROBLEM USING SPHDET

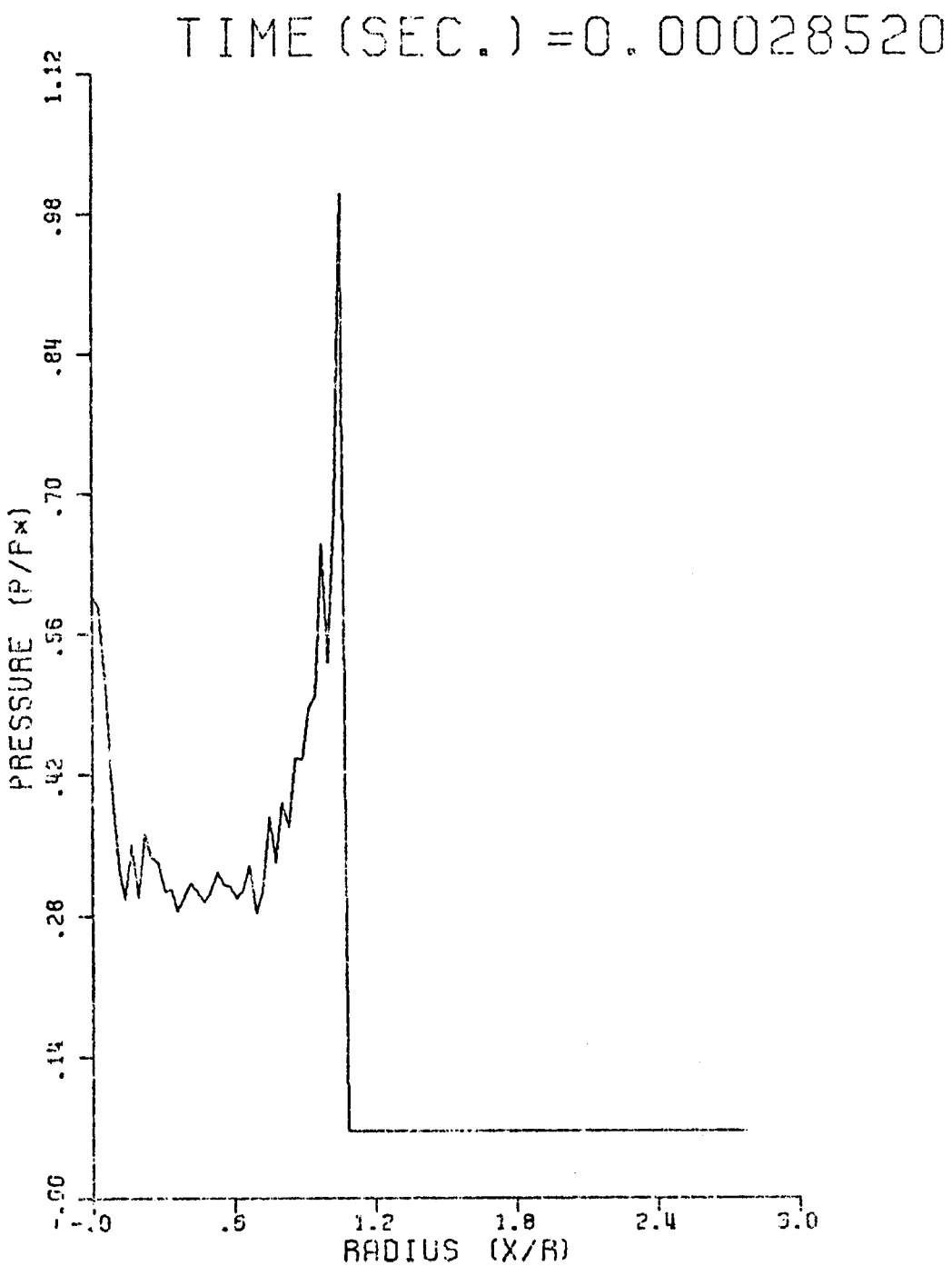

FIGURE 4.4.4: NON-DIMENSIONAL PRESSURE DISTRIBUTION FOR THE ONE-DIMENSIONAL SPHERICAL PROBLEM USING THE AXISYMMETRIC ALGORITHM

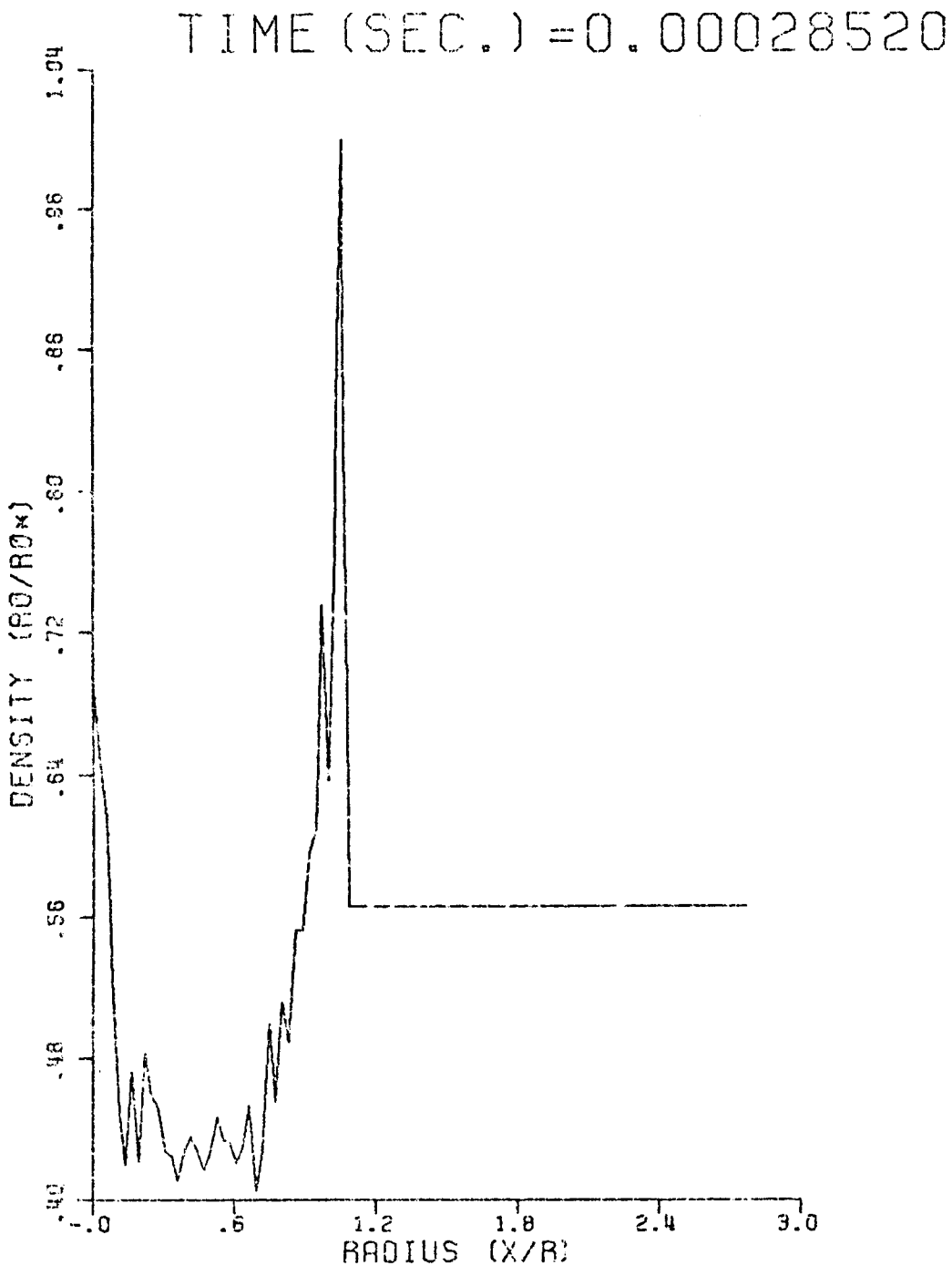

FIGURE 4.4.5: NON-DIMENSIONAL DENSITY DISTRIBUTION FOR THE ONE-DIMENSIONAL SPHERICAL PROBLEM USING THE AXISYMMETRIC ALGORITHM

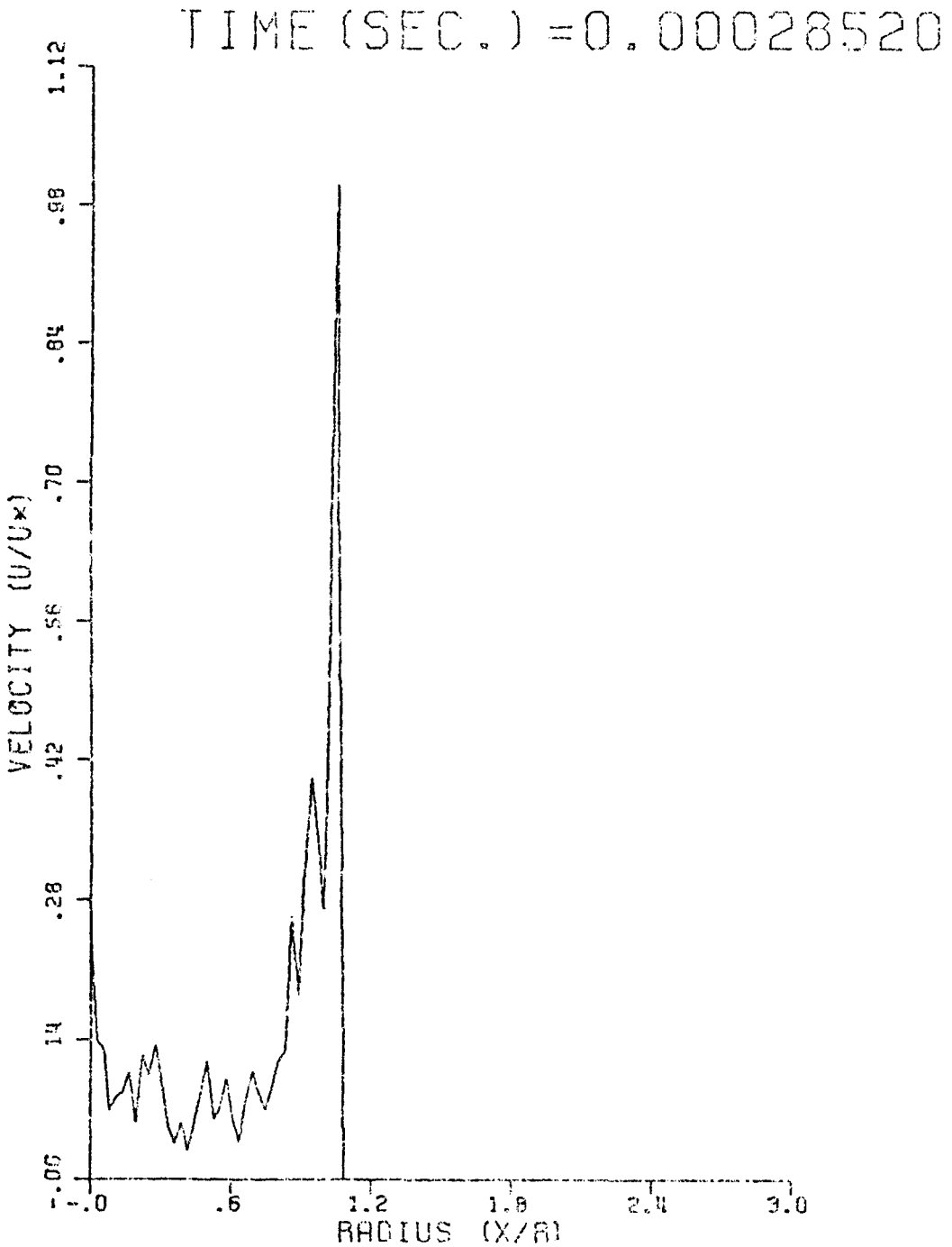

FIGURE 4.4.6: NON-DIMENSIONAL VELOCITY DISTRIBUTION FOR THE ONE-DIMENSIONAL SPHERICAL PROBLEM USING THE AXISYMMETRIC ALGORITHM

spherical code. However, more oscillations are observed in the results for the two-dimensional axisymmetric code. This behavior may be explained by the randomness of the technique; while in the one-dimensional case two half time steps are needed (i.e. two different pseudorandom numbers), for a two-dimensional geometry four quarter time steps are used (i.e. four different pseudorandom numbers). More computer runs are required to validate the two-dimensional program.

The computation time taken to solve this problem (101x101 grid points and 80 time steps) on an IBM-370 was approximately 40 CPU minutes.

4.5 Summary

The summary of the work done is presented in Table 4.5.1; different geometries have been studied (planar, spherical and axisymmetric). We validated the one-dimensional codes by comparing the results to the Taylor solutions. The axisymmetric code was validated by using it to solve the spherical geometry problem. The results for the pressure at the wall were obtained for the one-dimensional geometries and the interaction with the wall has been studied for the planar geometry.

The computer time depends on the code used. More iterations are needed in SPHDET than in CRTDET to correct for the inhomogeneous terms; hence, the CPU time per time step per grid point is larger in SPHDET (by a factor of 2). The efficiency of the TWODIM code has been improved by bypassing the calculations for those grid points ahead of the detonation front; this reduces the CPU time per time step and grid point by approximately 25%.

TABLE 4.5.1: DETONATION CONDITIONS AND RESULTS

GEOMETRY	H_2 CONCENTRATION	UNBURNT GAS[+] CONDITIONS	VALIDATION OF THE PROGRAMS	PRESSURE OF THE WALL	INTERACTION WITH THE WALL
Planar	Stoichiometric	(1)and(2)	yes*	yes	yes
Spherical	Stoichiometric	(1)and(2)	yes*	yes	no
Axisymmetric	Stoichiometric	(1)	yes**	yes	no

*By comparison with the Taylor solution.

**By comparison with the spherical solution.

+
(1) p_u=10100N/m^2,ρ_u=0.1188 kg/m^3

(2) p_u=1 atm,ρ_u=1.19kg/m^3

CHAPTER V

PRESSURE CALCULATIONS FOR THE INDIAN POINT CONTAINMENT

The two-dimensional axisymmetric program described in sections 3.4 and 4.4 was used to calculate pressure time histories inside the containment building of the Indian Point Nuclear Power Plant. The geometry of the containment is shown in Fig. 5.1. No obstacles inside the containment building were considered.

The program allows for detonation initiation at any point on the axis of the containment structure. No attempt was made to model the initial growth of the detonation. Instead it was assumed that the detonation progresses spherically to an arbitrary radius from the initiation point. This arbitrary radius was always selected less than the closest distance of the initiation point from the containment wall. The initial conditions behind the initial spherical detonation were taken as the conditions given by the Taylor [2.5] solution for the selected detonation radius [see section 2.4].

A uniform concentration of hydrogen was assumed inside the containment, so that the strength of the detonation is the same everywhere. For a uniformly dispersed detonable mixture and for a given initiation point, the pressure P at a point $\underline{x}$ inside the containment and at time t, is proportional to the initial uniform containment pressure P_o, and is a function of 1) the gas constant, $\gamma = C_p/C_v$; and 2) the ratio of the heat generated by the detonation, q (which is proportional to hydrogen concentration), to the product of the initial absolute containment

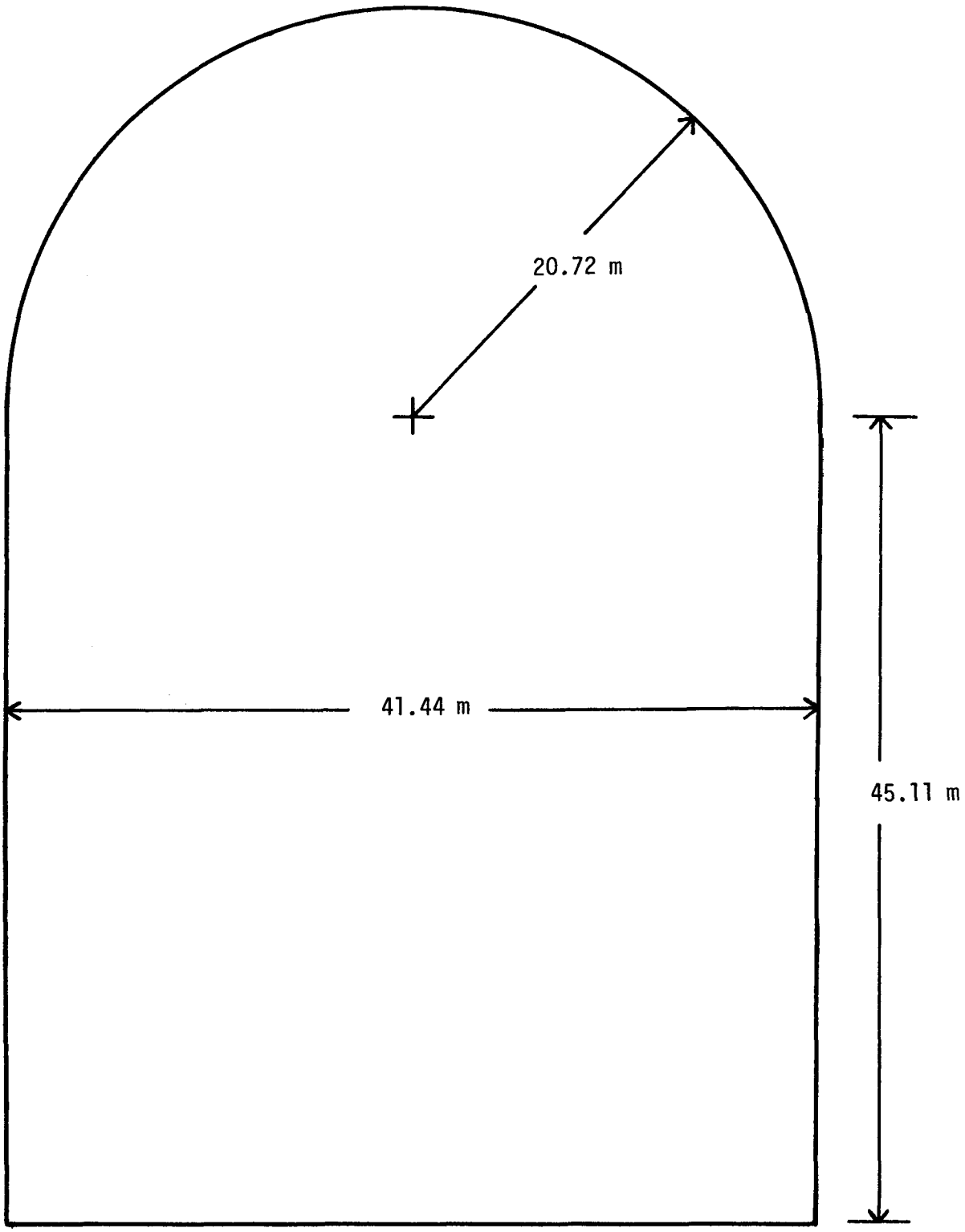

Fig. 5.1 - Geometry of the Containment of the Indian Point Nuclear Power Plant

temperature, T_o, and the universal gas constant R [2.1, 3.11]. Symbolically, and in terms of dimensionless quantities,

$$\frac{P(t,\underline{x})}{P_o} = f(\gamma , \frac{q}{RT_o}, \frac{tC_o}{L} , \frac{\underline{x}}{L}) \qquad (5.1)$$

where C_o is the speed of sound at the initial conditions and L is a characteristic linear scale of the containment. Eq. 5.1 is valid for geometrically similar containments.

In the pressure calculations performed, any variations in the gas constant, γ, were neglected and its value was taken equal to 1.4. For hydrogen concentrations less than or equal to stoichiometric, the dimensionless heat release rate q/RT_o is equal to:

$$\frac{q}{RT_o} = C_{H_2} \frac{288.5}{T_o} \qquad (5.2)$$

where C_{H_2} is the volume concentration of hydrogen, in percent, and the initial containment temperature, T_o, is in degrees Kelvin [1.1, 3.6]. The ranges of hydrogen concentration and initial temperatures that can realistically be expected in a containment following an accident, are shown in Fig. 5.2. Computer calculations were performed here for two values of the dimensionless heat release rate, equal to 17 and 23. Fig. 5.2 shows that these two values of q/RT_o cover an important portion of the range of possible hydrogen concentrations and initial temperatures.

The spatial discretization in the r-z plane had a variable grid size and consisted of 28 points in the radial (r) and 59 in the

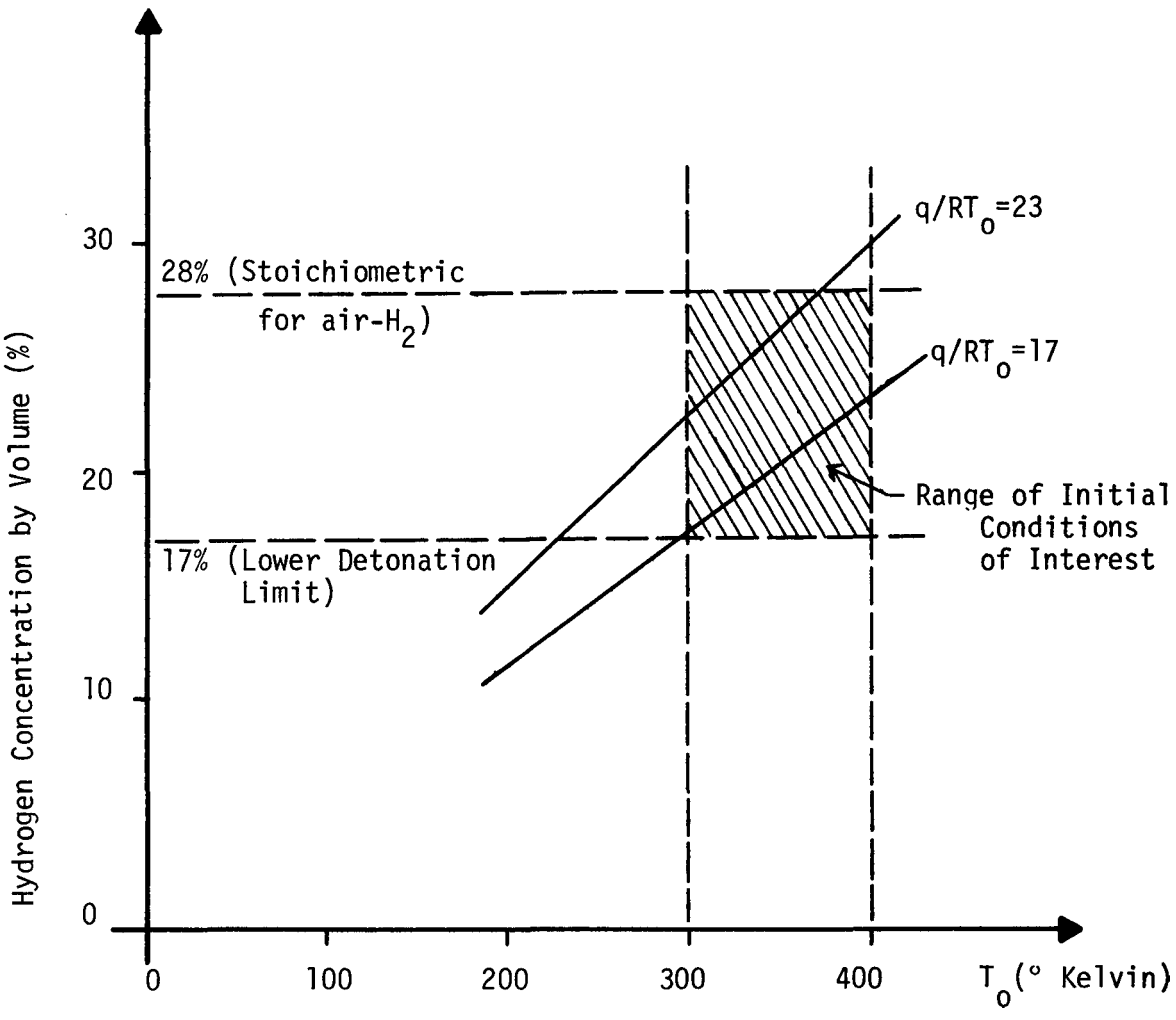

Fig. 5.2 - Range of Interest of Hydrogen Concentration and Initial Temperature in the Containment

vertical direction. Figure 5.3 presents the calculation grid for the Indian Point containment. The dome was approximated by a stepwise line, consisting of segments parallel to the r and z directions. Although a variable grip size can be used in the program for calculation efficiency, very large differences in the grip should be avoided, because they may induce fluctuations due to large differences in the characteristic Courant number $\frac{\Delta x}{\Delta t}$ (compare also with the discussion in section 4.1).

Preliminary computer runs were made to check the stability of the code and its ability to reproduce exactly the times of first arrival of the detonation front to the walls, which can be calculated easily.

Results were obtained for two initiation points, one at the center of the base mat and another at a point on the axis 34.5 m above the base, and for two values of the dimensionless heat release rate, 17 and 23. Calculated pressure time histories at several points on the wall are presented in Appendix E. All pressure values are normalized with respect to the initial containment pressure, P_o, and are given as a function of the dimensionless time tC_o/r, where r is the inside radius of the cylinder and the dome. In the present case, the non-dimensionalizing constant, r/C_o, equals 0.06 sec. Results typically show a series of decaying pressure peaks. The first peak is due to the first arrival of the detonation front. Subsequent peaks represent reflections of shocks which have been reflected before at the containment axis. Pressure peaks at nearby points occur at approximately the same

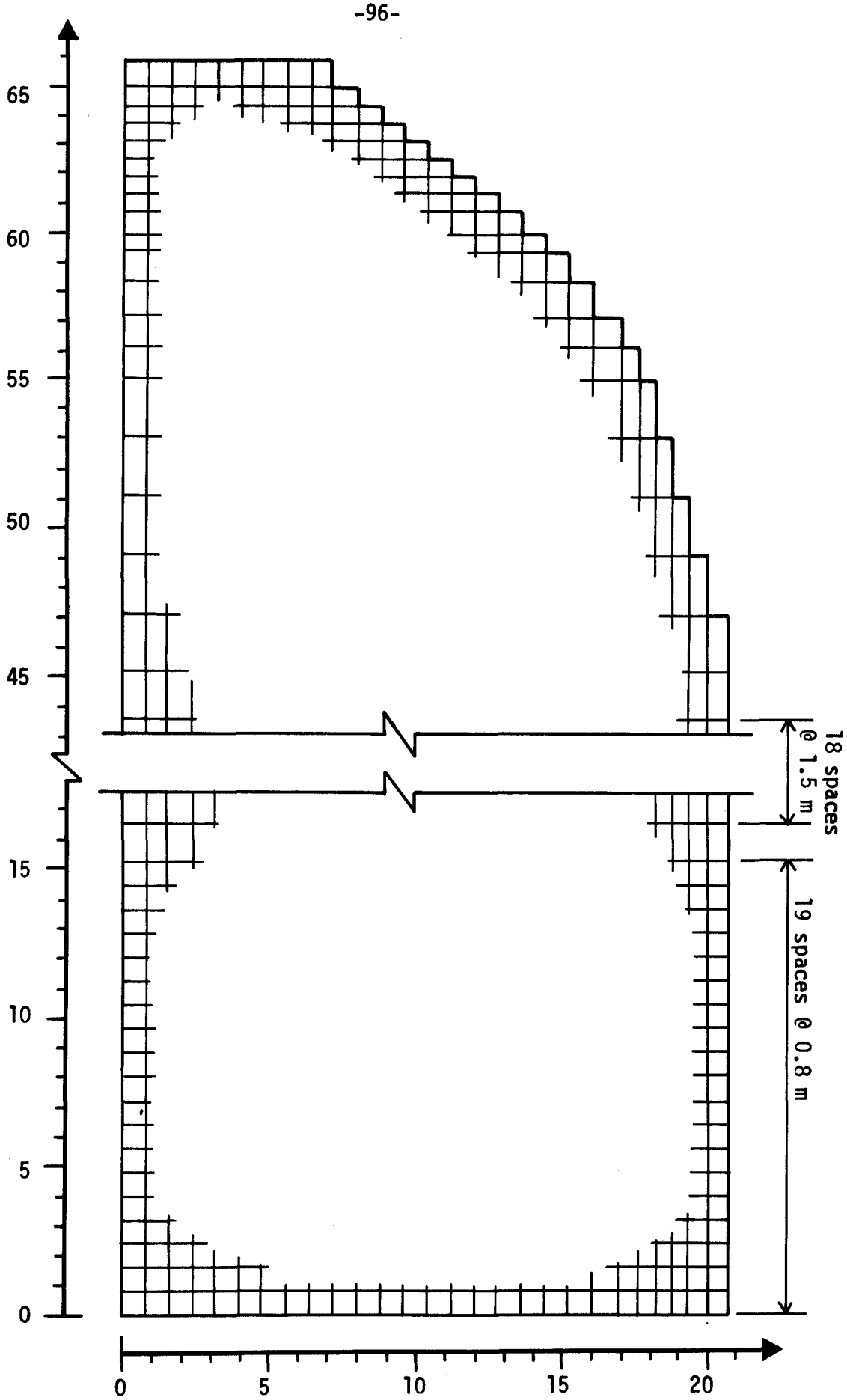

Fig. 5.3 - Calculation Grid for the Indian Point Containment

times. After a few reflections (3 or 4, at most), pressures decay to an almost constant value. Decay is faster for initiation at a point 34.5 m above the base than for initiation at the center of the base mat, because the stronger three-dimensionality of the shocks in the former case produces more scattering of the waves. For given initiation point, decay is faster for the larger of the two heat release rates, but peak pressures are slightly higher.

The pressure time histories obtained show considerable high frequency oscillations. These oscillations are believed to be numerical and can be attributed to: 1) the randomness built in the code by using the random choice technique; 2) the variable grid size; 3) the stepwise approximation of the dome geometry. (Notice that at the points of the dome there are, in general, more oscillations). Performing the computations with different time steps has shown that the high frequency oscillations do not affect the lower frequency trends in the pressure time histories, which are real and not numerical, and are important for the dynamic response of the structure.

The results reported herein agree qualitatively with those reported in Ref. [1.7]. The results in the latter reference were obtained by a Finite Difference code which introduces artificial damping and smooths sharp discontinuities. On the contrary the method used in this work preserves exactly the sharpness of the shock front, but introduces some artificial high frequency components. This fundamental difference between the two methods is the reason for the fact that significantly higher peak pressures are calculated by the present method.

CHAPTER VI

SUMMARY AND CONCLUSIONS

Computer codes for solving the hydrogen detonation problem in the containment of a nuclear reactor were developed and used. The compressible flow equations including detonation were solved using a new numerical technique due to Glimm.

The computer codes CRTDET, SPHDET and TWODIM have been developed and tested; they reproduce satisfactorily existing analytical results. CRTDET solves the one-dimensional planar problem. The one-dimensional spherical or cylindrical geometries are handled by SPHDET, which is very similar to CRTDET; it solves for the inhomogeneous terms in the equations of motion by using the operator splitting method. The computer program TWODIM is a natural extension of CRTDET and SPHDET, since it uses the same techniques used in these two codes; however, to account properly for the wave in the r and z directions, we used a splitting technique with a four-sweeps cycle; the duration for each sweep is $\frac{\Delta t}{2}$.

Pressure histories on the wall for a plane and spherical geometry have been calculated. Interactions with an elastic wall have been evaluated numerically only in a plane geometry. The results indicate that the effect of the motion of the wall on the pressure histories is negligible.

The two-dimensional axisymmetric program was validated by using it to predict pressure histories in a spherical geometry. Pressure

histories have been calculated for an actual nuclear containment building, that of the Indian Point Nuclear Power Plant. Hydrogen concentration in the containment volume was assumed uniform, any obstacles inside the containment were neglected, and a hydrogen detonation was postulated. The probability of such a detonation and the question of the initial detonation growth were considered out of the scope of the present work. The numerical results for wall pressures are presented in dimensionless form, which allows their use for different combinations of hydrogen concentrations and initial conditions. Three cases were considered in the calculations,which include two sets of dimensionless heat release rate and two initial points of the detonation: one at the center of the base mat and another 34.5 on the containment axis above the base. The results are in qualitative agreement with previous ones obtained by using the Finite Difference code CSQ. However, higher pressures (sometimes by a factor of two) are predicted in general by the present method. This can be attributed to the absence of artificial viscosity which allows a more accurate description of pressure discontinuities.

Due to multiple reflections, peak pressures at some points are very high (e.g.,fifty times the initial containment pressure), but they last for very short times, and the dynamic pressures decay to almost constant values within approximately 0.1 sec. for initiation 34.5 m above the base, or within approximately 0.2 sec for initiation at the center of the base. Decay was faster for the highest of the two non-dimensionless heat release rate values, but peak pressures were, in general, slightly higher. Due to multiple reflections, most pressure

histories exhibit three or four peaks. These peaks are not expected to cause resonance of the structure, because their interarrival times are too short in comparison to the top few natural periods of the containment.

NOMENCLATURE

Latin Alphabet

c	sound speed
c_b	sound speed in the burnt gas
c_{cj}	Chapman-Jouguet sound speed
c_u	sound speed in the unburnt gas
e	energy per unit volume
K	wall stiffness
M	mass of the wall
m	momentum flux
P	pressure exerted at the wall
p	gas pressure
p_b	pressure of the burnt gas
p_{cj}	Chapman-Jouguet pressure
p_u	pressure of the unburnt gas
Q	energy due to external sources or sinks
q	energy released by chemical reactions
t	time
U	wave velocity
u	particle velocity
u_b	particle velocity of the burnt gas
u_{cj}	particle velocity given the Chapman-Jouguet conditions
u_u	particle velocity of the unburnt gas

w_b burnt gas velocity in the Eulerian frame

w_u unburnt gas velocity in the Eulerian frame

w displacement of the wall

$\dot{w}$ velocity of the wall

$\ddot{w}$ acceleration of the wall

Greek Alphabet

ε_i internal energy per unit mass

η integer equal 2 for cylindrical coordinates, 3 for spherical

ϕ labeling integer equal 1 for unburnt gas and 0 otherwise

Γ Riemann invariant

γ gas constant equal to C_p/C_v

ψ defined by equations (A.7)

ξ random number

ξ' pseudorandom number

ρ gas density

ρ_{CJ} Chapman-Jouguet gas density

ρ_b density of the burnt gas

ρ_u density of the unburnt gas

Other symbols are defined in the text.

REFERENCES

1.1 Shapiro, Z. M. and Moffette, T. R., "Hydrogen Flammability Data and Application to PWR Loss-of-coolant Accident," WAPD-SC-545, 1957.

1.2 Zabetakis, M. G., "Safety with Cryogenic Fluids," Plenum Press, New York, N. Y., 1967.

1.3 U.S.N.R.C.,"U.S. Nuclear Regulatory Commission, Reactor Safety Study," WASH-1400, 1975.

1.4 Fardis, M. N., "Accident and Seismic Containment Reliability Including Statistical Uncertainty," Research Report R77-45, Department of Civil Engineering, M.I.T., Cambridge, MA, 1977.

1.5 Morrison, D.L, et al., "An Evaluation of the Applicability of Existing Data to the Analytical Description of a Nuclear Reactor Accident-core Melt-down Evaluation," Topical Report, Task 18, Battelle Memorial Institute, BMI-1910, 1971.

1.6 Carbiener, W. A., et al., "Physical Processes in Reactor Melt-down Accidents," Appendix VIII of the U.S.N.R.C. Reactor Safety Study, WASH-1400, 1975.

1.7 Byers, R.K., "CSQ Calculations of H_2 Detonations in Zion and Sequoyah," Presented at Workshop on the Impact of Hydrogen on Water Reactor Safety, Albuquerque, N.M., 1981

2.1 Landau L. D. and Lifshitz, E. M., Fluid Mechanics, Addison-Wesley, Reading,Massachusetts, 1959.

2.2 Williams, F. A., Combustion Theory, Addison Wesley, Reading, Massachusetts, 1965.

2.3 Courant R., and Friedrichs, K. O., "Supersonic Flow and Shock Waves," Interscience, New York, 1948.

2.4 Chorin, A. J. "Random Choice Solution of Hyperbolic Systems," Journal of Computational Physics, Vol. 22, pp. 517-533, 1976.

2.5 Taylor, G., "The Dynamics of the Combustion Products Behind the Plane and Spherical Detonation Fronts in Explosives," Proceedings of Royal Society A 200, pp. 235-247, 1950.

2.6 Barenblatt, G. I., et al., "Self-similar Explosion Waves of Variable Energy at the Front," Journal of Fluid Mechanics, Vol. 99, part 4, pp. 841-858, 1980.

3.1 Sod, G. A., "The Computer Implementation of Glimm's Method," UCID-17252, Lawrence Livermore Laboratory, University of California, 1976.

3.2 Boris, J. P. and Book, D.C., "Flux Corrected Transport.I.SHASTA, A Fluid Transport Algorithm that Works," Journal of Computational Physics, Vol. 11, pp. 38-69, 1973.

REFERENCES (CONTINUED)

3.3 Glimm, J., "Solutions in the Large for Nonlinear Hyperbolic Systems of Equations," Comm. Pure Applied Math., Vol. 18, p. 697, 1965.

3.4 Chorin, A. J., "Random Choice Methods with Application to Reacting Gas Flow," Journal of Computational Physics, Vol. 25, pp. 253-272, 1977.

3.5 Godunov, S.K., "Finite Difference Methods for Numerical Computation of Discontinuous Solution of the Equations of Fluid Dynamics," Mat. Sbornik, Vol. 47, p. 271, 1959.

3.6 Herzberg, M. "Flammability Limits for Hydrogen Detonations," Presented at Sandia Labs. Workshop in the Impact of Hydrogen on Water Reactor Safety, Albuquerque, N.M., 1981.

3.7 Sod, G. A., "A Numerical Study of a Converging Cylindrical Shock," Journal of Fluid Mechanics, Vol. 83, part 4, pp. 785-794, 1977.

3.8 Sod, G. A., "A Survey of Several Finite Difference Methods for Systems of Nonlinear Hyperbolic Conservation Laws," Journal of Computational Physics, Vol. 27, 1978.

3.9 Sod, G. A., "Automotive Engine Modeling with a Hybrid Random Choice Method, II," SAE Technical Paper Series, No. 800288, 1980.

3.10 Perry, R. W. and Kantrowitz, A., "The Production and Stability of Converging Shock Waves," Journal of Applied Physics, Vol. 22, p. 878, 1951.

3.11 Oswatitsh, K. Gas Dynamics, Academic Press, New York, p. 168, 1956.

APPENDIX A

THE GODUNOV METHOD

This method of calculation of the conditions behind the detonation front was first implemented by Godunov [3.5] and then modified by Chorin [2.4] and Sod [3.1]. The method is used by the computer codes developed herein, and is described in this Appendix for completeness.

Given the equation (3.1.4), we would like to find the properties ρ_*, u_*, p_* in state S_*. Let us define

$$M_r = (p_r - p_*)/(u_r - u_*), \qquad (A.1)$$

and

$$M_\ell = -(p_\ell - p_*)/(u_\ell - u_*). \qquad (A.2)$$

It can be easily shown that if the right wave is a shock,

$$M_r = -\rho_r(u_r - U_r) = -\rho_*(u_* - U_r), \qquad (A.3)$$

where ρ_* is the density in the region adjacent to the right shock and U_r is the velocity of the right shock.

Similarly, if the left wave is a shock,

$$M_\ell = \rho_\ell(u_\ell - U_\ell) = -\rho_*(u_* - U_\ell), \qquad (A.4)$$

where ρ_* is the density in the portion of S_* adjacent to the left shock and U_ℓ is the velocity of the left shock. M_r and M_ℓ can be can be written in the form

$$M_r = (p_r\rho_r)^{1/2}\ \psi(p_*/p_r), \tag{A.5}$$

$$M_\ell = (p_\ell\rho_\ell)^{1/2}\ \psi(p_*/p_\ell), \tag{A.6}$$

where

$$\psi(w) = \left(\frac{\gamma+1}{2}\,w + \frac{\gamma-1}{2}\right)^{1/2}, \qquad \text{for } w \geq 1, \tag{A.7}$$

$$= \frac{\gamma-1}{2\gamma^{1/2}}\ \frac{1-w}{1-w^{(\gamma-1)/2\gamma}}, \quad \text{for } w \leq 1.$$

Upon elimination of u_* from (A.1) and (A.2), we obtain

$$p_* = \frac{u_\ell - u_r + p_\ell/M_\ell + p_r/M_r}{1/M_\ell + 1/M_r}. \tag{A.8}$$

Equations (A.5), (A.6) and (A.8) are three equations in three unknowns for which there exists a real solution. The solution can be found iteratively by choosing a starting value p_*°(or M_r° or M_ℓ°), and then compute p_*^{q+1}, M_r^{q+1}, M_ℓ^{q+1}, $q \geq 0$ using

$$p^q = (u_\ell - u_r + p_r/M_r^q + p_\ell/M_\ell^q)/(1/M_r^q + 1/M_\ell^q), \tag{A.9b}$$

$$p_*^{q+1} = \max(\varepsilon_1,\ p^q), \tag{A.9b}$$

$$M_r^{q+1} = (p_r\rho_r)^{1/2}\ \psi(p_*^{q+1}/p_r), \tag{A.9c}$$

$$M_\ell^{q+1} = (p_\ell\rho_\ell)^{1/2}\ \psi(p_*^{q+1}/p_\ell). \tag{A.9d}$$

Equation (A.9b), where ε_1 is a very small number ($\sim 10^{-6}$), is used to prevent the pressure of becoming negative.

Once p_*, M_r and M_ℓ are found, we may obtain u_* by eliminating p_* from (A.1) and (A.2),

$$u_* = (p_\ell - p_r + M_r u_r + M_\ell u_\ell)/(M_r + M_\ell). \quad (A.10)$$

APPENDIX B

THE COMPUTER PROGRAM CRTDET

B.1 General Description

The program consists of the main program, the subroutine GLIMM and the output section. The overall idea behind the main program can be found in the flow chart of Figure B.1. The major steps to follow in order to run this program are

1. Select the grid spacing for each specific problem and adjust accordingly the values of N and DX;

2. Decide about the number of time steps necessary (NSTOP) and the time intervals for which a printed output of the properties is required (NPRINT);

3. Assign the parameters defining the initial conditons of the gas and the properties of the combustion. GAMMA and DELTA are respectively, the gas constant and the energy released by the combustion. PR, RR and UR are the initial conditions of the unburnt gas and PL, RL and UL are the C-J conditions of the burnt gas. On the other hand, the grid points behind the detonation front should be given their appropriate values obtained from the Taylor curves (Figures 2.4.1-2.4.3).

The subroutine GLIMM solves the Riemann problem for each grid point. The major part of this subroutine has been described by Sod (1978). However, the last section of the subroutine has been added to solve the detonation problem.

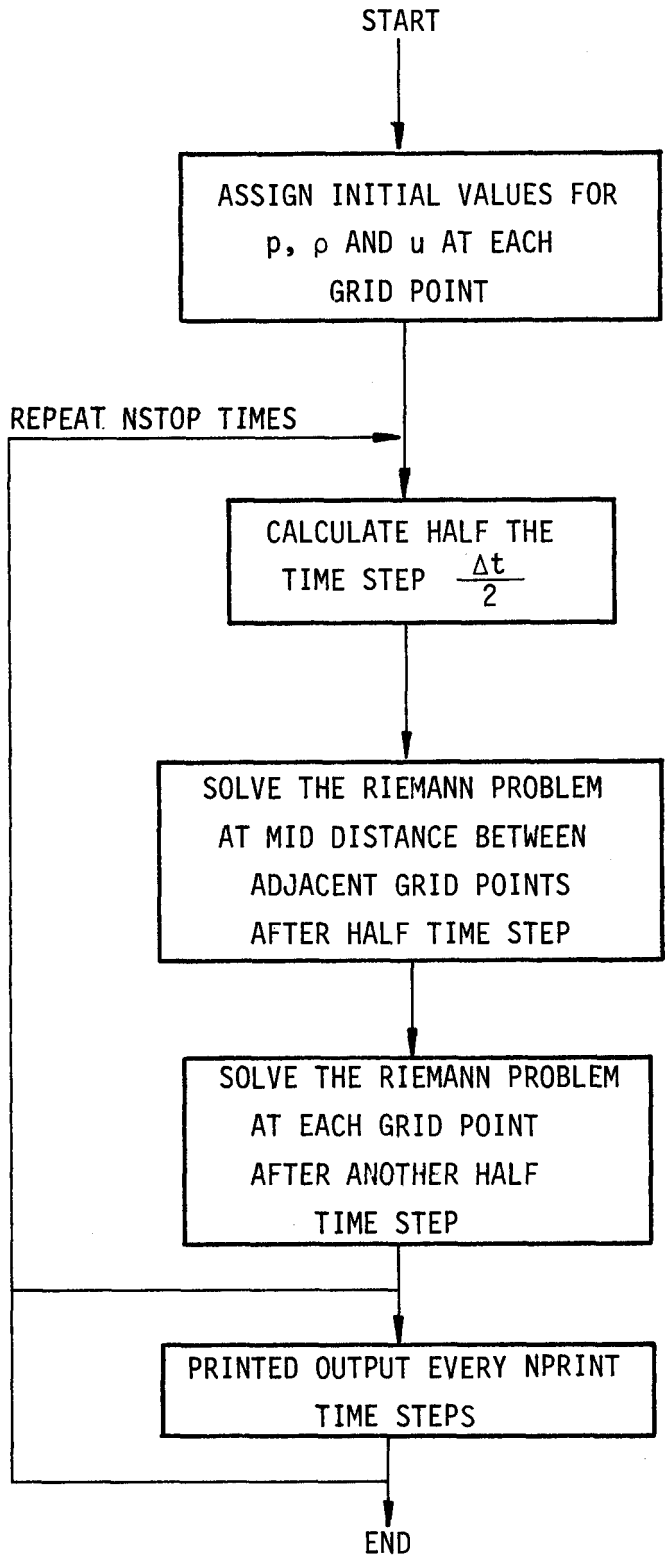

FIGURE B.1: FLOW CHART FOR CRTDET

B.2 Dictionary of the Key Terms in the Program

B	Defined in equation (2.4.7a)
C	Defined in equation (2.4.7b)
CL	Sound speed in the left state of the solution of the Riemann problem
CR	Sound speed in the right state of the solution of the Riemann problem
CSTAR	Sound speed in state S_* or C-J sound speed
DELTA	Chemical energy released by the combustion process
GAMMA	Gas constant = C_p/C_v
GGUBFS	Random number generator; IMSL function subroutine
ML	Defined in equation (A.2)
MR	Defined in equation (A.1)
MUSQ	Defined in equation (2.4.4)
N	Number of intervals generated by the grid points
NPRINT	Controls the output section; the properties at each grid point will be printed every NPRINT time steps
NSTOP	Number of time steps
PHI(I)	Variable indicating whether the gas is burnt or not at grid point I
PRE(I)	Pressure of the gas in N/m^2 at grid point I
PSI	Function subroutine defined by equation (A.7)
PSTAR	Pressure in state S_* or C-J pressure
RHO(I)	Density of the gas in kg/m^3 at grid point I
RSTAR	Density in state S_* or C-J density
SI	Pseudorandom number in the interval [0,1]
SIGMA	Coefficient in]0,1] to control the length of each time step

TIME	Total time in seconds elapsed since the origin of the detonation
UCJ	Detonation front velocity given C-J conditions
USTAR	Particle velocity in state S_* or particle C-J velocity
UX(I)	Particle velocity in m/s at grid point I
XI	Pseudorandom number in the interval $[-\frac{\Delta x}{2}, \frac{\Delta x}{2}]$

```
CCCCCCCCCCCCCCCCCCCCCCCCCCCCCCCCCCCCCCCCCCCCCCCCCCCCCCCCCCCCCCCCCCCCCC
C                                                                     C
C                        CRTDET                                       C
C                                                                     C
C      ONE DIMENSIONAL PROGRAM(CARTESIAN) TO CALCULATE                C
C      PRESSURE,DENSITY AND VELOCITY HISTORY IN A REACTIVE            C
C      MIXTURE                                                        C
C                                                                     C
CCCCCCCCCCCCCCCCCCCCCCCCCCCCCCCCCCCCCCCCCCCCCCCCCCCCCCCCCCCCCCCCCCCCCC
C
C
      COMMON//DT,GAMMA,RL,UL,PL,R,U,P,E,RR,UR,PR,XI,KPHI,DELTA
     1,KIM
      COMMON/OUT/TIME,N,DX,RHO(2001),PRE(2001),UX(2001)
     1,PHI(2001)
      COMMON/RAD/ETA
      COMMON/LIN/LAM
      REAL LAM
      DOUBLE PRECISION BLIP
      INTEGER TSTP,PHI
      NPRINT=25
      NSTOP=1000
      N=200
      NP1=N+1
      NM1=N-1
      DX=20.0/FLOAT(N)
      DT=0.01
      TIME=0.1/1787.7
      VMAX=0.
      NP=0
      GAMMA=1.4
      DELTA=1447716.8
      BLIP=0.0D0
      K1=11
      K2=7
      NU=2
      SIGMA=0.8
      ETA=1.
C
C     SET INITIAL CONDITIONS
C
      RL=2.10939
      PL=1539126.7
      UL=777.0
      RR=1.19242
      PR=101325.
      UR=0.
      DO 15 I=1,2
      PHI(I)=0
      RHO(I)=RL
```

```
      PRE(I)=PL
      UX(I)=UL
15    CONTINUE
      RHO(1)=0.91546
      PRE(1)=478350.0
      UX(1)=0.0
14    DO 16 I=3,NP1
      PHI(I)=1
      RHO(I)=RR
      PRE(I)=PR
      UX(I)=UR
16    CONTINUE
C
C     BEGIN TIME STEP
C
      DO 100 TSTP=1,NSTOP
      NP=NP+1
      DO 8 I=2,N
      VMAX1=ABS(UX(I))+SQRT(GAMMA*PRE(I)/RHO(I))
      IF(VMAX1.GT.VMAX) VMAX=VMAX1
8     CONTINUE
      DTT=SIGMA*DX/(2.*VMAX)
      IF(DTT.LT.DT) DT=DTT
      TIME=TIME+2.*DT
      LAM=0.5/VMAX
C
C     COMPUTE FIRST HALF STEP
C
C
C     GENERATE RANDOM SI USING CHORIN'S METHOD
C
      NU=MOD(NU+K2,K1)
      BLIP=BLIP+2.D0
      SI=(GGUBFS(BLIP)+FLOAT(NU))/FLOAT(K1)
C
C     XI LIES BETWEEN -DX/2 AND +DX/2
C
      DO 40 I=2,NP1
      XI=SI*DX-0.5*DX
      RR=RHO(I)
      UR=UX(I)
      PR=PRE(I)
      KPHI=PHI(I)
      IF(I.EQ.2)GO TO 43
      RL=RIM1
      PL=PIM1
      UL=UIM1
      GO TO 44
C
C     BOUNDARY CONDITION AT AXIS R=0
```

```
C
43    RL=RHO(1)
      UL=UX(1)
      PL=PRE(1)
      KIM=PHI(1)
      GO TO 44
C
C     COMPUTE FIRST HALF STEP OF GLIMM
C
44    CALL GLIMM
      RIM1=RHO(I)
      RHO(I)=R
      PIM1=PRE(I)
      PRE(I)=P
      UIM1=UX(I)
      UX(I)=U
      KIM=PHI(I)
      PHI(I)=KPHI
40    CONTINUE
C
C     COMPUTE SECOND HALF STEP
C
C
C     GENERATE RANDOM SI USING CHORIN'S METHOD
C
      NU=MOD(NU+K2,K1)
      SI=(GGUBFS(BLIP)+FLOAT(NU))/FLOAT(K1)
C
C     XI LIES BETWEEN -DX/2 AND +DX/2
C
      KIM=PHI(1)
      DO 60 I=1,NP1
      XI=SI*DX-0.5*DX
      RL=RHO(I)
      PL=PRE(I)
      UL=UX(I)
      IF(I.EQ.NP1) GO TO 63
      KPHI=PHI(I+1)
      RR=RHO(I+1)
      PR=PRE(I+1)
      UR=UX(I+1)
      IF(I.EQ.1) GO TO 62
      GO TO 64
C     BOUNDARY CONDITION AT R=1.
63    RR=RL
      UR=-UL
      PR=PL
      KPHI=PHI(I)
      XI=0.0
      GO TO 64
```

```
C
C       COMPUTE SECOND HALF STEP OF GLIMM
C
62      XI=0.0
        RL=RR
        UL=-UR
        PL=PR
64      CALL GLIMM
        RHO(I)=R
        PRE(I)=P
        UX(I)=U
        KIM=PHI(I+1)
        PHI(I)=KPHI
60      CONTINUE
        WRITE(15,20000) TIME
20000   FORMAT(1H1,7H TIME = ,F11.7)
        WRITE(15,20001) RHO(1),PRE(1)
        WRITE(15,20001) RHO(NP1),PRE(NP1)
20001   FORMAT(1H0,2F13.5)
        IF(NP.LT.NPRINT) GO TO 100
        NP=0
100     CONTINUE
        STOP
        END
C
C       SUBROUTINE GLIMM:TO SOLVE RIEMANN PROBLEM
C
        SUBROUTINE GLIMM
        COMMON//DT,GAMMA,RL,UL,PL,R,U,P,E,RR,UR,PR,XI,KPHI,DELTA
       1,KIM
        COMMON/RAD/ETA
        COMMON/LIN/LAM
        REAL MR,ML,MRP1,MLP1
        REAL LAM,MUSQ
        EPS=1.E-6
        IT=0
        ITSTOP=20
        KPHIP=KPHI*KIM
C
C       IF KPHI=1 , MIGHT HAVE A DETONATION
C
        IF(KPHI.EQ.1.AND.KPHIP.EQ.0) GO TO 111
C
C       CONSTRUCTION OF RIEMANN PROBLEM
C       ALFA IS THE CONVERGENCE FACTOR
C
        ALFA=1.
        ALFAM=1.-ALFA
C
C       INITIAL ML AND MR
```

```
C
      ML=100.
      MR=100.
      COEFL=SQRT(PL*RL)
      COEFR=SQRT(PR*RR)
C
C     COMPUTE INITIAL PSTAR USING LINEARIZED GODUNOV
C
      RAV=0.5*(RL+RR)
      PAV=0.5*(PL+PR)
      A=PAV/(RAV**GAMMA)
      R=RAV-LAM*(UR*RR-UL*RL)
      PSTAR=A*(R**GAMMA)
C
C     SOLVE RIEMANN PROBLEM USING GODUNOV'S ITERARIVE METHOD
C
10    IT=IT+1
C
C     IF PSTAR IS LESS THAN EPS THEN PSTAR IS SET EQUAL
C     TO 1.0E-6 TO PREVENT PSTAR FROM BECOMING NEGATIVE
C
      PSTAR=AMAX1(EPS,PSTAR)
C
C     COMPUTE MR AND ML AT STEP Q+1
C
20    MLP1=COEFL*PSI(PSTAR/PL,GAMMA)
      MRP1=COEFR*PSI(PSTAR/PR,GAMMA)
      DIFML=ABS(MLP1-ML)
      DIFMR=ABS(MRP1-MR)
      ML=MLP1
      MR=MRP1
C
C     COMPUTE NEW PRESSURE PSTAR
C
      PSTARP=PSTAR
      PSTAR=(UL-UR+PR/MR+PL/ML)/(1./ML+1./MR)
      PSTAR=ALFA*PSTAR+ALFAM*PSTARP
      IF(IT.LE.ITSTOP) GO TO 30
      IF(ABS(PSTAR-PSTARP).LT.EPS) GO TO 40
      IF(DIFML*DIFMR.LT.EPS) GO TO 40
      ALFA=ALFA/2.
      ALFAM=1.-ALFA
      IF(ALFAM.LT.EPS) GO TO 40
      IT=0
30    IF(DIFML.GT.EPS) GO TO 10
      IF(DIFMR.GT.EPS) GO TO 10
C
C     COMPUTE USTAR AT END OF GODUNOV ITERATION
C
40    USTAR=(PL-PR+MR*UR+ML*UL)/(ML+MR)
```

```
C
C       BEGIN GLIMM'S METHOD
C
        IREGL=1
        IF(PSTAR.LT.PL) IREGL=2
        IREGR=1
        IF(PSTAR.LT.PR) IREGR=2
        X=USTAR*DT
        IF(XI.GE.X) GO TO 200
C
C       LEFT SIDE
C
        IF(IREGL.EQ.2) GO TO 110
C
C       COMPUTE LEFT SHOCK SPEED
C
        U=UL-ML/RL
        X=U*DT
        IF(XI.GE.X) GO TO 100
C
C       LEFT OF LEFT SHOCK
C
        R=RL
        U=UL
        P=PL
        GO TO 500
C
C       RIGHT OF LEFT SHOCK
C
100     R=ML/(USTAR-U)
        U=USTAR
        P=PSTAR
        GO TO 500
C
C       COMPUTE SOUND SPEED IN LEFT STATE
C
110     CL=SQRT(GAMMA*PL/RL)
        X=(UL-CL)*DT
        IF(XI.GE.X) GO TO 120
C
C       LEFT OF LEFT FAN
C
        R=RL
        U=UL
        P=PL
        GO TO 500
C
C       COMPUTE CONSTANT OF ISENTROPIC LAW-A
C
120     A=PL/(RL**GAMMA)
```

```
C
C       COMPUTE DENSITY IN STATE STAR
C
        RSTAR=(PSTAR/A)**(1./GAMMA)
C
C       COMPUTE SOUND SPEED IN STATE STAR
C
        CSTAR=SQRT(GAMMA*PSTAR/RSTAR)
        X=(USTAR-CSTAR)*DT
        IF(XI.GE.X) GO TO 130
C
C       IN LEFT FAN
C
        U=(2./(GAMMA+1.))*(XI/DT+CL+0.5*(GAMMA-1.)*UL)
        RINT=CL+0.5*(GAMMA-1.)*(UL-U)
        R=(RINT*RINT/(A*GAMMA))**(1./(GAMMA-1.))
        P=A*(R**GAMMA)
        GO TO 500
C
C       RIGHT OF LEFT FAN
C
130     R=RSTAR
        U=USTAR
        P=PSTAR
        GO TO 500
C
C       RIGHT SIDE
C
200     IF(IREGR.EQ.2) GO TO 220
C
C       COMPUTE RIGHT SHOCK SPEED
C
        U=UR+MR/RR
        X=U*DT
        IF(XI.GE.X) GO TO 210
C
C       LEFT OF RIGHT SHOCK
C
        R=-MR/(USTAR-U)
        U=USTAR
        P=PSTAR
        GO TO 500
C
C       RIGHT OF RIGHT SHOCK
C
210     R=RR
        U=UR
        P=PR
        GO TO 500
C
```

```
C       COMPUTE CONSTANT OF ISENTROPIC LAW-A
C
220     A=PR/(RR**GAMMA)
C
C       COMPUTE DENSITY IN STATE STAR
C
        RSTAR=(PSTAR/A)**(1./GAMMA)
C
C       COMPUTE SOUND SPEED IN STATE STAR
C
        CSTAR=SQRT(GAMMA*PSTAR/RSTAR)
        X=(USTAR+CSTAR)*DT
        IF(XI.GE.X) GO TO 230
C
C       LEFT OF RIGHT FAN
C
        R=RSTAR
        U=USTAR
        P=PSTAR
        GO TO 500
C
C       COMPUTE SOUND SPEED IN RIGHT STATE
C
230     CR=SQRT(GAMMA*PR/RR)
        X=(UR+CR)*DT
        IF(XI.GE.X) GO TO 240
C
C       IN RIGHT FAN
C
        U=(2./(GAMMA+1.))*(XI/DT-CR+0.5*(GAMMA-1.)*UR)
        RINT=CR+0.5*(GAMMA-1.)*(U-UR)
        R=(RINT*RINT/(A*GAMMA))**(1./(GAMMA-1.))
        P=A*(R**GAMMA)
        GO TO 500
C
C       RIGHT OF RIGHT FAN
C
240     R=RR
        U=UR
        P=PR
        GO TO 500
C
C       DETONATION CONDITIONS
C
C
C       CALCULATE CONDITIONS JUST BEHIND CJ DETONATION
C
111     B=-PR-DELTA*(GAMMA-1.)*RR
        MUSQ=(GAMMA-1.)/(GAMMA+1.)
        C=(PR*PR)+2.*MUSQ*PR*RR*DELTA
```

```
      PSTAR=-B+SQRT((B*B)-C)
      RSTAR=(PSTAR*(GAMMA+1.)-PR)*RR/(GAMMA*PSTAR)
      UCJ=SQRT(GAMMA*PSTAR*RSTAR)/RR+UR
      CSTAR=SQRT(GAMMA*PSTAR/RSTAR)
      USTAR=UCJ-CSTAR
      USTAR=777.0
      PSTAR=1539126.7
      RSTAR=2.10939
      CSTAR=SQRT(GAMMA*PSTAR/RSTAR)
      UCJ=USTAR+CSTAR
C
C     BEGIN GLIMM'S METHOD
C
      X=UCJ*DT
      IF(XI.GE.X) GO TO 222
      IF(ETA.LT.3.5) GO TO 333
C
C     COMPUTE SOUND SPEED IN LEFT STATE
C
      CL=SQRT(GAMMA*PL/RL)
      X=(UL-CL)*DT
      IF(XI.GE.X) GO TO 444
C
C     LEFT OF RAREFACTION FAN
C
      R=RL
      U=UL
      P=PL
      KPHI=0
      GO TO 500
C
C     COMPUTE CONSTANT OF ISENTROPIC LAW-A
C
444   A=PSTAR/(RSTAR**GAMMA)
C
C     IN RIGHT FAN
C
      U=(2./(GAMMA+1.))*(XI/DT-CSTAR+0.5*(GAMMA-1.)*USTAR)
      RINT=CSTAR+0.5*(GAMMA-1.)*(U-USTAR)
      R=(RINT*RINT/(A*GAMMA))**(1./(GAMMA-1.))
      P=A*(R**GAMMA)
      KPHI=0
      GO TO 500
C
C     RIGHT OF DETONATION
C
333   U=USTAR
      P=PSTAR
      R=RSTAR
      KPHI=0
```

```
      GO TO 500
222   U=UR
      P=PR
      R=RR
500   CONTINUE
      RETURN
      END
C
C     FUNCTION PSI
C
      FUNCTION PSI(X,GAMMA)
      EPS=1.0E-6
      IF(ABS(1.-X).GT.EPS) GO TO 100
      PSI=SQRT(GAMMA)
      RETURN
100   COEF1=0.5*(GAMMA+1.)
      COEF2=0.5*(GAMMA-1.)
      COEF3=COEF2/GAMMA
      IF(X.GE.1.) GO TO 200
      PSI=COEF2*(1.-X)/(SQRT(GAMMA)*(1.-(X**COEF3)))
      RETURN
200   PSI=SQRT(COEF1*X+COEF2)
      RETURN
      END
C
C     SUBROUTINE OUTPUT:OUTPUT SECTION OF THE PROGRAM
C
      SUBROUTINE OUTPUT
      COMMON//DT,GAMMA,RL,UL,PL,R,U,P,E,RR,UR,PR,XI,KPHI,DELTA
     1,KIM
      COMMON/OUT/TIME,N,DX,RHO(2001),PRE(2001),UX(2001)
     1,PHI(2001)
      INTEGER PHI
      NP1=N+1
      WRITE(6,10000) TIME
      WRITE(6,10001)
      DO 20 I=1,NP1
      X=FLOAT(I-1)*DX
      R=RHO(I)
      U=UX(I)
      P=PRE(I)
      K=PHI(I)
      WRITE(6,10002) X,R,U,P,K
20    CONTINUE
      RETURN
10000 FORMAT(1H1,7H TIME = ,F11.7)
10001 FORMAT(1H ,3H  X,6X,5HDENSE,8X,3HVEL,10X,4HPRES,10X,3HPHI)
10002 FORMAT(1H0,F6.3,3F13.5,I2)
      END
```

APPENDIX C

THE COMPUTER PROGRAM SPHDET

The computer program SPHDET is very similar to CRTDET; however, the subroutine INHOM has been added to make the correction for the inhomogeneous terms in the equations of gas dynamics in one dimensional spherical or cylindrical coordinate system. This subroutine is called after the solution of the Riemann problem has been advanced one time step in the time space. It uses the method described in section 3.3.

Actually the one-dimensional cartesian, cylindrical and spherical problems can be solved by SPHDET by taking ETA equal to 1, 2, and 3 respectively.

```
CCCCCCCCCCCCCCCCCCCCCCCCCCCCCCCCCCCCCCCCCCCCCCCCCCCCCCCCCCCCCCCCCCCCCC
C                                                                     C
C                          SPHDET                                     C
C                                                                     C
C      ONE DIMENSIONAL PROGRAM(CYL. OR SPHE.) TO CALCULATE            C
C      PRESSURE,DENSITY AND VELOCITY HISTORY IN A REACTIVE            C
C      MIXTURE                                                        C
C                                                                     C
CCCCCCCCCCCCCCCCCCCCCCCCCCCCCCCCCCCCCCCCCCCCCCCCCCCCCCCCCCCCCCCCCCCCCC
       COMMON//DT,GAMMA,RL,UL,PL,R,U,P,E,RR,UR,PR,KPHI,DELTA,KIM
       COMMON/OUT/TIME,N,DX,RHO(111),PRE(111),UX(111),PHI(111)
       COMMON/RAD/ETA
       COMMON/LIN/LAM
       REAL LAM
       DOUBLE PRECISION BLIP
       INTEGER TSTP,PHI
       NPRINT=20
       NSTOP=100
       N=100
       NP1=N+1
       NM1=N-1
       DX=1.0/FLOAT(N)
       DT=0.01
       TIME=0.19/1787.85
       VMAX=0.
       NP=0
       GAMMA=1.4
       DELTA=1447711.2
       BLIP=10.0D0
       K1=11
       K2=7
       NU=2
       SIGMA=0.8
       ETA=3.
C
C      SET INITIAL CONDITIONS
C
       RL=0.2102
       PL=153419.
       UL=777.
       RR=0.11886
       PR=10100.
       UR=0.
       DO 15 I=1,20
       PHI(I)=0
       RHO(I)=RL
       PRE(I)=PL
       UX(I)=UL
15     CONTINUE
       RHO(1)=0.0841
```

```
PRE(1)=42550.91
UX(1)=0.0
RHO(2)=0.0841
PRE(2)=42550.91
UX(2)=0.0
RHO(3)=0.0841
PRE(3)=42550.91
UX(3)=0.
RHO(4)=0.0841
PRE(4)=42550.91
UX(4)=0.
RHO(5)=0.0841
PRE(5)=42550.91
UX(5)=0.
RHO(6)=0.0841
PRE(6)=42550.91
UX(6)=0.0
RHO(7)=0.0841
PRE(7)=42550.91
UX(7)=0.0
RHO(8)=0.0841
PRE(8)=42550.91
UX(8)=0.0
RHO(9)=0.0841
PRE(9)=42550.91
UX(9)=0.0
RHO(10)=0.0841
PRE(10)=42550.91
UX(10)=0.0
RHO(11)=0.08565
PRE(11)=43264.16
UX(11)=23.29
RHO(12)=0.08933
PRE(12)=45642.15
UX(12)=62.06
RHO(13)=0.09354
PRE(13)=49477.62
UX(13)=100.98
RHO(14)=0.09984
PRE(14)=54463.75
UX(14)=139.82
RHO(15)=0.10720
PRE(15)=60216.95
UX(15)=191.87
RHO(16)=0.11661
PRE(16)=67504.36
UX(16)=252.45
RHO(17)=0.12822
PRE(17)=77476.59
UX(17)=322.36
```

```
      RHO(18)=0.14188
      PRE(18)=88983.02
      UX(18)=419.46
      RHO(19)=0.16395
      PRE(19)=105859.11
      UX(19)=532.10
14    DO 16 I=21,NP1
      PHI(I)=1
      RHO(I)=RR
      PRE(I)=PR
      UX(I)=UR
16    CONTINUE
C
C     BEGIN TIME STEP
C
      DO 100 TSTP=1,NSTOP
      NP=NP+1
      DO 8 I=2,N
      VMAX1=ABS(UX(I))+SQRT(GAMMA*PRE(I)/RHO(I))
      IF(VMAX1.GT.VMAX) VMAX=VMAX1
8     CONTINUE
      DTT=SIGMA*DX/(2.*VMAX)
      IF(DTT.LT.DT) DT=DTT
      TIME=TIME+2.*DT
      LAM=0.5/VMAX
C
C     COMPUTE FIRST HALF STEP
C
C
C     GENERATE RANDOM SI USING CHORIN'S METHOD
C
      NU=MOD(NU+K2,K1)
      BLIP=BLIP+1.D0
      SI=(GGUBFS(BLIP)+FLOAT(NU))/FLOAT(K1)
C
C     XI LIES BETWEEN -DX/2 AND +DX/2
C
      DO 40 I=2,NP1
      XI1=SI*DX-0.5*DX
      RR=RHO(I)
      UR=UX(I)
      PR=PRE(I)
      KPHI=PHI(I)
      IF(I.EQ.2)GO TO 43
      RL=RIM1
      PL=PIM1
      UL=UIM1
      GO TO 44
C
C     BOUNDARY CONDITION AT AXIS R=0
```

```
C
43    RL=RHO(1)
      UL=UX(1)
      PL=PRE(1)
      KIM=PHI(1)
      GO TO 44
C
C     COMPUTE FIRST HALF STEP OF GLIMM
C
44    CALL GLIMM(XI1)
      RIM1=RHO(I)
      RHO(I)=R
      PIM1=PRE(I)
      PRE(I)=P
      UIM1=UX(I)
      UX(I)=U
      KIM=PHI(I)
      PHI(I)=KPHI
40    CONTINUE
C
C     COMPUTE SECOND HALF STEP
C
C
C     GENERATE RANDOM SI USING CHORIN'S METHOD
C
      NU=MOD(NU+K2,K1)
      SI=(GGUBFS(BLIP)+FLOAT(NU))/FLOAT(K1)
C
C     XI LIES BETWEEN -DX/2 AND +DX/2
C
      KIM=PHI(1)
      DO 60 I=1,NP1
      XI2=SI*DX-0.5*DX
      RL=RHO(I)
      PL=PRE(I)
      UL=UX(I)
      IF(I.EQ.NP1) GO TO 63
      KPHI=PHI(I+1)
      RR=RHO(I+1)
      PR=PRE(I+1)
      UR=UX(I+1)
      IF(I.EQ.1) GO TO 62
      GO TO 64
C     BOUNDARY CONDITION AT R=1.
63    RR=RL
      UR=-UL
      PR=PL
      KPHI=PHI(I)
      XI2=0.0
      GO TO 64
```

```
C
C       COMPUTE SECOND HALF STEP OF GLIMM
C
62      XI2=ABS(XI2)
        IF(XI1.LT.0.) XI2=XI1+0.5*DX
        RL=RR
        UL=-UR
        PL=PR
64      CALL GLIMM(XI2)
        RHO(I)=R
        PRE(I)=P
        UX(I)=U
        KIM=PHI(I+1)
        PHI(I)=KPHI
60      CONTINUE
        CALL INHOM
        WRITE(15,20000) TIME
20000   FORMAT(1H1,7H TIME = ,F11.7)
        WRITE(15,20001) RHO(1),PRE(1)
        WRITE(15,20001) RHO(NP1),PRE(NP1)
20001   FORMAT(1H0,2F13.5)
        IF(NP.LT.NPRINT) GO TO 100
        NP=0
        CALL OUTPUT
100     CONTINUE
        STOP
        END
C
C       SUBROUTINE GLIMM:TO SOLVE RIEMANN PROBLEM
C
        SUBROUTINE GLIMM(XI)
        COMMON//DT,GAMMA,RL,UL,PL,R,U,P,E,RR,UR,PR,KPHI,DELTA,KIM
        COMMON/RAD/ETA
        COMMON/LIN/LAM
        REAL MR,ML,MRP1,MLP1
        REAL LAM,MUSQ
        EPS=1.E-6
        IT=0
        ITSTOP=20
        KPHIP=KPHI*KIM
C
C       IF KPHI=1 , MIGHT HAVE A DETONATION
C
        IF(KPHI.EQ.1.AND.KPHIP.EQ.0) GO TO 111
C
C       CONSTRUCTION OF RIEMANN PROBLEM
C       ALFA IS THE CONVERGENCE FACTOR
C
        ALFA=1.
        ALFAM=1.-ALFA
```

```
C
C       INITIAL ML AND MR
C
        ML=100.
        MR=100.
        COEFL=SQRT(PL*RL)
        COEFR=SQRT(PR*RR)
C
C       COMPUTE INITIAL PSTAR USING LINEARIZED GODUNOV
C
        RAV=0.5*(RL+RR)
        PAV=0.5*(PL+PR)
        A=PAV/(RAV**GAMMA)
        R=RAV-LAM*(UR*RR-UL*RL)
        PSTAR=A*(R**GAMMA)
C
C       SOLVE RIEMANN PROBLEM USING GODUNOV'S ITERARIVE METHOD
C
10      IT=IT+1
C
C       IF PSTAR IS LESS THAN EPS THEN PSTAR IS SET EQUAL
C       TO 1.0E-6 TO PREVENT PSTAR FROM BECOMING NEGATIVE
C
        PSTAR=AMAX1(EPS,PSTAR)
C
C       COMPUTE MR AND ML AT STEP Q+1
C
20      MLP1=COEFL*PSI(PSTAR/PL,GAMMA)
        MRP1=COEFR*PSI(PSTAR/PR,GAMMA)
        DIFML=ABS(MLP1-ML)
        DIFMR=ABS(MRP1-MR)
        ML=MLP1
        MR=MRP1
C
C       COMPUTE NEW PRESSURE PSTAR
C
        PSTARP=PSTAR
        PSTAR=(UL-UR+PR/MR+PL/ML)/(1./ML+1./MR)
        PSTAR=ALFA*PSTAR+ALFAM*PSTARP
        IF(IT.LE.ITSTOP) GO TO 30
        IF(ABS(PSTAR-PSTARP).LT.EPS) GO TO 40
        IF(DIFML*DIFMR.LT.EPS) GO TO 40
        ALFA=ALFA/2.
        ALFAM=1.-ALFA
        IF(ALFAM.LT.EPS) GO TO 40
        IT=0
30      IF(DIFML.GT.EPS) GO TO 10
        IF(DIFMR.GT.EPS) GO TO 10
C
C       COMPUTE USTAR AT END OF GODUNOV ITERATION
```

```
C
40    USTAR=(PL-PR+MR*UR+ML*UL)/(ML+MR)
C
C     BEGIN GLIMM'S METHOD
C
      IREGL=1
      IF(PSTAR.LT.PL) IREGL=2
      IREGR=1
      IF(PSTAR.LT.PR) IREGR=2
      X=USTAR*DT
      IF(XI.GE.X) GO TO 200
C
C     LEFT SIDE
C
      IF(IREGL.EQ.2) GO TO 110
C
C     COMPUTE LEFT SHOCK SPEED
C
      U=UL-ML/RL
      X=U*DT
      IF(XI.GE.X) GO TO 100
C
C     LEFT OF LEFT SHOCK
C
      R=RL
      U=UL
      P=PL
      GO TO 500
C
C     RIGHT OF LEFT SHOCK
C
100   R=ML/(USTAR-U)
      U=USTAR
      P=PSTAR
      GO TO 500
C
C     COMPUTE SOUND SPEED IN LEFT STATE
C
110   CL=SQRT(GAMMA*PL/RL)
      X=(UL-CL)*DT
      IF(XI.GE.X) GO TO 120
C
C     LEFT OF LEFT FAN
C
      R=RL
      U=UL
      P=PL
      GO TO 500
C
C     COMPUTE CONSTANT OF ISENTROPIC LAW-A
```

```
C
120   A=PL/(RL**GAMMA)
C
C     COMPUTE DENSITY IN STATE STAR
C
      RSTAR=(PSTAR/A)**(1./GAMMA)
C
C     COMPUTE SOUND SPEED IN STATE STAR
C
      CSTAR=SQRT(GAMMA*PSTAR/RSTAR)
      X=(USTAR-CSTAR)*DT
      IF(XI.GE.X) GO TO 130
C
C     IN LEFT FAN
C
      U=(2./(GAMMA+1.))*(XI/DT+CL+0.5*(GAMMA-1.)*UL)
      RINT=CL+0.5*(GAMMA-1.)*(UL-U)
      R=(RINT*RINT/(A*GAMMA))**(1./(GAMMA-1.))
      P=A*(R**GAMMA)
      GO TO 500
C
C     RIGHT OF LEFT FAN
C
130   R=RSTAR
      U=USTAR
      P=PSTAR
      GO TO 500
C
C     RIGHT SIDE
C
200   IF(IREGR.EQ.2) GO TO 220
C
C     COMPUTE RIGHT SHOCK SPEED
C
      U=UR+MR/RR
      X=U*DT
      IF(XI.GE.X) GO TO 210
C
C     LEFT OF RIGHT SHOCK
C
      R=-MR/(USTAR-U)
      U=USTAR
      P=PSTAR
      GO TO 500
C
C     RIGHT OF RIGHT SHOCK
C
210   R=RR
      U=UR
      P=PR
```

```
      GO TO 500
C
C     COMPUTE CONSTANT OF ISENTROPIC LAW-A
C
220   A=PR/(RR**GAMMA)
C
C     COMPUTE DENSITY IN STATE STAR
C
      RSTAR=(PSTAR/A)**(1./GAMMA)
C
C     COMPUTE SOUND SPEED IN STATE STAR
C
      CSTAR=SQRT(GAMMA*PSTAR/RSTAR)
      X=(USTAR+CSTAR)*DT
      IF(XI.GE.X) GO TO 230
C
C     LEFT OF RIGHT FAN
C
      R=RSTAR
      U=USTAR
      P=PSTAR
      GO TO 500
C
C     COMPUTE SOUND SPEED IN RIGHT STATE
C
230   CR=SQRT(GAMMA*PR/RR)
      X=(UR+CR)*DT
      IF(XI.GE.X) GO TO 240
C
C     IN RIGHT FAN
C
      U=(2./(GAMMA+1.))*(XI/DT-CR+0.5*(GAMMA-1.)*UR)
      RINT=CR+0.5*(GAMMA-1.)*(U-UR)
      R=(RINT*RINT/(A*GAMMA))**(1./(GAMMA-1.))
      P=A*(R**GAMMA)
      GO TO 500
C
C     RIGHT OF RIGHT FAN
C
240   R=RR
      U=UR
      P=PR
      GO TO 500
C
C     DETONATION CONDITIONS
C
C
C     CALCULATE CONDITIONS JUST BEHIND CJ DETONATION
C
111   B=-PR-DELTA*(GAMMA-1.)*RR
```

```
      MUSQ=(GAMMA-1.)/(GAMMA+1.)
      C=(PR*PR)+2.*MUSQ*PR*RR*DELTA
      PSTAR=-B+SQRT((B*B)-C)
      RSTAR=(PSTAR*(GAMMA+1.)-PR)*RR/(GAMMA*PSTAR)
      UCJ=SQRT(GAMMA*PSTAR*RSTAR)/RR+UR
      CSTAR=SQRT(GAMMA*PSTAR/RSTAR)
      USTAR=UCJ-CSTAR
C
C     BEGIN GLIMM'S METHOD
C
      X=UCJ*DT
      IF(XI.GE.X) GO TO 222
C
C     LEFT OF DETONATION
C
333   U=USTAR
      P=PSTAR
      R=RSTAR
      KPHI=0
      GO TO 500
222   U=UR
      P=PR
      R=RR
500   CONTINUE
      RETURN
      END
C
C     FUNCTION PSI
C
      FUNCTION PSI(X,GAMMA)
      EPS=1.0E-6
      IF(ABS(1.-X).GT.EPS) GO TO 100
      PSI=SQRT(GAMMA)
      RETURN
100   COEF1=0.5*(GAMMA+1.)
      COEF2=0.5*(GAMMA-1.)
      COEF3=COEF2/GAMMA
      IF(X.GE.1.) GO TO 200
      PSI=COEF2*(1.-X)/(SQRT(GAMMA)*(1.-(X**COEF3)))
      RETURN
200   PSI=SQRT(COEF1*X+COEF2)
      RETURN
      END
C
C     SUBROUTINE INHOM,TO CALCULATE THE NON-HOMOGENEOUS
C     DIFFERENTIAL EQUATION
C
      SUBROUTINE INHOM
      COMMON//DT,GAMMA,RL,UL,PL,R,U,P,E,RR,UR,PR,KPHI,DELTA,KIM
      COMMON/OUT/TIME,N,DX,RHO(111),PRE(111),UX(111),PHI(111)
```

```
      COMMON/RAD/ETA
      REAL MOM
      INTEGER PHI
      NP1=N+1
      DO 100 I=2,NP1
      X=FLOAT(I-1)*DX
      R=RHO(I)
      U=UX(I)
      P=PRE(I)
      KPHI=PHI(I)
      KPHIP=PHI(I+1)
      KIP=KPHI*KPHIP
      IF(KPHIP.EQ.1.AND.KIP.EQ.0) GO TO 10
      E=P/(GAMMA-1.)+0.5*R*U*U+KPHI*DELTA*R
      DEN=R-2.*DT*(ETA-1.)*R*U/X
      MOM=R*U-R*U*2.*DT*(ETA-1.)*U/X
      E=E-2.*DT*(ETA-1.)*U*(E+P)/X
      RHO(I)=DEN
      UX(I)=MOM/DEN
      PRE(I)=(GAMMA-1.)*(E-KPHI*DELTA*DEN-0.5*MOM*MOM/DEN)
11    GO TO 100
10    RHO(I)=R
      UX(I)=U
      PRE(I)=P
100   CONTINUE
      RETURN
      END
C
C     SUBROUTINE OUTPUT:OUTPUT SECTION OF THE PROGRAM
C
      SUBROUTINE OUTPUT
      COMMON//DT,GAMMA,RL,UL,PL,R,U,P,E,RR,UR,PR,KPHI,DELTA,KIM
      COMMON/OUT/TIME,N,DX,RHO(111),PRE(111),UX(111),PHI(111)
      INTEGER PHI
      NP1=N+1
      WRITE(6,10000) TIME
      WRITE(6,10001)
      DO 20 I=1,NP1
      X=FLOAT(I-1)*DX
      R=RHO(I)
      U=UX(I)
      P=PRE(I)
      K=PHI(I)
      WRITE(6,10002) X,R,U,P,K
20    CONTINUE
      RETURN
10000 FORMAT(1H1,7H TIME = ,F11.7)
10001 FORMAT(1H ,3H  X,6X,5HDENSE,8X,3HVEL,10X,4HPRES,10X,3HPHI)
10002 FORMAT(1H0,F6.3,3F13.5,I2)
      END
```

APPENDIX D

THE COMPUTER PROGRAM TWODIM

D.1 Description of the Program

The major parts of the program are similar to the previous two programs i.e., the main program, the subroutine GLIMM, the subroutine INHOM and the output section. However, two subroutines have been added. Subroutine LABEL defines the boundaries for the problem, it simulates the curved walls of a containment by a stepwise line; it also identifies the grid points which fall outside the boundaries. Subroutine SPLINE is a third order polynomial approximation of the Taylor curves in spherical coordinates.

The general flow chart of the main section of the program can be found in Figure D.1. The data file cards are explained in Table D.1.

D.2 Dictionary of Key Terms in TWODIM

The terms which have been defined in section B.2 are not repeated here

AP(12), BP(12), CP(12), DP(12), AR(12), BR(12), CR(12), DR(12), AU(12), BU(12),	Coefficient of the third order polynomial approximating the Taylor curves for the pressure, density and velocity
DETDIS	Initial distance the detonation front had reached:

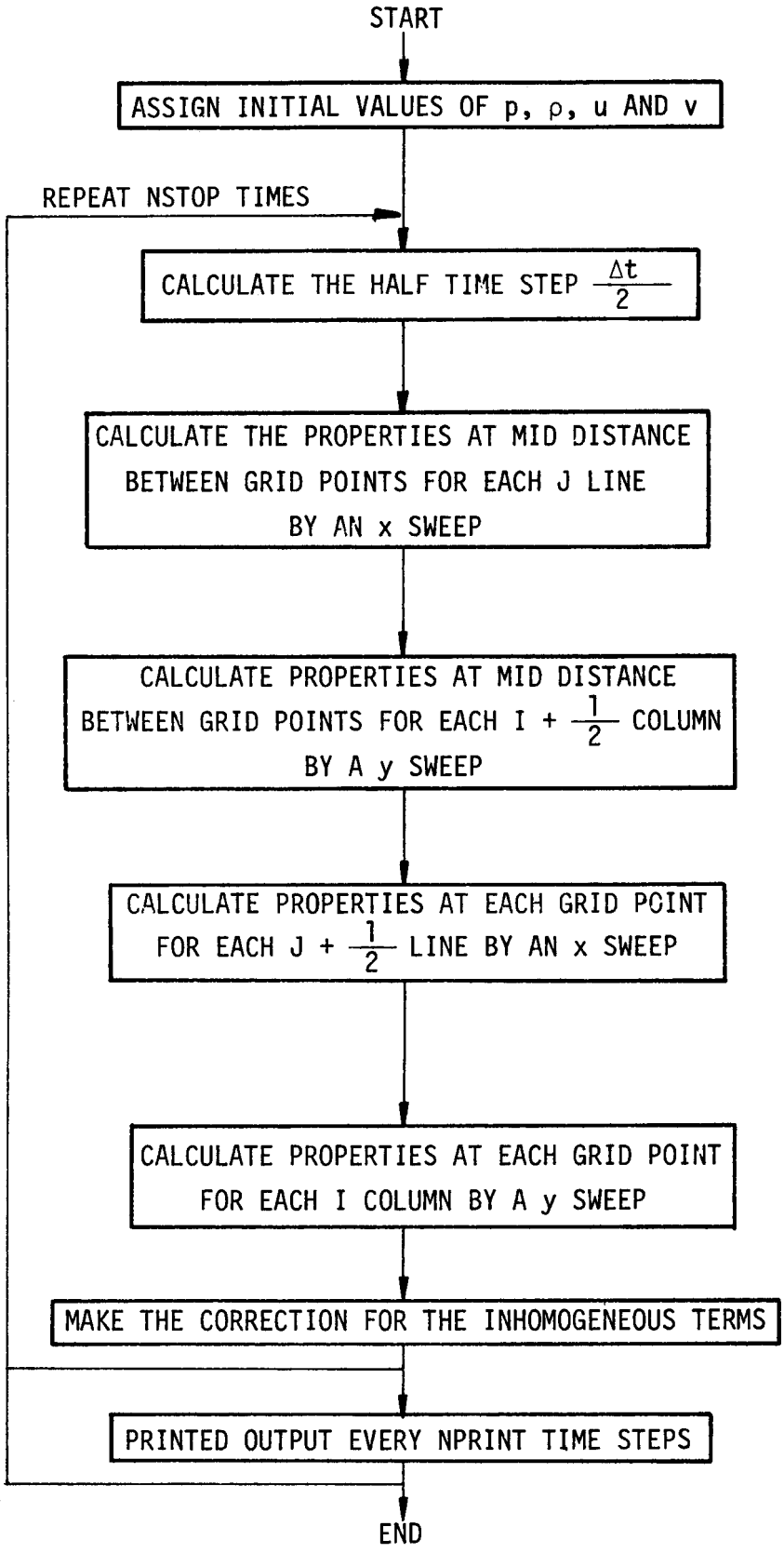

FIGURE D.1: FLOW CHART FOR TWODIM

TABLE D.1: DATA FILE

NO. OF CARDS	FORTRAN NAME[FORMAT]	COLUMN N°	
1	NPRINT [I4]	1-4 last digit in column 4	
	NSTOP [I4]	5-8 last digit in column 8	
1	NX[I3]	1-3 last digit in column 3	
	NY[I3]	4-6 last digit in column 6	
$\left[\frac{NX}{10}\right]^{*} + 1$	X(I)[10F7.3]	X(1)	1-7
		X(2)	8-14
		⋮	⋮
		X(10)	64-70
		X(11)	1-7
		⋮	
		X(NX)	
$\left[\frac{NY}{10}\right]^{*} + 1$	Y(I)[10F7.3]	Y(1)	1-7
		Y(2)	8-14
		⋮	
		Y(10)	64-70
		Y(11)	1-7
		⋮	
		Y(NY)	
1	SXDXY[F10.4]	1-10	
1	DETDIS[F7.3]	1-7	
1	JCYL[I3]	1-3 last digit in column 3	

*$[\![X]\!]$ ≡ largest integer < X

IDUM(I,J)	Dummy variable which identifies whether the grid point is an internal, external or boundary point.
JCYL	Last grid point in the y-direction before the wall of the containment starts to curve
LABEL	Subroutine which defines the wall boundaries of the containment
NX	Number of grid points in the x-direction
NY	Number of grid points in the y-direction
SDXY	Smallest grid interval in the x and in the y directions
SPLINE	Subroutine which generates the coefficients of the third order fit polynomial
SX(12)	Selected points on the absissa axis of the Taylor curves
UX(I,J)	X-component of the velocity at grid point (I,J)
VY(I,J)	Y-component of the velocity at grid poing (I,J)
X(I)	Grid distance from the origin in the x-direction
Y(I)	Grid distance from the origin in the y-direction
YP(12),YR(12),YU(12)	Ordinate corresponding to SX in the spherical Taylor curves for the pressure, density and velocity

```
C      TWO DIMENSIONAL AXISYMMETRIC PROGRAM TO CALCULATE
C      PRESSURE,DENSITY AND VELOCITY HISTORY IN A REACTIVE MIXTURE
C
       COMMON//DT,GAMMA,RL,UL,PL,R,U,V,P,E,RR,UR,PR,KPHI,DELTA,KIM,
      &        V1
       COMMON/OUT/TIME,NX,NY,RHO(101,101),PRE(101,101),UX(101,101)
       COMMON/OWT/PHI(101,101)
       COMMON/AWT/VY(101,101),X(101),Y(101),DIST(101,101),
      &           IDUM(101,101)
       COMMON/RAD/ETA
       COMMON/LIN/LAM
       COMMON/INI/RCHJ,PCHJ,UCHJ
       DIMENSION SX(12),YP(12),AP(12),BP(12),CP(12),DP(12)
       DIMENSION YR(12),AR(12),BR(12),CR(12),DR(12)
       DIMENSION YU(12),AU(12),BU(12),CU(12),DU(12)
       DATA SX/.501,.6,.7,.75,.8,.85,.9,.92,.94,.96,.98,1./
       DATA YP/.2773,.3075,.3675,.405,.45,.515,.59,.62,.67,.725,.8,
      &        1./
       DATA YR/.4,.43,.485,.52,.565,.6175,.68,.715,.76,.815,.88,1./
       DATA YU/.0,.1,.2,.265,.345,.43,.55,.61,.66,.73,.83,1./
       CALL SPLINE(SX,YP,AP,BP,CP,DP)
       CALL SPLINE(SX,YR,AR,BR,CR,DR)
       CALL SPLINE(SX,YU,AU,BU,CU,DU)
       REAL LAM
       DOUBLE PRECISION BLIP
       INTEGER TSTP,PHI
       READ(5,9999) NPRINT,NSTOP
9999   FORMAT(2I4)
       READ (5,8888) C1
 8888  FORMAT(F12.5)
C
C      READ THE DIMENSION OF THE GRID IN THE X AND Y DIRECTIONS
C
       READ(5,10000)NX,NY
10000  FORMAT(2I3)
       NXM1=NX-1
       NYM1=NY-1
C
C      READ THE GRID LOCATION
C
       READ(5,10001) (X(I),I=1,NX)
       READ(5,10001) (Y(J),J=1,NY)
10001  FORMAT(10F7.3)
       READ(5,10002) SDXY
10002  FORMAT(F10.4)
       DT1=0.00001
       TIME=0.0
       VMAX=0.
       NP=0
       GAMMA=1.4
       DELTA=1447711.2
       BLIP=0.0D0
```

```
      K1=11
      K2=7
      NU=2
      SIGMA=1.0
C     ETA IS A DUMMY CONTROL
      ETA=3.
C
C     READ THE INITIAL INITIATION RADIUS
C
      READ(5,10003) DETDIS
10003 FORMAT(F7.3)
C
C     SET INITIAL CONDITIONS
C
      READ(5,10004)RCHJ
      READ(5,10004)PCHJ
      READ(5,10004)UCHJ
      READ(5,10004)RIN
      READ(5,10004)PIN
      READ(5,10004)UIN
10004 FORMAT(F13.5)
      RL=RCHJ
      PL=PCHJ
      UL=UCHJ
      VL=0.
      RR=RIN
      PR=PIN
      UR=UIN
      VR=0.
      READ(5,10006) YO
10006 FORMAT(F7.3)
      READ(5,10007) NYO
10007 FORMAT(I3)
      DO 10 I=1,NX
      DO 10 J=1,NY
      DIST(I,J)=SQRT(X(I)**2.+(Y(J)-YO)*(Y(J)-YO))
      IF(DIST(I,J).GT.DETDIS) GO TO 11
      PHI(I,J)=0
      DDET=DIST(I,J)/DETDIS
      IF(DDET.GT.SX(1)) GO TO 1
      PRE(I,J)=YP(1)*PL
      RHO(I,J)=YR(1)*RL
      UX(I,J)=YU(1)*UL
      GO TO 29
1     DO 9 K=2,12
      IF(DDET.GT.SX(K)) GO TO 9
      XX=DDET-SX(K-1)
      PRE(I,J)=AP(K-1)*XX*XX*XX+BP(K-1)*XX*XX+CP(K-1)*XX+DP(K-1)
      PRE(I,J)=PRE(I,J)*PL
      RHO(I,J)=AR(K-1)*XX*XX*XX+BR(K-1)*XX*XX+CR(K-1)*XX+DR(K-1)
      RHO(I,J)=RHO(I,J)*RL
      UX(I,J)=AU(K-1)*XX*XX*XX+BU(K-1)*XX*XX+CU(K-1)*XX+DU(K-1)
```

```
      UX(I,J)=UX(I,J)*UL
      GO TO 29
9     CONTINUE
29    IF(I.EQ.1.AND.J.EQ.NYO) GO TO 12
      GO TO 13
12    VY(I,J)=UX(I,J)
      GO TO 10
13    U=UX(I,J)
      UX(I,J)=U*X(I)/DIST(I,J)
      VY(I,J)=U*(Y(J)-YO)/DIST(I,J)
      GO TO 10
11    RHO(I,J)=RR
      PRE(I,J)=PR
      UX(I,J)=UR
      VY(I,J)=VR
      PHI(I,J)=1
10    CONTINUE
      READ(5,10005) JCYL
10005 FORMAT(I3)
      CALL LABEL(NX,NY,JCYL)
      DO 333 I=1,NXM1
      DO 333 J=1,NYM1
      IF(IDUM(I,J).EQ.4) GO TO 333
      IF(PHI(I+1,J).EQ.1.AND.PHI(I,J).EQ.0) IDUM(I,J)=3
      IF(PHI(I,J+1).EQ.1.AND.PHI(I,J).EQ.0) IDUM(I,J)=3
333   CONTINUE
C
C     BEGIN TIME STEP
C
      DO 100 TSTP=1,NSTOP
      NP=NP+1
      DO 30 I=1,NX
      DO 30 J=1,NY

      VMAX1=SQRT(UX(I,J)*UX(I,J)+VY(I,J)*VY(I,J))+SQRT(GAMMA*PRE(I,J)/
     &RHO(I,J))
      IF(VMAX1.GT.VMAX) VMAX=VMAX1
30    CONTINUE
C       SET INITIAL VALUE OF DT
      DT=0.01
C     FIND THE HALF TIME STEP DT
C
      DTT=SIGMA*SDXY/(2.*VMAX)
      IF(DTT.LT.DT) DT=DTT
      DT=AMAX1(DT,DT1)
      TIME=TIME+2.*DT
      LAM=0.5/VMAX
C
C     COMPUTE FIRST QUARTER STEP. X-SWEEP
C
C
C     GENERATE RANDOM SI USING CHORIN'S METHOD
C
```

```
      NU=MOD(NU+K2,K1)
      BLIP=BLIP+1.D0
      SI=(GGUBFS(BLIP)+FLOAT(NU))/FLOAT(K1)
C
      DO 40 J=1,NY
      DO 40 I=2,NX
      DX=(X(I)-X(I-1))
      XI1=SI*DX-0.5*DX
      IF(IDUM(I,J).EQ.0) GO TO 40
      RR=RHO(I,J)
      UR=UX(I,J)
      PR=PRE(I,J)
      KPHI=PHI(I,J)
      V1=VY(I,J)
      IF(I.EQ.2) GO TO 43
      RL=RIM1
      PL=PIM1
      UL=UIM1
      V=VIM1
      GO TO 44
43    RL=RHO(1,J)
      UL=UX(1,J)
      PL=PRE(1,J)
      KIM=PHI(1,J)
      V=VY(1,J)
44    CALL GLIMM(XI1)
      RIM1=RHO(I,J)
      RHO(I,J)=R
      PIM1=PRE(I,J)
      PRE(I,J)=P
      UIM1=UX(I,J)
      UX(I,J)=U
      VIM1=VY(I,J)
      VY(I,J)=V
      KIM=PHI(I,J)
      PHI(I,J)=KPHI
40    CONTINUE
C
C     COMPUTE SECOND QUARTER STEP. Y-SWEEP
C
C
C     GENERATE RANDOM SI USING CHORIN'S METHOD
C
      NU=MOD(NU+K2,K1)
      SI=(GGUBFS(BLIP)+FLOAT(NU))/FLOAT(K1)
C
      DO 50 I=2,NX
      DO 50 J=2,NY
      DY=(Y(J)-Y(J-1))
      XI2=SI*DY-0.5*DY
      IF(IDUM(I,J).EQ.0) GO TO 50
      RR=RHO(I,J)
```

```
      UR=VY(I,J)
      PR=PRE(I,J)
      KPHI=PHI(I,J)
      V1=UX(I,J)
      IF(J.EQ.2) GO TO 53
      RL=RIM1
      PL=PIM1
      UL=UIM1
      V=VIM1
      GO TO 54
53    RL=RHO(I,1)
      UL=VY(I,1)
      PL=PRE(I,1)
      KIM=PHI(I,1)
      V=UX(I,1)
54    CALL GLIMM(XI2)
      RIM1=RHO(I,J)
      RHO(I,J)=R
      PIM1=PRE(I,J)
      PRE(I,J)=P
      UIM1=VY(I,J)
      VY(I,J)=U
      VIM1=UX(I,J)
      UX(I,J)=V
      KIM=PHI(I,J)
      PHI(I,J)=KPHI
50    CONTINUE
C
C     COMPUTE THIRD QUARTER STEP. X-SWEEP
C
C
C     GENERATE RANDOM SI USING CHORIN'S METHOD
C
      NU=MOD(NU+K2,K1)
      SI=(GGUBFS(BLIP)+FLOAT(NU))/FLOAT(K1)
C
      DO 60 J=2,NY
      DO 60 I=1,NX
      IF(IDUM(I,J).EQ.0) GO TO 60
      RL=RHO(I,J)
      PL=PRE(I,J)
      UL=UX(I,J)
      V=VY(I,J)
      IF(I.EQ.NX) GO TO 63
      IF(IDUM(I+1,J).EQ.0) GO TO 63
      DXR=(X(I+1)-X(I))*0.5
      IF(I.EQ.1) DXL=DXR
      IF(I.NE.1) DXL=(X(I)-X(I-1))*0.5
      XI3=(DXR+DXL)*SI-DXL
      KPHI=PHI(I+1,J)
      RR=RHO(I+1,J)
      PR=PRE(I+1,J)
```

```
      UR=UX(I+1,J)
      V1=VY(I+1,J)
      IF(I.EQ.1) GO TO 62
      GO TO 64
C
C     BOUNDARY CONDITIONS AT WALL
C
63    RR=RL
      UR=-UL
      PR=PL
      KPHI=PHI(I,J)
      XI3=-ABS(XI3)
      GO TO 64
C
C     BOUNDARY CONDITIONS AT CENTERLINE
C
62    XI3=ABS(XI3)
      RL=RR
      PL=PR
      UL=-UR
       KIM=PHI(2,J)
       PHI(1,J)=PHI(2,J)
      V=VY(I+1,J)
      VY(I,J)=VY(I+1,J)
64    CALL GLIMM(XI3)
      RHO(I,J)=R
      PRE(I,J)=P
      UX(I,J)=U
      IF(I.NE.NX) KIM=PHI(I+1,J)
      PHI(I,J)=KPHI
      VY(I,J)=V
60    CONTINUE
C
C     COMPUTE FOURTH QUARTER STEP. Y-SWEEP
C
C
C     GENERATE RANDOM SI USING CHORIN'S METHOD
C
      NU=MOD(NU+K2,K1)
      SI=(GGUBFS(BLIP)+FLOAT(NU))/FLOAT(K1)
C
      DO 70 I=1,NX
      DO 70 J=1,NY
      IF(IDUM(I,J).EQ.0) GO TO 70
      RL=RHO(I,J)
      PL=PRE(I,J)
      UL=VY(I,J)
      V=UX(I,J)
      IF(J.EQ.NY) GO TO 73
      IF(IDUM(I,J+1).EQ.0) GO TO 73
      DYR=(Y(J+1)-Y(J))*0.5
      IF(J.EQ.1) DYL=DYR
```

```
      IF(J.NE.1) DYL=(Y(J)-Y(J-1))*0.5
      XI4=(DYR+DYL)*SI-DYL
      KPHI=PHI(I,J+1)
      RR=RHO(I,J+1)
      PR=PRE(I,J+1)
      UR=VY(I,J+1)
      V1=UX(I,J+1)
      IF(J.EQ.1) GO TO 72
      GO TO 74
C
C     BOUNDARY CONDITIONS AT THE UPPER WALL
C
73    RR=RL
      UR=-UL
      PR=PL
      KPHI=PHI(I,J)
      XI4=-ABS(XI4)
      GO TO 74
C
C     BOUNDARY CONDITIONS AT THE LOWER WALL
C
72    XI4=ABS(XI4)
      RL=RR
      PL=PR
      UL=-UR
      KIM=PHI(I,2)
      PHI(I,1)=PHI(I,2)
      V=UX(I,J+1)
      UX(I,J)=UX(I,J+1)
74    CALL GLIMM(XI4)
      RHO(I,J)=R
      PRE(I,J)=P
      VY(I,J)=U
      IF(J.NE.NY) KIM=PHI(I,J+1)
      PHI(I,J)=KPHI
      UX(I,J)=V
70    CONTINUE
      CALL LABEL(NX,NY,JCYL)
      DO 777 I=1,NXM1
      DO 777 J=1,NYM1
      IF(IDUM(I,J).EQ.4) GO TO 777
      IF(PHI(I+1,J).EQ.1.AND.PHI(I,J).EQ.0) IDUM(I,J)=3
      IF(PHI(I,J+1).EQ.1.AND.PHI(I,J).EQ.0) IDUM(I,J)=3
777   CONTINUE
      CALL INHOM
      WRITE(6,300) TIME,PRE(NX,1),PRE(NX,8),PRE(NX,16),PRE(NX,21),
     *PRE(NX,26),PRE(NX,30),PRE(NX,34),PRE(NX,38),PRE(NX,41),
     *PRE(24,46),PRE(20,50),PRE(15,55),PRE(10,60),PRE(5,65),
     *PRE(1,65),PRE(1,1),PRE(1,24),PRE(1,34),PRE(1,44),PRE(1,54)
300   FORMAT(1X,E9.3,1X,10(E9.3,1X),/,10X,10(E9.3,1X))
      IF(NP.LT.NPRINT) GO TO 100
      NP=0
```

```
100   CONTINUE
      STOP
      END
C
C     SUBROUTINE GLIMM:TO SOLVE RIEMANN PROBLEM
C
      SUBROUTINE GLIMM(XI)
      COMMON//DT,GAMMA,RL,UL,PL,R,U,V,P,E,RR,UR,PR,KPHI,DELTA,KIM,
     &       V1
      COMMON/RAD/ETA
      COMMON/LIN/LAM
      COMMON/INI/RCHJ,PCHJ,UCHJ
      REAL MR,ML,MRP1,MLP1
      REAL LAM,MUSQ
      EPS=1.E-6
      EPS1=1.E-3
      IT=0
      ITSTOP=20
      KPHIP=KPHI*KIM
C
C     IF KPHI=1 , MIGHT HAVE A DETONATION
C
      IF(KPHI.EQ.1.AND.KPHIP.EQ.0) GO TO 111
      IF(KIM.EQ.1.AND.KPHIP.EQ.0) GO TO 111
C
C     CONSTRUCTION OF RIEMANN PROBLEM
C     ALFA IS THE CONVERGENCE FACTOR
C
      ALFA=1.
      ALFAM=1.-ALFA
C
C     INITIAL ML AND MR
C
      ML=100.
      MR=100.
      COEFL=SQRT(PL*RL)
      COEFR=SQRT(PR*RR)
C
C     COMPUTE INITIAL PSTAR USING LINEARIZED GODUNOV
C
      RAV=0.5*(RL+RR)
      PAV=0.5*(PL+PR)
      A=PAV/(RAV**GAMMA)
      R=RAV-LAM*(UR*RR-UL*RL)
      PSTAR=A*(R**GAMMA)
C
C     SOLVE RIEMANN PROBLEM USING GODUNOV'S ITERARIVE METHOD
C
10    IT=IT+1
C
C     IF PSTAR IS LESS THAN EPS1THEN PSTAR IS SET EQUAL
C     TO 1.0E-3 TO PREVENT PSTAR FROM BECOMING NEGATIVE
```

```
C
      PSTAR=AMAX1(EPS1,PSTAR)
C
C     COMPUTE MR AND ML AT STEP Q+1
C
20    MLP1=COEFL*PSI(PSTAR/PL,GAMMA)
      MRP1=COEFR*PSI(PSTAR/PR,GAMMA)
      DIFML=ABS(1.-(MLP1/ML))
      DIFMR=ABS(1.-(MRP1/MR))
      ML=MLP1
      MR=MRP1
C
C     COMPUTE NEW PRESSURE PSTAR
C
      PSTARP=PSTAR
      PSTAR=(UL-UR+PR/MR+PL/ML)/(1./ML+1./MR)
      PSTAR=ALFA*PSTAR+ALFAM*PSTARP
      IF(IT.LE.ITSTOP) GO TO 30
      DIFPS=ABS(1.-(PSTARP/PSTAR))
      IF(DIFPS.LT.EPS1) GO TO 40
      IF(DIFML*DIFMR.LT.EPS1) GO TO 40
      ALFA=ALFA/2.
      ALFAM=1.-ALFA
      IF(ALFAM.LT.EPS1) GO TO 40
      IT=0
30    IF(DIFML.GT.EPS1) GO TO 10
      IF(DIFMR.GT.EPS1) GO TO 10
C
C     COMPUTE USTAR AT END OF GODUNOV ITERATION
C
40    PSTAR=AMAX1(EPS1,PSTAR)
      USTAR=(PL-PR+MR*UR+ML*UL)/(ML+MR)
C
C     BEGIN GLIMM'S METHOD
C
      IREGL=1
      IF(PSTAR.LT.PL) IREGL=2
      IREGR=1
      IF(PSTAR.LT.PR) IREGR=2
      X=USTAR*DT
      IF(XI.GE.X) GO TO 200
C
C     LEFT SIDE
C
      IF(IREGL.EQ.2) GO TO 110
C
C     COMPUTE LEFT SHOCK SPEED
C
      U=UL-ML/RL
      X=U*DT
      IF(XI.GE.X) GO TO 100
C
```

```
C     LEFT OF LEFT SHOCK
C
      R=RL
      U=UL
      P=PL
      GO TO 500
C
C     RIGHT OF LEFT SHOCK
C
100   R=ML/(USTAR-U)
      U=USTAR
      P=PSTAR
      GO TO 500
C
C     COMPUTE SOUND SPEED IN LEFT STATE
C
110   CL=SQRT(GAMMA*PL/RL)
      X=(UL-CL)*DT
      IF(XI.GE.X) GO TO 120
C
C     LEFT OF LEFT FAN
C
      R=RL
      U=UL
      P=PL
      GO TO 500
C
C     COMPUTE CONSTANT OF ISENTROPIC LAW-A
C
120   A=PL/(RL**GAMMA)
C
C     COMPUTE DENSITY IN STATE STAR
C
      RSTAR=(PSTAR/A)**(1./GAMMA)
C
C     COMPUTE SOUND SPEED IN STATE STAR
C
      CSTAR=SQRT(GAMMA*PSTAR/RSTAR)
      X=(USTAR-CSTAR)*DT
      IF(XI.GE.X) GO TO 130
C
C     IN LEFT FAN
C
      U=(2./(GAMMA+1.))*(XI/DT+CL+0.5*(GAMMA-1.)*UL)
      RINT=CL+0.5*(GAMMA-1.)*(UL-U)
      R=(RINT*RINT/(A*GAMMA))**(1./(GAMMA-1.))
      P=A*(R**GAMMA)
      GO TO 500
C
C     RIGHT OF LEFT FAN
C
130   R=RSTAR
```

```
      U=USTAR
      P=PSTAR
      GO TO 500
C
C     RIGHT SIDE
C
200   IF(IREGR.EQ.2) GO TO 220
C
C     COMPUTE RIGHT SHOCK SPEED
C
      U=UR+MR/RR
      X=U*DT
      IF(XI.GE.X) GO TO 210
C
C     LEFT OF RIGHT SHOCK
C
      R=-MR/(USTAR-U)
      U=USTAR
      P=PSTAR
      GO TO 500
C
C     RIGHT OF RIGHT SHOCK
C
210   R=RR
      U=UR
      P=PR
      GO TO 500
C
C     COMPUTE CONSTANT OF ISENTROPIC LAW-A
C
220   A=PR/(RR**GAMMA)
C
C     COMPUTE DENSITY IN STATE STAR
C
      RSTAR=(PSTAR/A)**(1./GAMMA)
C
C     COMPUTE SOUND SPEED IN STATE STAR
C
      CSTAR=SQRT(GAMMA*PSTAR/RSTAR)
      X=(USTAR+CSTAR)*DT
      IF(XI.GE.X) GO TO 230
C
C     LEFT OF RIGHT FAN
C
      R=RSTAR
      U=USTAR
      P=PSTAR
      GO TO 500
C
C     COMPUTE SOUND SPEED IN RIGHT STATE
C
230   CR=SQRT(GAMMA*PR/RR)
```

```
      X=(UR+CR)*DT
      IF(XI.GE.X) GO TO 240
C
C     IN RIGHT FAN
C
      U=(2./(GAMMA+1.))*(XI/DT-CR+0.5*(GAMMA-1.)*UR)
      RINT=CR+0.5*(GAMMA-1.)*(U-UR)
      R=(RINT*RINT/(A*GAMMA))**(1./(GAMMA-1.))
      P=A*(R**GAMMA)
      GO TO 500
C
C     RIGHT OF RIGHT FAN
C
240   R=RR
      U=UR
      P=PR
      GO TO 500
C
C     DETONATION CONDITIONS
C
C
C     CALCULATE CONDITIONS JUST BEHIND CJ DETONATION
C
111   B=-PR-DELTA*(GAMMA-1.)*RR
      MUSQ=(GAMMA-1.)/(GAMMA+1.)
      C=(PR*PR)+2.*MUSQ*PR*RR*DELTA
      PSTAR=-B+SQRT((B*B)-C)
      RSTAR=(PSTAR*(GAMMA+1.)-PR)*RR/(GAMMA*PSTAR)
      UCJ=SQRT(GAMMA*PSTAR*RSTAR)/RR+UR
      CSTAR=SQRT(GAMMA*PSTAR/RSTAR)
      USTAR=UCJ-CSTAR
      PSTAR=PCHJ
      USTAR=SQRT(ABS(UCHJ*UCHJ-V*V))
      RSTAR=RCHJ
      CSTAR=SQRT(GAMMA*PSTAR/RSTAR)
      UCJ=(USTAR/UCHJ)*(CSTAR+UCHJ)
      IF(KIM.EQ.1) GO TO 555
C
C     BEGIN GLIMM'S METHOD
C
      X=UCJ*DT
      IF(XI.GE.X) GO TO 222
      IF(ETA.LT.3.5) GO TO 333
C
C     COMPUTE SOUND SPEED IN LEFT STATE
C     NEXT STATEMENTS TO333 NOT USED
C
      CL=SQRT(GAMMA*PL/RL)
      X=(UL+CL)*DT
      IF(XI.GE.X) GO TO 444
C
C     LEFT OF RAREFACTION FAN
```

```
C
      R=RL
      U=UL
      P=PL
      KPHI=0
      GO TO 500
C
C     COMPUTE CONSTANT OF ISENTROPIC LAW-A
C
444   A=PSTAR/(RSTAR**GAMMA)
C
C     IN RIGHT FAN
C
      U=(2./(GAMMA+1.))*(XI/DT-CSTAR+0.5*(GAMMA-1.)*USTAR)
      RINT=CSTAR+0.5*(GAMMA-1.)*(U-USTAR)
      R=(RINT*RINT/(A*GAMMA))**(1./(GAMMA-1.))
      P=A*(R**GAMMA)
      KPHI=0
      GO TO 500
C
C     RIGHT OF DETONATION
C
333   U=USTAR
      P=PCHJ
      R=RCHJ
      KPHI=0
      GO TO 500
222   U=UR
      P=PR
      R=RR
      V=0
      GO TO 500
C
C     DETONATION FROM RIGHT TO LEFT
C
555   USTAR=SQRT(ABS(UCHJ*UCHJ-V1*V1))
      UCJ=(USTAR/UCHJ)*(CSTAR+UCHJ)
       X=-UCJ*DT
      IF(XI.LE.X) GO TO 556
      IF(ETA.LT.3.5) GO TO 557
557   U=-USTAR
      P=PCHJ
      R=RCHJ
      V=V1
      KPHI=0
      GO TO 500
556   U=UL
      P=PL
      R=RL
      KPHI=1
      V=0
500   CONTINUE
```

```
      RETURN
      END
C
C     FUNCTION PSI
C
      FUNCTION PSI(X,GAMMA)
      EPS=1.0E-6
      IF(ABS(1.-X).GT.EPS) GO TO 100
      PSI=SQRT(GAMMA)
      RETURN
100   COEF1=0.5*(GAMMA+1.)
      COEF2=0.5*(GAMMA-1.)
      COEF3=COEF2/GAMMA
      IF(X.GE.1.) GO TO 200
      PSI=COEF2*(1.-X)/(SQRT(GAMMA)*(1.-(X**COEF3)))
      RETURN
200   PSI=SQRT(COEF1*X+COEF2)
      RETURN
      END
C
C     SUBROUTINE INHOM,TO CALCULATE THE NON-HOMOGENEOUS
C     DIFFERENTIAL EQUATION
C
      SUBROUTINE INHOM
      COMMON//DT,GAMMA,RL,UL,PL,R,U,V,P,E,RR,UR,PR,KPHI,DELTA,KIM
      COMMON/OUT/TIME,NX,NY,RHO(101,101),PRE(101,101),UX(101,101)
      COMMON/OWT/PHI(101,101)
      COMMON/AWT/VY(101,101),X(101),Y(101),DIST(101,101),
     &           IDUM(101,101)
      REAL MOMX,MOMY
      INTEGER PHI
      EPS2=1.E-3
      DO 100 J=1,NY
      DO 100 I=2,NX
      XX=X(I)
      R=RHO(I,J)
      U=UX(I,J)
      P=PRE(I,J)
      V=VY(I,J)
      KPHI=PHI(I,J)
      KPHIP=PHI(I+1,J)
      KPHIPY=PHI(I,J+1)
      IF(J.NE.1) KPHIPP=PHI(I,J-1)
      KIP=KPHI*KPHIP
      KIPY=KPHI*KPHIPY
      IF(J.NE.1) KIPP=KPHI*KPHIPP
      IF(KPHIP.EQ.1.AND.KIP.EQ.0) GO TO 10
      IF(KPHIPY.EQ.1.AND.KIPY.EQ.0) GO TO 10
      IF(J.NE.1.AND.KPHIPP.EQ.1.AND.KIPP.EQ.0) GO TO 10
      E=P/(GAMMA-1.)+0.5*R*U*U+KPHI*DELTA*R+0.5*R*V*V
      DEN=R-2.*DT*R*U/XX
      MOMX=R*U-R*U*2.*DT*U/XX
```

```
      MOMY=R*V-2.*DT*R*U*V/XX
      E=E-2.*DT*U*(E+P)/XX
      RHO(I,J)=DEN
      UX(I,J)=MOMX/DEN
      VY(I,J)=MOMY/DEN
      POP=(GAMMA-1.)*(E-KPHI*DELTA*DEN-0.5*MOMX*MOMX/DEN-0.5*MOMY*M
     &OMY/DEN)
      PRE(I,J)=AMAX1(EPS2,POP)
11    GO TO 100
10    RHO(I,J)=R
      UX(I,J)=U
      VY(I,J)=V
      PRE(I,J)=P
100   CONTINUE
      RETURN
      END
C
C     SUBROUTINE SMOOTH TO DAMP THE OSCILLATIONS
C
      SUBROUTINE SMOOTH(C1)
      COMMON/OUT/TIME,NX,NY,RHO(101,101),PRE(101,101),UX(101,101)
      COMMON/OWT/PHI(101,101)
      COMMON/AWT/VY(101,101),X(101),Y(101),DIST(101,101),
     &           IDUM(101,101)
      DO 1 J=1,NY
      RP=RHO(1,J)
      UP=UX(1,J)
      PP=PRE(1,J)
      VP=VY(1,J)
      NXM1=NX-1
      DO 1 I=2,NXM1
      IF(IDUM(I+1,J).EQ.0) GO TO 1
      R=RHO(I,J)
      U=UX(I,J)
      V=VY(I,J)
      P=PRE(I,J)
      R1DEL=RHO(I,J)-RP
      U1DEL=UX(I,J)-UP
      P1DEL=PRE(I,J)-PP
      V1DEL=VY(I,J)-VP
      R2DEL=RHO(I+1,J)-R
      U2DEL=UX(I+1,J)-U
      P2DEL=PRE(I+1,J)-P
      V2DEL=VY(I+1,J)-V
      R=R+C1*(ABS(U2DEL)*R2DEL-ABS(U1DEL)*R1DEL)
      U=U+C1*(ABS(U2DEL)*U2DEL-ABS(U1DEL)*U1DEL)
      P=P+C1*(ABS(U2DEL)*P2DEL-ABS(U1DEL)*P1DEL)
      V=V+C1*(ABS(U2DEL)*V2DEL-ABS(U1DEL)*V1DEL)
      RP=RHO(I,J)
      RHO(I,J)=R
      UP=UX(I,J)
      UX(I,J)=U
```

```
      PP=PRE(I,J)
      PRE(I,J)=P
      VP=VY(I,J)
      VY(I,J)=V
1     CONTINUE
      NYM1=NY-1
      DO 2 I=1,NX
      RP=RHO(I,1)
      UP=UX(I,1)
      PP=PRE(I,1)
      VP=VY(I,1)
      DO 2 J=2,NYM1
      IF(IDUM(I,J+1).EQ.0) GO TO 2
      R=RHO(I,J)
      U=UX(I,J)
      P=PRE(I,J)
      V=VY(I,J)
      R1DEL=RHO(I,J)-RP
      U1DEL=UX(I,J)-UP
      P1DEL=PRE(I,J)-PP
      V1DEL=VY(I,J)-VP
      R2DEL=RHO(I,J+1)-R
      U2DEL=UX(I,J+1)-U
      P2DEL=PRE(I,J+1)-P
      V2DEL=VY(I,J+1)-V
      R=R+C1*(ABS(V2DEL)*R2DEL-ABS(V1DEL)*R1DEL)
      U=U+C1*(ABS(V2DEL)*U2DEL-ABS(V1DEL)*U1DEL)
      P=P+C1*(ABS(V2DEL)*P2DEL-ABS(V1DEL)*P1DEL)
      V=V+C1*(ABS(V2DEL)*V2DEL-ABS(V1DEL)*V1DEL)
      RP=RHO(I,J)
      RHO(I,J)=R
      UP=UX(I,J)
      UX(I,J)=U
      PP=PRE(I,J)
      PRE(I,J)=P
      VP=VY(I,J)
      VY(I,J)=V
2     CONTINUE
      RETURN
      END
C     SUBROUTINE LABEL TO IDENTIFY THE GRID POINTS
C
      SUBROUTINE LABELF(NX,NY,JCYL)
      COMMON/AWT/VY(101,101),X(101),Y(101),DIST(101,101),
     &           IDUM(101,101)
      DO 1 J=1,NY
      DO 1 I=1,NX
      IDUM(I,J)=1
1     IF(I.EQ.NX.OR.J.EQ.NY) IDUM(I,J)=4
      IX1=30
      IX2=24
      IX3=20
```

```
      IX4=12
      IY1=12
      IY2=20
      IY3=24
      IY4=30
      DO 2 I=IX2,NX
      DO 2 J=IY1,IY2
      IDUM(I,J)=0
      IF(I.EQ.IX2) IDUM(I,J)=4
2     IF(J.EQ.IY1.AND.I.LE.IX1) IDUM(I,J)=4
      DO 3 I=IX3,NX
      DO 3 J=IY2,IY3
      IDUM(I,J)=0
      IF(I.EQ.IX3) IDUM(I,J)=4
3     IF(J.EQ.IY2.AND.I.LE.IX2) IDUM(I,J)=4
      DO 4 I=IX4,NX
      DO 4 J=IY3,IY4
      IDUM(I,J)=0
      IF(I.EQ.IX4) IDUM(I,J)=4
4     IF(J.EQ.IY3.AND.I.LE.IX3) IDUM(I,J)=4
      RETURN
      END
C
C     SUBROUTINE LABEL TO IDENTIFY THE GRID  POINTS
C
      SUBROUTINE LABEL(NX,NY,JCYL)
      COMMON/AWT/VY(101,101),X(101),Y(101),DIST(101,101),
     &           IDUM(101,101)
      DO 1 J=1,NY
      DO 1 I=1,NX
      IDUM(I,J)=1
1     IF(I.EQ.NX.OR.J.EQ.NY) IDUM(I,J)=4
      NXF=NX+1
      JCYLF=JCYL-1
      NYM1=NY-1
      DO 2 I=1,NX
      IM=NXF-I
      JCYLF=JCYLF+1
      IF(JCYLF.GT.NYM1) GO TO 11
      DO 2 J=JCYLF,NYM1
      IDUM(IM,J+1)=0
      IDUM(IM-1,J)=4
2     IDUM(IM-1,J+1)=4
11    RETURN
      END
C
C     SUBROUTINE OUTPUT:OUTPUT SECTION OF THE PROGRAM
C
      SUBROUTINE OUTPUT
      COMMON//DT,GAMMA,RL,UL,PL,R,U,V,P,E,RR,UR,PR,KPHI,DELTA,KIM
      COMMON/OUT/TIME,NX,NY,RHO(101,101),PRE(101,101),UX(101,101)
      COMMON/OWT/PHI(101,101)
```

```
      COMMON/AWT/VY(101,101),X(101),Y(101),DIST(101,101),
     &           IDUM(101,101)
      INTEGER PHI
      WRITE(6,20000) TIME
      DO 20 J=1,NY,3
      JM=NY+1-J
      WRITE(6,20001) Y(JM),(RHO(I,JM),I=1,NX,3)
      WRITE(6,20002) (UX(I,JM),I=1,NX,3)
      WRITE(6,20002) (VY(I,JM),I=1,NX,3)
      WRITE(6,20003) (PRE(I,JM),I=1,NX,3)
      WRITE(6,20004) (PHI(I,JM),I=1,NX,3)
      WRITE(6,20004) (IDUM(I,JM),I=1,NX,3)
20    CONTINUE
      WRITE(6,20005) (X(I),I=1,NX,3)
      WRITE(15,20000) TIME
      WRITE(15,30000)
      DO 30 J=1,NY
      WRITE(15,30001) Y(J),RHO(NX,J),UX(NX,J),VY(NX,J),PRE(NX,J),
     &PHI(NX,J)
30    CONTINUE
      RETURN
20000 FORMAT(1X,' TIME = ',F11.7/)
20001 FORMAT(1X,F7.3,11(F9.5,2X))
20002 FORMAT(8X,11(F9.4,2X))
20003 FORMAT(8X,11(F9.1,2X))
20004 FORMAT(12X,11(I1,10X))
20005 FORMAT(8X,11(F9.3,2X))
30000 FORMAT(1H ,3H  X,6X,5HDENSE,8X,3HVEL,10X,4HPRES,10X,3HPHI)
30001 FORMAT(1H0,F6.3,4F13.5,I2)
      END
C
C     SUBROUTINE SPLINE:FINDS THE THIRD ORDER FIT COEFFICIENTS
C     FOR THE TAYLOR CURVES IN SPHERICAL COORDINATES
C
      SUBROUTINE SPLINE(X,Y,A,B,C,D)
      DIMENSION X(12),Y(12),H(11),RHS(10),W(10,10),A(12),B(12)
      DIMENSION C(12),D(12),AS(10),BS(10),CS(10),G(12)
      DO 2 I=1,11
      J=I+1
2     H(I)=X(J)-X(I)
      DO 3 I=1,10
      J=I+1
      K=I+2
3     RHS(I)=3.*(((Y(K)-Y(J))/H(J))-((Y(J)-Y(I))/H(I)))
      DO 4 I=1,10
      DO 4 J=1,10
4     W(I,J)=0.0
      DO 5 I=1,10
      J=I+1
      W(I,I)=2.*(H(I)+H(J))
      IF(J.EQ.11) GO TO 6
      W(I,J)=H(J)
```

```
5       W(J,I)=W(I,J)
6       AS(1)=W(1,1)
        BS(1)=W(1,2)
        CS(1)=RHS(1)
        BS(10)=0.0
        DO 7 I=2,10
        J=I+1
        K=I-1
        AS(I)=(W(I,K)*BS(K))-(AS(K)*W(I,I))
        CS(I)=(W(I,K)*CS(K))-(RHS(I)*AS(K))
        IF(I.EQ.10) GO TO 7
        BS(I)=-AS(K)*W(I,J)
7       CONTINUE
        B(10)=CS(10)/AS(10)
        DO 8 I=2,10
        J=11-I
        K=J+1
8       B(J)=(CS(J)-(BS(J)*B(K)))/AS(J)
        DO 9 I=1,10
        J=I+1
9       G(J)=B(I)
        G(1)=0.0
        G(12)=0.0
        DO 12 I=1,12
12      B(I)=G(I)
        DO 10 I=1,11
        J=I+1
        A(I)=(B(J)-B(I))/3./H(I)
        C(I)=((Y(J)-Y(I))/H(I))-((H(I)*(B(J)+(2.*B(I))))/3.)
10      D(I)=Y(I)
        RETURN
        END
```

APPENDIX E

PRESSURE TIME HISTORIES AT THE WALL OF THE INDIAN POINT CONTAINMENT

Pressure time histories at selected points on the wall of the Indian Point containment are presented in this Appendix. Wall pressures are normalized with respect to the initial pressure in the containment, P_o, and are shown as a function of dimensionless time since initiation, tC_o/r, where C_o is the speed of sound at the initial conditions and r is the radius of the cylinder and the dome. In the Indian Point Containment r equals 20.7 m and at atmospheric initial conditions r/C_o = 0.06 sec. Results are shown for two initiation points and two dimensionless heat release rates, q/RT_0 = 17 and 23.

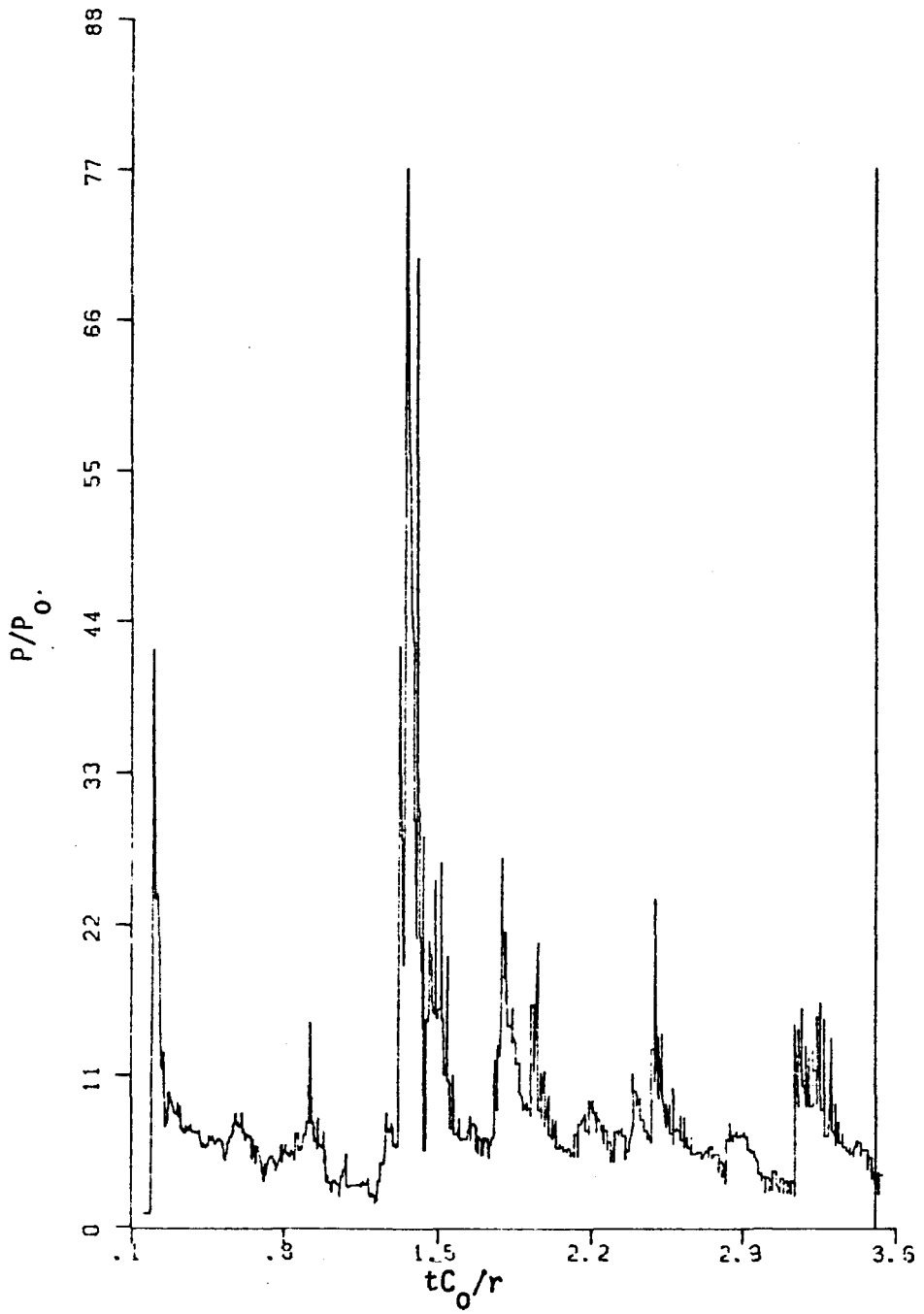

Fig. E.1 - Wall Pressure History at the Junction of the Base and the Cylinder (q/RT_o = 17; Initiation at Base Center)

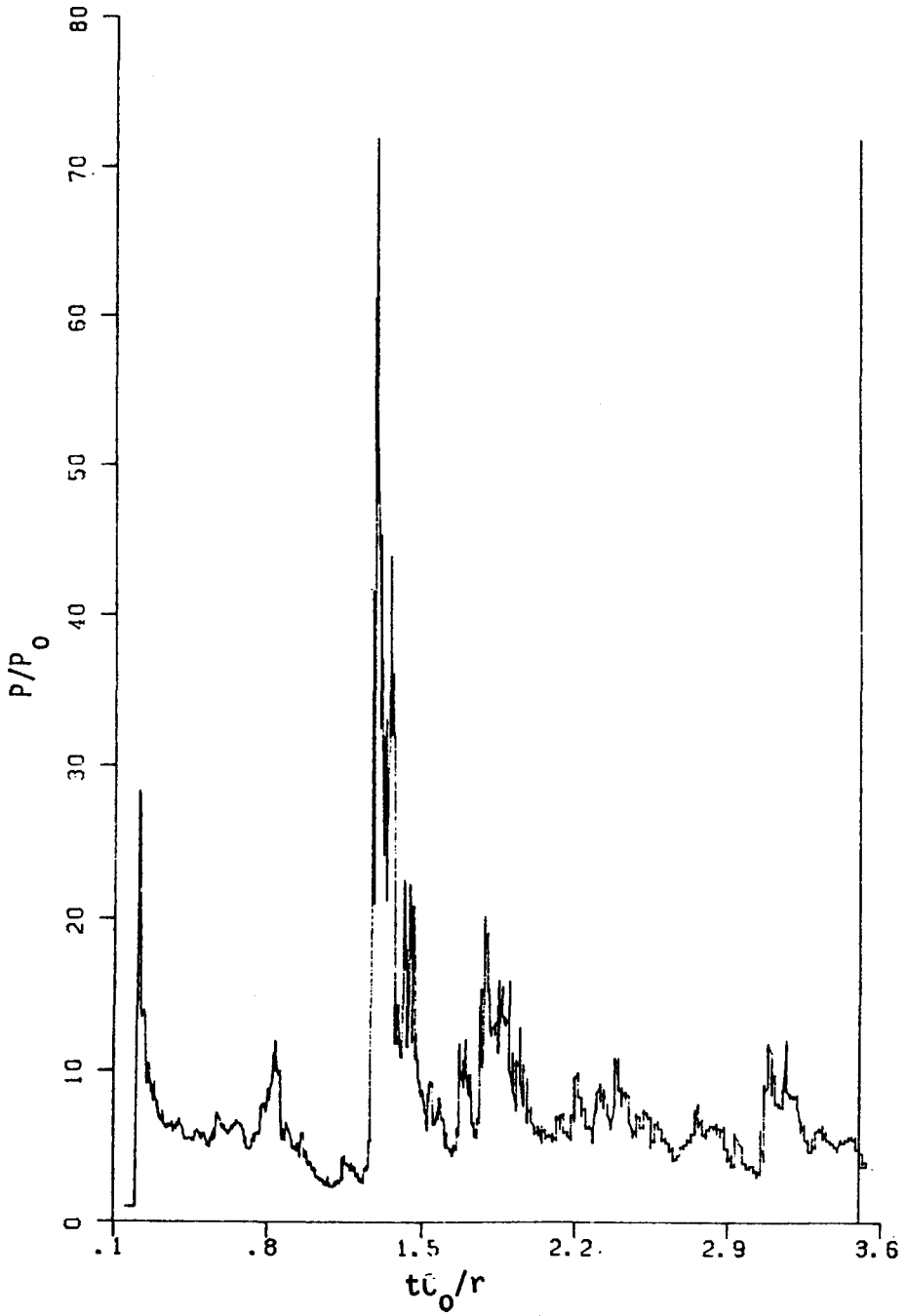

Fig. E.2 - Wall Pressure History at Elevation 6.0 m of the Cylinder (q/RT_0 = 17; Initiation at Base Center)

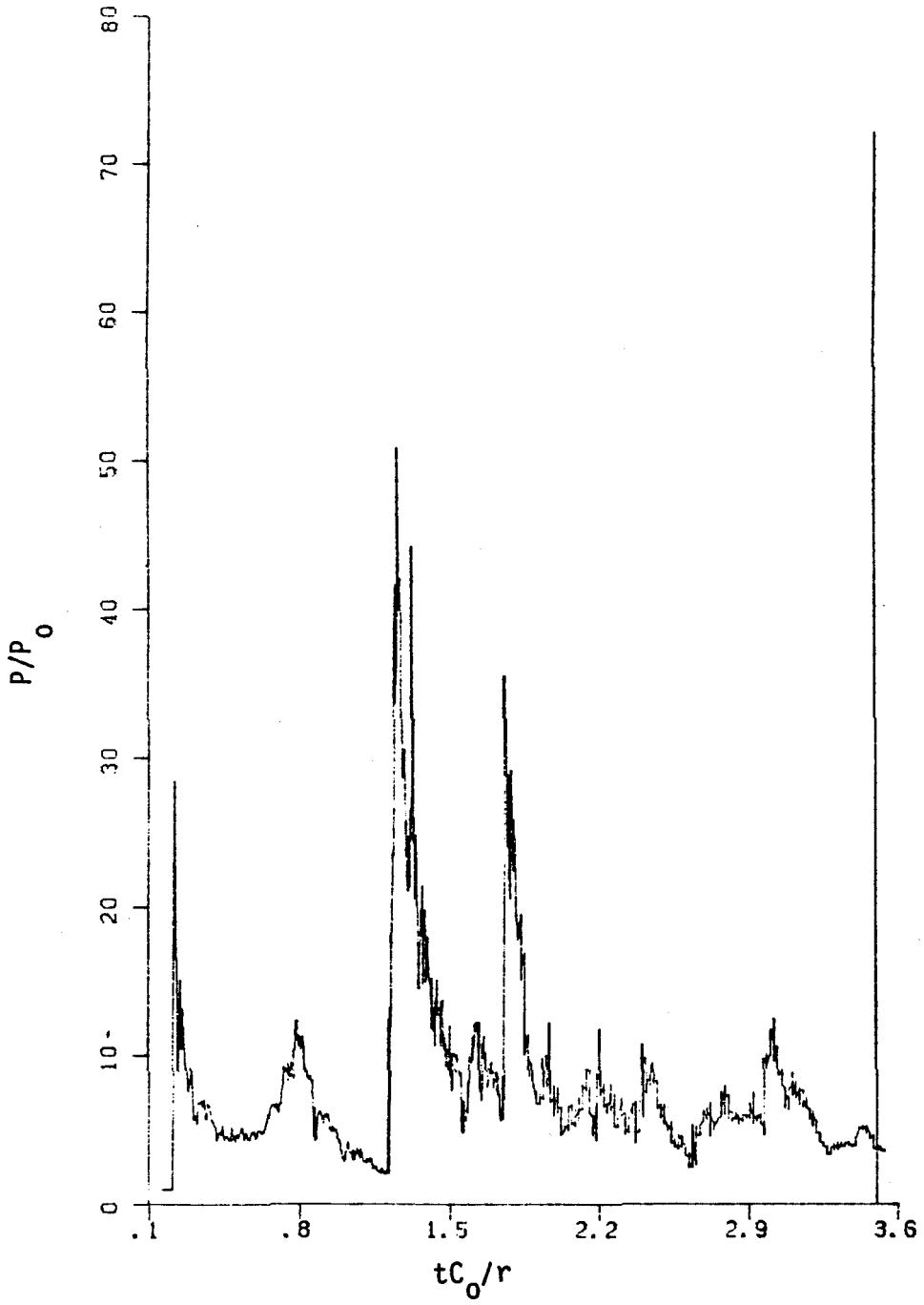

Fig. E.3 - Wall Pressure History at Elevation 12.0 m of the Cylinder (q/RT_o = 17; Initiation at Base Center)

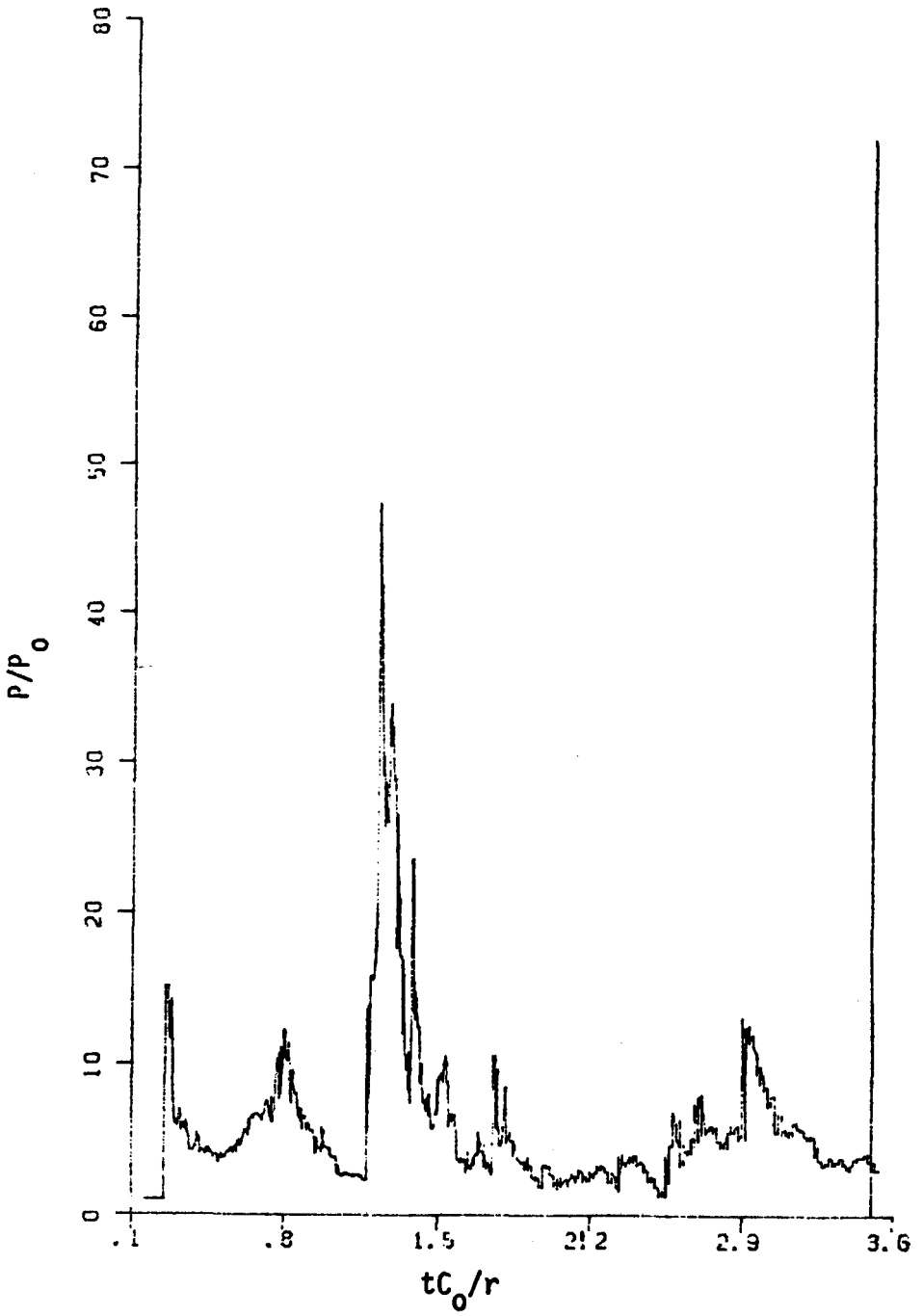

Fig. E.4 - Wall Pressure History at Elevation 18.0 m of the Cylinder (q/RT_0 = 17; Initiation at Base Center)

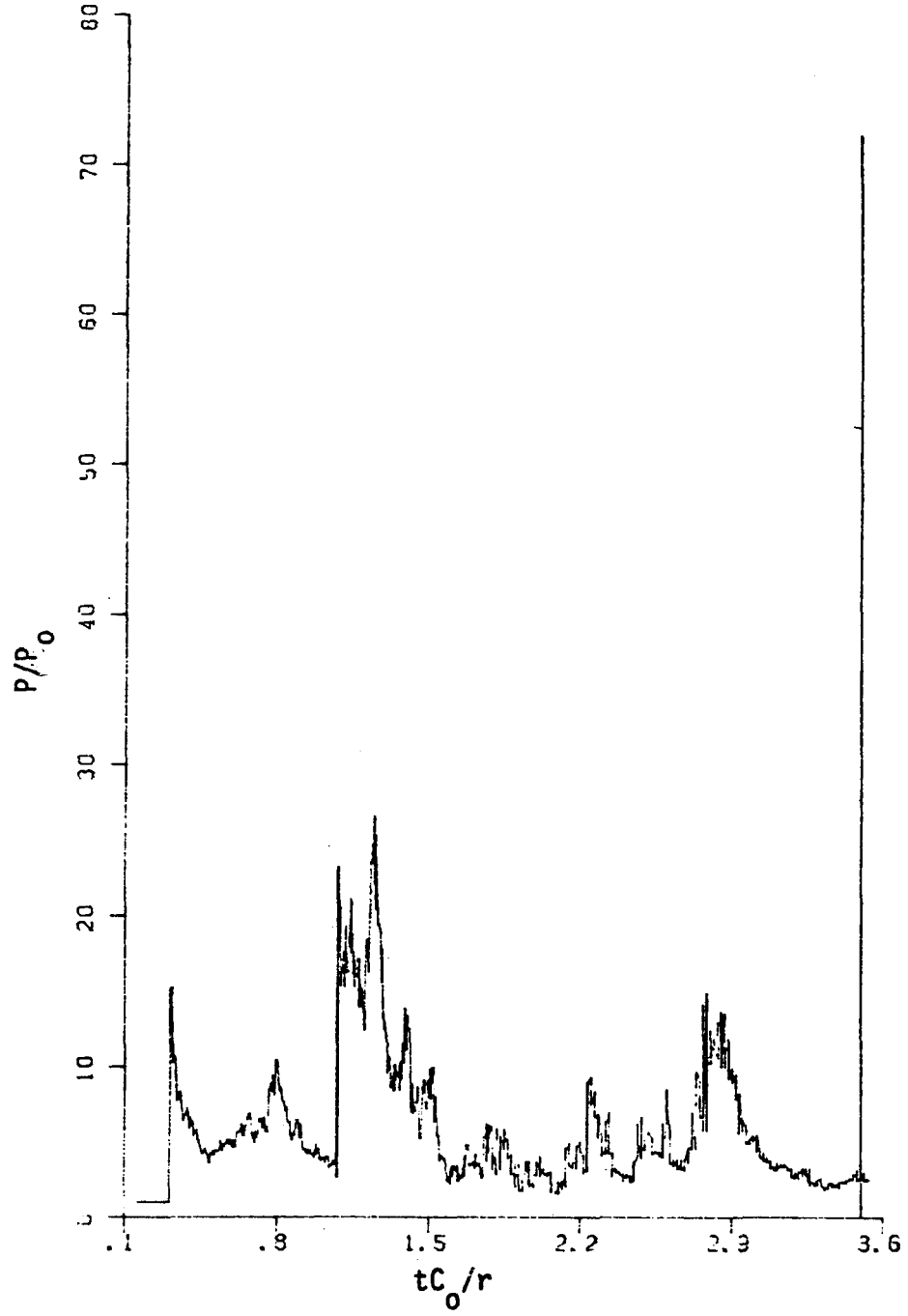

Fig. E.5 - Wall Pressure History at Elevation 24.0 m of the Cylinder (q/RT_o = 17; Initiation at Base Center)

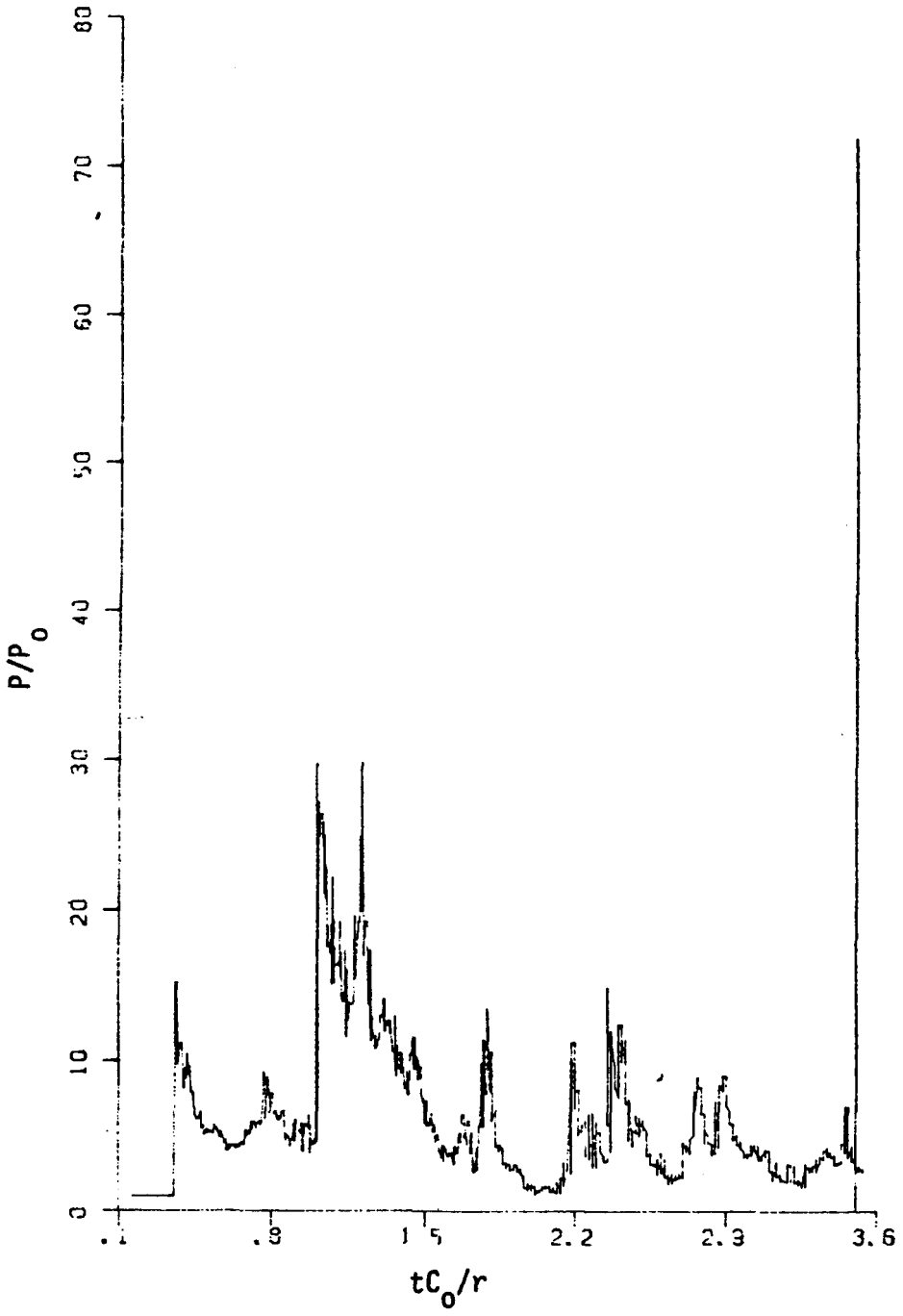

Fig. E.6 - Wall Pressure History at Elevation 30.0 m of the Cylinder (q/RT_0 = 17; Initiation at Base Center)

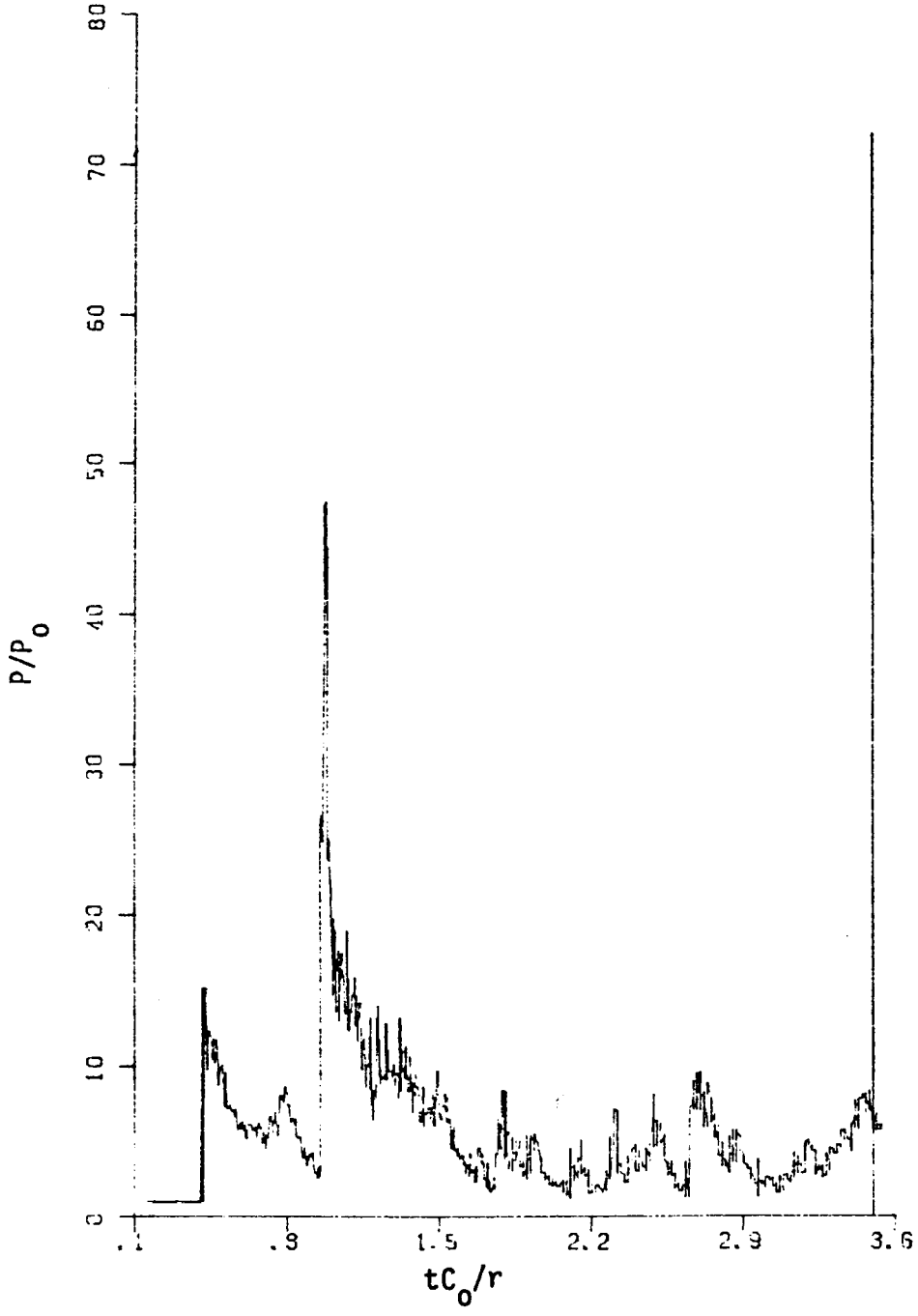

Fig. E.7 - Wall Pressure History at Elevation 36.0 m of the Cylinder (q/RT_o = 17; Initiation at Base Center)

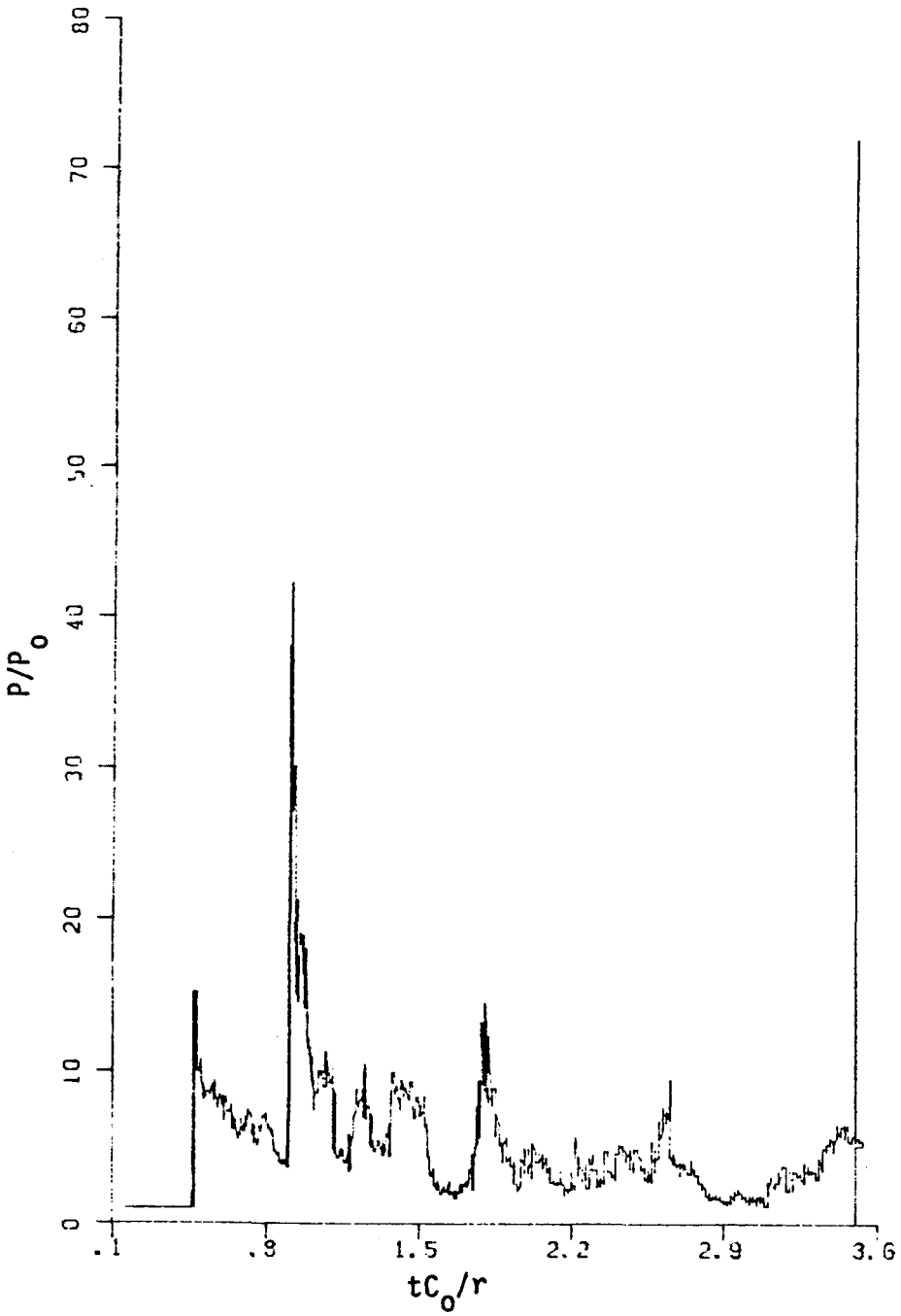

Fig. E.8 - Wall Pressure History at Elevation 42.0 m of the Cylinder (q/RT_o = 17; Initiation at Base Center)

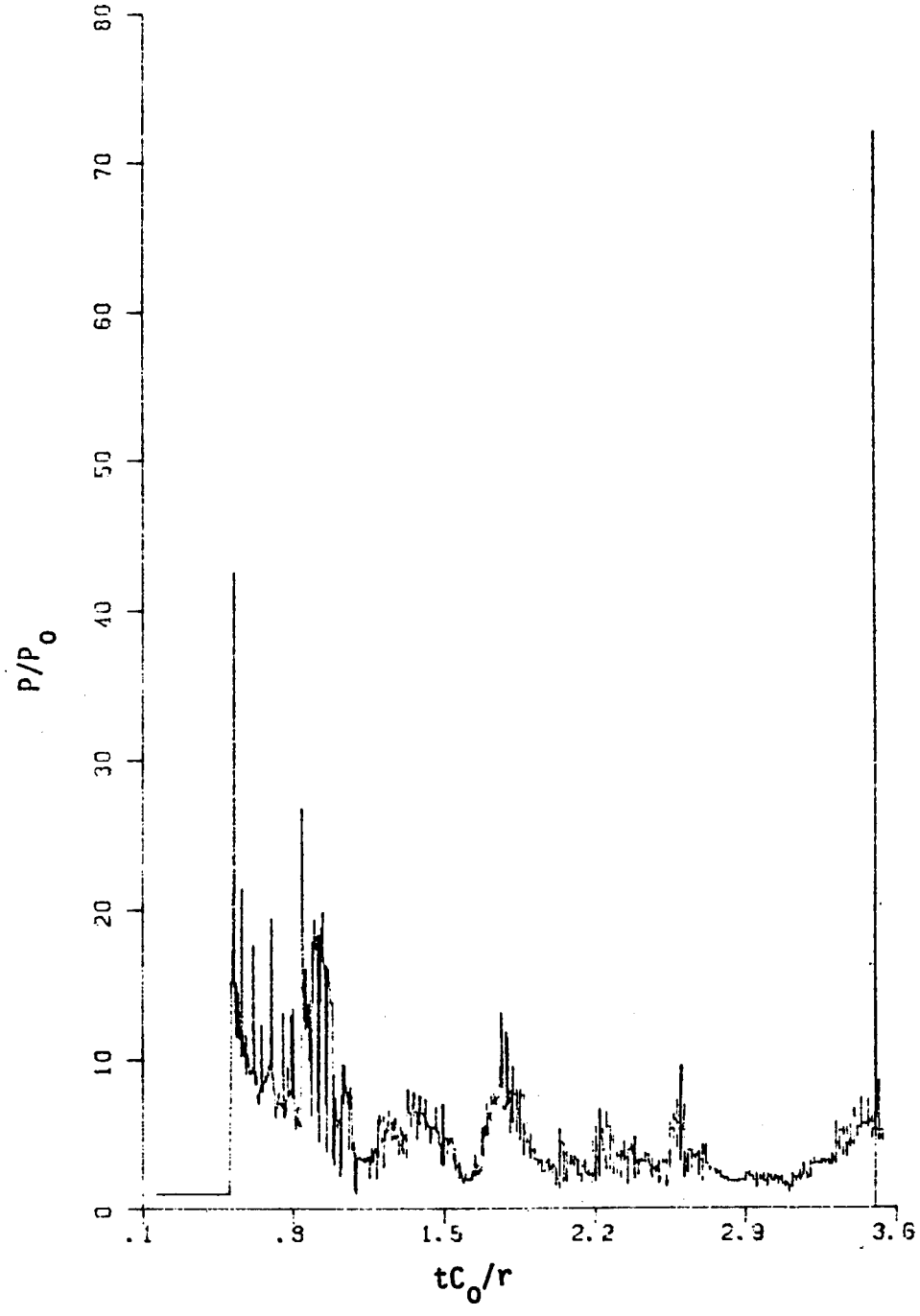

Fig. E.9 - Dome Pressure History at Elevation 47.0 m and Radius 20.7 m (q/RT_o = 17; Initiation at Base Center)

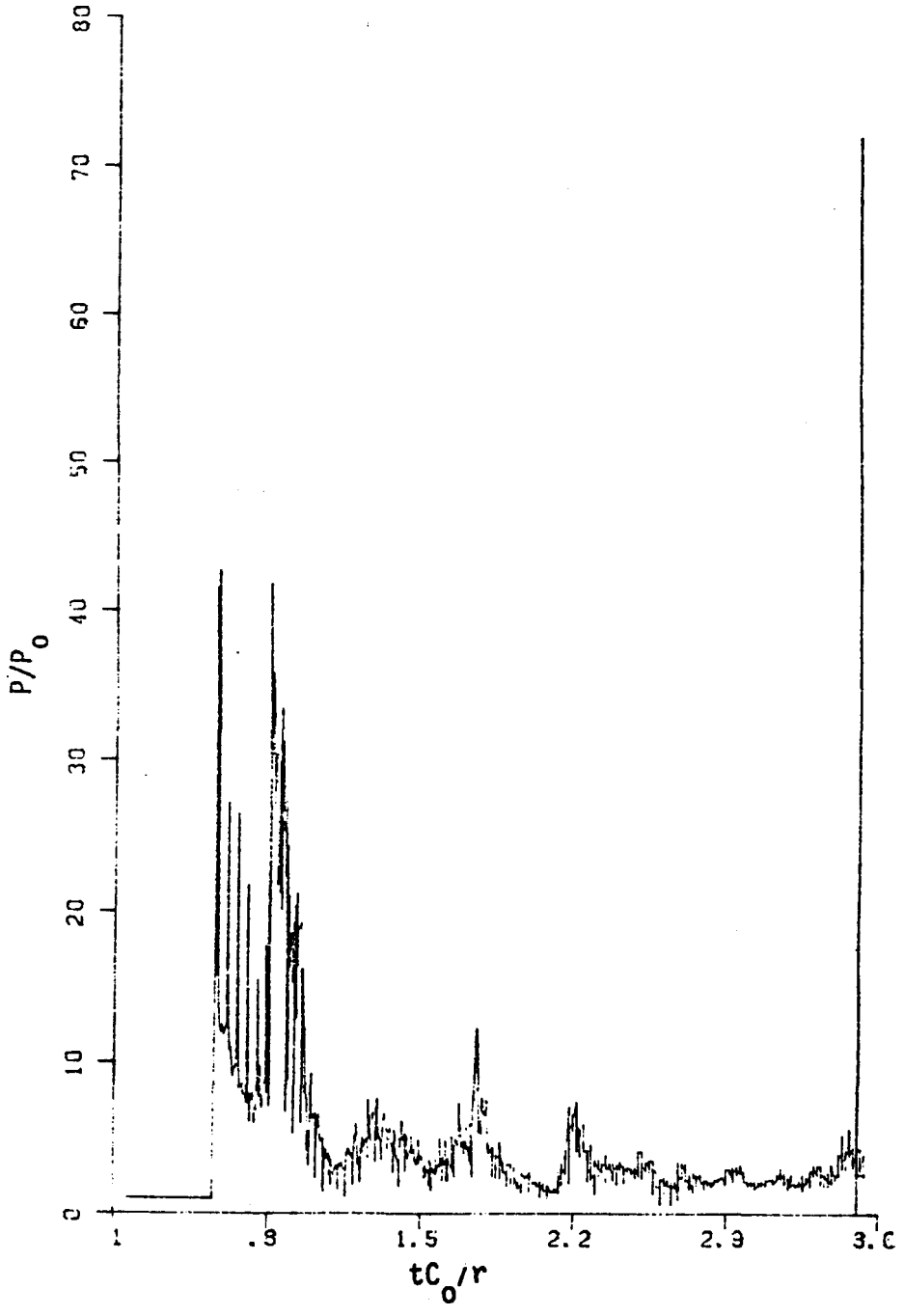

Fig. E.10 - Dome Pressure History at Elevation 51.0 and Radius 19.4 m (q/RT_o = 17; Initation at Base Center)

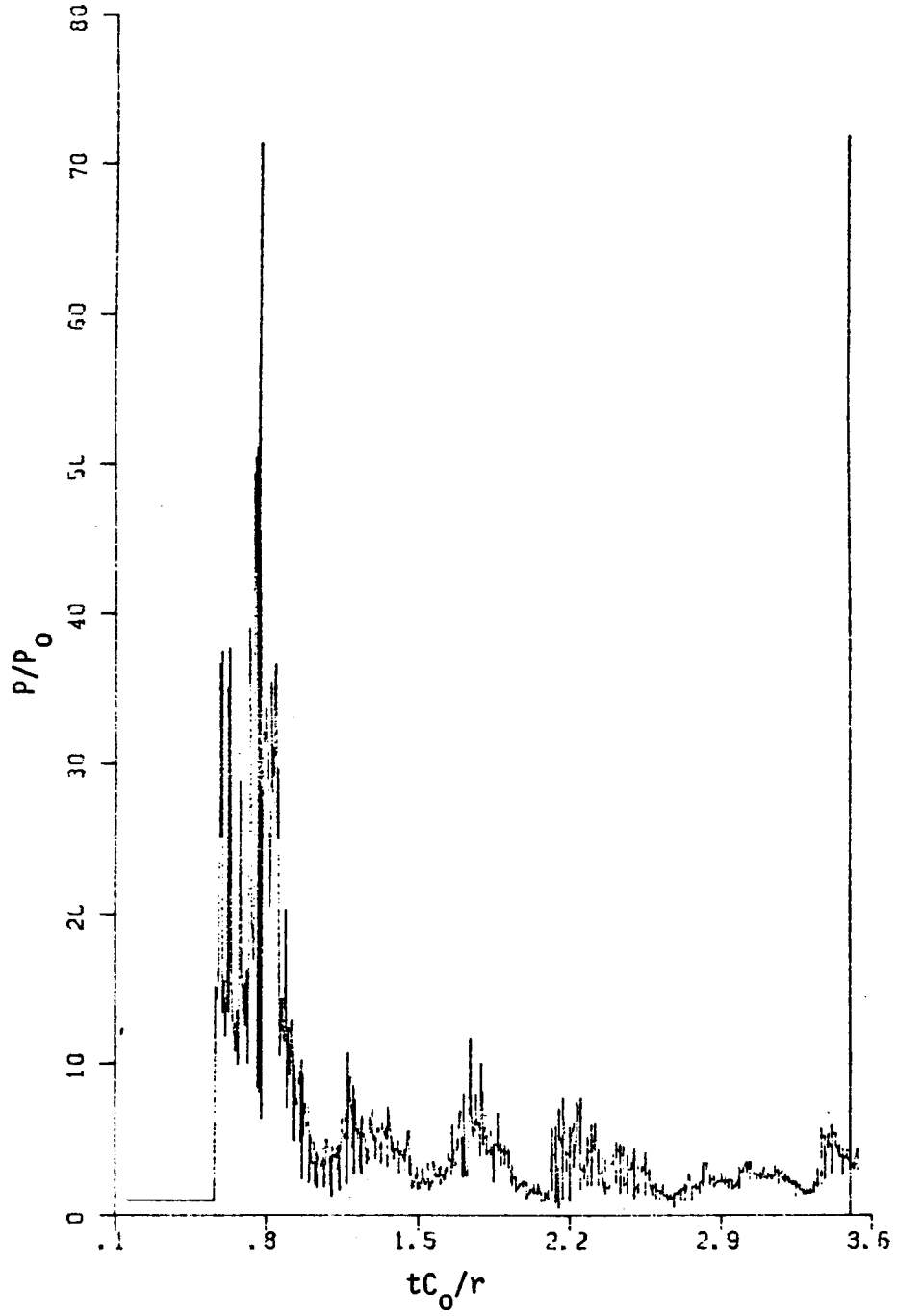

Fig. E.11 - Dome Pressure History at Elevation 56.0 and Radius 17.6 m (q/RT_o = 17; Initiation at Base Center)

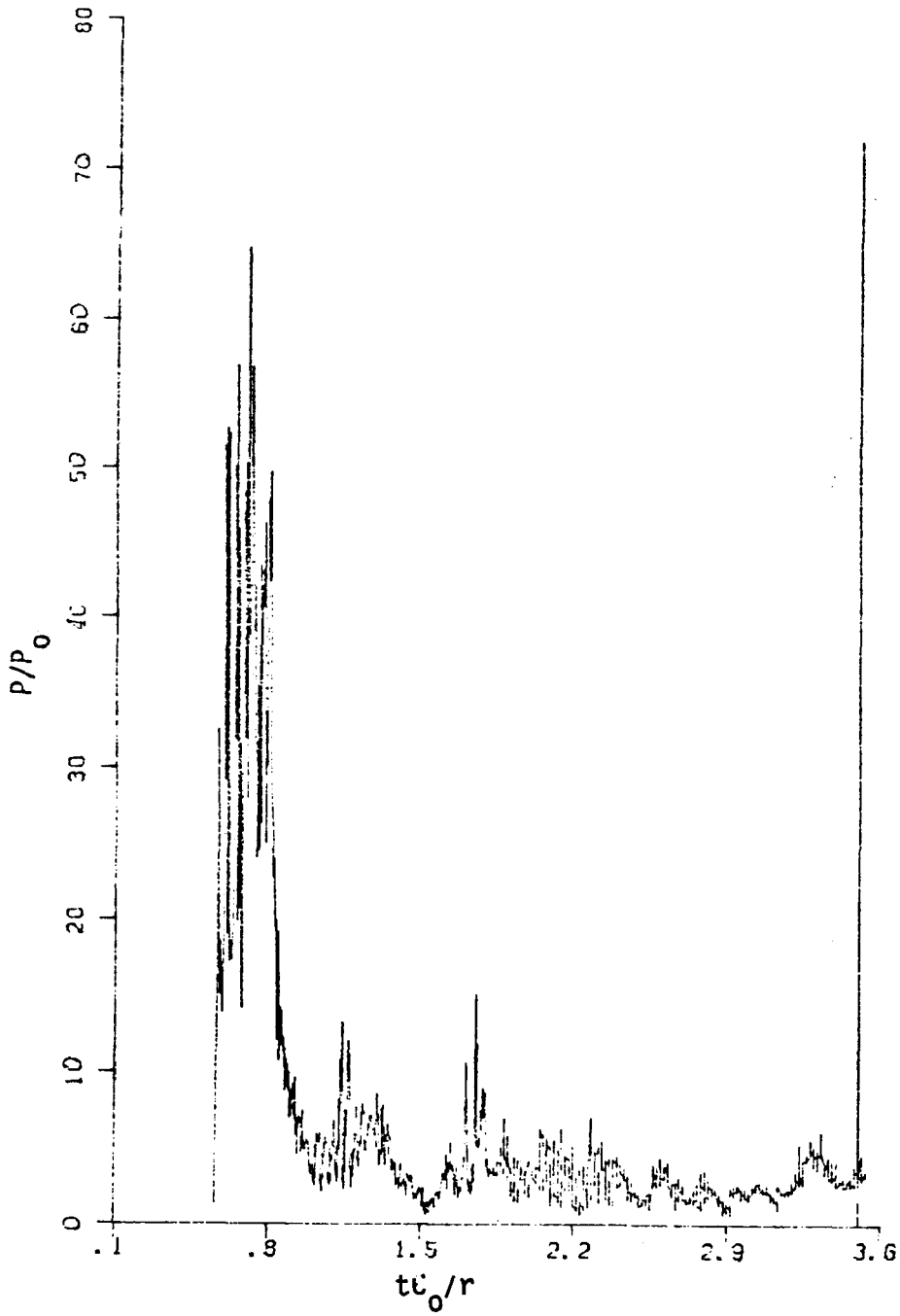

Fig. E.12 - Dome Pressure History at Elevation 61.0 and Radius 13.6 m (q/RT_o = 17; Initiation at Base Center)

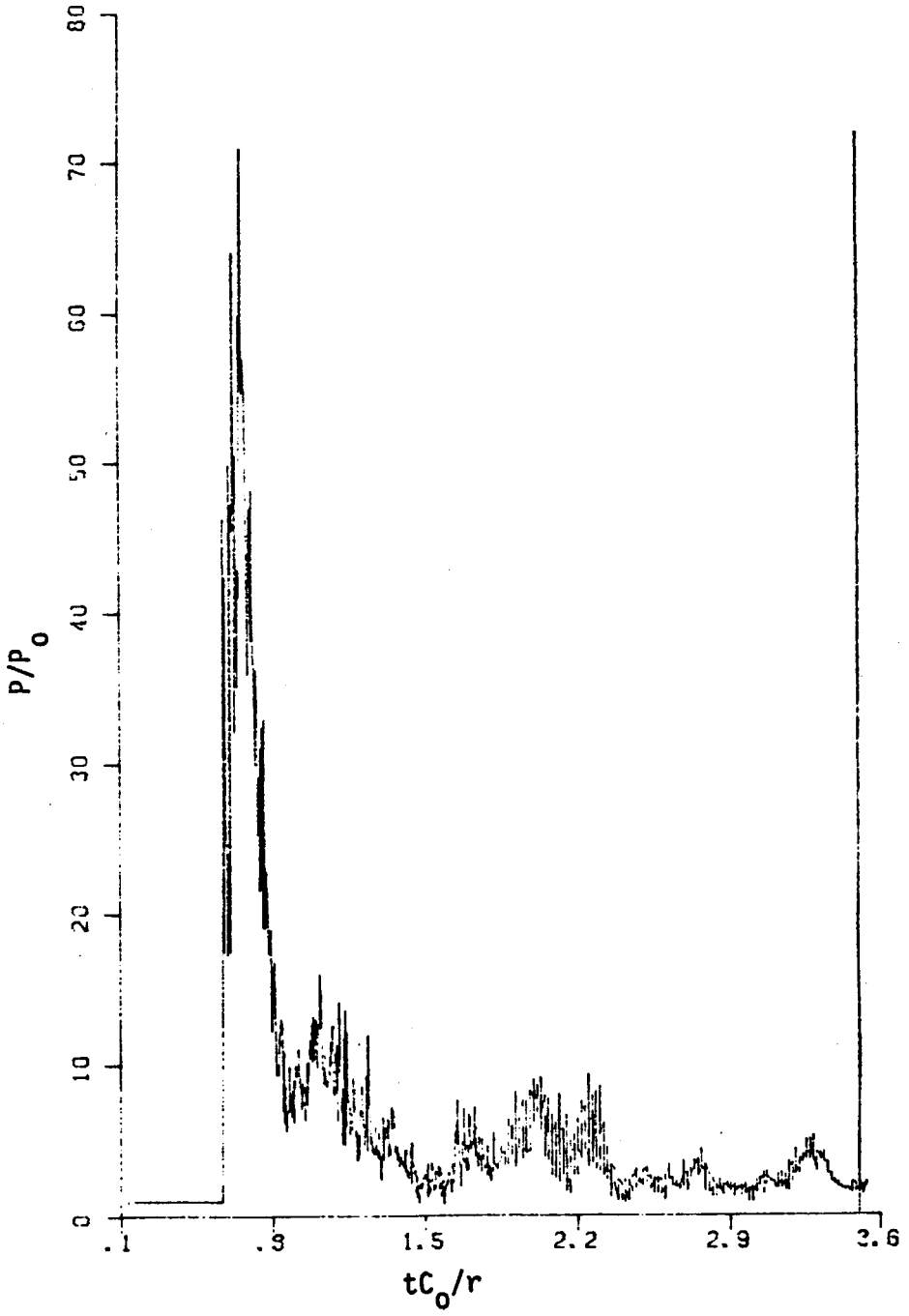

Fig. E.13 - Dome Pressure History at Elevation 64.0 m and Radius 9.6 m (q/RT_o = 17; Initiation at Base Center)

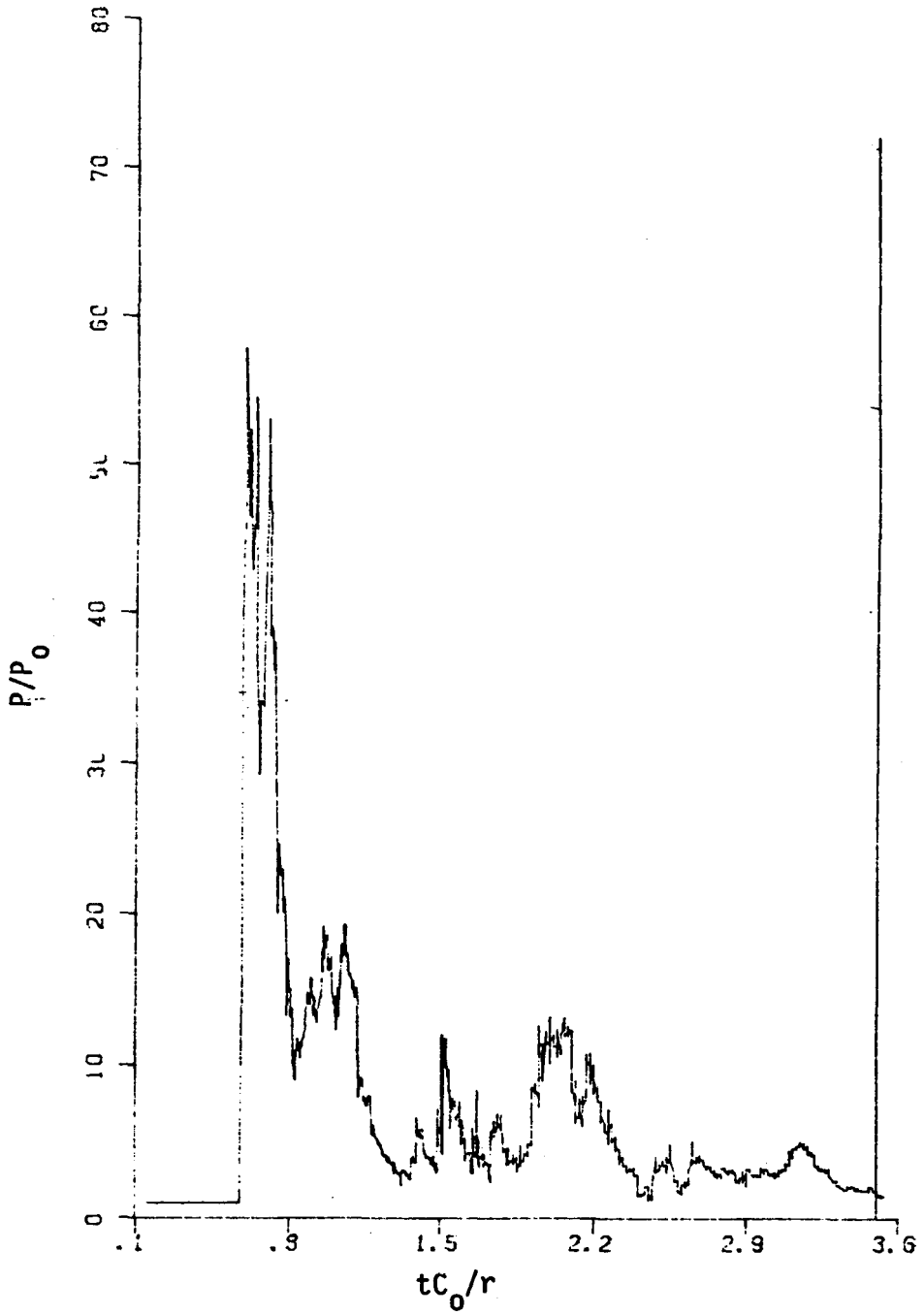

Fig. E.14 - Dome Pressure History at Elevation 66.0 m and Radius 9.6 m (η/RT_o = 17; Initiation at Base Center)

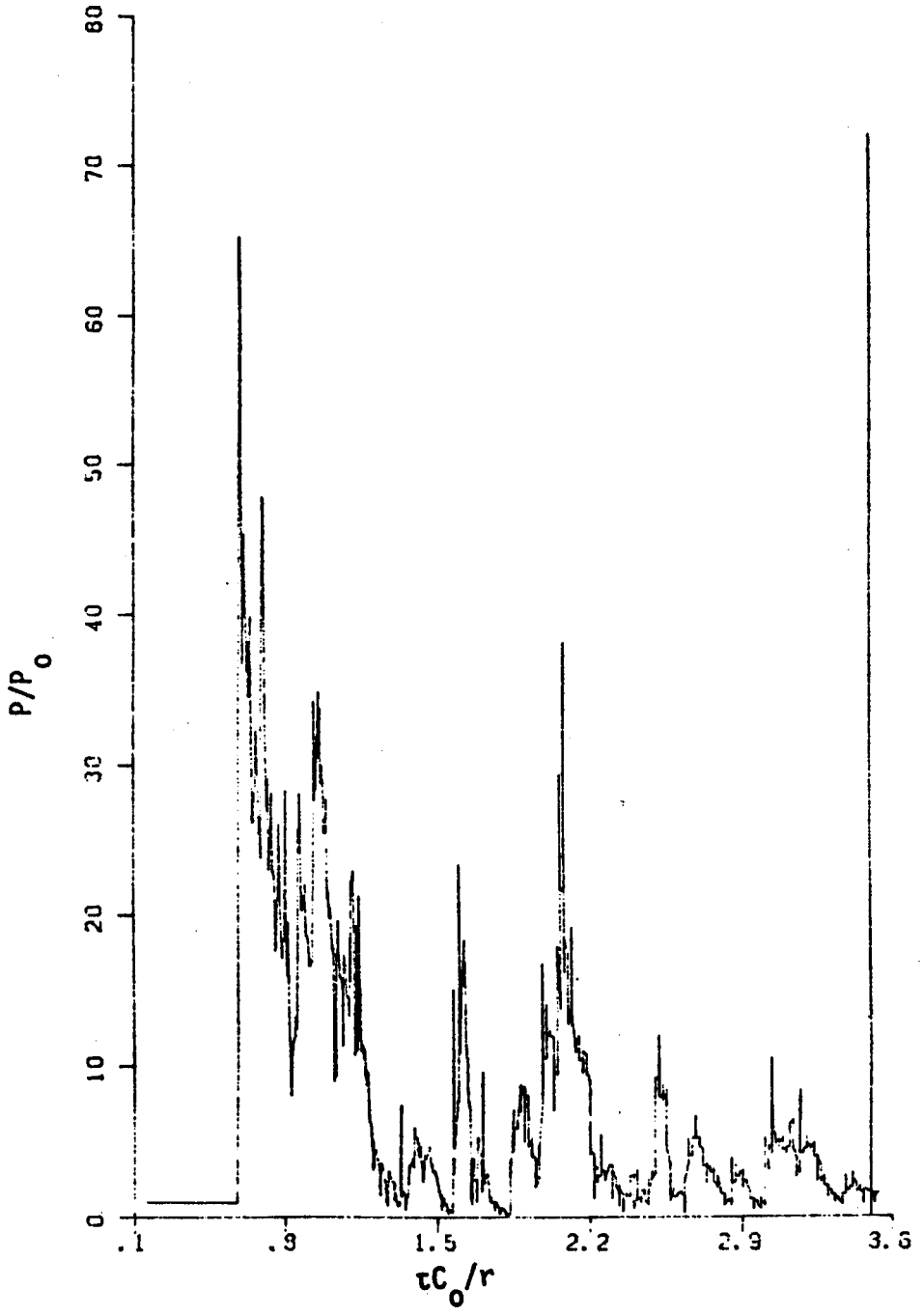

Fig. E.15 - Pressure History at the Apex of the Dome (q/RT_o = 17; Initiation at Base Center)

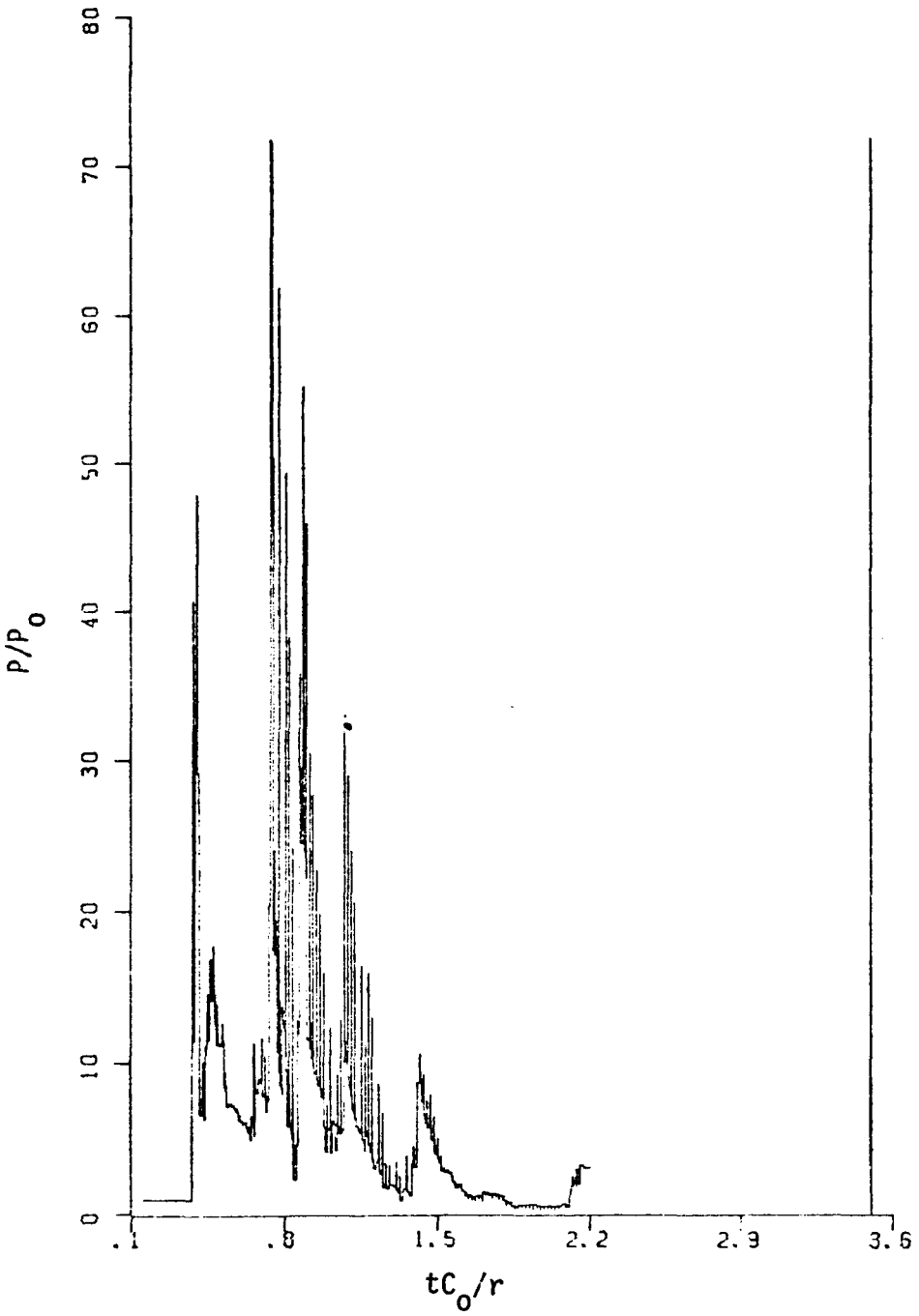

Fig. E.16 - Wall Pressure History at the Junction of the Base and the Cylinder (q/RT_o = 17; Initiation 34.5 Above Base)

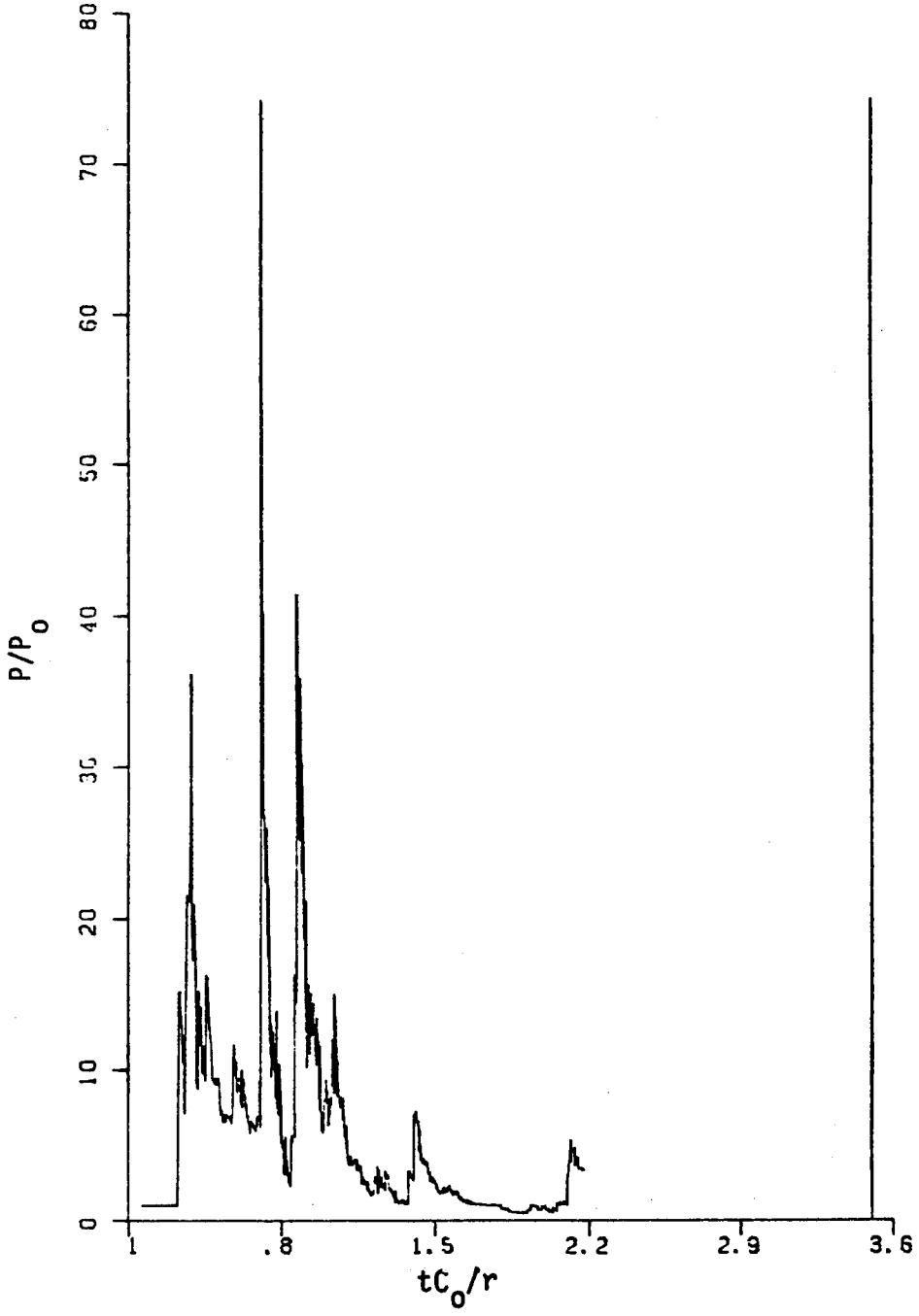

Fig. E.17 - Wall Pressure History at Elevation 6.0 m of the Cylinder (q/RT_o = 17; Initiation 34.5 m Above Base)

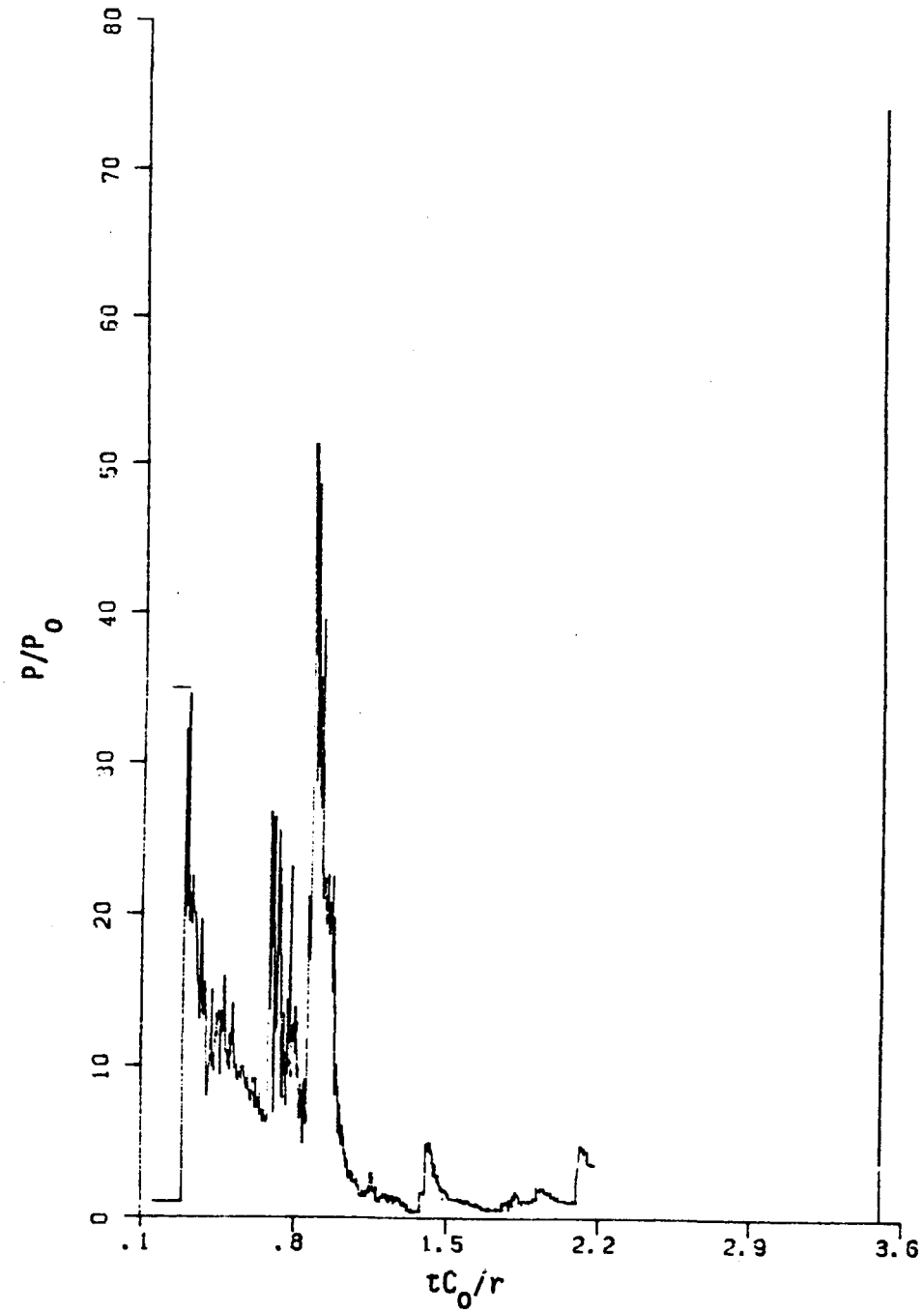

Fig. E.18 - Wall Pressure History at Elevation 12.0 m of the Cylinder (q/RT_o = 17; Initiation 34.5 Above Base)

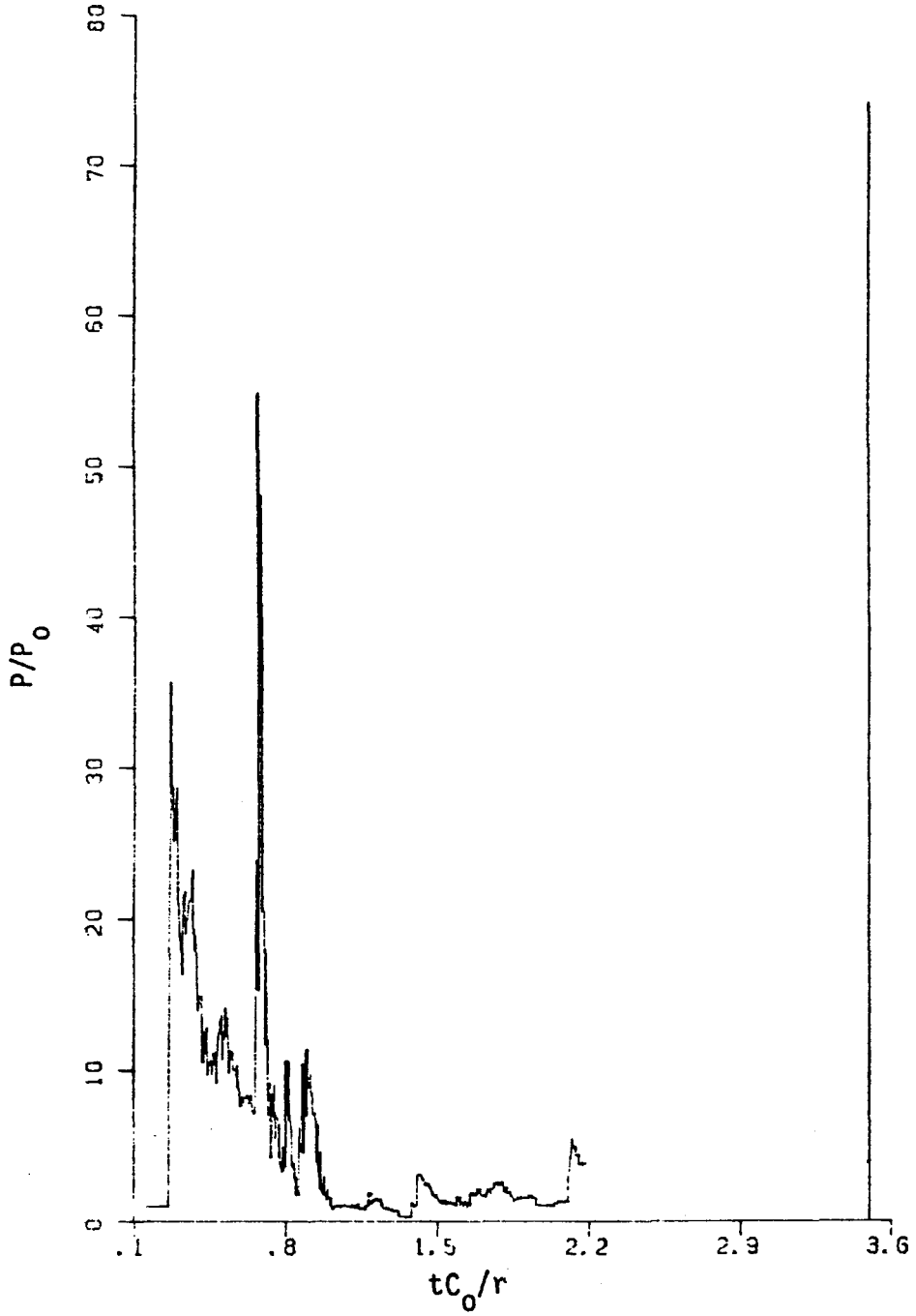

Fig. E.19 - Wall Pressure History at Elevation 18.0 m of the Cylinder (q/RT_o = 17; Initiation 34.5 m Above Base)

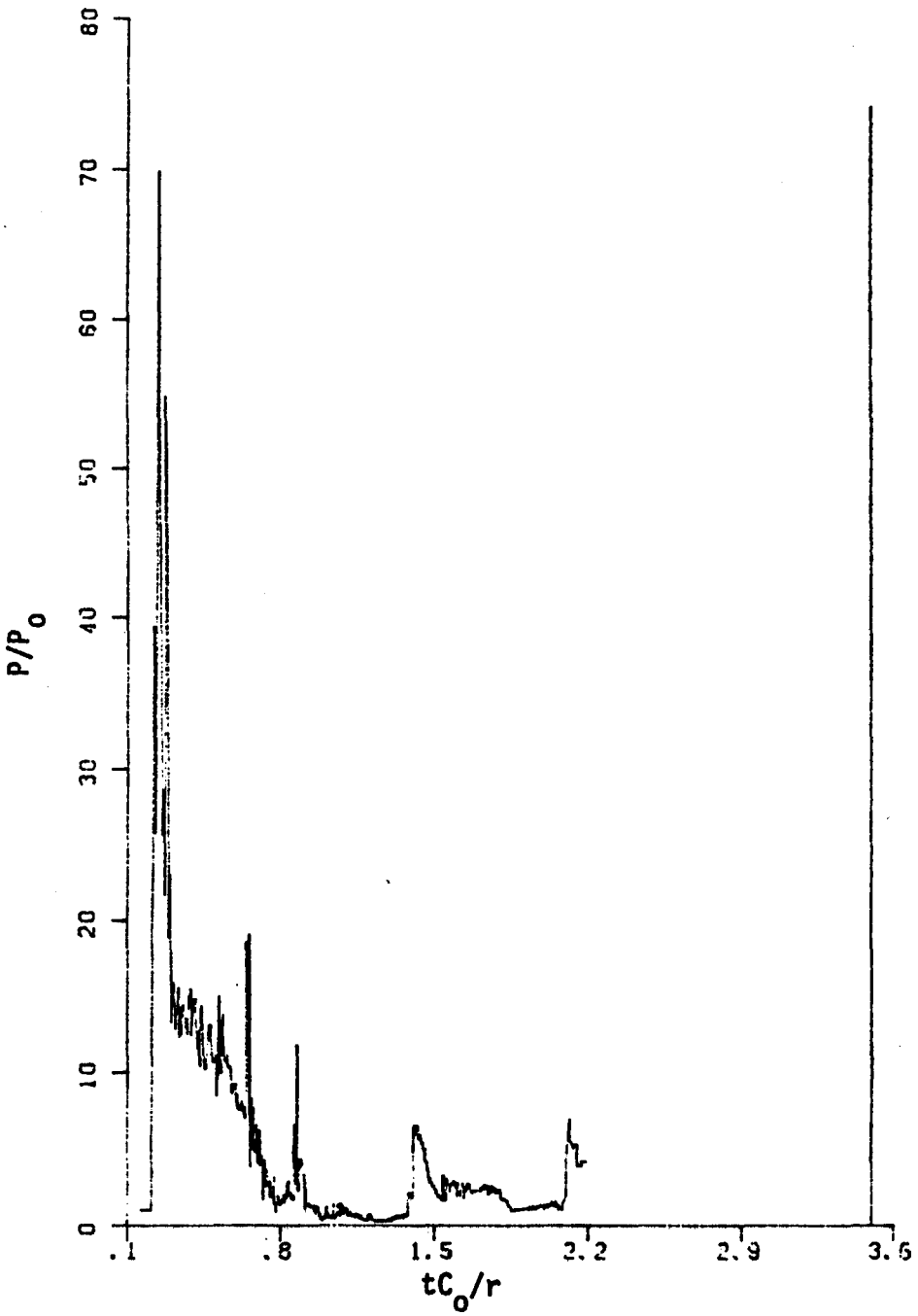

Fig. E.20 - Wall Pressure History at Elevation 24.0 m of the Cylinder (a/RT_0 = 17; Initiation 34.5 m Above Base)

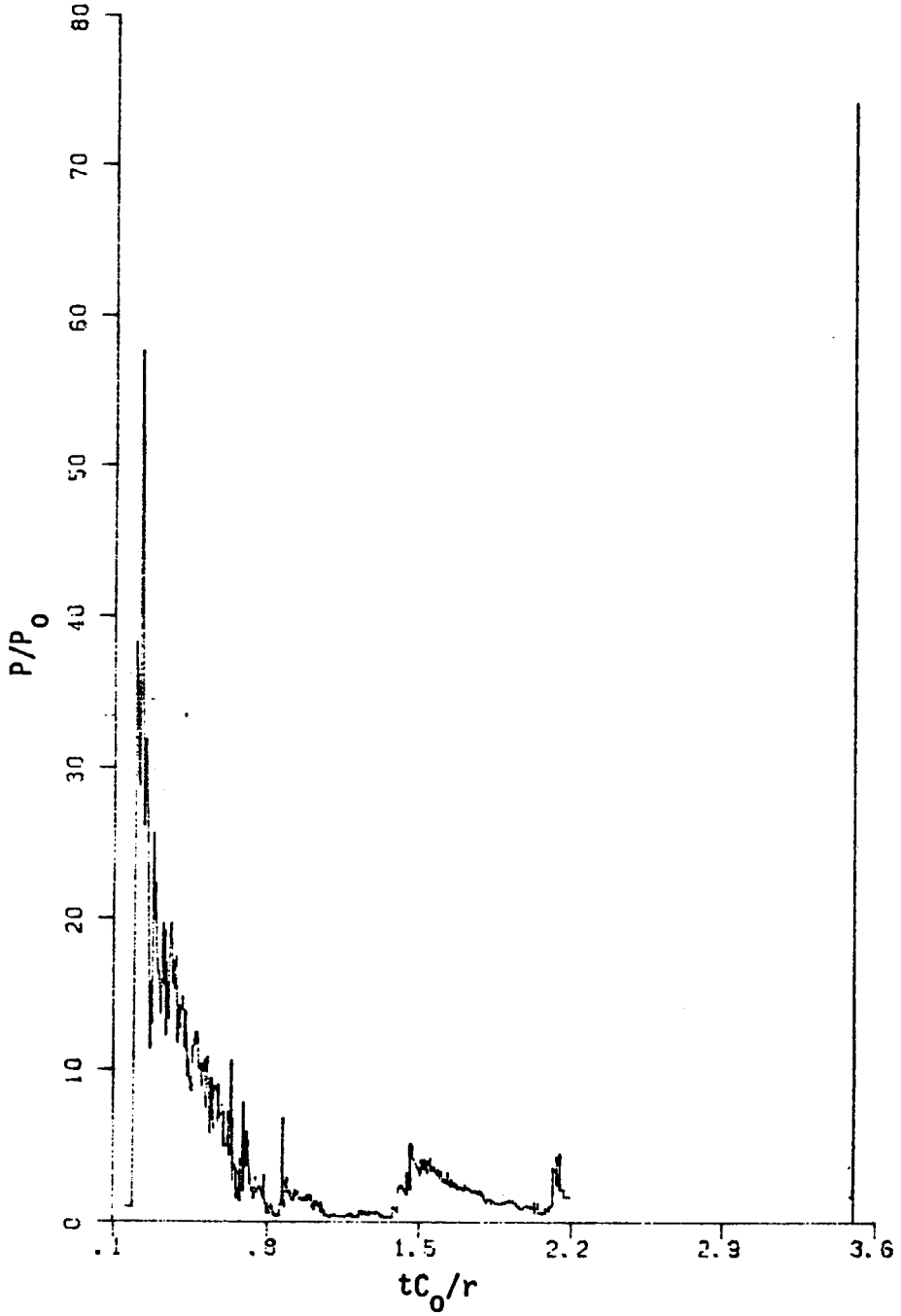

Fig. E.21 - Wall Pressure History at Elevation 30.0 m of the Cylinder (q/RT_o = 17; Initiation 34.5 m Above Base)

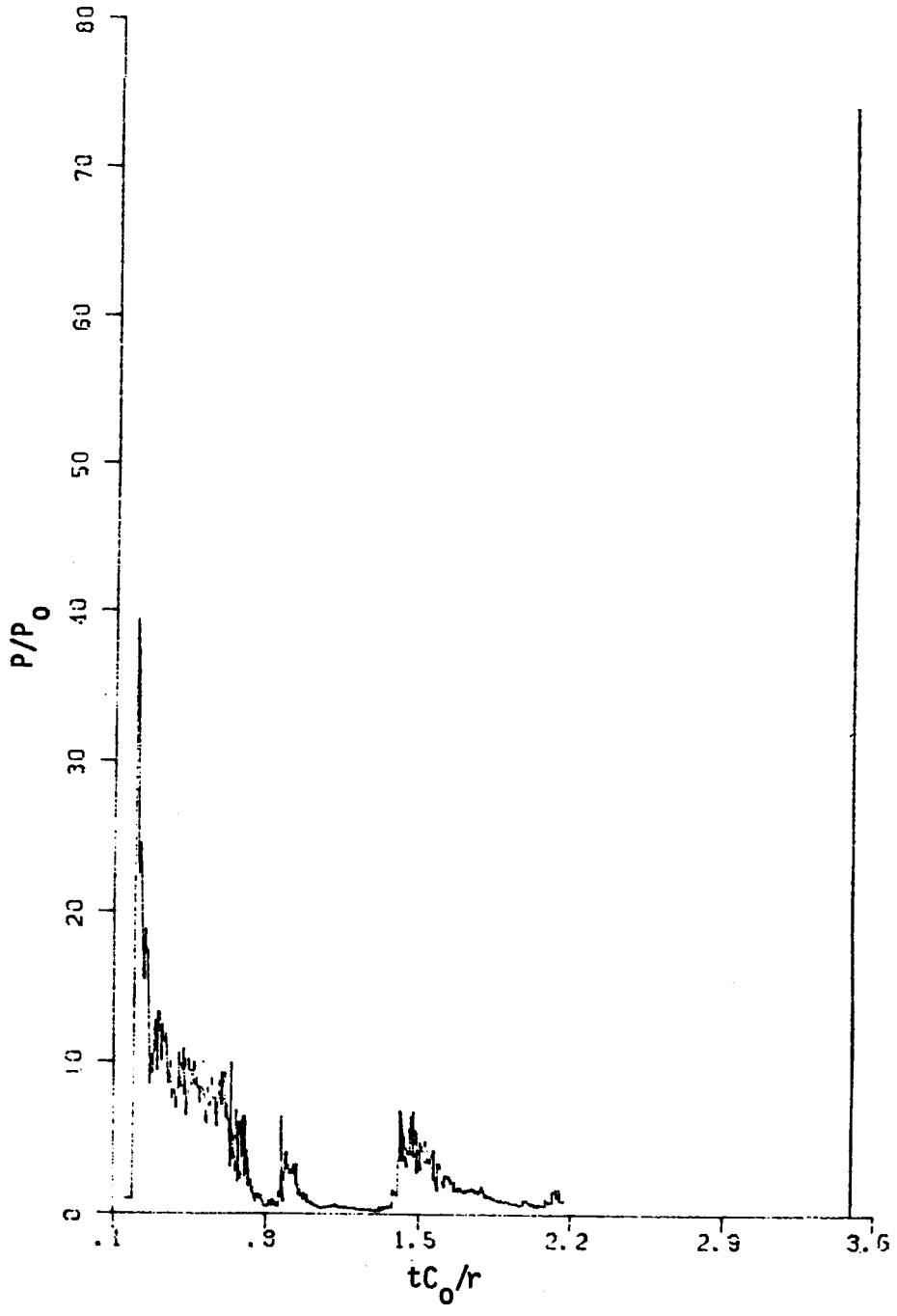

Fig. E.22 - Wall Pressure History at Elevation 36.0 m of the Cylinder (q/RT_0 = 17; Initiation 34.5 m Above Base)

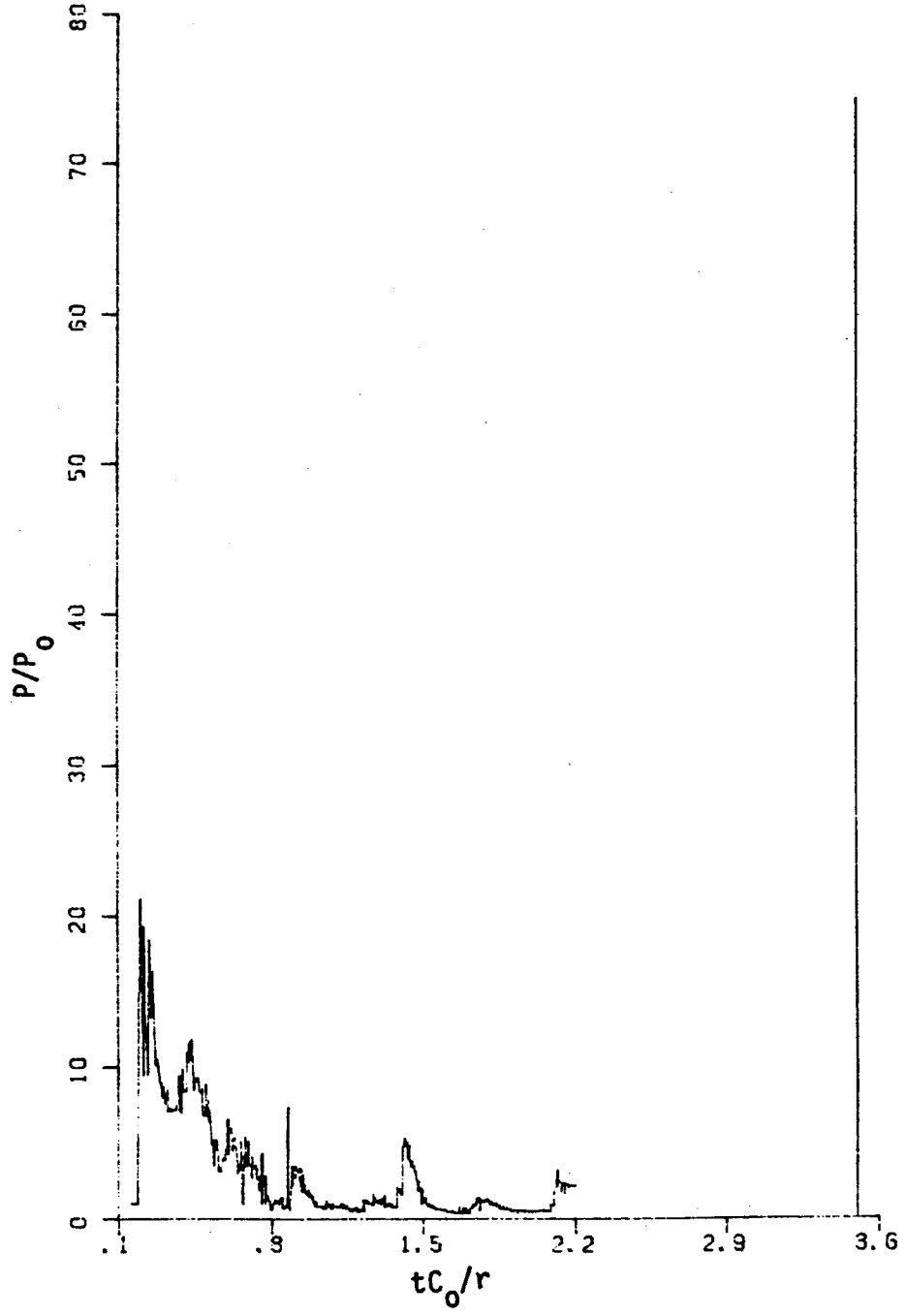

Fig. E.23 - Wall Pressure History at Elevation 42.0 m of the Cylinder (q/RT_o = 17; Initiation 34.5 m Above Base)

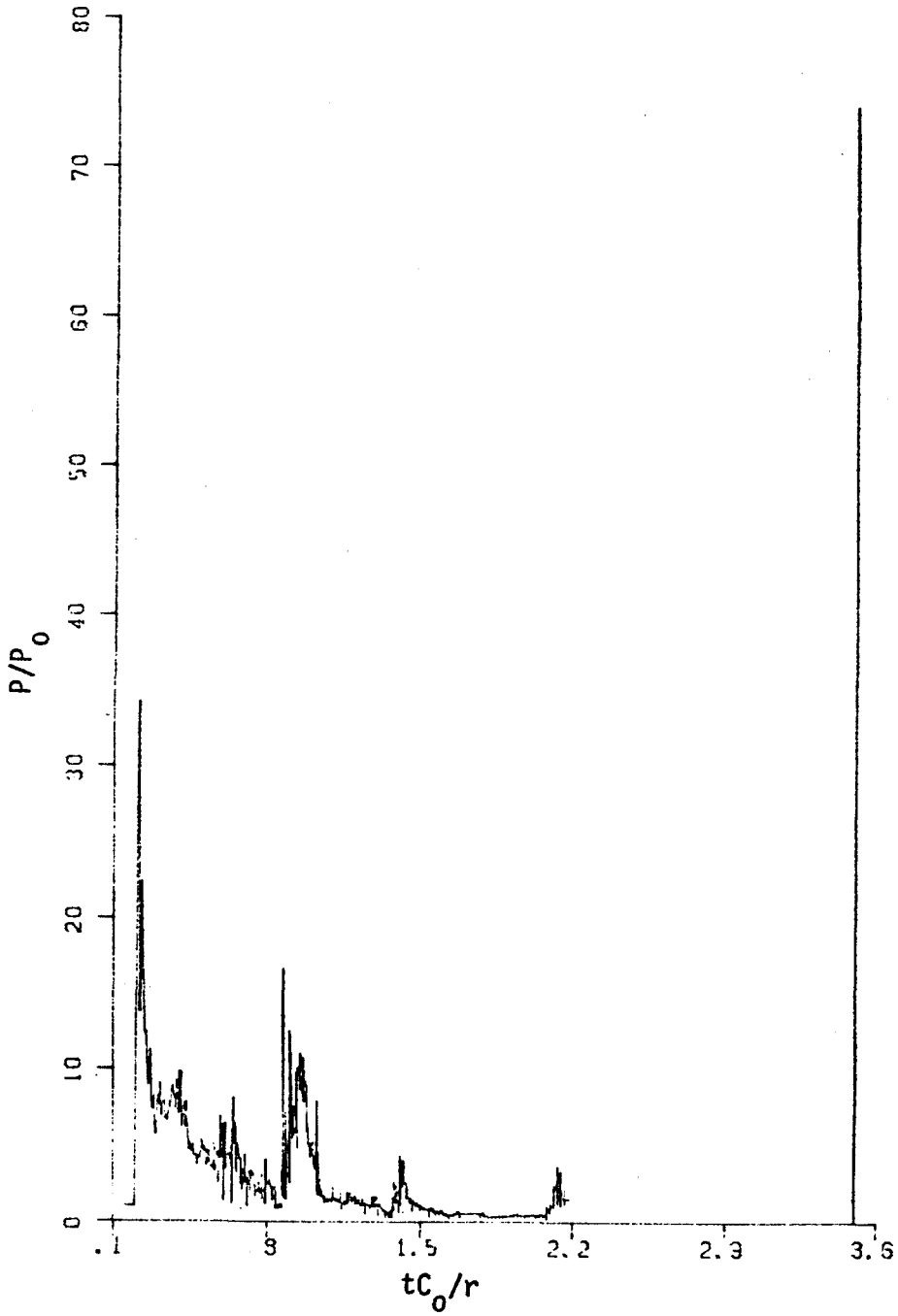

Fig. E.24 - Dome Pressure History at Elevation 47.0 m and Radius 20.7 m (q/RT_o = 17; Initiation 34.5 m Above Base)

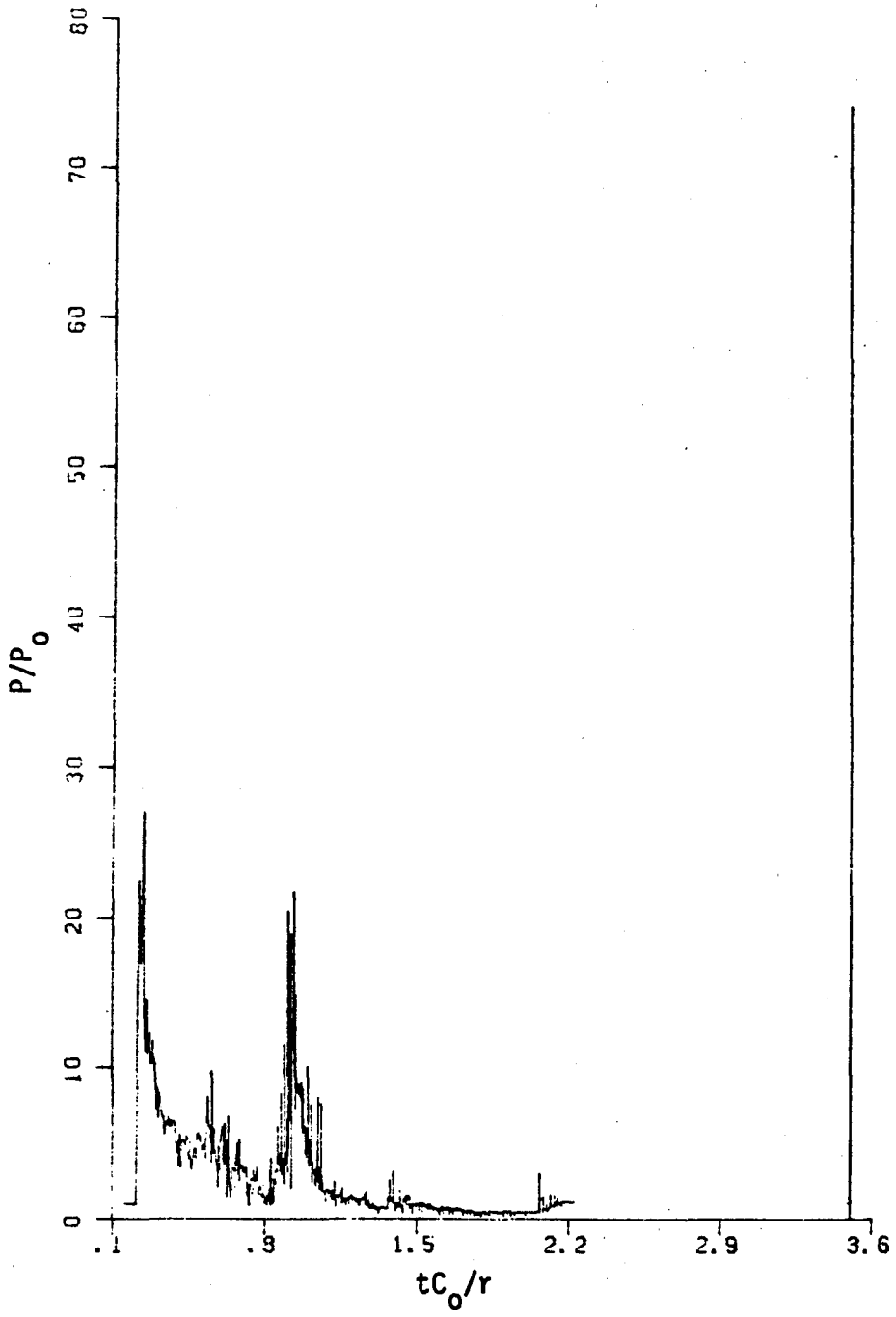

Fig. E.25 - Dome Pressure History at Elevation 51.0 m and Radius 19.4 m (q/RT_o = 17; Initiation 34.5 m Above Base)

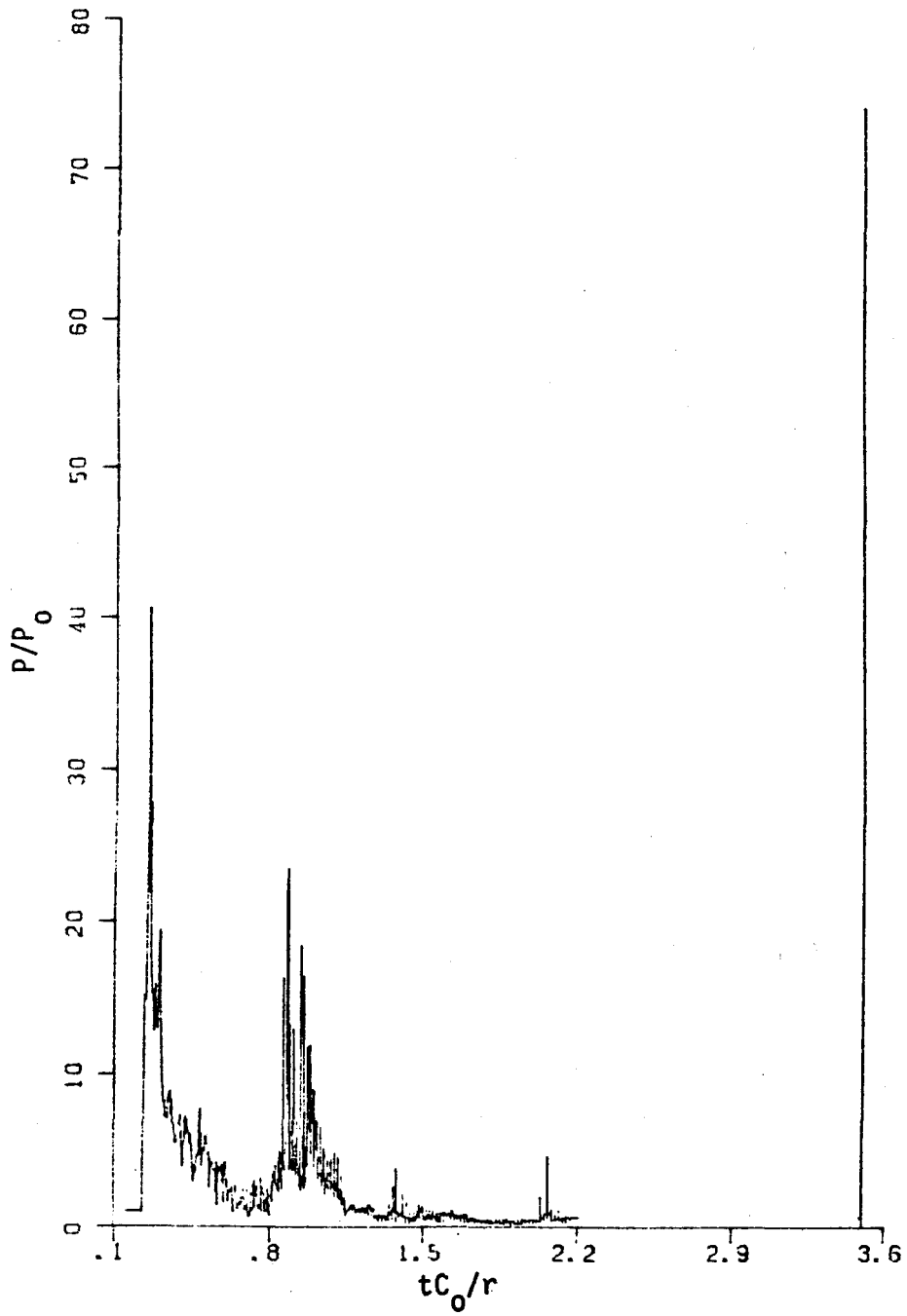

Fig. E.26 - Dome Pressure History at Elevation 56.0 m and Radius 17.1 m (q/RT_o = 17; Initiation 34.5 m Above Base)

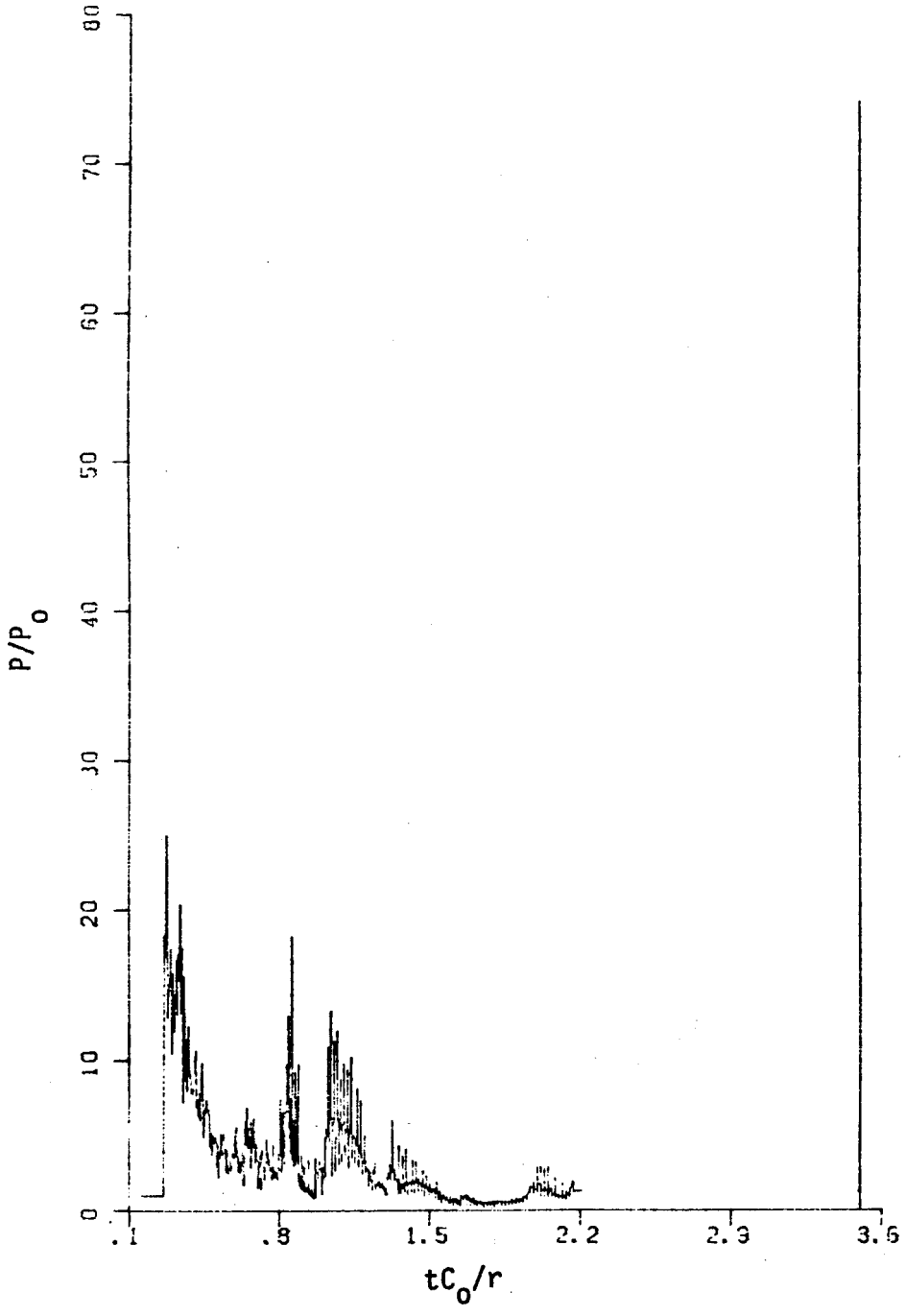

Fig. E.27 - Dome Pressure History at Elevation 61.0 m and Radius 13.6 m (q/RT_o = 17; Initiation 34.5 m Above Base)

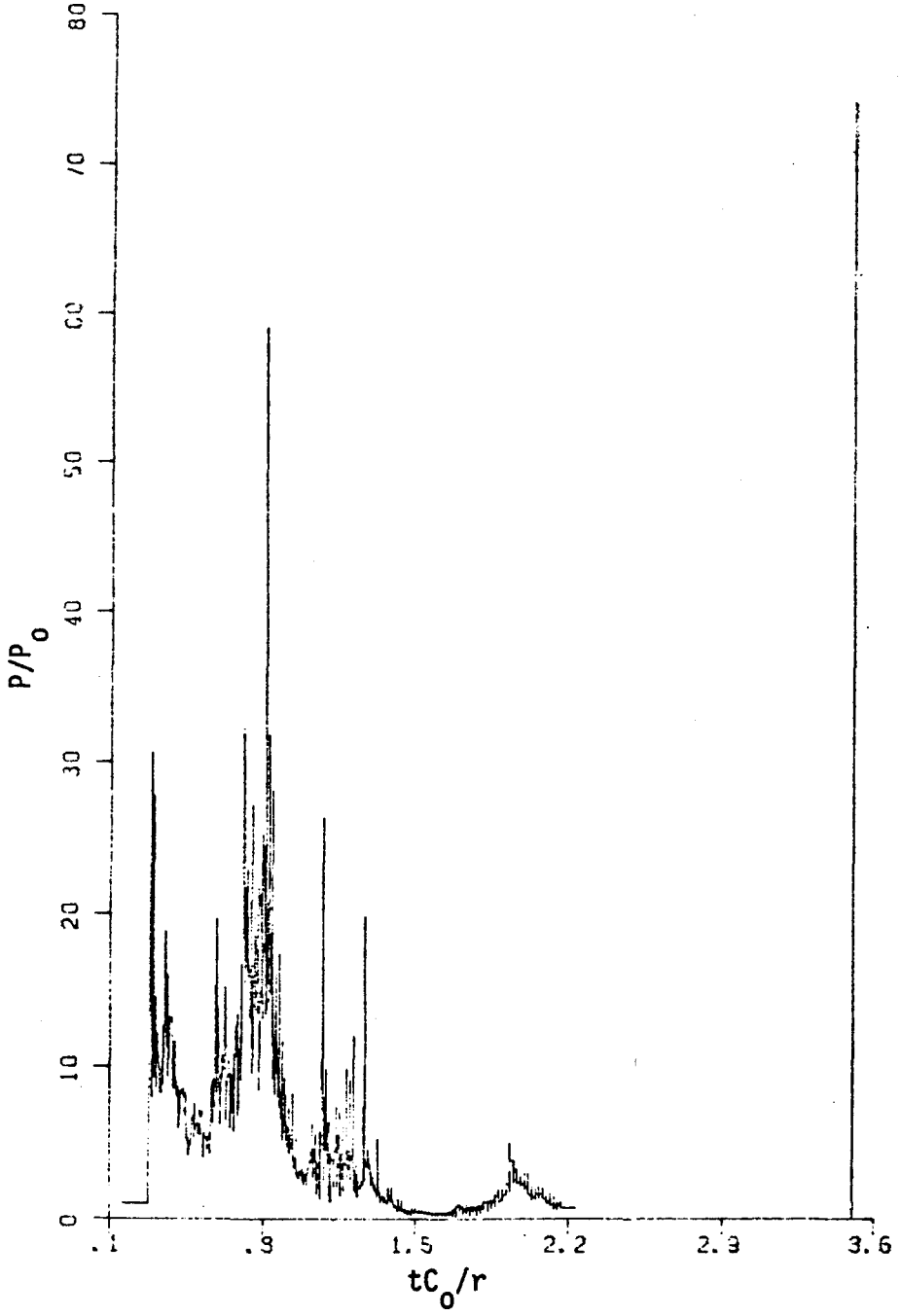

Fig. E.28 - Dome Pressure History at Elevation 64.0 m and Radius 9.6 m (q/RT_o = 17; Initiation 34.5 m Above Base)

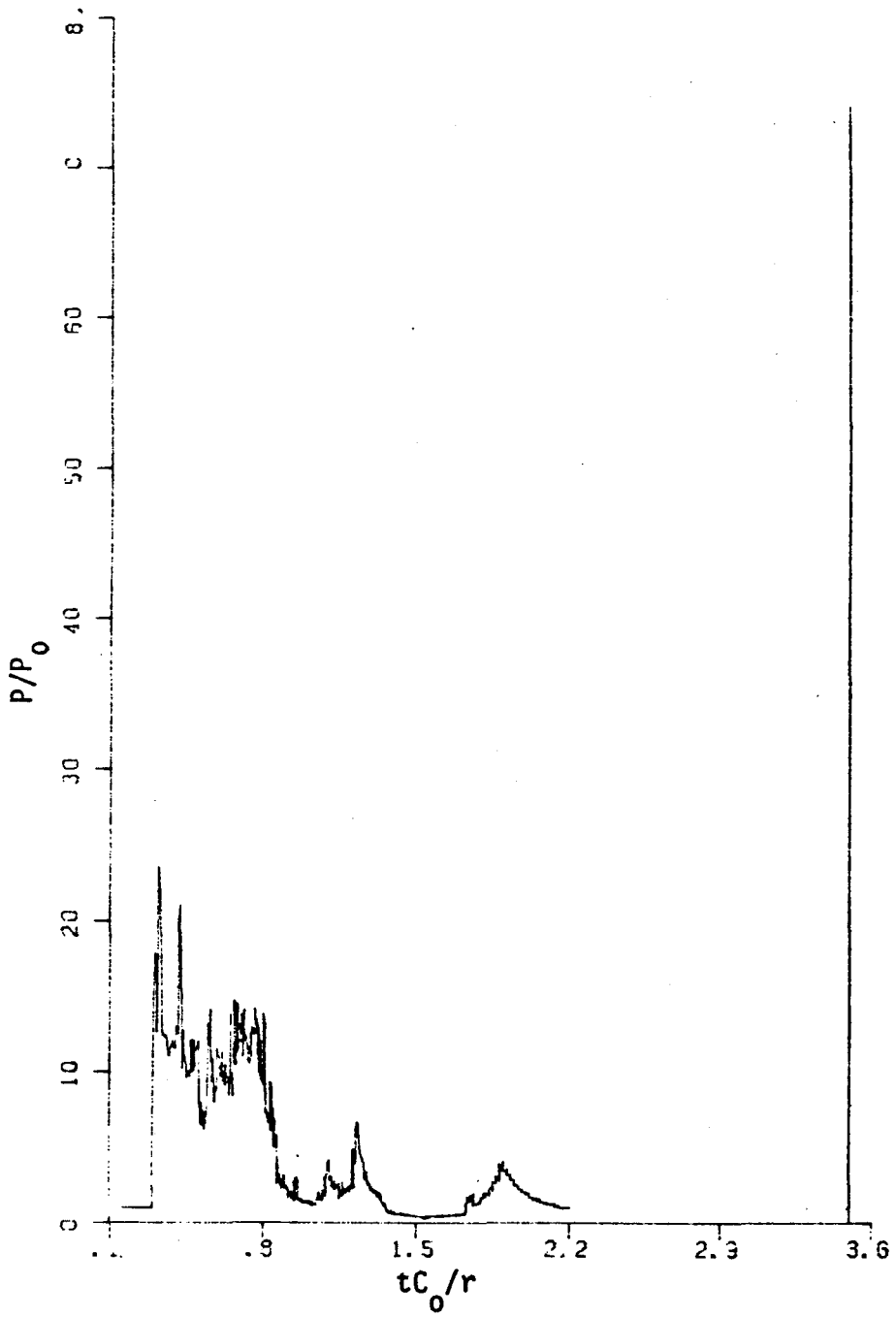

Fig. E.29 - Dome Pressure History at Elevation 66.0 and Radius 5.6 m (q/RT_o = 17; Initiation 34.5 m Above Base Center)

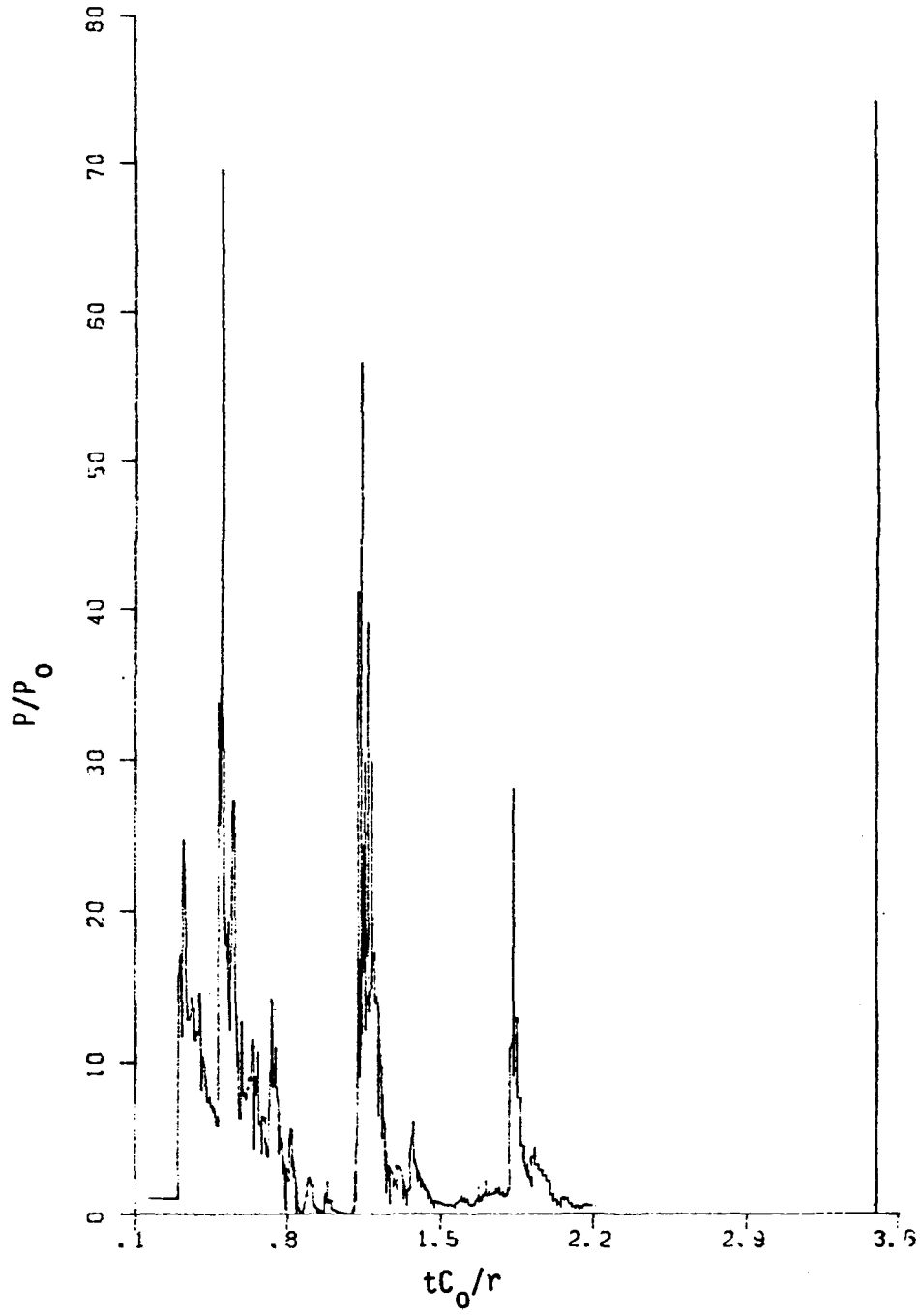

Fig. E.30 - Pressure History at the Apex of the Dome (q/RT_o = 17; Initation 34.5 m Above Base)

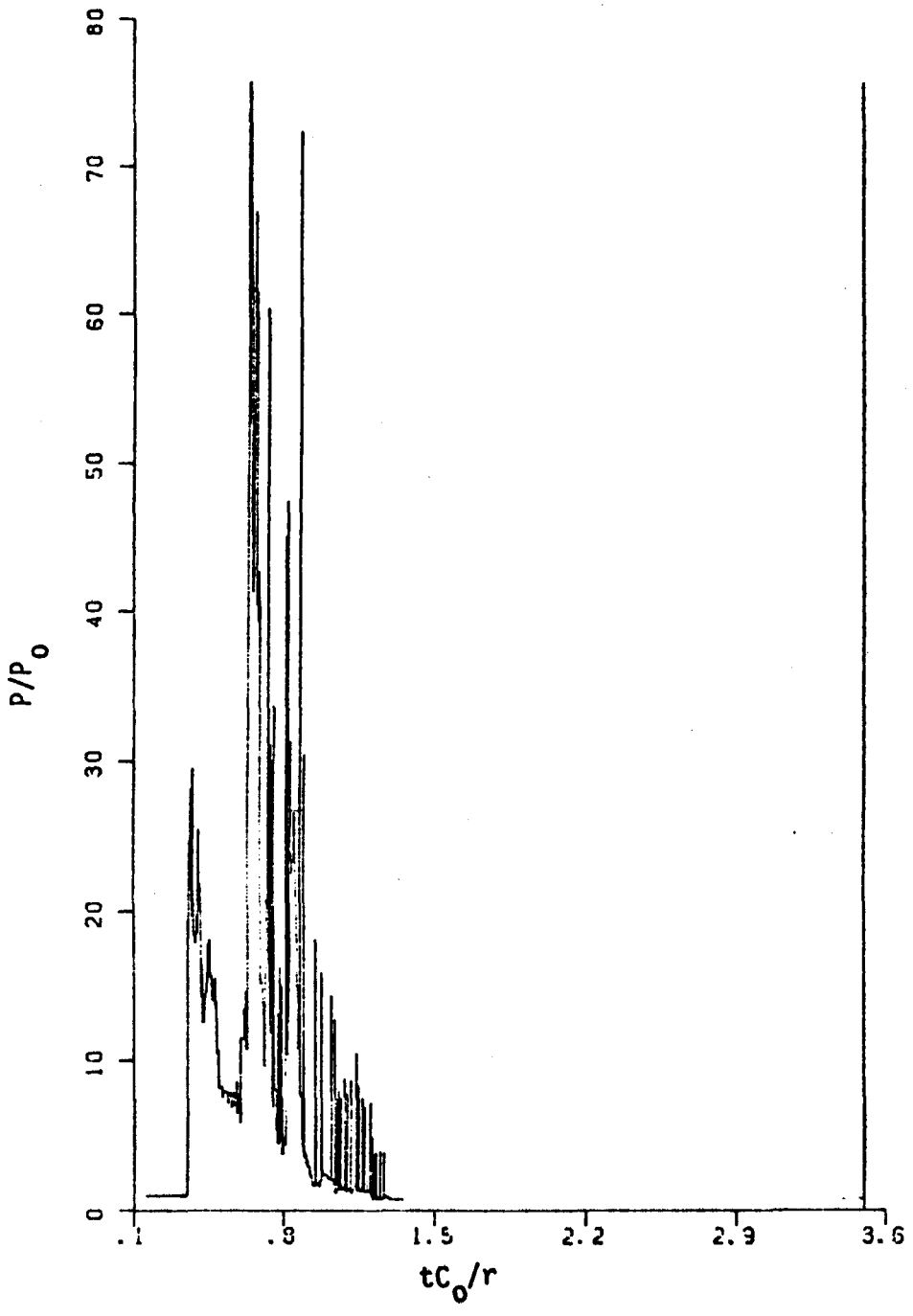

Fig. E.31 - Wall Pressure History at the Junction of the Base and the Cylinder (q/RT_o = 23; Initiation 34.5 m Above Base)

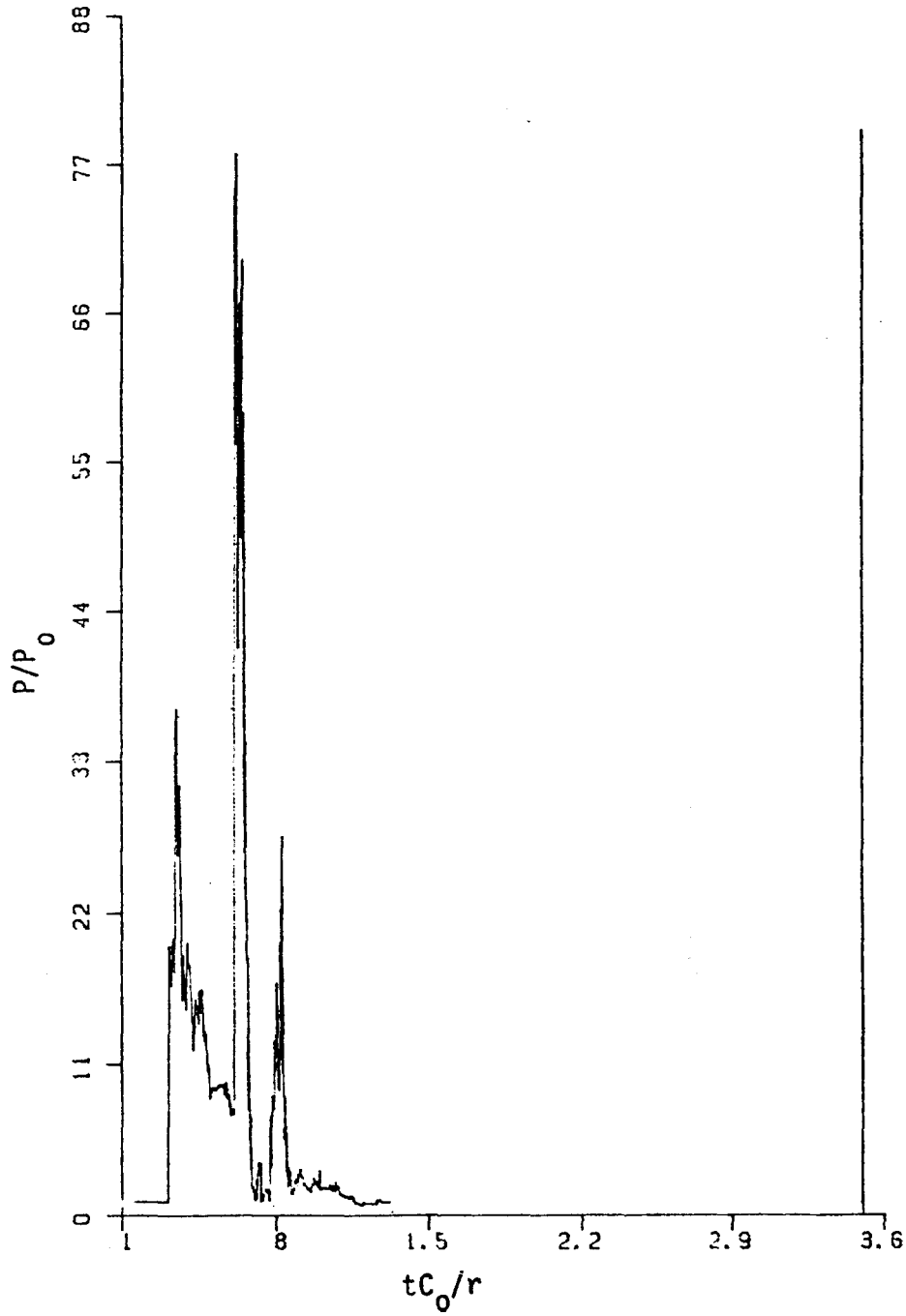

Fig. E.32 - Wall Pressure History at Elevation 6.0 m of the Cylinder (q/RT_1 = 23; Initiation 34.5 m Above Base)

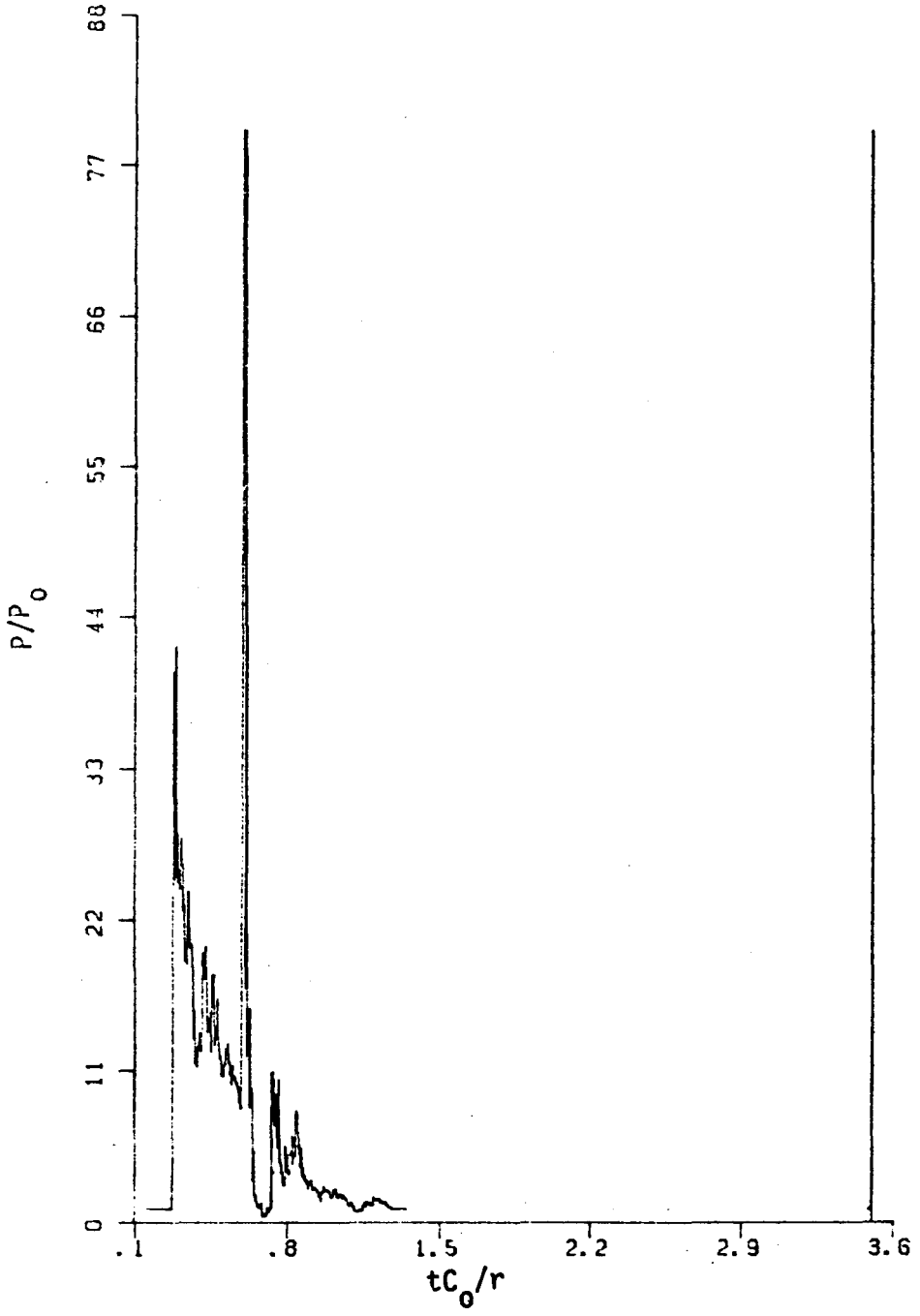

E.33 - Wall Pressure History at Elevation 12.0m of the Cylinder (q/RT_o = 23; Initiation 34.5 m Above Base)

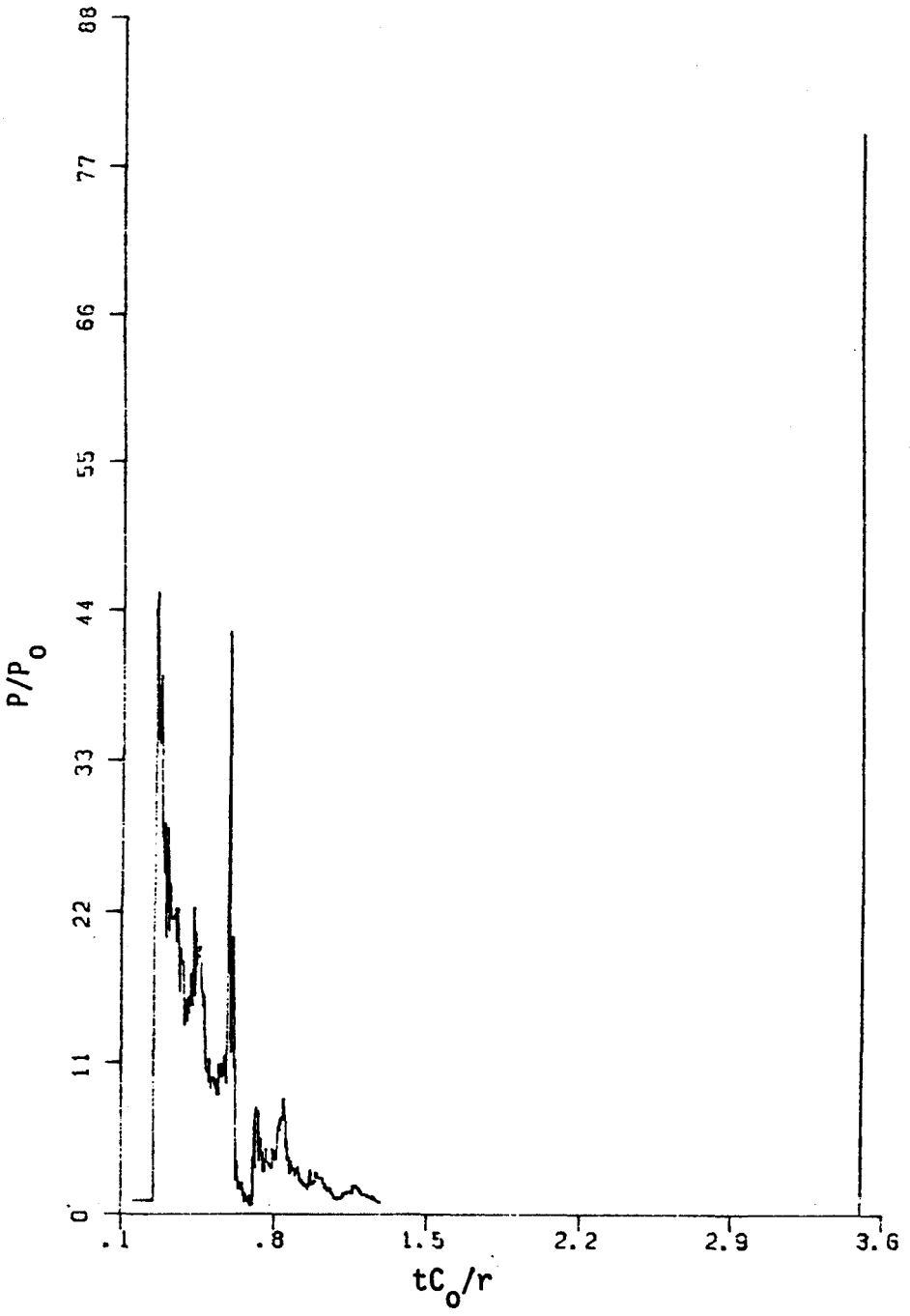

E.34 - Wall Pressure History at Elevation 18.0 m of the Cylinder (q/RT_o = 23; Initiation 34.5 m Above Base)

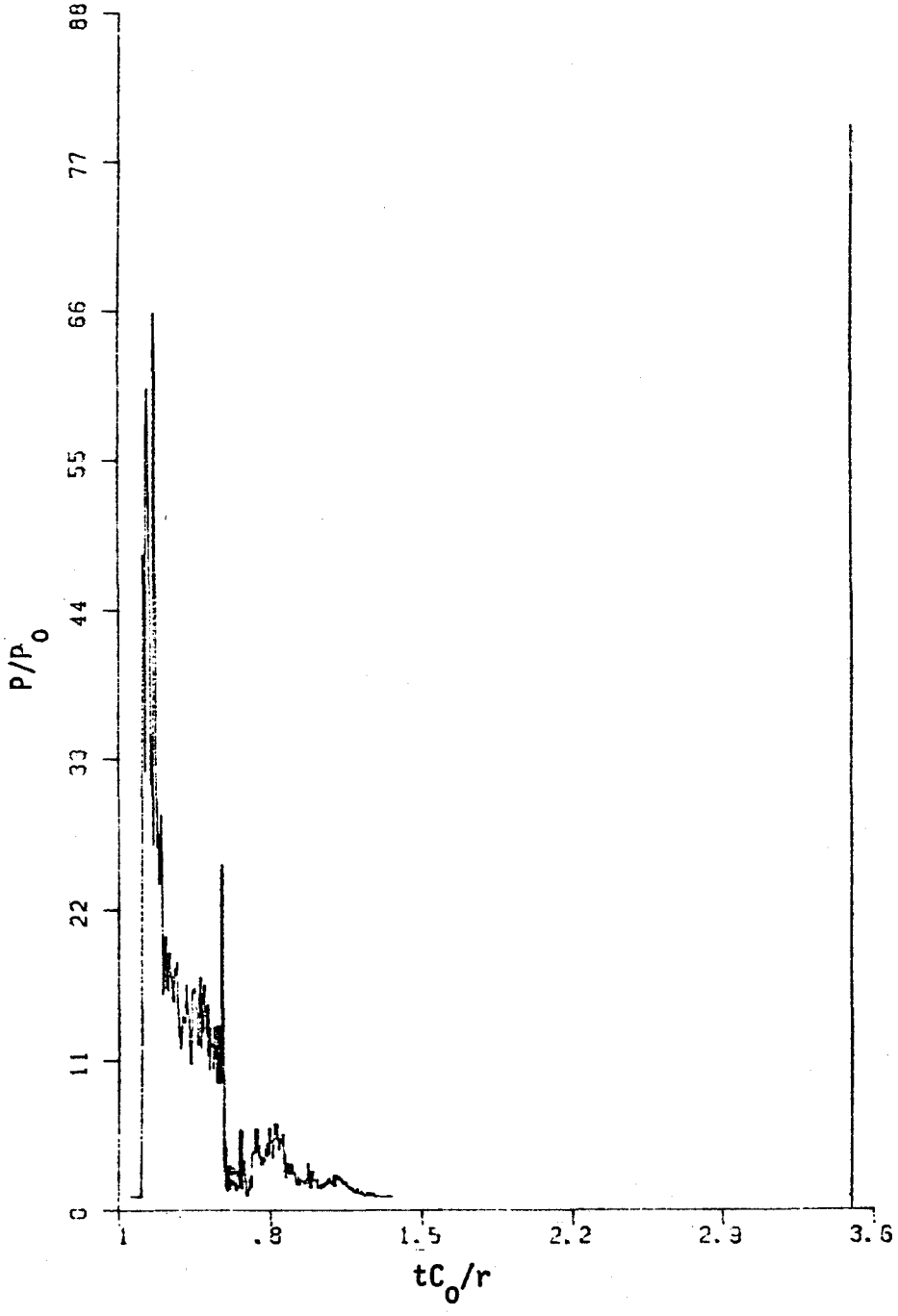

Fig. E.35 - Wall Pressure History at Elevation 24.0 m of the Cylinder (q/RT_o = 23; Initiation 34.5 m Above Base)

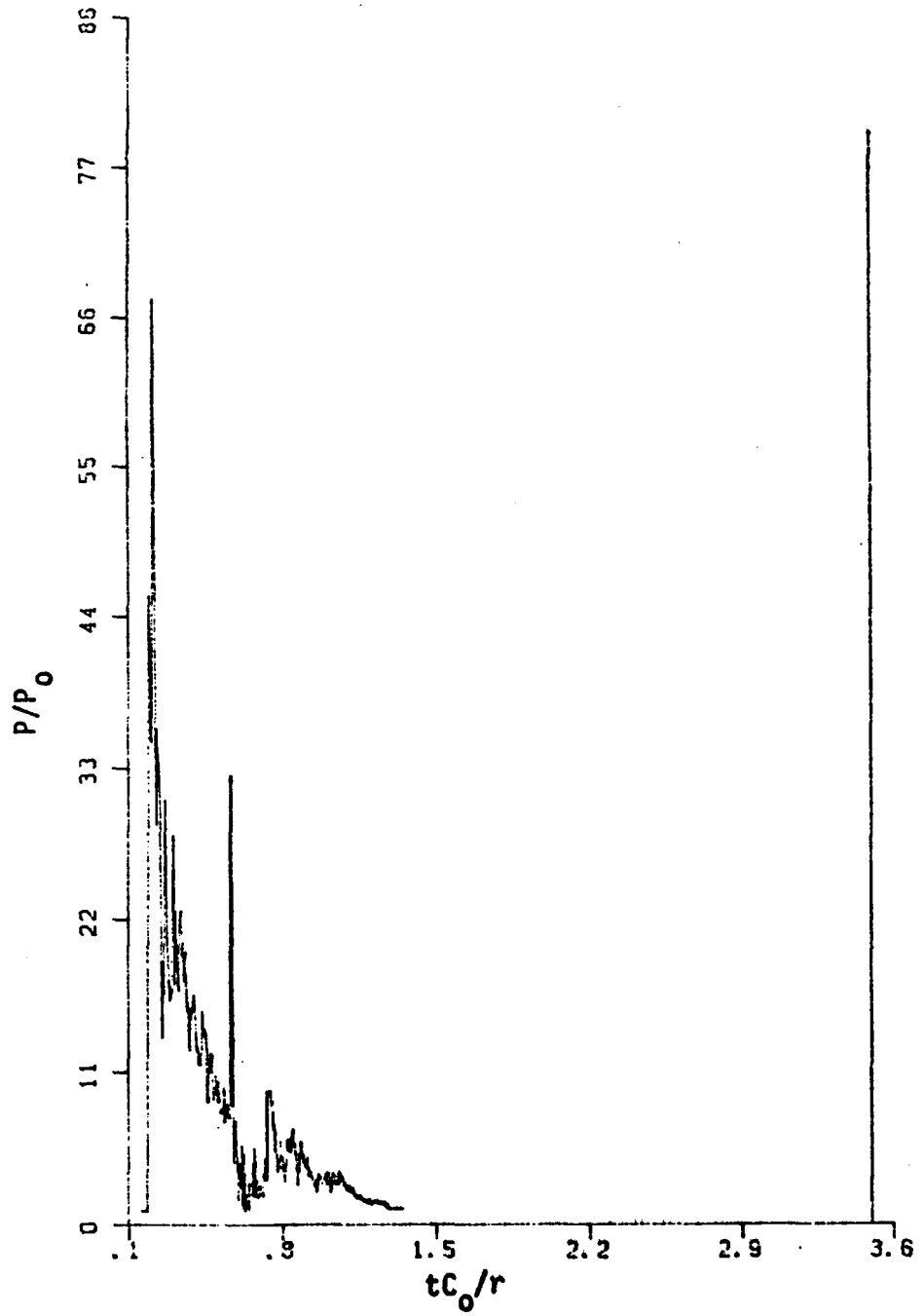

Fig. E.36 - Wall Pressure History at Elevation 30.0 m of the Cylinder (q/RT_o = 23; Initiation 34.5 m Above Base)

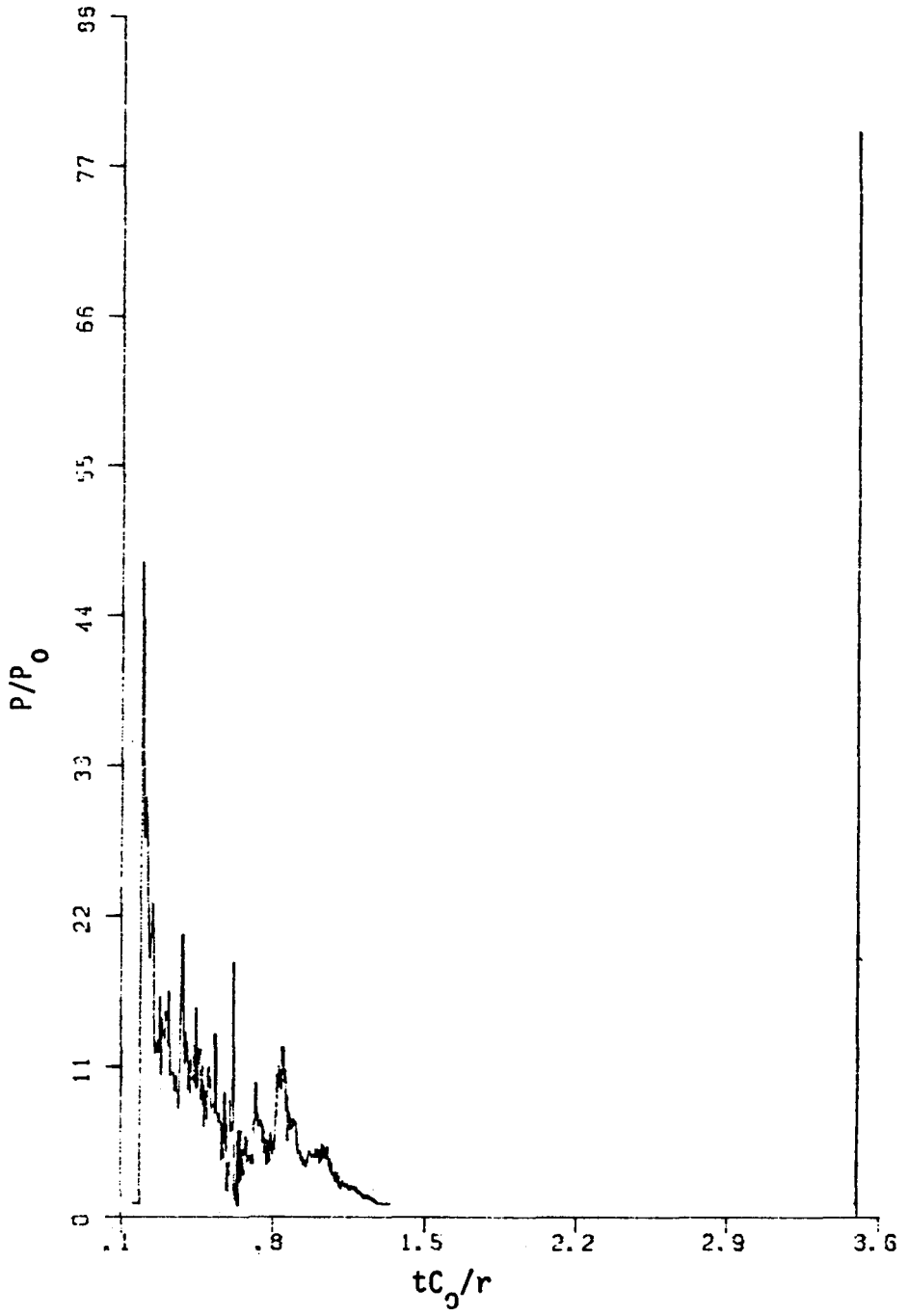

Fig. E.37 - Wall Pressure History at Elevation 36.0 m of the Cylinder (q/RT_0 = 23; Initiation 34.5 m Above Base)

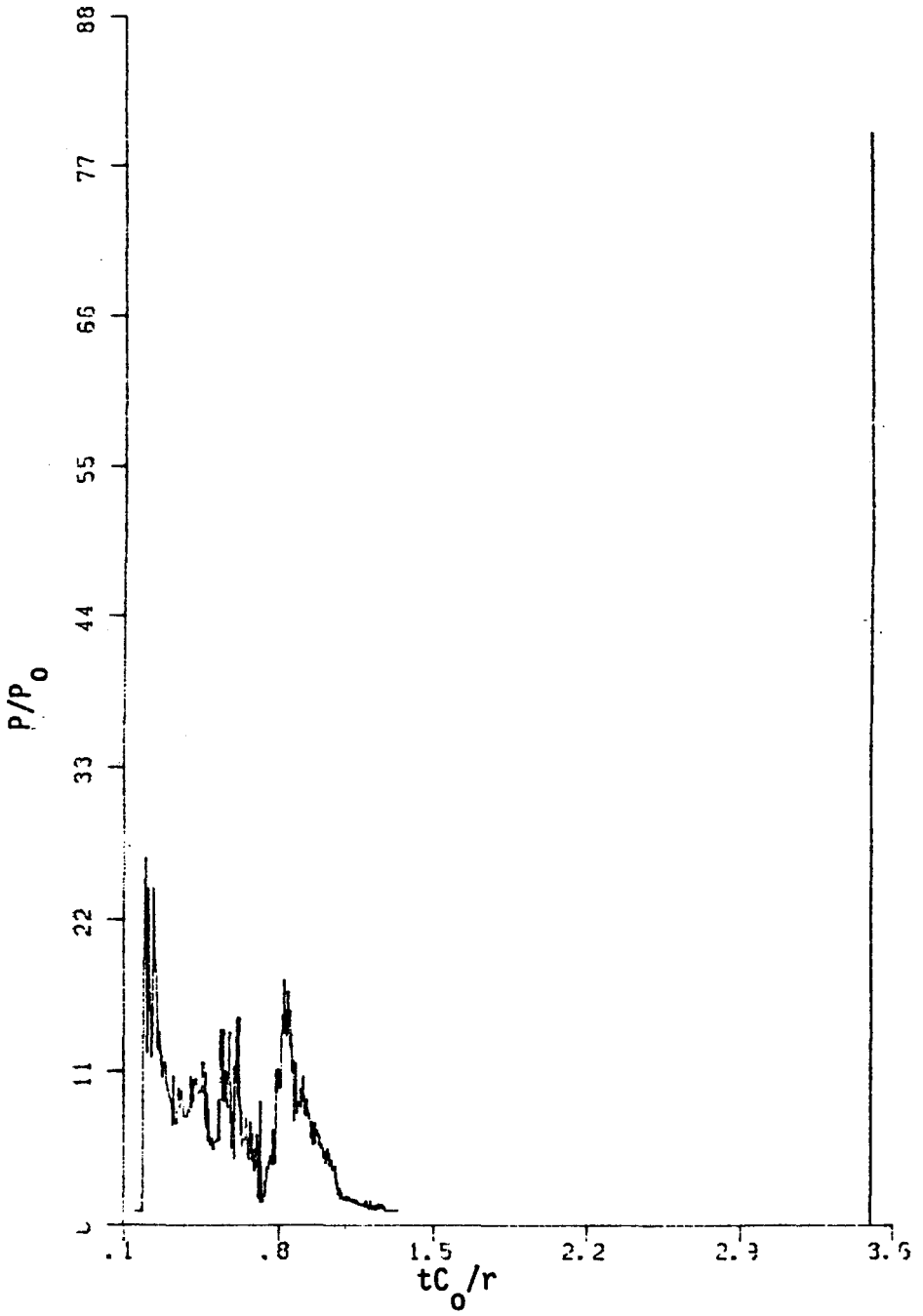

Fig. E.38 - Wall Pressure History at Elevation 42.0 m of the Cylinder (q/RT_o = 23; Initiation 34.5 Above Base)

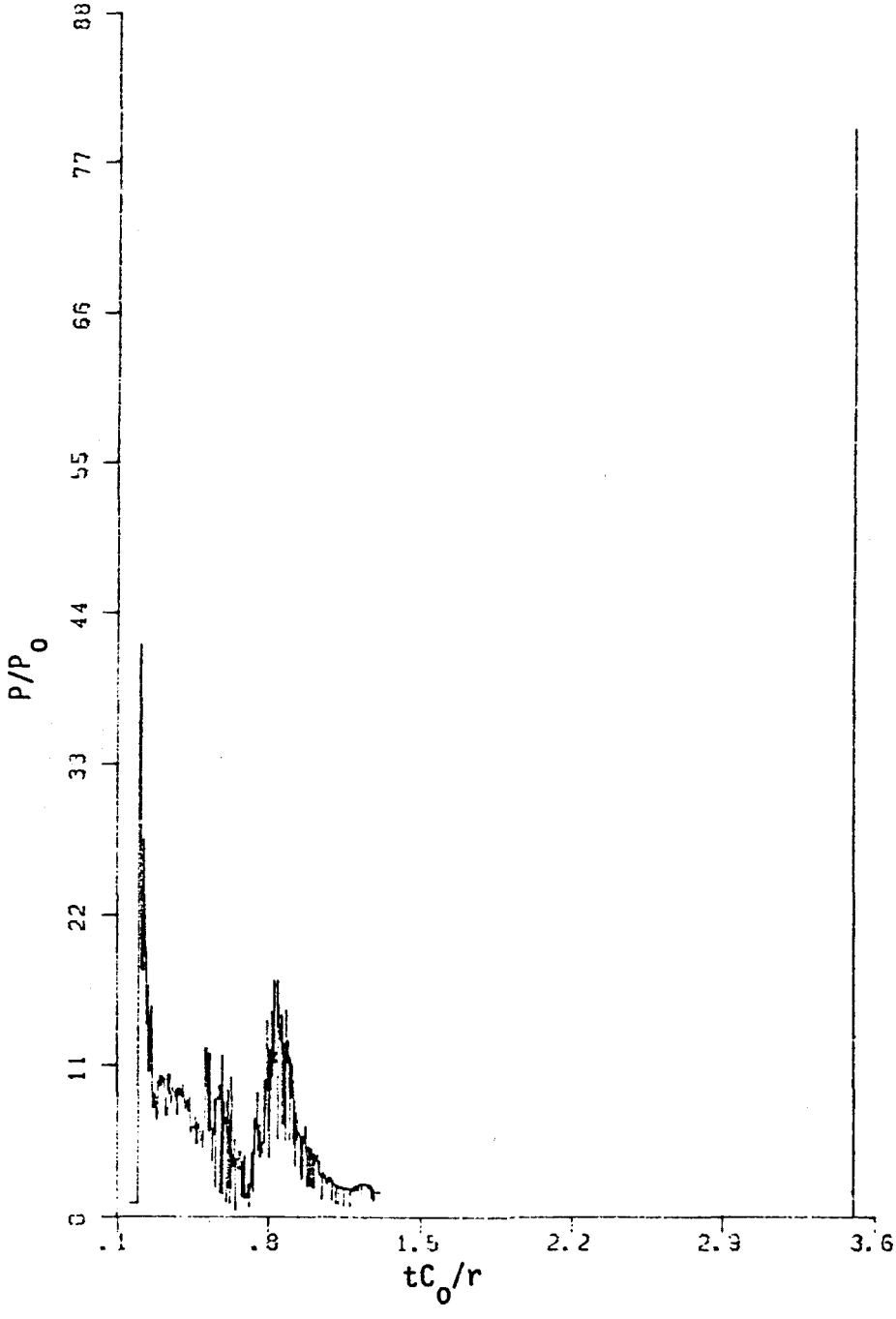

Fig. E.39 - Dome Pressure History at Elevation 47.0 m and Radius 20.7 m (q/RT_0 = 23; Initiation 34.5 m Above Base)

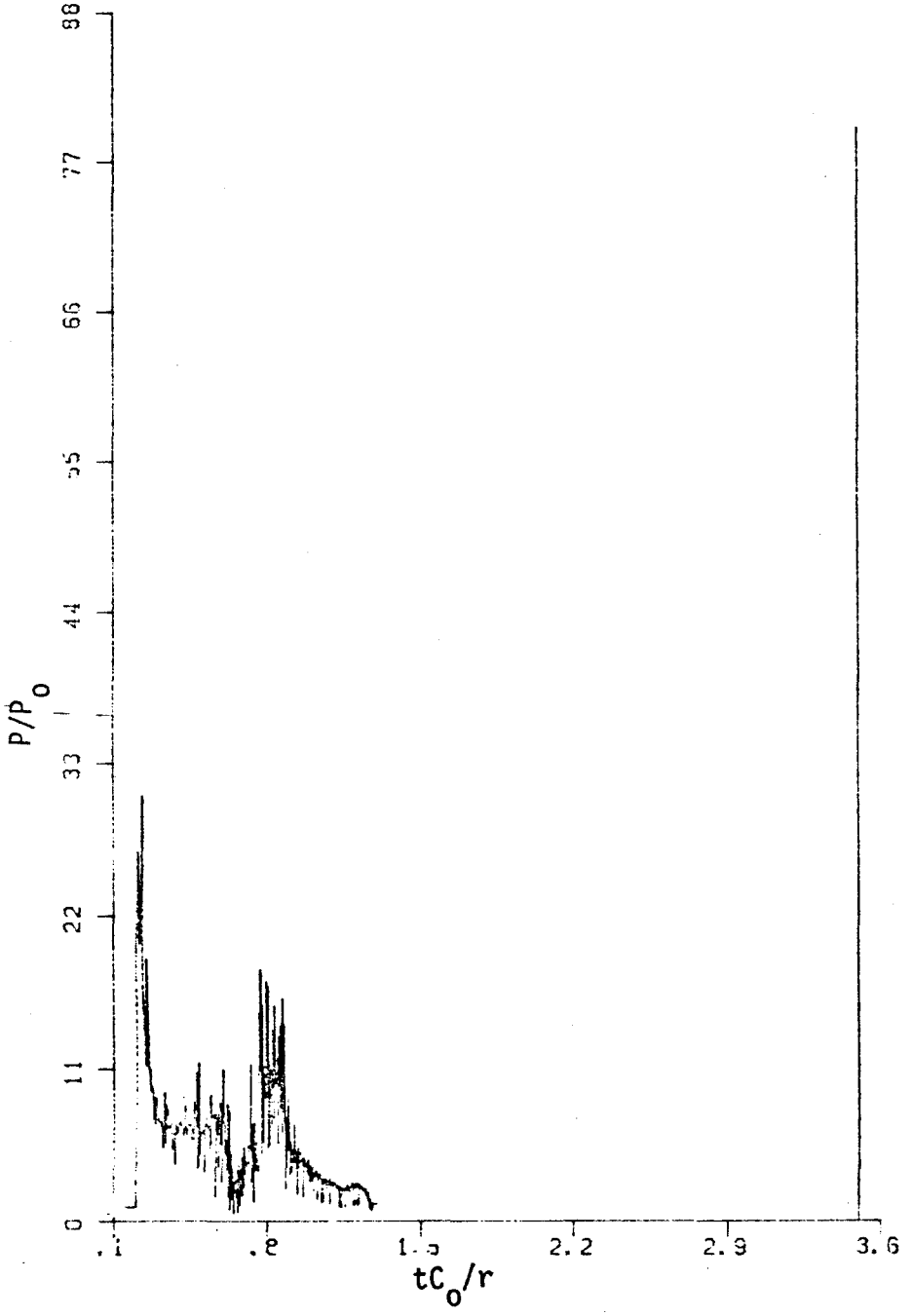

Fig. E.40 - Dome Pressure History at Elevation 51.0 m and Radius 19.4 m (a/RT_o = 23; Initiation 34.5 m Above Base)

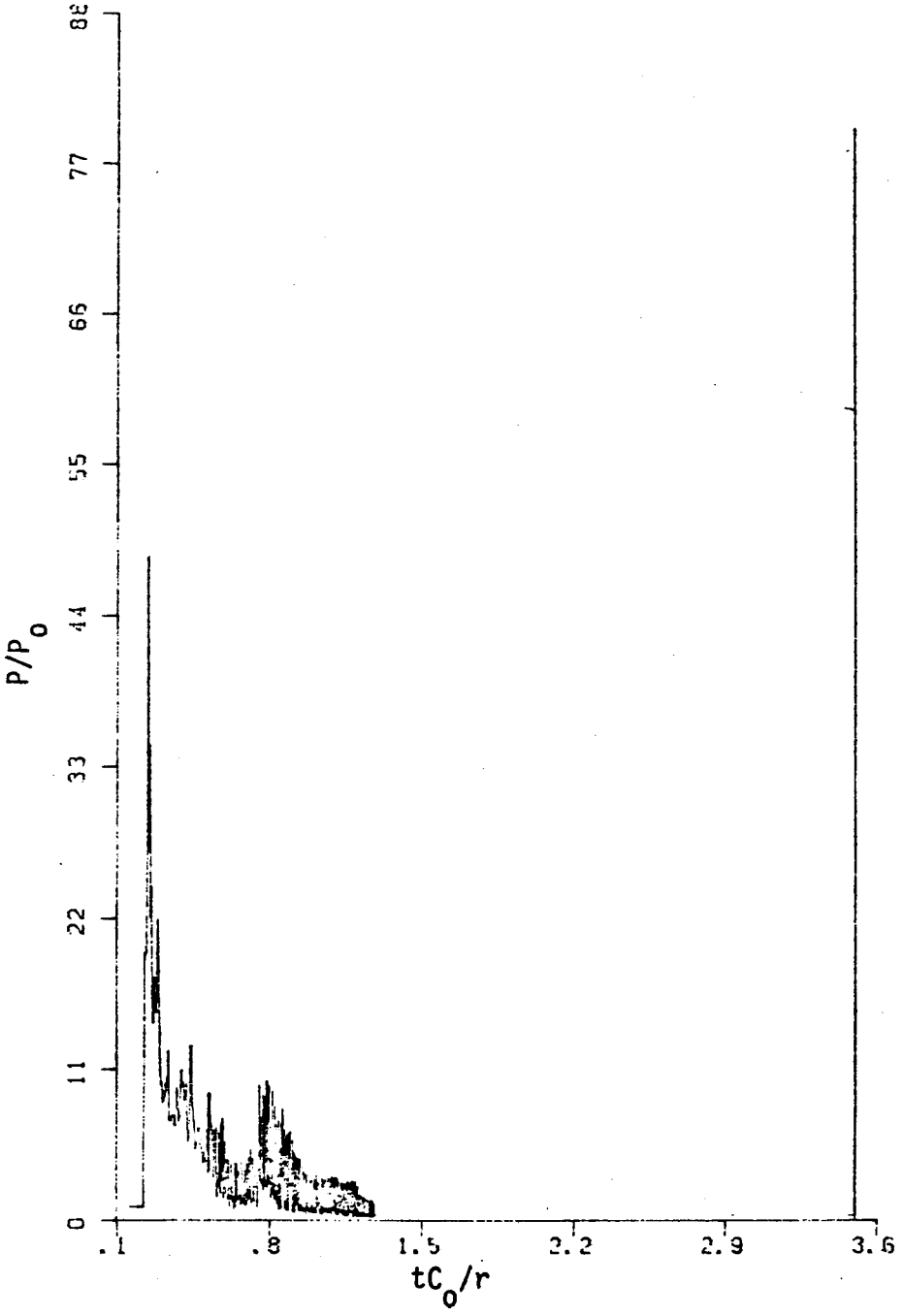

Fig. E.41 - Dome Pressure History at Elevation 56.0 m and Radius 17.6 m (q/RT_o = 23; Initiation 34.5 m Above Base)

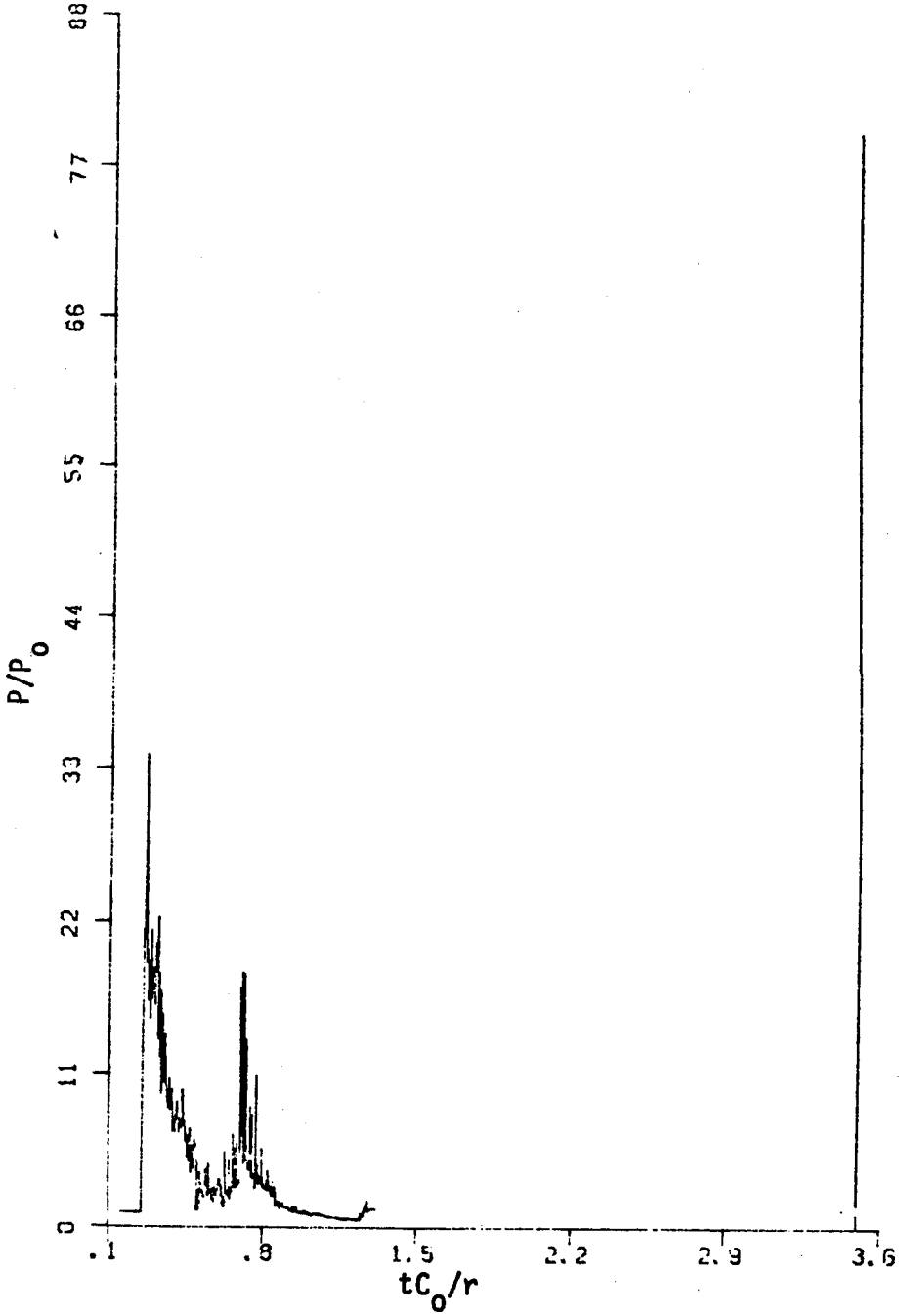

Fig. E.42 - Dome Pressure History at Elevation 61.0 m and Radius 13.6 m (q/RT_o = 23; Initiation 34.5 m Above Base)

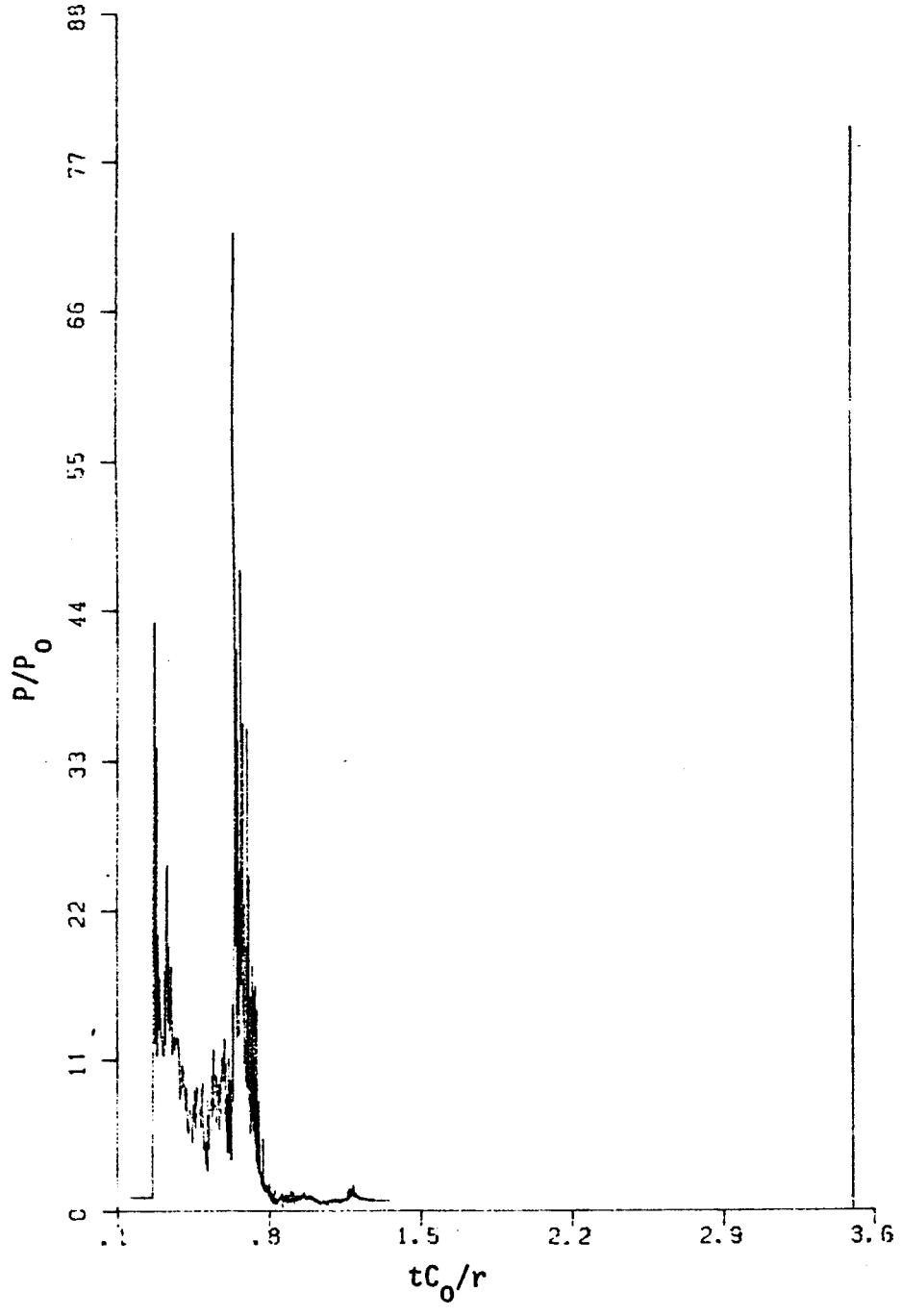

Fig. E.43 - Dome Pressure History at Elevation 64.0 m and Radius 9.6 m (q/RT_o = 23; Initiation 34.5 m Above Base)

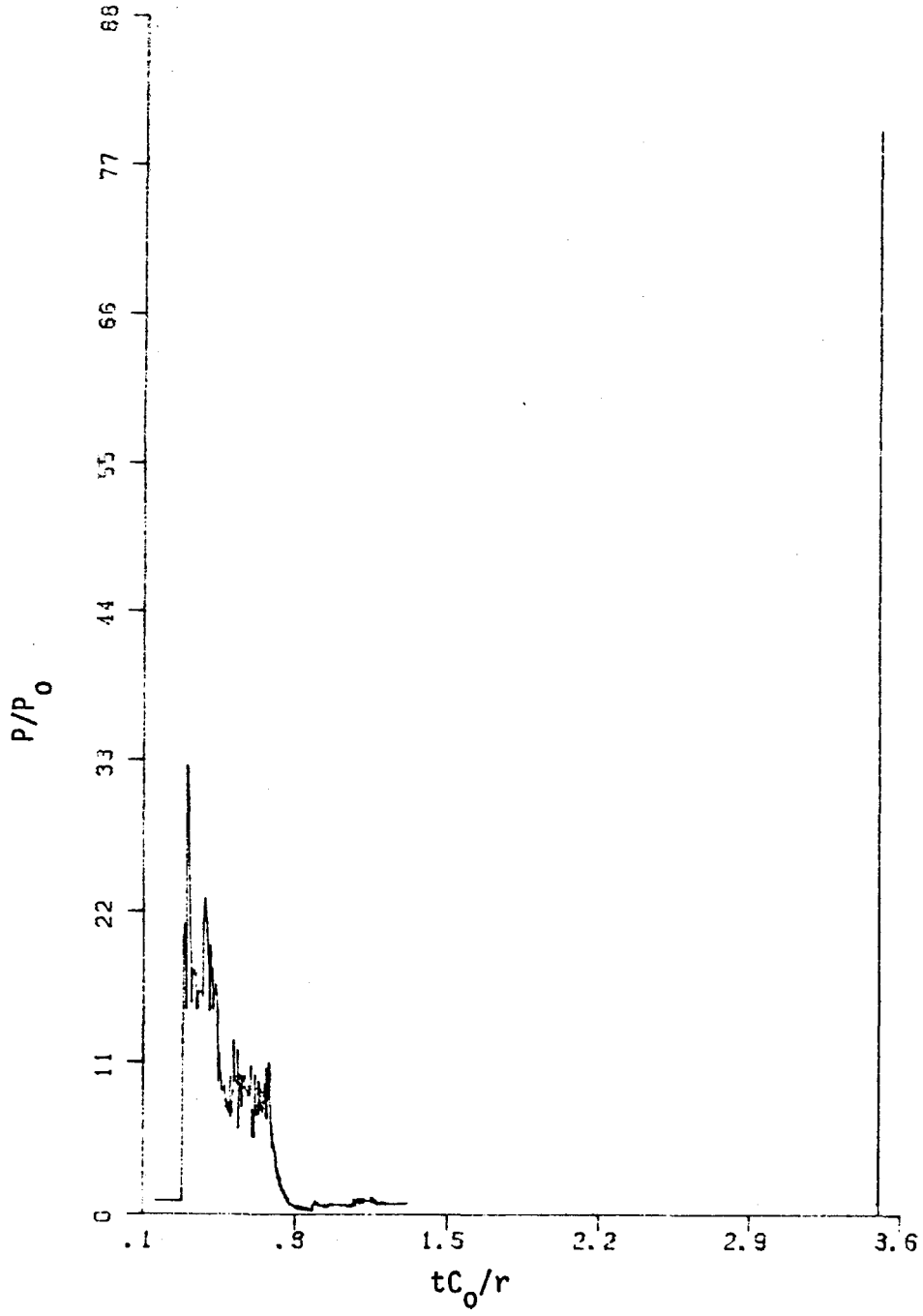

Fig. E.44 - Dome Pressure History at Elevation 66.0 m and Radius 5.6 m (q/RT_0 = 23; Initiation 34.5 m Above Base)

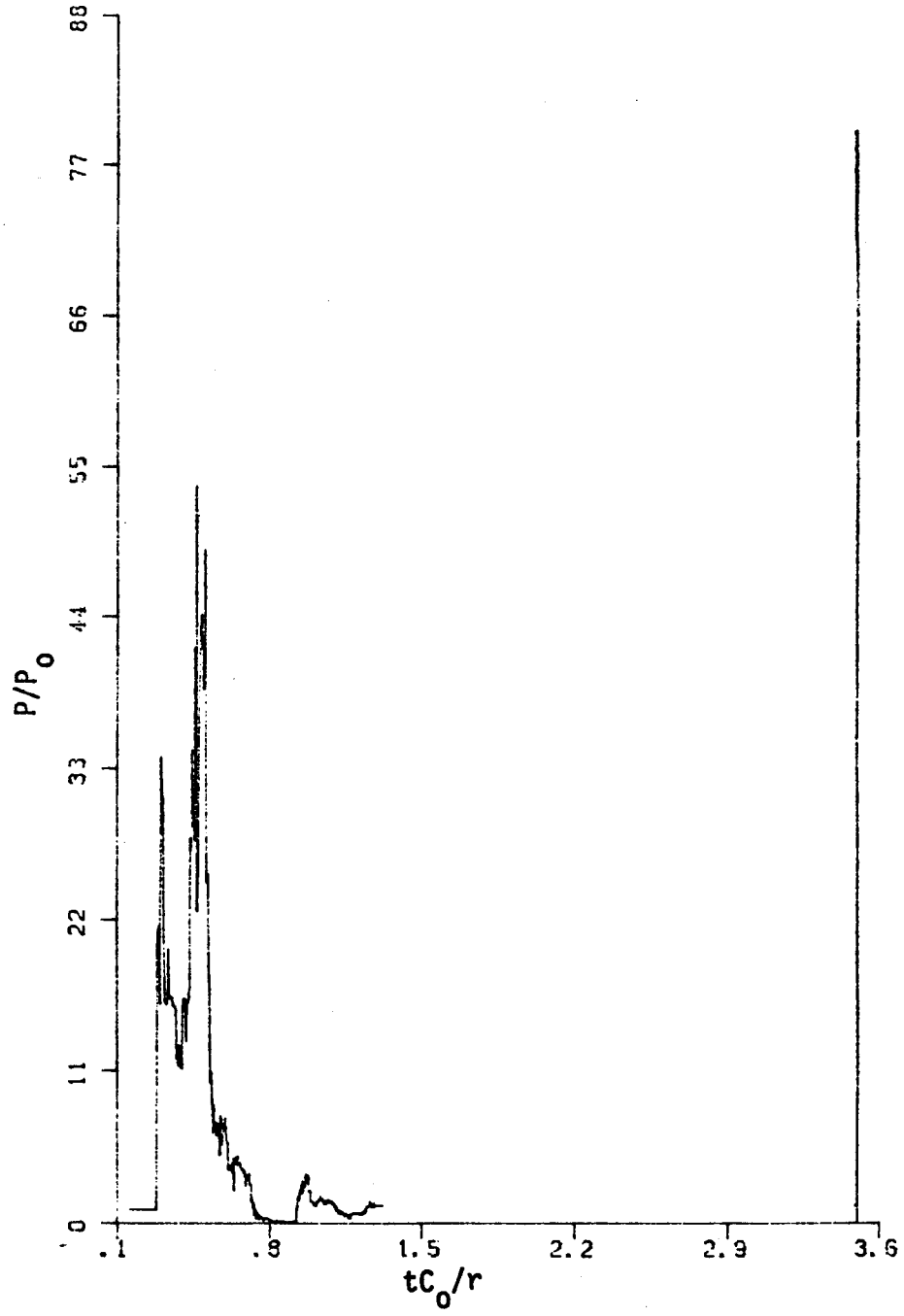

Fig. E.45 - Pressure History at the Apex of the Dome (q/RT_o = 23; Initiation 34.5 m Above Base)

*U.S. GOVERNMENT PRINTING OFFICE:1982 361-297/2047 1-3

NRC FORM 335 (7-77) U.S. NUCLEAR REGULATORY COMMISSION

BIBLIOGRAPHIC DATA SHEET

1. REPORT NUMBER *(Assigned by DDC)*: NUREG/CR-2897

4. TITLE AND SUBTITLE *(Add Volume No., if appropriate)*: Calculations of Hydrogen Detonations in Nuclear Containments by the Random Choice Method

2. *(Leave blank)*

3. RECIPIENT'S ACCESSION NO.

7. AUTHOR(S): Michael A. Delichatsios, Marcel B. Genadry, Michael N. Fardis

5. DATE REPORT COMPLETED: MONTH December YEAR 1981

9. PERFORMING ORGANIZATION NAME AND MAILING ADDRESS *(Include Zip Code)*:
Michael N. Fardis
Dept. of Civil Engineering
Massachusetts Institute of Technology
Cambridge, Massachusetts 02139

DATE REPORT ISSUED: MONTH September YEAR 1982

6. *(Leave blank)*

8. *(Leave blank)*

12. SPONSORING ORGANIZATION NAME AND MAILING ADDRESS *(Include Zip Code)*:
Division of Engineering Technology
Office of Nuclear Regulatory Research
USNRC
Washington, DC 20555

10. PROJECT/TASK/WORK UNIT NO.

11. CONTRACT NO.: B7085

13. TYPE OF REPORT: Formal Technical Report

PERIOD COVERED *(Inclusive dates)*: 9/80 - 12/81

15. SUPPLEMENTARY NOTES

14. *(Leave blank)*

16. ABSTRACT *(200 words or less)*

Computer codes simulating hydrogen detonators in planar, cylindrical, spherical and two-dimensional axisymmetric geometries were developed. The computational method is based on the Random Choice Technique which can handle accurately sharp discontinuities. The detonation front is represented as a discontinuity changing the still unburnt gas to a completely burnt one, according to the Chapman-Jouguet conditions. Results for one-dimensional geometries show good agreement with available analytical solutions. The one-dimensional code was modified to include coupling with an elastically deformable wall and used to demonstrate that for typical concrete containment structures interaction of the waves with wall deformations has insignificant effects on the wave properties, and can be neglected. The two-dimensional axisymmetric code was used to calculate pressure time histories at the wall of a cylindrical containment capped with a semi-spherical dome, dimensionally similar to the Indian Point Nuclear Power Plant. The detonations simulated had initiation at either the center of the base mat or at a point on the axis at approximately two-thirds the cylinder height, and were for two different intensities. Computed pressures included repeated reflections at the walls and died out within a few tenths of a second.

17. KEY WORDS AND DOCUMENT ANALYSIS

17a. DESCRIPTORS

17b. IDENTIFIERS/OPEN-ENDED TERMS

18. AVAILABILITY STATEMENT: Unlimited

19 SECURITY CLASS *(This report)*: Unclassified

21 NO OF PAGES

20 SECURITY CLASS *(This page)*

22 PRICE: $